Sheffield Hallam University

A Sheffield Hallam University thesis

ProQuest Number: 10694449

ProQuest 10694449

STUDIES OF BRONZE ELECTRODEPOSITION.

by

BRIAN   ERIC   DODDS   BSc.

A THESIS SUBMITTED TO THE COUNCIL FOR NATIONAL
ACADEMIC AWARDS IN PARTIAL FULFILMENT OF THE
REQUIREMENTS FOR THE DEGREE OF MASTER OF
PHILOSOPHY.

Collaborating Establishment: Goldrite Limited
                             Sheffield
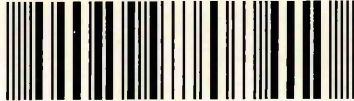
Sponsoring Establishment: Materials Research Institute
                          Sheffield City Polytechnic

DATE: OCTOBER 1992.

PREFACE.

The results obtained and theories developed during the course of this work are to the best of my knowledge original, except where reference is made to the work of others.
No part of this thesis has been submitted for a degree at any other university or polytechnic.

B.E.Dodds

October 1992.

INTRODUCTION

The aim of the work carried out in this thesis was to study the behaviour of a cyanide-stannate bronze plating bath with a view to constructing a model of the process. This model would then serve as the basis for the development of a predictive control system which could be used to control the bath to produce bronze deposits having desired chemical and physical properties.

Alloy deposits have advantages over deposits of pure metals, alloys exhibit a wide range of properties in both the "as plated" and heat treated conditions.

Bronze is an alloy which is used extensively for industrial and aesthetic purposes, there are strong possibilities for bronze plate to replace nickel plate for certain applications where the plated article comes into contact with humans.

The properties of alloy deposits are highly dependent upon their chemical compositions and so the ability to produce alloy deposits with consistent compositions is highly desirable.

A study of a typical bronze plating solution is of general interest. Thus a cyanide-stannate bronze plating solution was used for these studies. The copper and tin in this type of bath exist as different complexes and are normally deposited with different valencies. This makes the cyanide-stannate type of bronze plating solution a good example to study. If a predictive control system can be developed for this type of bath it should be feasible to do the same for less complicated

alloy plating solutions.

The usual way adopted to control alloy deposits is to perform bath analysis and adjust the bath composition accordingly. The best outcome that could be expected from this is for the bath composition to fluctuate above and below its optimum value. The degree of control exerted on the bath composition depends upon the frequency of bath analysis.

A more precise method of controlling the bath composition and the alloy deposits produced from such a bath would be to construct a predictive model based upon a fundamental understanding of the bath's behaviour.

Aspects of the baths operation to be studied included the effects of temperature, current density, current mode, anode material and bath composition upon the composition and properties of the bronze deposits produced.

The current modes studied were conventional and pulsed currents. Pulsed currents were investigated as it was known that by using a superimposed pulsed current with certain systems produced deposits with enhanced properties.

Anode materials to be investigated were inert, copper, tin and bronze which covers all the practical possibilities for anodic material.

ABSTRACT.

Studies have been carried out on a bronze plating solution using conventional current and pulsed current electrolyses at various bath temperatures and anode and cathode current densities under galvanostatic conditions. The results from these tests have been interpreted and a set of optimum bath conditions has been decided upon to achieve deposits of a desired composition and properties.

Further studies have been carried out to determine the effect of bath composition, anode material and pulse frequency on the composition and structure of the deposits obtained.

The deposits produced were analysed chemically by atomic absorption and X-ray fluorescence methods and studied structurally by X-ray diffraction.

By application of the experimental data to the optimum plating conditions already specified a rudimentary mass balance for the system has been calculated. The possibility of developing a predictive control system for the bronze bath has been discussed in relationship to the mass balance.

Contents.

1.0 Literature Review.

1.1 Alloy Plating.

Alloy plating has certain advantages and disadvantages over the plating of pure metals. The main advantage is that alloys exhibit many phases and properties that a single metal does not have, Figure (1). Alloys are also responsive to heat treatment and a wide range of useful properties can be obtained by using the appropriate alloy system with or without heat treatment of the as plated alloy deposit.

A major drawback to alloy deposition is that many useful alloys have parent metals with widely differing standard electrode potentials, (E^o values). This is illustrated in Table (1) and clearly shows that under normal circumstances a gold-cobalt alloy could not be deposited (1). Gold is the most noble metal and its co-deposition with other less noble metals would not be expected. Gold has an E^o value of +1.70v and cobalt has an E^o value of -0.277v. To bring about co-deposition of these two metals their potentials must be equalised and the potential of the gold made more negative (less noble). There are two main ways this can be accomplished. Firstly, diluting a solution will move the electrode potential to a more negative (base) value as can be seen from Table (2). This however has only limited scope, as diluting the more noble metals concentration to 10^{-20}M only gives a negative shift in the E value of 0.59v. In turn, having such a dilute solution would make controlling the deposit composition virtually impossible. This is because removing even the slightest amount of alloy would alter the

concentration of the noble metal and the ratio of the metals in solution so drastically.

The second and most widely used method involves complexing the noble metal with a suitable complexant. The instability constant for each complex gives a measure to the degree of complex dissociation, a list of instability constants is given in Table (3).

The main types of complexants used are cyanides although other complexants are used to some extent. Indeed, alloy plating only became commercially viable with the advent of cyanide complexing. The previous statements may be explained by considering the following:

If a metal is immersed in a solution of its own ions a potential difference occurs between metal and solution which is described by the Nernst equation:

$$E = E^\circ - \frac{RT}{nF} \ln (a_m / a_{mn+})$$

Where E° = Standard Electrode Potential

R = Gas constant.

T = Temperature in Kelvin.

n = Number of electrons involved per gram atom.

F = Faraday constant (96,487 Coulombs).

a_m and a_{mn+} = Activity of Products and Reactants.

Thus, assuming that (a_m = 1), the following is obtained:

$$E = E^\circ + \frac{0.059}{n} \log a_{mn+}$$

From this equation it can seen that diluting the

solution will move the electrode potential to more negative values.

Using the example of gold and cobalt to demonstrate the effect of complexing. The respective E^o values for gold and cobalt are; (+ 1.70v and - 0.277v). For co-deposition to occur we need to lower the gold potential to that for cobalt, by using the Nernst equation we can find the required values.

$$- 0.277 = 1.70 + 0.059 \log [Au^+]$$

$$[Au^+] = 10^{-34}M$$

This can be achieved by cyanide complexing if excess cyanide is maintained, as the instability constant for the gold cyanide complex $Au(CN)_2^-$ is 5×10^{-39} .

$$(Au(CN)_2)^- = Au^+ + 2CN^-$$
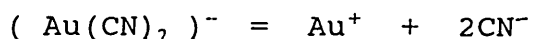
$$K = \frac{[Au^+] \ [CN^-]^2}{[Au(CN)_2^-]} = 5 \times 10^{-39}$$

However, whether or not alloy deposition occurs is determined by more than just the relative electrode potentials of the pure metals for any particular alloy system. The determining factor is the deposition potential determined by the polarization processes (2). These processes are affected by factors such as bath temperature, bath agitation, cathode current density and metal ion concentration. The metal ions may arrive at the cathode surface by transport due to the applied potential, by diffusion, or by convection within the bath. When charged metal ions or complexes arrive at the cathode increasing the potential causes an increase in the ion discharge rate which in turn causes an increase in current. The

concentration difference between the bulk solution and the cathode layer increases, this causes an increase in the rate of diffusion. When ions arriving at the cathode by diffusion are immediately discharged the limiting current density is said to have been reached. This is because the number of ions being discharged under these conditions is determined exclusively by the diffusion rate. Thus, any further increase in potential will cause no increase in current. In an alloy plating bath comprising of metals of different nobilities, diffusion rates, concentrations, limiting current densities and complexants, the interrelationship between these parameters plays a large part in determining the alloy deposit composition.

Five main types of alloy deposition have been categorised by Brenner (3),(4), these are as follows:

1. Regular solutions, these are diffusion controlled and contain uncomplexed metal ions of metals with vastly different nobilities.

2. Irregular solutions under cathode potential control where the static potential is affected by complexing alone, such as a cyanide bath for brass deposition.

3. Equilibrium solutions where at low current densities the metal ratio in the bath and deposit are directly related, such as acid plated lead-tin alloys.

4. Anomalous solutions where the less noble metal deposits preferentially.

5. Solutions where a metal which will not deposit

alone can be co-deposited as an alloy.(e g. tungsten or molybdenum with iron).

Types one, two and three above are classed as normal systems. The proportions of each metal in the deposit can be estimated from the polarization curves for each individual metal.

Two general types of system are observed as can be seen from Figure (2). The first is where the polarization curves for the metals have similar slopes. In this case the deposit weight ratio is given by i_1z_1 / i_2z_2 ; where i_1 and i_2 are the individual current densities and z_1 and z_2 their electrochemical equivalents (1).

The second case is where the polarization curves intersect and at this point $i_1 = i_2$ and the weight ratio in the deposit must be proportional to z_1 / z_2 . At more positive potentials the ratio is less while at more negative potentials the ratio is more. The overall deposition rate ($i_1z_1 + i_2z_2$) also varying with potential.

The deposition process involves the cathodic discharge of a metal bearing ion to form a growing deposit surface. This may be regarded as a series of steps in which the ion moves towards the electrode surface and is finally discharged. The events thought to occur during this process when a metal is deposited from one of its complexes are schematically depicted in Figure (3). This may be summarised by four main steps (2).

1. Ion migration to the cathode through the electrode double layer to the electrode surface and loss of hydration molecules.

2. Ion adsorbed as an adion onto the metal surface or incorporation into an intermediate surface film.

3. The adion diffuses across the surface to a site of minimum surface energy.

4. Ionic discharge and electron transfer.

The cathode attracts mainly positively charged ions into the Helmholtz double layer which is a region adjacent to the cathode surface. In addition the cathode also attracts negatively charged complex ions such as the $Cu(CN)_2^-$, $Cu(CN)_3^{2-}$ and $Cu(CN)_4^{3-}$ ions which are present in bronze cyanide plating solutions. These are polarised in the electric field of the cathode. The ligands around the metal become distorted and this assists diffusion of the complex ion into the Helmholtz double layer. When finally within this layer the complex breaks up with its component ligand ions or molecules being set free. The metal is released as a positively charged metal cation and is deposited onto the cathode as a metal atom.

Direct deposition from anions at a cathode surface is unlikely unless a neutral surface film can be formed, discharge may then proceed as follows.

$$Cu(CN)_2^- + e \rightarrow Cu^0 + 2CN^-$$
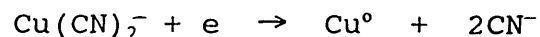
If the complex is regarded as a cation reservoir, where following dissociation of the complex indirect discharge occurs, a better explanation may be derived. Thus:

$$Cu(CN)_2^- \rightarrow Cu^+ + 2CN^-$$

$$Cu^+ + e \rightarrow Cu^0$$
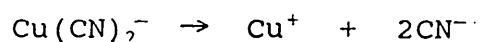
The static potential in a series of copper cyanide

complexes will depend upon which of the complexes is predominant at any time. In simple solutions metal cation depletion usually occurs due to concentration polarisation. In complex baths metal cation depletion may lead to complex concentration. Also, large potential changes which vary with current density may be caused due to complex concentration in the cathode layer.

Examination of the instability constants for the copper complexes shows large variations and for this reason it is difficult to assess exactly which reactions are occurring at any one time.

$$Cu(CN)_2^- = Cu^+ + 2CN^-$$

Complex ion: [Cu(CN)$_2^-$]

    Instability Constant = 1×10^{-16}

$$Cu(CN)_3^{2-} = Cu^+ + 3CN^-$$
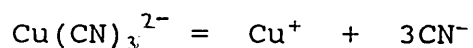
Complex ion: [Cu(CN)$_3^{2-}$]

    Instability Constant = 5.6×10^{-28}

$$Cu(CN)_4^{3-} = Cu^+ + 4CN^-$$
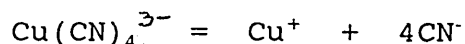
Complex ion: [Cu(CN)$_4^{3-}$]

    Instability Constant = 1×10^{-27}

Concentration polarization occurs in the deposition of tin from an alkaline stannate with a rise in pH accompanying tin deposition due to hydroxyl ion formation.

$$SnO_3^{2-} + 3H_2O + 4e \rightarrow Sn^\circ + 6OH^-$$
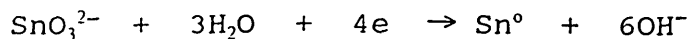
The above process occurs in two stages. Firstly, an irreversible stage where tin changes from a tetravalent to a divalent state. The second stage being the conversion of the divalent form to metallic tin.

$$Sn(OH)_6^{2-} + 2e \rightarrow Sn(OH)_4^{2-} + 2OH^-$$

$$Sn(OH)_4^{2-} + 2e \rightarrow Sn^\circ + 4OH^-$$
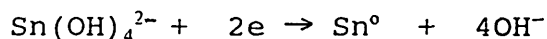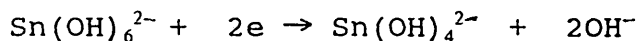
This suggests that tin metal would redissolve in excess hydroxyl ion concentrations in solutions having very high pH values.

1.2 Pulse Plating.

Although considered by some to be a relatively new concept, pulse plating has in fact been used in one form or another since Coehn (5) produced coherent deposits of zinc at the end of the last century. The reason for it being considered a new process is that advances made in electronic control equipment have given much greater scope to the process.

The main reasons for using pulsed or modulated current as it is sometimes referred to is that it may, depending upon the species being deposited, improve the deposits physical properties. Some of the properties that pulse plating has been claimed to improve are as follows:(6).

1. Decreased porosity due mainly to grain refinement,

- 8 -

each pulse producing a new nucleation site.

2. Improved adhesion, this is due to the peak voltage being so great that it helps to break down any passive layers which may form on the cathode.

3. Improved deposit distribution, due to the effects of high current density areas associated with D.C plating being reduced by the use of pulse.

4. Greater macro-throwing power obtained in recesses, plated through holes and other complex shapes.

5. Improved covering power using pulse due to its greater micro-throwing power. This means the coating thickness needed to obtain a given property may be reduced by a factor of one half.

6. During plating the formation of an oxide layer on the anode surface can inhibit its dissolution. Additives are usually required to prevent this occurring. However, the higher peak voltages employed in pulse plating prevent this and remove the need for additives.

7. Improved physical properties such as increased density, ductility, wear and corrosion resistance have all been observed.

8. It is possible to deposit alloys with a specific composition and structure which may not be possible using conventional D.C plating.

9. A limited increase in deposition rate may be achieved using pulsed current.

10. Pulsing can reduce the co-deposition of impurities and eliminate voids and nodules encountered in D.C

plating. This helps reduce the stress in deposits.

There are various forms of pulsed current which can be used as shown in Figure (4). There are also a number of variations possible for the other pulse conditions such as duty cycle, on / off ratio, applied voltage and current. This makes pulse plating a very versatile process and the correct choice of these parameters should enable a deposit of predetermined characteristics to be engineered (6).

1.3 Pulsed Alloy Deposition.

Possibly one of the earliest relevant attempts to alloy plate using pulsed current was by J. Winkler Jr (7) who was granted a patent on his work. By selecting a time and a magnitude for the applied pulse it was found that the alloy composition could be controlled independently of bath composition. This was found to be true for other alloy systems and pulsed current has been used in the deposition of alloys such as Ni-Cr, Ag-Sn, Pb-Sn, Cr-Co, Ni-P, Au-Co, and Cu-Zn to mention a few of the more common alloy systems deposited.

Unfortunately relatively little work has been published on pulsed deposition of bronze. Therefore, it is perhaps relevant to look at the analogous brass alloy system upon which work has been published.

Gardam and Tidswell (8) obtained results from using pulsed electrolysis on a brass solution which suggested that by altering the on-time, or the current density employed, a wide range of colours could be obtained for the deposit. These ranged from green through yellow and orange to red by simply varying one or both of the aforementioned

parameters, this effect is shown in Table (4). This work was performed before the advent of modern pulse generators however and the pulse duration used was very long by modern standards.

The same effect was also found to occur in pulse plated gold-copper alloys (8), the deposits varying from green to pink in colour as shown in Figure (5). If these two examples of deposits from cyanide baths containing copper and another metal are mirrored in a cyanide-bronze plating solution, it could be postulated that by varying the current density along with other plating parameters a predetermined deposit composition and structure should be obtainable from a bronze plating bath.

Work has however been performed upon a ternary alloy containing copper, tin and zinc (9). The work involved a comparison of pulsed deposits to conventionally plated deposits. It was found that although the tin and zinc content of the deposits was high, twenty five and twenty per cent respectively, a single phase structure was obtained. It was also observed that although pulsed electrolysis had no effect upon deposit composition, different phases to those observed in conventionally produced deposits were present in pulse plated deposits.

1.4 The Effect of Pulse upon Deposit Structure.

The effect of pulse plating parameters upon deposit morphology and structure can be complicated. It is highly dependent upon the type of alloy being produced and the bath composition. In alloy plating the competing deposition reactions are greatly affected by changes in current

density and applied voltage (6). For deposition of a binary alloy containing metals M1 and M2 the effect of current and voltage changes can be seen in Figure (6). If the slope of the polarization curve increases faster for deposition of metal 1 than for metal 2, the current efficiency for metal 1 will usually increase with increasing current density. Similarly when deposition is accompanied by hydrogen evolution, if the polarization curve for metal deposition increases faster than that for hydrogen evolution. The current efficiency for metal deposition will usually increase with increasing pulse current density. This effect can be anomalous when using very short pulsed electrolysis. The reason for this is that hydrogen tends to desorb during the off-time, to build up a new adsorbed hydrogen layer at the beginning of a new pulse cycle requires a certain amount of energy. If this is a substantial part of the total energy imparted by each pulse the current efficiency for metal deposition can actually decrease, even if the slope of the polarization curves would suggest otherwise.

The crystallisation mechanisms operating during the deposition process are either nucleation and formation of new crystals or growth of existing crystals Figure (7). These two processes are in direct competition during deposition and have a large influence upon the structure and physical properties of the deposit. Crystal growth is favoured by high surface diffusion rates, low overpotentials and low concentrations of adatoms. Nucleation is favoured by low diffusion rates, high overpotentials and high adatom concentrations. Large

overpotentials and current densities occur during pulse plating and fine grained and amorphous structures are commonly obtained. (10), (11), (12).

1.5 Bronze Plating Baths.

A comprehensive review of alloy plating baths has been carried out by Brenner (3),(4). The types of bath used for plating bronze can be divided into two main categories, those based on cyanide, or non-cyanide baths which are either alkaline or acidic in nature.

In cyanide baths copper is present as the cyanide complex and tin may be present as any one of a different number of species. The most widely used types of bath are ones based on copper cyanide and either potassium stannate or tin pyrophosphate.

The first mention of bronze plating in the literature was of a bath containing copper as the cyanide complex together with potassium stannate. This was developed by Ruolz (13) in 1842 and the constituents of his bath were similar to those used in a modern plating bath for bronze deposition. Other early researchers experimented with baths containing copper and tin salts such as chlorides, tartrates, oxides and carbonates with varying degrees of success.

The first scientifically detailed studies of the bronze plating process were made in 1914 and 1915 by Treadwell and Bekh (14) and Kremann and his co-workers (15). They studied several kinds of bath which were essentially cyanide baths with additions of tin salts such as tartrates and sulphostannates. Following these studies

these workers patented their respective processes.

The next major development in bronze plating came in the mid-thirties when Baier and Macnaughton (16) carried out investigations into bronze plating and ten years later in 1946 when Angeles et al (17) experimented with speculum plating. These studies put the plating of copper-tin alloys onto a sound practical basis.

Bronze plating became more important from a commercial standpoint after both the second world war and the Korean war due to shortages of nickel. This led to the bronze coating of steel for both decorative and corrosion purposes and also as sub-coats for chrome plating.

Recently, concern about the skin allergies which can occur from contact with products containing nickel have caused a renewed interest in bronze as a substitute for nickel in certain applications. Several companies are currently developing modern bronze plating baths with the aim of using these instead of nickel plating where the product is to come into contact with human skin (18).

1.6 The Cyanide-Stannate Plating Bath.

This type of bath is probably the most widely studied and the one with the most commercial significance. The bath compositions include copper as a cyanide and either sodium or potassium cyanides, hydroxides and stannates in various amounts, depending upon the composition of deposit required. Brightening agents play an important role in these baths and they can affect plating efficiencies and the deposits physical properties. The types of brighteners used can be inorganic or organic in nature. Common

inorganic brighteners are metals such as lead or nickel, or alternatively Rochelle salt may be used. Some operators prefer to use baths which include potassium salts, this allows higher current densities to be used and these baths operate with higher cathode current efficiencies.

There are two main versions of this type of bath in use for bronze plating. One of these is used to produce bronze deposits containing tin up to fifteen per cent. The second type is to produce an alloy called speculum which can contain up to forty five per cent tin.

The main difference in these bath compositions is that a speculum plating bath contains much more tin in solution than a conventional bronze plating bath. A dual anode system of copper and tin in parallel is used in a speculum plating bath. This bath operates at lower current densities than conventional bronze plating baths.

Although work had been done using this type of plating bath as long ago as 1916, it was not brought to successful commercial use until after 1936. Many workers have studied the effects of varying the operating conditions of such baths.(16,17,19,20)

Their findings may be summarised as follows.

1.6.1 Effect of Temperature.

Varying the temperature was found to have a marked effect upon the composition of deposits obtained and also upon the cathode current efficiency for deposition of the alloys.

Increasing temperature greatly increases the cathode current efficiency and so an elevated operating temperature

would seem an obvious choice. However, one major drawback with this is that sodium cyanide decomposes much faster at temperatures above 65°C . To achieve an acceptably high cathode current efficiency with an acceptable degree of bath deterioration this type of bath is often operated at temperatures between 60°C and 70°C.

It has been found that increasing the temperature of the bath favours the deposition of tin, hence increasing the tin content of the deposits. At temperatures above 80°C the tin content of deposits is quite high but at temperatures below 40°C tin does not co-deposit readily, alloys deposited consisting mainly of copper.

1.6.2 The Effect of Current Density.

Cathode current efficiency was found to decrease sharply with increasing current density and these plating baths cannot be operated economically at high current densities. However, these baths do operate at higher current densities than conventional brass plating baths with a typical range being from 20 to 100mA cm^{-2} as opposed to 10 to 50mA cm^{-2} for brass plating baths.

The alloy composition obtained at different current densities was found to vary but in a non-uniform way. Some researchers reported increasing current density to increase the tin content of deposits but other workers in this area found the opposite effect.(7,10)

1.6.3 The Effect of Hydroxide-Cyanide Concentrations.

Conditions in the cyanide-stannate bath can be controlled to some extent by changing the free cyanide to free hydroxide ratio within the bath. It is easier to alter

the cyanide to hydroxide ratio than to effect control of the metal ratio in the bath. There is however a practical limit to this method of control. With increasing concentration within the bath a marked decrease in cathode current efficiency occurs.

It was found that increasing the free hydroxide content of a bath greatly lowered the deposition rate for tin but hardly affected that for copper. However, increasing the free cyanide content was found to greatly decrease the deposition rate for copper and have a much smaller effect on the deposition rate for tin. This can be summarised as follows, increasing the hydroxide content decreases the tin content and increasing the cyanide content increases the tin content of deposits.

1.6.4 The Effect of Metal Concentration in the Bath.

Workers have shown that tin is less readily deposited from bronze plating baths than copper (16,17) . This is reflected in the percentage tin content of deposits being much less than the percentage tin content in the bath. Large increases in the percentage of tin in the bath only increase the amount of tin in the deposit by a few per cent. Using baths with high metal contents has the advantage that high cathode current efficiencies can be obtained even at high current densities. However, the use of concentrated solutions promotes larger losses due to drag out.

1.6.5 The Effect of Carbonate in Plating Baths.

Carbonates have been found to form in various ways in plating baths. They can be formed by reaction of

atmospheric carbon dioxide with alkaline hydroxides, or by its reaction with decomposing cyanides in the presence of oxygen. Carbonates can also form at the anode by decomposition of cyanides, or formates which may be formed as a result of hydrolysis of cyanides.

Removal of carbonate from plating baths is inconvenient and costly involving chemical methods or freezing out. Freezing out as the name suggests involves cooling the bath to low temperatures around zero, when the carbonate is removed. This obviously involves loss of production and is not applicable to potassium carbonate due to its high solubility. Chemical methods involve the addition of other salts such as calcium nitrate or oxide for a cheap method, or barium salts which are the most effective but expensive way to precipitate out the carbonate.

The effect of increasing levels of carbonate in bronze plating baths has been studied (21). It has been found that a certain amount of carbonate has a beneficial effect by increasing conductivity and so increasing the throwing power of the bath. Potassium carbonate contents up to 100g l^{-1} have been found to increase the throwing power of bronze baths. Further increases in potassium carbonate content above this value caused a decrease in throwing power (22).

Increasing potassium carbonate levels in the plating bath caused a decrease in the cathode current efficiency. For practical purposes the level of carbonate in plating baths is allowed to drift between acceptable upper and lower values.

1.6.6 Anodes used for Bronze Plating.

These fall into three types and depend upon the deposits required, bath composition and operating conditions. A dual copper and tin anode system is used for speculum plating, whereas copper, bronze and particularly inert anodes are used for bronze plating.

Bronze anodes can be used which contain up to about twelve per cent tin. Above this value an insoluble phase is present and non-uniform dissolution occurs. This type of anode also has to be heat treated to obtain a uniform structure prior to use (16). These anodes are operated at low current densities of less than 60mA cm^{-2}, otherwise they passivate and efficiency for dissolution of the anodes rapidly decreases. In practice the anode current density is kept well below this figure. The anodes dissolve with high efficiency and tin enters the solution as a stannate and not the detrimental stannite which causes mossy tin deposits to be produced.

Copper anodes may be used on their own for bronze plating or as part of a dual circuit with tin anodes in speculum plating. A difficulty encountered when using copper anodes is that tin has a tendency to deposit on the copper when the bath is idle. This is not a problem if the bath down time is short and the film thin as it is easily dissolved off. However, after long down times thick films can develop which are difficult to dissolve and can lead to the formation of the detrimental stannite ion.

The modern trend is to use inert anodes which present none of the dissolution problems of the other types of soluble anode. The metal content of the bath is replenished

by additions of the metals as their respective chemicals to maintain the metal ratio in the bath. However, this results in the bath having a relatively short life.

Some physical disintegration of soluble anodes has been observed during the operation of bronze plating baths. However, this phenomena and its effect upon both the bath operation and the deposits produced has received scant attention. In practice the problem has been dealt with by bagging the anodes during operation. However, the disintegration of sacrificial anodes used for cathodic protection has received some attention, (23).

1.6.7 Electrode Reactions.

The cyanide-stannate type of bronze plating bath contains copper and tin as a cyanide and stannate respectively. This means that the electrode reactions are not quite as straightforward as in a simple plating bath. It is generally accepted that tin is deposited from solution by way of simple ions which are formed by hydrolysis or dissociation of the complex, (15).

$$SnO_3^{2-} + 3H_2O \rightarrow Sn^{4+} + 6OH^- \qquad (i)$$

then:

$$Sn^{4+} + 4e \rightarrow Sn^o \qquad (ii)$$

Alternatively this reaction may occur due to the direct discharge of the complex ion.

$$SnO_3^{2-} + 3H_2O + 4e \rightarrow Sn^o + 6OH^- \qquad (iii)$$
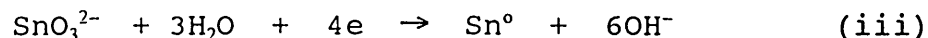
The above reaction shows that for every one atom of tin deposited six hydroxyl ions are formed. This produces an excessive concentration of hydroxyl ions in the cathode diffusion layer when compared to that within the bath. This in turn affects the cathode reaction.

For the deposition of copper from the cyanide complex the dissociation of the ion is given by:

$$Cu(CN)_3^{2-} \rightarrow Cu^+ + 3CN^- \qquad \text{(iv)}$$
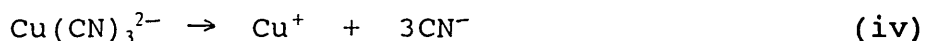
This reaction (iv) is not as straightforward as it may appear and altering the free cyanide concentration in the solution has an unusual effect upon the electrode potential. As the solution becomes diluted it would be reasonable to assume that the electrode potential would become more negative, or less noble as for electrodes in solutions of simple ions. However, the electrode potential for copper becomes more positive (more noble), as the cyanide solution becomes more dilute. One theory postulated for the variation in electrode potential with free cyanide concentration is that different electrode reactions occur as the cyanide concentration changes. The observed potential thus being a mixture of the potentials related to more than one discharge reaction.

One of the reactions which occurs in strong cyanide solutions is due to the direct reaction of the cyanide ion, water and metal to liberate hydrogen from the water:

$$Cu + 4CN^- + H_2O \rightarrow Cu(CN)_4^{3-} + 1/2 \; H_2 + OH^- \qquad \text{(v)}$$
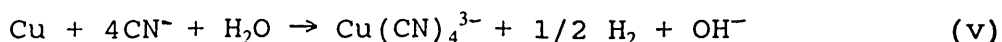
The other reactions put forward are based on the fact that copper forms a series of complex cyanides having different potential values. The series of complexes formed as the cyanide concentration is increased might be as follows:

$$Cu(CN)_2^- \rightarrow Cu(CN)_3^{2-} \rightarrow Cu(CN)_4^{3-} \qquad \text{(vi)}$$
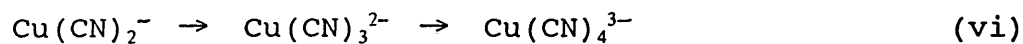
All of these complexes are known to exist in solution and their potential increases as the number of cyanide ligands increases. Thus the potential becomes more negative as the cyanide content of the bath increases.

1.7 Other Cyanide Baths for Bronze Plating.

Although the cyanide-stannate type of bath is probably of most commercial significance other baths containing cyanide and another complex other than a stannate have been used. These are of varying degrees of significance and fall into four main types, baths containing the tin as a pyrophosphate, phosphate, sulphide, or oxalate. The most important of these by far is the pyrophosphate bath, all the others being much less significant.

1.7.1 The Cyanide-Pyrophosphate Bath.

This type of bath is second only to the cyanide-stannate bath in commercial importance and is extensively used in the United States. The developers of this bath claim it has several advantages over the cyanide-stannate bath (24,25).

It is claimed to be a more stable bath with greater levelling power giving brighter deposits having better corrosion resistance. The baths used consist of varying

amounts of potassium cyanide, potassium pyrophosphate, copper cyanide, potassium orthophosphate, stannous sulphate and hide glue. The last two of these components functioning as brighteners and enhancing deposit adhesion. The bath is operated at temperatures from 60°C to 85°C at a pH of 9.

1.7.2 The Cyanide-Phosphate Bath.

A bath of this type was investigated by Yoneda (26) who was granted a Japanese patent . The bath originally contained copper and tin as phosphates, potassium cyanide and either glucose or dextrin as brighteners. The pH range was 8 to 14, this means the tin may actually have been present as a stannate or stannite and the copper as a cyanide complex.

1.7.3 The Cyanide-Sulphide Bath.

Treadwell and Bekh (14) investigated a bath containing copper as a cyanide and an excess of sodium sulphide to convert the tin into a sulphostannate. The relative nobilities of copper and tin are reversed in this bath relative to those in the cyanide stannate type of bath. At low current densities only tin is deposited. To obtain co-deposition sodium sulphide was added to a copper cyanide plating solution. They reported deposits from this bath as being of good quality.

1.7.4 The Cyanide-Oxalate Bath.

Good results were claimed for this type of bath by Treadwell and Bekh (14) . They used a bath containing potassium hydroxide, potassium stannic chloride, potassium cyanide, potassium oxalate and copper sulphate. The bath was operated at 40°C and was caustic in nature which meant

the tin could have been present as a stannate.

1.8 Non-Cyanide Plating Baths.

These baths can be either acidic or alkaline in nature
and are of varying degrees of commercial significance.

1.8.1 Acid Plating Baths.

There are four main types of acid bronze plating bath;
these are, an acid sulphate bath, an oxalate bath and a
fluoroborate type bath, all of which are electrolytic.
There is also an acidic immersion bath which is not
electrolytic.

1.8.2 Acid Sulphate Bath.

Studies have been made of deposits obtained from acid
sulphate solutions by Loshkarev and Grechykhina (27) . They
reported that thin, fine grained deposits containing ten to
eighty per cent tin were obtained. However, they paid
little attention to the composition or physical nature of
the deposits they obtained otherwise.

1.8.3 Immersion Plating Bath.

This consists of a solution of copper sulphate,
stannous sulphate and sulphuric acid. The bath operates
with a tin to copper ratio of six to one and produces
deposits having a tin to copper ratio of one to three. This
bath has been used for some years to immersion coat steel
wire.

1.8.4 Fluoroborate Bath.

Deposits claimed to be similar to those obtained from
a cyanide-stannate bath were produced by Balachandra (28).
The bath he used contained excess fluoroboric acid and
various additives to produce smooth deposits. The bath was

operated at 23°C using a dual anode system and produced deposits containing between ten and fifty per cent copper.

More recent work was carried out by Teichimann and Mayer on the deposition of tin and its alloys from a bath containing fluoroborate, an acid, usually sulphuric acid to give the correct pH, plus various wetting agents and brighteners. These baths were operated at temperatures between 10°C and 40°C , with the optimum being around 20°C. The deposits were claimed to be of good quality and two U.K patents (29,30) were granted to the developers.

1.8.5 Oxalate Bath.

Work has been performed upon this type of bath, it has been found that it is of no commercial significance. It also has inherent disadvantages which make it difficult to use.

The oxalic acid content of the bath is critical, too high a concentration causes the copper complex to precipitate, too low a concentration causes the tin complex to become insoluble. Very tight control of the bath environment is required to obtain good deposits. Insoluble anodes oxidised the oxalate to carbon dioxide and bronze anodes with high tin contents would not dissolve cleanly. Another disadvantage was that these baths are unstable in air since stannous oxalate is oxidised to the stannic complex.

1.8.6 Alkaline Baths.

This type of bath is probably the least useful, with the exception of a bath developed by Vaid and Rama Char (31). There are three main types of bath in this category,

a pyrophosphate bath, a tartrate bath and a hydroxide bath.

1.8.7 Pyrophosphate Bath.

A bronze plating bath containing stannous and copper pyrophosphate was claimed to give good deposits by Langbein and Brant (32).

Vaid and Rama Char (31) developed a bath containing these salts which they claimed had commercial possibilities. The bath operated at 60°C and a pH of around 9, and good quality deposits were reported having copper contents ranging from twelve to ninety five per cent.

1.8.8 Tartrate Bath.

An alkaline tartrate bath was studied in detail by Kremann et al (33), the bath was difficult to operate and the deposits obtained of poor quality. The bath decomposed during electrolysis precipitating cuprous compounds at the anode. The deposits were less ductile than those obtained from a cyanide bath and were found to contain up to one per cent of oxygen.

1.8.9 Hydroxide Bath.

A bath made up of tin chloride, copper sulphate, potassium hydroxide and glue was used by Yagi (34). Deposits were obtained from the bath operating at 50°C and very low current densities. However, the bath was deemed to be of no commercial use.

1.9 Structure of Bronze Deposits.

A study of the thermal equilibrium diagram for the copper-tin system Figure (1) shows it to be relatively complicated. There are a large number of phases possible which are not necessarily the equilibrium phase present at

room temperature. Even up to about fifty per cent tin which covers the range of bronze and speculum commercially produced, a large number of non-equilibrium and intermetallic type phases can exist.

To complicate matters further, electrodeposition is a non-equilibrium process and as a consequence phases which are not normally stable at room temperature can be present in an electrodeposited alloy. Various researchers (14,20,35,36,37) have examined the microstructure of bronze deposits and are in agreement that a uniform, fine grained structure is obtained.

Treadwell and Bekh (14) and also Curry (35) reported deposits to appear homogeneous, Curry also reported an alloy of seventeen per cent tin to contain almost equal amounts of two phases. Studies carried out by Menzies and Ng (36) showed that current density had an effect upon the structures of deposits. Examination by electron microscopy revealed that deposits formed at a low current density of 5mA cm^{-2} exhibited spiral and pyramidal type growths with sharp edges. As current density was increased to above 30mA cm^{-2} the deposits obtained became more featureless with a much finer grain size.

Early X-ray diffraction studies by Bechard (20) and later by Raub and Sautter (37) confirmed that phases in the electrodeposited alloy existed over a wider range of compositions than those to be found in thermally produced alloys.

Hardness studies of bronze deposits have been carried out by various investigators and Raub and Sautter (37)

showed the hardness of electrodeposited bronze alloys to reach a maximum of about 550 VHN at forty per cent tin (speculum). This was in agreement with studies performed by Ramanathan (38) who obtained a maximum hardness of 520 VHN at forty per cent tin. He also found that deposit composition had a marked effect upon the hardness. Menzies and Ng (36) found that the microhardness of deposits increased at all corresponding current densities with increasing plating bath temperature. They also found that at a given current density the microhardness increased with increased bath temperature.

The maximum hardness which they obtained in any deposit was found in a deposit obtained from a bath at 70°C even though this deposit did not have the highest tin content. They concluded that hardness in deposits may also be related to plating temperature and not entirely to composition or structure.

An important factor in determining a coating's properties is the stress which exists within the coating. This may determine the adhesion characteristics of the coating to the substrate and also whether or not any subsequent surface treatments will adhere to the coating. Internal stresses in coatings can be caused by numerous factors. These can vary from the substrate material having a different structure to the coating being deposited, to the plating conditions used to deposit the coatings (2).

Some of the plating variables which may affect the internal stress in a deposit are, bath composition, bath pH, bath additives, bath temperature, co-deposition of

impurities or hydrogen and current density used.

Deposits of the same metal from different baths may have different internal stresses depending upon whether or not it was plated from an alkaline or an acidic bath.

The effect of bath pH upon internal stresses in nickel deposits is well documented (3). Nickel deposits obtained from plating baths having pH 5 or less have low internal stress, whereas increases in pH levels above this value greatly increases the stress in the deposits.

Using additives in plating baths can promote internal tensile or compressive stresses and this depends greatly on the types of additive used. The use of brighteners which contain triple bonds, such as butynediol and quinone usually increase internal stresses. Stress reducing agents such as benzene, saccharin or additives containing sulfonamides may be used. These may even transform a tensile stress into a slight compressive stress. Use of these additives requires stringent control.

Plating bath temperature is an important factor in determining a deposit's internal stresses. Generally, increasing the plating bath temperature causes a reduction in the internal tensile stress of deposits.

Co-deposition of hydrogen or impurities generally increases internal tensile stress by causing lattice distortion or voids.

Increasing current density causes an increase in internal tensile stress in deposits. For example, when using a sulphamate bath for nickel deposition the use of low current densities produces deposits with slight

compressive stress. When the current density is increased to high values this produces deposits having slight tensile stress.

Methods used for measuring the stress in deposits depend upon the stresses to be measured being of a macro or micro-crystalline nature. A method for measuring the stress in deposits was developed by Kushner (39) and a popular method for measuring micro-stresses is by line broadening measurements of X-ray diffraction traces (40),(41).

1.10 Control of Plating Baths.

To control a commercial bronze plating bath which is to be operated over a long period of time presents complex problems. Many of the operating conditions change with time the main one of these being the bath composition. As the bath is progressively worked the metal content and the ratio of metals in the bath changes. At the same time the ratio of free cyanide to free hydroxide changes from its original value. Also, the concentrations of various other species in the plating solution may increase or decrease with bath usage.

The effect upon deposit composition of various parameters such as current density, temperature, metal content etc have been reported with little regard to the anodes being employed. Clearly if soluble anodes or dual anodes are used these plating variables would have a different effect upon the deposit than if an inert anode system was employed.

Also, the anodic and cathodic current efficiencies must be interrelated, this relationship will depend upon

the anode system employed.

The manufacturers of commercially operated bronze baths have adopted various approaches to control (42). The pH of these baths is a critical factor and all operate at high pH values between 12 and 13. The cathode current density employed in all these baths is low, up to a maximum of 5mA cm^{-2}. However, a variation occurs in the type of anodes recommended and the temperature ranges quoted. Some manufacturers recommend copper anodes, while others recommend stainless steel, carbon or platinised titanium. Bath temperatures can vary from 25°C to 50°C for one available bath to 60°C to 70°C for another. The temperature range can be wildly different, one supplier recommending a range of 25°C to 50°C and another recommending a temperature range of 43°C to 47°C.

Copper replenishment in the bath is by addition of chemicals or a mixture of chemicals and soluble anodes where these are used. The other major elements in these deposits, tin and zinc are added in all cases in the form of chemicals.

The control parameters for many of these baths are tenuous. The same manufacturer of two bronze baths states that pH control is critical for one bath while not being important in the other bath.

Another manufacturer states that the bath pH is independent of hydroxide content while others place greater emphasis upon hydroxide control.

Although much work has been performed to study the factors determining the composition of bronze deposits and

plating bath control, these factors have largely been considered in isolation. No in depth studies have been carried out which consider the plating system as a whole.

A modern approach to plating bath and deposit control is to try and utilise so called intelligent systems. (43,44,45,46,47,48,49,50). The conventional way to maintain a bath in specification is by using suitable anodes and adding chemicals when required. This method involves frequent bath analysis to ensure that the composition of the bath does not drift out of specification. Even with regular analysis the best outcome is that the bath composition will gently oscillate above and below its optimum values. If the interval between analyses is long then these variations from the optimum value become large and the bath can move well out of specification.

Modern systems attempt to automate the control of plating baths and so negate the requirement for the bath to be analysed as often. By setting the control parameters to their optimum and programming in an acceptable standard deviation for each variable the plating bath can be rigidly controlled. This ensures consistent deposit composition and thickness and reduces the quantity of plated of rejects incurred (43).

Most of these systems operate on a closed loop principle where information from the bath is constantly being monitored and the plating conditions adjusted to correct any deviations from the optimum (44).

The degree of control exerted upon the plating operation is dependent upon the sophistication of the

equipment and software employed (45). The systems giving the tightest control usually being those which use the greatest sampling and most advanced software.

Statistical process control is used to identify trends in the process and help to control the maintenance schedule. To apply statistical control methods to a process "normal distributions" are found for many of the bath parameters. Parameters which can be quantified in this way are;

a) Metal concentration in the bath.

b) Chemical concentrations in the bath.

c) Concentration of additives to the bath.

d) Current densities.

e) Cathode and anode efficiencies.

f) Bath pH.

g) Bath temperature.

The steps which must be followed in implementing statistical process control can be summarised as follows:

1)   Select the parameter to be controlled.

2)   Accumulate sufficient data points.

3)   Calculate the mean and standard deviation.

4)   Select limits for warning and action (95% and 99.8%).

5)   Decide upon acceptable error margins.

6)   Calculate the number of samples to be used for the moving average.

7)   Adjust the sampling frequency to obtain the desired response time.

8)   Calculate the limits for the moving average means.

9)   Plot the moving averages and standard deviations.

10) Frequently update population mean and standard deviations.

11) Refine limits, reduce risk of errors and frequency of samples based upon cost estimates.

12) Adjust the replenishment schedules to maintain the most constant composition.

13) Establish correlations between bath operation and product quality.

The use of advanced predictive control methods is limited at the present time to the deposition of single metals. It has recieved most attention from the manufacturers of electrical circuits and contacts where the thickness of the precious metal deposit is of prime importance (43).

The advantages or disadvantages of using advanced control systems depends upon each operators individual circumstances. For operators with low production rates and low reject levels the initial cost of the equipment might be prohibitive. However, for operators with high production levels who require stringent bath control the savings possible due to less rejects will quickly offset the initial outlay incurred.

2. Experimental Procedure.

The experimental procedures covered in this section can be divided into five main categories:

a) Preliminary procedures required to ensure that the main electrolyses were performed under constant conditions, (Sections 2.1, 2.1.2).

b) Preparation of bronze anode material, (Sections 2.2, 2.2.1, 2.2.2, 2.2.3, 2.2.4). Plating bath preparation (Section 2.3) and preparation of substrate material (Section 2.4).

c) Electrolyses carried out to determine the effects of operating parameters upon the cathodic processes (Sections 2.5, 2.6, 2.7, 2.8, 2.9).

d) Electrolyses to determine the effects of operating parameters upon the anodic processes (Sections 2.10.1, 2.10.2). The anodic and cathodic determinations were performed using the apparatus shown in Figure 8.

e) The techniques used to analyse and examine the structure of the deposits (Sections 2.11, 2.11.1, 2.11.2, 2.11.3, 2.11.4).

2.1 Evaporation Tests.

The losses due to evaporation from a bronze plating solution at commercial operating temperatures of 60 and 70°C are significant. These losses must be made up by suitable additions of water to the bath during operation. In practice it may be possible to adjust the bath composition by additions of the appropriate chemicals to the water used to make up for evaporation losses.

Tests were performed to measure the

evaporation rate from a bronze plating bath at different temperatures. For these tests two litres of the plating solution were placed into a two litre polypropylene beaker which was held in a twenty eight litre capacity thermostatically controlled water bath. The rate of evaporation from the bath was determined by measuring the volume of water lost over a suitable period of time.

2.1.2 Determination of Chemical Losses due to Drag Out.

During the life of a commercial plating bath a significant amount of its component chemicals may be lost due to physical removal or drag out. This will alter the concentration of metals in the bath and the concentration has to be corrected by adding extra chemicals.

To determine the amount of metals lost by this process a Hull cell panel of known dimensions was placed in two litres of bronze plating solution at a typical operating temperature of 70°C. This was removed from the solution and washed in a litre of distilled water. This process was done repeatedly to simulate cathode removal from a plating bath. The resultant solution was concentrated and analysed to determine the amounts of copper and tin present.

2.2 Production of Cast Bronze Anodes and Analytical Standards.

Suitable tin and bronze anode material is not commercially available. To facilitate tests using soluble tin and bronze anodes, these materials had to be prepared. A series of bronze alloys was prepared for use in calibrating the Philips XRF spectrometer, which was to be

used to analyse the bronze deposits.

2.2.1 Charge Preparation.

Suitable charges were prepared by weighing out the appropriate amounts of high purity copper and tin for each alloy composition. The charge weights were calculated to produce sufficient alloy to fill both the mould cavity and feeder head being cast. The weights of each metal used and the analysis of each alloy obtained are given in Table (5).

2.2.2 Casting Procedure.

Attempts to melt copper and tin simultaneously lead to the loss of a large proportion of tin before the copper has melted. This results from the differences in melting points of tin and copper which are 232°C and 1083°C respectively.

This problem was overcome by preheating to 1200°C a Salamander (clay/graphite) crucible in a gas fired furnace. The total copper charge weight was placed into this crucible and melted as quickly as possible. When all the copper had melted the total tin charge was added to the melt and stirred into it using a ceramic rod. The mixture was reheated for a short time to obtain a sufficient fluidity of the alloy to enable casting. The crucible was removed from the furnace and the alloy stirred to homogenise it, any surface oxide was removed prior to casting the alloy into pre-prepared sand moulds.

2.2.3 Production of Sand Moulds.

Mansfield Red sand containing 5% moisture and 5% Bentonite clay as a binding agent was mixed in a miller

and sieved to produce a fine particle size. This was subsequently moulded around suitable wooden patterns. The pattern used for anode material measured 5cm x 1.5cm x 15cm, the one used for the analytical standards being 5cm diameter and 20cm long. Both patterns had feeder heads of 50% of their respective volumes to offset any shrinkage problems. The moulds were placed in a core drying oven at 140°C in readiness for casting.

2.2.4 Post Casting Heat Treatment.

When the castings had cooled to room temperature they were stripped from the moulds, shot blasted using fine glass beads and given a suitable heat treatment. The pure tin and bronze castings were annealed for one hour at 100°C and 600°C respectively. This broke down the as cast structure and transformed the bronze anode material into a single phase alpha structure. Material was subsequently machined to remove surface oxidation before it was then cut and/or rolled down to the appropriate shape and size. For anode material this was the same size as the mild steel cathodes,(60mm x 20mm x 1.5mm). Analytical standards were machined to 40mm diameter and 20mm thick.

2.3 Plating Bath Preparation.

The composition of the bronze plating solution used throughout this work is given in Table (6). This composition gave copper and tin contents of 24.84 g l^{-1} and 17.1 g l^{-1} respectively. The overall percentages of copper and tin in the solution were 59.2% and 40.8% respectively.

Solutions were prepared in four litre

batches by adding the appropriate chemicals in turn to three litres of distilled water at a temperature of 65°C. The solution was agitated until the chemicals had completely dissolved.

The volume of the solution was adjusted to four litres by adding distilled water. Two grams of activated charcoal was added and the solution agitated continuously for a further two hours during which the temperature was maintained at 65°C. The solution was then allowed to cool to room temperature before its volume was again corrected to four litres. It was then filtered through a Whatmans number 40 filter paper into storage containers. The solution was filtered again prior to using.

2.4 Choice and Preparation of Substrate Material.

Iron was chosen as a suitable substrate material as it had the advantage of not interfering with the subsequent chemical analysis of the deposits.

Mild steel specimens approximately sized (60mm x 20mm x 1.5mm) were initially cropped from sheet before being machined square to fit into a specially prepared holder to facilitate polishing.

The samples were shot blasted using fine glass beads to remove any loose mill scale present. Using the sample holder, the specimens were polished using progressively finer grades of silicon carbide paper to a six hundred grade finish. The samples were then cleaned and finally polished using diamond paste to a one micron finish. At this stage the samples were ultrasonically cleaned and degreased in Arklone. After this the samples

were dried and placed into resealable plastic bags and stored in a desiccator until required for testing.

2.5 Production of Bronze Plated Samples.

Prepared mild steel test pieces were bronze plated using the apparatus shown in Figure (8). The mild steel samples were suspended centrally between two inert platinised titanium electrodes(100mm x 50mm). A total specimen area of 10cm^2 was immersed in the bronze plating solution. Two litres of solution were used and this was agitated using a circular, non-vortexing, magnetic stirrer.

Three series of electrolyses were carried out, one using conventional direct current and two using pulsed direct current. The two series using pulse had an on to off ratio of 1:9, this meant that during the test the current was applied for ten per cent and off for ninety per cent of the total time. The pulse frequencies used were 100Hz and 1000Hz to give a long and short pulse respectively. The tests were devised to use the same number of coulombs (180) for each individual electrolysis. Cathode current densities employed ranged from 5 to 70mA cm^{-2}. The tests were performed in a non-sequential order to help avoid any misinterpretation of results. (i.e.50,40,10,70,20,60,30,5mA cm^{-2}).

For conventional direct current plating tests a Farnell (30v,4A) power supply was used and connected directly to the anodes and cathode. For pulsed electrolyses the power supply was connected to a JCT PDM 2040/1 pulse plating unit which supplied a pulsed current of selected duty cycle and frequency to the plating cell. The applied

- 40 -

pulse was checked by inserting a differential oscilloscope into the circuit. This arrangement is shown schematically in Figure (9). Test temperatures in the range 30 to 70°C were employed, again in a non-sequential fashion.

Fresh two litre batches of plating solution were used for each individual series of electrolyses. Regular checks were made on the bath temperature and pH. Temperatures were maintained to 1°C above or below the set value and the bath pH was kept to within 0.1 of its original value of 12.8.

The amount of metal deposited from the solution was monitored and kept to within five per cent of the original total metal content of the bath. Two litres of unused plating solution had a total metal content of 83.9 grams and therefore a maximum of 4.2 grams of alloy was plated out from it.

The procedure for plating mild steel test pieces was as follows:

1. Area of specimen to be plated ($10cm^2$) marked off.

2. Specimen weighed.

3. Specimen anodically cleaned at 40°C and 40mA cm^2 for two minutes in a mild cyanide based cleaner. (Kleenax).

4. Washed thoroughly in distilled water.

5. Immediately plated using test conditions preset using a spare dummy electrode.

6. Specimen thoroughly washed after plating.

7. Dried.

8. Reweighed.

9. Analysed.

10. Samples placed in marked resealable plastic bags and stored in a desiccator.

2.6 Initial Deposition Tests.

Three series of electrolyses using direct current, pulsed d.c. at 1000Hz frequency (1ms duty cycle) and pulsed d.c. at 100Hz frequency (10ms duty cycle) were carried out to study cathode current efficiency. In all cases the bath temperature and pH were controlled within the limits previously mentioned. These initial electrolyses used the original plating solution whose composition is given in Table(6). Conditions for these tests encompassed the full range of temperatures and current densities previously mentioned.

The results of these initial electrolyses suggested the optimum operating conditions for bronze deposition to be at a bath temperature of 60°C or 70°C and current densities between 10 and 30mA cm^{-2}. Further deposition tests were therefore carried out under conditions corresponding to these.

2.7 Deposition Tests Using Longer and Shorter Pulsed Currents.

This short series of tests employed a shorter pulsed current of 4000Hz and a longer pulsed current of 20Hz frequency. The bath was operated at temperatures of 30°C to 70°C and current densities of 10 and 20mA cm^{-2}.

2.8 Deposition Tests Using Diluted Plating Solutions.

Past work suggested that not only the copper to tin ratio in the bath could determine deposit composition, but also the total metal content. A series of

tests was carried out in solutions operated at 60°C using a current density of 20mA cm^{-2}.

The first series of electrolyses used the basic plating solution diluted by 15%, 25% and 35% respectively. For this series of tests no extra cyanide or hydroxide was added to the diluted solutions. Thus although the free cyanide to hydroxide ratio remained constant in this series, their concentrations changed compared to those in the basic undiluted solution used in the main work.

A second series of electrolyses using similarly diluted solutions was performed. However, in this series additions of potassium cyanide and potassium hydroxide were made to the solutions. This was done in order to have the same free cyanide and hydroxide concentrations as in the undiluted basic solution. The compositions of these solutions is given in Tables(7,8,9).

2.9 Deposition of Copper/Tin/Zinc Alloys.

During the course of this work a number of commercial bronze plating solutions were introduced on to the market which produced ternary copper / tin / zinc deposits. A limited number of experiments were carried out using a modified basic plating solution in which 15mol% of the copper cyanide was replaced by zinc cyanide. A second series of electrolyses was performed using this modified solution diluted by 25%. Direct current and short pulse (1000Hz) electrolyses were carried out at bath temperatures of 60°C and 70°C using current densities of 20mA cm^{-2}. The compositions of these solutions is given in Tables (10,11).

2.10 Anodic Dissolution Studies.

2.10.1 Procedure for Measurement of Anode Dissolution.

The electrical circuit used for this series of tests was similar to that used in the cathodic efficiency tests. However, in this case a single anode was positioned centrally between two cathodes. The anode materials used were pure copper, pure tin and bronze, the latter containing approximately ten per cent tin. Fresh two litre batches of the basic plating solution were used for each series of electrolyses. For these tests the bath was operated at temperatures from 30°C to 70°C.

The anode current density range investigated was based upon the assumption that the optimum cathode current density for the deposition process was 20mA cm^{-2}. It was also based on the fact that most plating processes operate with an anode to cathode ratio of approximately 2:1. Thus anode current efficiencies for copper and bronze anodes were investigated at anode current densities up to 40mA cm^{-2}. However, it was already known that when using tin anodes in bronze plating baths, the anodic efficiency decreases at anode current densities above 25mA cm^{-2}. Also, at anode current densities below 15mA cm^{-2} stannite formation had been observed. The efficiency of tin anode dissolution was therefore only investigated at anode current densities between 15 and 25mA cm^{-2}.

These electrolyses were performed using direct current, short pulsed (1000Hz) and long pulsed (100Hz) currents.

In these experiments an anode area of 10cm^2 was

immersed in the plating bath. The mild steel cathodes positioned either side of the anode had their reverse side stopped off using Lacomet. This gave an effective cathode area of 5cm^2 on each side of the anode.

A typical procedure for each test was as follows:

1. Abrade anode with 240 grade silicon carbide paper.

2. Wash and dry anode.

3. Degrease anode in acetone.

4. Weigh anode.

5. Centrally position anode between cathodes.

5a. Tin anodes placed in solution with a suitable potential already applied in order to film the anode.

6. After plating wash anodes and cathodes, dry and reweigh.

7. Determine composition of cathodic deposit.

2.10.2 Bagged Anode Efficiency Tests.

The previous tests indicated that some anodes appeared to dissolve with an anode current efficiency of greater than one hundred per cent. Furthermore, small particles of anode material appeared to have dropped off and could often be seen in the plating solution. Further tests were carried out using bagged anodes. These tests used copper and bronze anodes operating under conditions which previously had produced apparent anodic efficiencies of greater than one hundred per cent. Typically this would be, direct current at 60°C and 10mA cm^{-2} current density.

At the end of experiments anodes were removed

from the bags, washed, dried and reweighed. The bags were then thoroughly washed to remove traces of plating salts and finally cleaned in boiling water. A solution of 50% Hydrochloric, 10% Nitric acid was then used at 60°C to dissolve out any traces of anode material trapped in the bag. The resultant solution was then analysed using atomic absorption spectrometry.

2.11 Chemical Analysis.

Three types of analytical technique were used to determine the chemical composition of the plated samples. These were:

1. Energy Dispersive X-Rays (EDX), employed when using the JEOL 840JXA scanning electron microprobe.

2. Atomic Absorption Spectrometry, used for bulk analysis of standards and anode material.

3. X-Ray Fluorescence Spectrometry, used for the majority of plated samples. This enabled further testing of deposits to be carried out.

2.11.1 Atomic Absorption Spectrometry.

All bronze anode material and cast standards were analysed using an IL aa/ae 357 spectrophotometer. The following conditions were observed during analysis:

1. Flame mixture of nitrous oxide / acetylene.

2. Solution uptake rate of 6ml per minute.

3a. Slit width for copper 0.5 micrometers.

3b. Slit width for tin 0.5 micrometers.

4a. Wavelength for copper 249.2 nanometres.

4b. Wavelength for tin 235.5 nanometres.

A series of standards was initially made up using

pure copper and pure tin to cover an appropriate range of analyses. This was accomplished by dissolving one gram of copper and one gram of tin separately in 200ml of a 50% Hydrochloric, 10% Nitric acid mixture at 60°C. These solutions were made up to a volume of one litre using a 10% Hydrochloric acid solution. Mixtures of these two solutions allowed a range of copper and tin analyses to be done on bronze alloys having a range of compositions.

The spectrometer was set to give zero counts using triple distilled water. Samples and standards were tested alternately and from the readings obtained a graph of metal concentration versus absorption constructed. A new calibration curve was determined prior to analysing each series of unknown deposits.

2.11.2 X-Ray Fluorescence Spectrometry.

This is a widely used analytical technique both industrially and for research applications. For the plated samples it had the advantage over atomic absorption of leaving the samples intact for further tests.

All plated samples were analysed by this method once calibration curves for copper and tin had been constructed in the software running the machine. This was achieved using the cast bronze standards whose analysis was known from atomic absorption tests. This enabled each unknown deposit to be analysed in thirty seconds as opposed to thirty minutes without calibration, with no loss in accuracy. Throughout testing, standards of known composition were analysed alternately with the unknown samples. The conditions used for analysing samples on the

Philips X-Ray PW1480 Spectrometer were as follows:

1. Excitation voltage 100Kv.

2. Excitation current 50mA.

3. Sample spinner IN.

4. Test duration 30seconds.

5. Molybdenum / Scandium tube.

2.11.3 Scanning Electron Microscopy.

Samples analysed using the JEOL 840JXA scanning electron microprobe were mounted in conductive bakelite and polished to a one micron finish. A total of six areas per sample were analysed and the results quantified using the standard ZAF4 programme. Samples to be examined for structure were etched in alcoholic ferric chloride prior to examination.

2.11.4 X-Ray Diffraction.

Many physical properties of materials can be determined from their X-Ray diffraction patterns such as phases present, particle size, degree of texturing, if any, and whether or not a material is amorphous or crystalline in nature. All samples analysed using the Philips X-Ray diffractometer were in the as plated condition. The following test conditions were observed:

1. Excitation voltage 35Kv.

2. Excitation current 45mA.

3. Scan rate one degree per minute.

4. Scan cycle 20 to 100 degrees.

5. Copper K_{alpha} radiation used.

Monochromatic copper K_{alpha} was considered suitable

as the majority of bronze samples to be tested comprised mainly of copper. This type of radiation penetrated the samples well with little interference. If other types of radiation had been used such as molybdenum this could have been a problem.

3.0 Experimental Results.

The results presented in this section can be divided into four categories:

a)   The variation of cathode current efficiencies with operating parameters and current mode, (Sections 3.2, 3.2.1, 3.2.2, 3.2.3).

b)   The anode current efficiencies as a function of operating parameters and current mode, (Sections 3.3, 3.3.1, 3.3.2, 3.3.3, 3.3.4).

c)   The composition of deposits as a function of operating conditions and current mode, (Sections 3.4, 3.4.1, 3.4.2, 3.4.3) and anode material used and bath composition, (Sections 3.4.4, 3.4.5, 3.4.6).

d)   The structure of the bronze deposits, (Section 3.5).

3.1   Evaporation Losses From Plating Bath.

The rate of evaporation of water from the surface of the plating bath as a function of temperature is shown in Figure (10). It can be seen that the rate of evaporation increases with increasing temperature. In fact, at bath temperatures of 60°C and 70°C the evaporation rate is considerable being 50ml and 70ml per minute respectively for each square metre of surface area of the bath.

3.1.1   Chemical Removal From Bath by Drag Out.

The results of tests to determine the drag out of metals from a plating bath due to cathode removal are shown in Figure (11). It can be seen that removing a cathode surface area of one square metre results in the loss of 2.34 grams of copper and 1.61 grams of tin as drag out. Since the plating solution contained 24.84 grams per

litre of copper and 17.1 grams per litre of tin the volume of plating solution lost due to the cathode removal can be calculated.i.e:

a).Based upon copper removal due to drag out.

$$\text{Drag out volume} = \underline{2.34 \times 1000} \text{ ml m}^{-2} = \underline{94.2 \text{ ml}}$$
$$24.84$$

or   b).Based upon tin removal due to drag out.

$$\text{Drag out volume} = \underline{1.61 \times 1000} \text{ ml m}^{-2} = \underline{94.1 \text{ ml}}$$
$$17.1$$

This gives an average value of 94.15 ml of drag out per square metre of cathode area removed from the bath.

The amount of each chemical lost from the bath due to this drag out can be calculated since their original concentrations are known Table (6).

Potassium Stannate:

$$\text{Weight Lost} = \underline{43 \times 94.15} \text{ g} = \underline{4.0463 \text{ grams}}$$
$$1000$$

Potassium Cyanide:

$$\text{Weight Lost} = \underline{72 \times 94.15} \text{ g} = \underline{6.775 \text{ grams}}$$
$$1000$$

Copper Cyanide:

$$\text{Weight Lost} = \underline{35 \times 94.15} \text{ g} = \underline{3.295 \text{ grams}}$$
$$1000$$

Potassium Hydroxide:

$$\text{Weight Lost} = \underline{10.5 \times 94.15} \text{ g} = \underline{0.99 \text{ grams}}$$
$$1000$$

3.2   Determination of Cathode Current Efficiencies.

The results of plating experiments to determine cathode current efficiencies are shown in

Tables(12-26). These results provided the mass of alloy deposited and their respective chemical compositions. The cathode current efficiencies for copper and tin were calculated directly by applying Faraday's Laws to the experimental results obtained.

The efficiencies for copper and tin deposition were calculated directly and the efficiency for hydrogen discharge was assumed to be one hundred per cent minus the sum of the efficiencies for copper and tin deposition. The results of these calculations are given in Tables (27 to 41).

3.2.1 Method of Calculating Cathodic Efficiencies.

For a process operating at one hundred per cent efficiency Faraday's Law may be represented by the expression:

$$w = zit \qquad \qquad (i)$$

Where w= weight of metal deposited (grams).

z= electrochemical equivalent.

i= current used (amperes).

t= time of test (seconds).

This expression may be rewritten as:

$$w = \frac{itA}{nF} \qquad \qquad (ii)$$

Where A = Atomic mass

n = valency or oxidation number of metal involved

F = The Faraday. = (96,500 Coulombs)

- 52 -

The cathode current efficiency of a process may be defined as.

$$\underline{\text{Current used to actually deposit metal}} \times 100\% \quad \text{(iii)}$$
$$\text{Total available current used}$$

Thus for a binary alloy involving two metals M1 and M2 respectively the percentage cathode current efficiency for metal deposition is given by:

$$\underline{\text{Current to deposit M1+Current to deposit M2}} \times 100\% \quad \text{(iv)}$$
$$\text{Total available current used}$$

For any given electrolysis the theoretical currents i_{M1} and i_{M2} required to deposit metals M1 and M2 respectively are obtained by rearranging Equation(ii). Therefore;

$$i_{M1} = \frac{W_1 nF}{tA} \quad \text{and} \quad i_{M2} = \frac{W_2 nF}{tA} \quad \text{(v)}$$

Since W,n,F,t and A are known or available from experimental data i_{M1} and i_{M2} may be calculated for the respective individual metals.

Using these values in equation (iii) allows the current efficiency for individual component metals and total efficiency for alloy deposition to be obtained. The current efficiency for hydrogen discharge may then be calculated.(Assuming any current not used for metal

deposition has been used to discharge hydrogen).

Taking data from Table (16) a typical example of efficiency calculations is as follows:

1) Cathode current density   = 40mA cm^{-2}

2) Area plated   = 10cm^2

3) Total current used   = 0.4Amps

4) Test duration   = 450seconds

5) Total weight gain   = 0.0845grams

6) Analysis: 86.78% Copper . 13.22% Tin.

From the total weight gain and chemical analysis the weight of each metal deposited can be calculated.Thus;

Weight of copper deposited = 0.0845 x 0.8678 = 0.0733g

Weight of tin deposited = 0.0845 x 0.1322   = 0.0122g

Using these values the efficiencies for each metal may be calculated:

Copper Efficiency.

Valency = 1. Using equation (ii) we have the following

$$0.0733 = \frac{I_{Cu}t \times 63.546}{1 \times 96,500}$$

Therefore: $I_{Cu}t$ = 111.31 Amp seconds.

%Efficiency = $\frac{\text{Actual current used}}{\text{Total current available}}$ x 100%

$$= \underline{111.31} \qquad \text{x } 100\% \qquad = \underline{61.84\%}$$
$$0.4 \text{ x } 450$$

Tin Efficiency.

Valency = 4. Using equation (ii) again we have

$$0.0122 = \underline{I_{Sn}t \text{ x } 118.71}$$
$$4 \text{ x } 96,500$$

Therefore: $I_{Sn}t$ = 36.42 Amp seconds.

$$\%\text{Efficiency} = \underline{36.42} \qquad \text{x } 100\% \qquad = \underline{20.23\%}$$
$$0.4 \text{ x } 450$$

The total cathodic efficiency is the sum of the calculated efficiencies for copper and tin.Thus;

Total Cathodic Efficiency = 61.84 + 20.23 $\quad$ = $\underline{82.07\%}$

Assuming lost efficiency is due to hydrogen discharge,the hydrogen efficiency is 100 - 82.07 $\qquad$ = $\underline{17.93\%}$

3.2.2 Cathodic Current Efficiencies.

Conventional D.C Plating.

The cathode current efficiencies for copper, tin, hydrogen and total metal deposition obtained using conventional plating at different bath temperatures are shown in Figures(12 to 16), as a function of current density.

The efficiency for copper deposition can be seen to fall off with increasing current density for all

temperatures investigated. Furthermore comparison of Figures (12 to 16) shows that this decrease in current efficiency with increasing current density becomes less pronounced at high bath temperatures.

The current efficiency for tin deposition decreases with increasing current density for electrolyses performed at 30°C and 40°C Figures (12 & 13). However, for electrolyses carried out at bath temperatures above 40°C the current density/current efficiency relationship exhibits a maximum value Figures (14 to 16). The current efficiency for tin deposition at any given current density increases with increasing plating temperature, as can be seen by comparing Figures(12 to 16). The maximum efficiency for tin deposition observed throughout the work was approximately twenty per cent which was obtained using a current density of 20mA cm^{-2} and a bath temperature of 70°C.

Comparison of Figures (12 to 16) show that the current efficiency for hydrogen discharge decreases with increasing bath temperature, but increases with increasing current density. At 30°C and 40°C the efficiency for hydrogen discharge is greater than that for tin deposition for all current densities investigated Figures (12 & 13). However, for bath temperatures above 40°C,whether or not the efficiency for hydrogen discharge exceeds that for tin deposition depends upon the current density being used. Furthermore, comparison of Figures(14 to 16) shows that the current density above which the efficiency for hydrogen discharge is greater than that for tin deposition, increases with increasing temperature.

The current density above which the current efficiency for hydrogen discharge exceeds that for copper deposition increases with increasing bath temperature. Thus, the current densities above which the efficiency for hydrogen discharge is greater than that for copper deposition are, 10mA cm^{-2} and 60mA cm^{-2} at temperatures of 30°C and 50°C respectively. Figures (12 & 14). At temperatures greater than 50°C the efficiency for copper deposition is always greater than that for hydrogen discharge at all current densities investigated Figures(15 & 16).

Short Pulsed D.C (1000Hz).

The current efficiencies obtained for copper, tin, hydrogen and total metal deposition, using short pulsed direct current at different bath temperatures, are shown in Figures (17 to 21) as a function of current density. Similar trends to those obtained when using conventional direct current are observed. However, there are some dissimilarities the most noticeable ones being:-

a) The efficiencies for tin deposition are lower at all corresponding conditions of temperature and current density when using short pulsed current.

b) The efficiency for total metal deposition at 60°C and 70°C Figures (20 & 21) and low current densities of 5 and 10mA cm^{-2}, is higher using pulse than when using conventional direct current.

c) The efficiency for total metal deposition only exceeds that for hydrogen discharge, over the entire current density range investigated, at a bath temperature

of 70°C using short pulse. This is in contrast to using conventional current where this occurs at bath temperatures above 50°C.

Long Pulsed D.C (100Hz).

The efficiencies for copper, tin, hydrogen and total metal deposition using long pulsed current are shown in Figures (22 to 26), as a function of current density for various bath temperatures.

Similar trends can be seen in the current density, bath temperature, efficiency interrelationships as were found in the corresponding results obtained from conventional and short pulsed electrolyses.

Furthermore, the efficiencies for total metal deposition are lower in general using long pulse than when using short pulse or conventional electrolysis under corresponding test conditions. An exception to this being when long or short pulse is used at a current density of 5mA cm^{-2} and bath temperatures of 60°C and 70°C.

3.2.3 Effect of Varying Pulse Frequency on Efficiencies.

The current efficiency for copper and tin deposition and hydrogen discharge as a function of pulse frequency are shown in Figures (27 to 30). These efficiencies were carried out at temperatures of 60°C and 70°C and current densities of 10 and 20mA cm^{-2}.

In all cases the efficiency for copper deposition increased with increasing pulse frequencies between twenty and one thousand Hertz. Further increases in frequency caused only slight or no increase in efficiency.

The current efficiency for tin deposition was lower

- 58 -

than that for copper deposition under all corresponding conditions. However, the current efficiency for tin deposition as a function of pulse frequency exhibited a maximum value corresponding to one thousand Hertz.

The current efficiency for hydrogen discharge decreased with increasing pulse frequency for electrolysis performed at 60°C and 20mA cm^{-2} current density,Figure(28) For the other test conditions investigated the efficiency for hydrogen discharge initially decreased up to a pulse frequency of one thousand Hertz before increasing slightly with increasing pulse frequencies, Figures(27,29 & 30).

The current efficiency for copper deposition at 70°C was higher than that obtained at 60°C for all corresponding conditions of current density and frequency. In contrast the current efficiency for hydrogen discharge at 70°C was lower than at 60°C under all corresponding conditions of current density and frequency, Figures (27 & 29) and (28 & 30) respectively.

The current efficiencies for tin deposition at 60°C and 70°C were similar in nature. However, the efficiencies obtained using a current density of 20mA cm^{-2} were slightly higher than those obtained for 10mA cm^{-2} under corresponding deposition conditions of temperature and frequency.

3.3 Measurement of Anodic Current Efficiencies.

The results of the electrolyses carried out to determine anode current efficiencies using conventional and pulsed currents are given in Tables (42 to 83). These results are based upon weight loss measurements using copper, tin and bronze anodes.

3.3.1 Electrolyses Using Copper Anodes.

Details of experiments performed to determine apparent anodic efficiencies using copper anodes under various operating conditions are given in Tables(42 to 56). These apparent efficiencies for copper anode dissolution as a function of current density for bath temperatures from 30°C to 70°C are shown in Figures (31 to 35). The results from using conventional, long and short pulsed electrolyses are presented together in these figures.

With one exception, where long pulsed current was used at 30°C, the apparent current efficiencies obtained for copper anode dissolution are high and approximately one hundred per cent. This is for current densities ranging from 5 to 40mA cm^{-2}. Indeed in many cases the observed current efficiencies based upon weight loss measurements were greater than one hundred per cent.

The anodic efficiencies for copper dissolution using long pulsed electrolysis at 30°C follow a similar pattern to those obtained for conventional and short pulse between 5 and 20mA cm^{-2}. However, at current densities greater than 20mA cm^{-2} there is a sharp decrease in current efficiency when using long pulsed current.

3.3.2 Electrolyses Using Bronze Anodes.

Details of the experiments performed to determine anodic efficiencies using bronze anodes are given in Tables (57 to 71). These apparent efficiencies are again based upon weight loss measurements. A typical example of how the efficiencies for bronze anode dissolution were calculated is shown below using data from Table (57).

1. Current Density   = 5mA cm^{-2}.

2. Area Plated   = 10cm^2.

3. Time of Test   = 7200seconds.

4. Weight Lost from Anode = 0.2376grams.

5. Anode analysis . 90.03% Cu. 9.97% Sn.

6. Atomic mass of copper = 63.546.

7. Atomic mass of tin   = 118.71.

Thus, knowing the anode composition and weight of anode lost during the test, the weight of copper and tin lost from the anode can be calculated.

Weight of copper lost = 0.9003 x 0.2376 = 0.2139g

Weight of tin lost   = 0.0997 x 0.2376 = 0.0237g

Copper Efficiency.

$$\text{valency} = 1: \qquad 0.2139 = \frac{I_{Cu}t \times 63.546}{1 \times 96,500}$$

Therefore $I_{Cu}t$ = 324.8 Amp seconds.

$$\text{Efficiency} = \frac{324.8 \times 100}{0.05 \times 7200} = 90.23\%$$

Tin Efficiency.

$$\text{valency} = 4: \qquad 0.0237 = \frac{I_{Sn}t \times 118.71}{4 \times 96,500}$$

Therefore $I_{Sn}t$ = 77.06 Amp seconds.

$$\text{Efficiency} = \frac{77.06 \times 100}{0.05 \times 7200} = 21.4\%$$

Total Apparent Anodic Efficiency = 90.23 + 21.4 = 111.63%

The apparent anodic efficiencies for the dissolution of bronze anodes as a function of current density are shown in Figures (36 to 40). These are for conventional and pulsed

electrolyses at bath temperatures ranging from 30°C to 70°C.

At the lowest current density used of 5mA cm^{-2} the apparent efficiencies obtained were consistently above one hundred per cent at all temperatures investigated. Using this current density at temperatures between 30°C and 50°C caused an increase in the apparent current efficiency as the bath temperature increased Figure (41). This was the case for conventional and both types of pulsed current used.

At temperatures between 30°C and 50°C the apparent current efficiencies observed for all modes of electrolysis decreased markedly with increasing current density; however at higher bath temperatures this effect was less noticeable, Figures (36 to 38).

The results of experiments performed at 60°C and 70°C are shown in Figures (39 & 40) respectively. With two exceptions these show the apparent efficiencies to be high and above one hundred per cent. The apparent efficiency obtained at 60°C using long pulse (100Hz) is unusually low at a current density of 30mA cm^{-2} being only forty eight per cent. Similarly using conventional current at 70°C and a current density of 30mA cm^{-2} gives an apparent efficiency of only fifty five per cent.

3.3.3 Electrolyses Using Tin Anodes.

The anodic behaviour of tin anodes in a bronze plating bath was found to be complex. This is confirmed by the results obtained from tests carried out between 30°C and 70°C using conventional and pulsed currents, Tables (72

to 83).

No weight loss was observed for tin anodes during electrolyses at 30°C using conventional or pulsed currents. Figures (42 to 45) show the apparent anodic efficiencies for tin dissolution as a function of current density for temperatures from 40°C to 70°C. Electrolyses were carried out using conventional and pulsed currents. All the efficiencies for tin dissolution were calculated assuming that tin entered solution with a valency of four.

In the current density range 15 to 25mA cm^{-2} the apparent efficiency for tin dissolution decreased as the current density increased. Electrolyses carried out using long pulsed current at 40°C and 50°C showed anodic current efficiencies to be low, typically less than five per cent, Figures (42 & 43). Further electrolyses at 60°C and 70°C using this current mode resulted in passivation of the tin anodes. During this process the anodes became coated with a black film and gained, rather than lost weight.

The anodic behaviour of tin during electrolyses carried out with short pulsed current between 50°C and 70°C and a current density of 17.5mA cm^{-2} was distinctive. During these electrolyses the tin anodes became coated with a mossy black deposit which was easily washed off after removal from the bath. The apparent current efficiency for the anodic dissolution process, calculated assuming a tin valency of four, was anomalously high at over two hundred per cent.

The apparent anodic efficiency for tin using conventional current varied between five and fifty per cent

depending upon the conditions of electrolysis used, Figures (42 to 45). Comparison of these figures suggests that the anodic efficiency for tin dissolution increases with increasing bath temperature from 40°C to 70°C for any given current density. This is true for electrolyses carried out using conventional and short pulsed currents and can be seen when the apparent anodic efficiencies are plotted as a function of bath temperature.Figures(46 & 47).

The surfaces of the tin anodes were inspected after the electrolyses and typical examples are shown in Figures (48a,b,& c). These show an anode which had passivated during dissolution Figure (48c) and developed a black coating which could not be washed off. One anode which developed a mossy black deposit during electrolysis which was easily removed by washing Figure (48b). The anode shown in Figure (48a) is from an electrolysis during which the anode developed a slight yellow patina and gave a good rate of dissolution.

3.3.4 Electrolyses Using Bagged Anodes.

The results of electrolyses carried out at 60°C using conventional current and bagged anodes are given in Table (84). Electrolyses were carried out using an anode current density of 10mA cm^{-2} for three hours.

In this table the apparent anodic efficiencies given for copper and bronze anode dissolution are based upon the total loss in weight from each anode which occurred during electrolysis. The true efficiencies were obtained by taking the weight of anode material trapped in the bags away from the total metal weight lost during

electrolysis.

The anomalously high apparent anodic current efficiencies
of over one hundred per cent are clearly due to physical
disintegration of the anodes and in each case the true
efficiencies are less than one hundred per cent.

3.4 Effect of Operating Parameters on Deposit Composition.

Figures(49 to 51) show the variation in tin content
of deposits as a function of current density, using pulsed
and conventional currents at different temperatures.
Comparison of these figures shows that deposits having the
highest tin contents were produced using a conventional
current at a current density of 20mA cm^{-2} and bath
temperature of 70°C. In all cases using pulsed current
yielded deposits with a lower tin content than those
produced by conventional electrolysis operated at the same
current density and temperature.

3.4.1 Conventional Current Electrolyses.

In the case of samples produced by conventional
current electrolysis, increasing bath temperature caused an
increase in tin content at any given current density Figure
(49). At all temperatures investigated except 30°C the tin
content of deposits as a function of current density showed
a maximum. The current density corresponding to this
maximum depended upon bath temperature and was 10mA cm^{-2} for
40°C and 50°C and 30mA cm^{-2} for bath temperatures of 60°C and
70°C. The decrease in tin content from the maximum observed
value with increasing current density was least noticeable
at 70°C and became more pronounced with decreasing bath
temperature. The tin content of deposits obtained from the

bath operated at 30°C decreased continuously with increasing current density for the whole range investigated.

3.4.2 Pulsed Current Electrolyses.

The deposits obtained using pulsed current electrolysis at 100Hz and 1000Hz were lower in tin than the corresponding deposits obtained using conventional plating Figures (49 to 51). The maximum tin content of deposits produced by pulse plating was approximately eight per cent compared to thirteen per cent for deposits produced by conventional plating. The general relationship between tin content and current density when using pulsed current showed the tin content to decrease as current density increased Figures (50 & 51). However, the relationship obtained when using short pulsed current at 70°C was similar to the relationships obtained using conventional current from 40°C to 70°C Figures(49 & 50). In general the tin content of deposits produced by long and short pulsed electrolysis decreased with decreasing bath temperature for any given current density Figures (51 & 50). The only exception to this being when short pulse was used at 70°C as previously mentioned.

3.4.3 Effect of Pulse Frequency on Deposit Composition.

The tin content of deposits obtained at 60°C and 70°C using current densities of 10mA cm^{-2} and 20mA cm^{-2} is shown in Figures (52 & 53) as a function of pulse frequency. For each case investigated the tin content showed a maximum value with increasing frequency. Initially the increase in tin content up to its maximum value with

increasing frequency was rapid . After this point
increasing pulse frequency caused tin contents to decrease.
However, this decrease was only slight.

The tin content of deposits as a function of bath
temperature is shown in Figure (54). A current density of
20mA cm^{-2} was used at different pulsed frequencies. When
using a frequency of 20Hz tin contents increased with
increasing bath temperatures from 30°C to 70°C. A maximum
was observed in the relationship between tin content and
temperature when pulse frequencies of 100Hz, 1000Hz and
4000Hz were used. The maximum tin content of any deposit
obtained from this series of electrolyses was approximately
six per cent. This was obtained from a bath at 60°C using
a pulse frequency of 1000Hz.

3.4.4 Effect of Anode Material on Deposit Composition.

The type of anode material used was found to
affect the composition of the cathodic deposits obtained
from both conventional and pulsed current electrolyses. The
effect of using copper, tin, bronze and inert anodes upon
deposit composition at different temperatures are shown in
Figures (55,56,57). These electrolyses were carried out
using a current density of 20mA cm^{-2}.

Conventional Current.

Figure (55) shows that when inert anodes are used
in conjunction with conventional current the tin content of
the deposits obtained increases linearly with increasing
temperature. Similarly the deposits produced using bronze
anodes showed an increase in tin content with increasing
temperature. However, this increase was non-linear and

generally the tin contents were lower than those obtained when using inert anodes. When copper or tin anodes were used the tin content as a function of bath temperature showed a maximum.

Short Pulsed Current (1000Hz).

The tin content of deposits as a function of bath temperature when using short pulse and different anodes is complex in all cases Figure (56). However, the tin content of deposits produced when using inert anodes generally increased with increasing temperature.

Long Pulsed Current (100Hz).

The tin content of deposits produced using long pulse generally increased with increasing bath temperature when copper, bronze or inert anodes were used. However, this increase was less marked than when conventional current was used and was non-linear in all cases. (c.f.Figures 55 & 57). The variation in tin content with bath temperature for electrolyses using tin anodes was complex and showed a minimum value at around 50°C. Increasing the bath temperatures above this point caused a slight increase in deposits tin content.

3.4.5 Effect of Bath Concentration on Deposit Composition.

A series of electrolyses was carried out using the basic plating solution diluted by increasing amounts of water. The composition of each of these diluted solutions is given in Table(6a). The composition of deposits obtained from these solutions at 60°C using conventional and pulsed currents at 20mA cm^{-2} current density is given in Table (85). The results show the tin content of deposits to decrease as

the concentration of plating solution decreases. This was marked when using conventional current. Bath dilution resulted in the tin content of deposits decreasing from ten to approximately three per cent.

The effect of using increasingly diluted plating solutions, Tables(7 to 9), in which the free cyanide and hydroxide were maintained at the same levels as in the basic plating solution is given in Table (86). This shows the tin content of deposits obtained at 60°C using conventional and pulsed currents at 20mA cm^{-2} current density.

The tin content of deposits decreased as solutions became increasingly dilute. This was again most marked when conventional current was used. The highest tin content for any given plating conditions was obtained when using conventional current. The lowest tin content was produced when long pulse current (100Hz) was used.

3.4.6 Effect of Replacing some Copper with Zinc in Bath.

Electrolyses were performed using plating solutions whose compositions are given in Tables (10 & 11). These solutions were based on the basic bronze plating solution but also contained some zinc.

The analyses of deposits obtained from the undiluted solution containing zinc are given in Table (87). These deposits were produced using conventional and pulsed current at 60°C and 70°C and a current density of 20mA cm^{-2}. Although the zinc content of these deposits was low (0.8% to 1.7%), the tin contents were relatively high (15% to 22.7%). This particular solution was unstable however and

- 69 -

developed a milky appearance from the time it was made up.

The analyses of deposits obtained from a diluted version of the zinc plating solution using identical plating conditions are given in Table(88). These deposits all had low zinc contents (1.5% to 1.7%), but relatively high tin contents (12.7% to 14%). The tin content of these deposits was lower than those obtained under corresponding conditions using the undiluted zinc plating solution. However, the diluted zinc containing plating solution was found to be stable in contrast to the undiluted solution mentioned previously.

3.4.7 Composition of Commercial Bronze Deposits.

The analyses of deposits obtained from commercial bronze plating baths supplied by Messrs Lea Ronal and Schlötter were determined. The compositions are given in Table (89). The tin content of these deposits varies considerably from (8.3% to 18.6%). The zinc contents are all low with one notable exception. Deposits also contained small but significant amounts of nickel ranging from (0.2% to 2.1%).

3.5 Structural Studies of Bronze Deposits.

Deposits produced by conventional current and pulsed current electrolyses at various temperatures and current densities were studied by X-ray diffraction, Figures(58 to 68). The structures of these deposits was complex and greatly depended upon the tin content of each deposit examined.

Deposits with low tin contents (less than 7%) had structures which consisted mainly of the alpha phase,

Figures (58 to 61). As the tin content of the deposits increased above this value a complex combination of phases was observed.

In addition to the alpha phase, various amounts of beta and epsilon were present, Figures (62 to 68). Generally the amounts of these phases increased and the amount of alpha decreased with increasing tin content above seven per cent. The deposits with the highest tin contents, above ten per cent, exhibited structures which consisted mainly of the beta and epsilon phases, Figures (67 & 68).

Allied to this complex behaviour some deposits also exhibited an amorphous component to their structure, Figures (64 & 65). This was found in deposits which were produced under conditions of current density and temperature giving the highest current efficiencies for tin deposition.

Measurements to determine the effects of tin content upon the lattice parameter were carried out, Table (90). These show that as the tin content of deposits increases an increase in the lattice parameter also occurs, Figure (69). This is the case up to about eight or nine per cent tin where a change in slope indicates that the alpha phase had become saturated and reached its maximum lattice parameter of 3.7 Angstroms. This change in slope indicates a phase boundary as is shown in Figure (70) and coincides with the beta and epsilon phases becoming the main phases present in the deposits.

4.0 Discussion.

It is evident that to control the bronze plating bath in order to obtain deposits of consistent composition and properties is problematic. The numerous variables involved in the plating process and their interrelationships with each other require careful consideration before any definitive predictive control model is developed.

Any control system considered would have to ensure the production of sound bronze deposits having the desired physical and chemical properties. This would typically be deposits having tin contents in excess of ten per cent.

4.1 Plating Bath Temperature.

Increasing the plating bath temperature from 30°C to 70°C increased the cathodic current efficiencies for copper and tin deposition in all cases investigated. This is in agreement with previous work (36). Also, the cathodic discharge of hydrogen decreased with increasing bath temperature for any given conditions of current density and current mode. This might be explained by the fact that temperature affects the hydrogen overpotential at a different rate to that for tin or copper deposition (2).

Increasing the bath temperature also increased the tin content of deposits obtained under corresponding plating conditions. Deposits having the highest tin contents were produced at temperatures of 60°C and 70°C for all current modes investigated, this is in agreement with earlier work especially that of Menzies and Ng.

Both the true and apparent current efficiencies for anode dissolution increased with increasing bath

- 72 -

temperature for all the soluble anode systems investigated. Efficiencies for dissolution of copper and bronze soluble anodes were high even at the lowest temperatures investigated. However, efficiencies for tin anodic dissolution only attained significant values at bath temperatures of 60°C and 70°C.

This suggests that the optimum temperature for the operation of the plating bath is between 60°C and 70°C for both the anodic and cathodic processes.

4.2 Cathode Current Density.

The optimum cathode current density for the process is more difficult to define. The highest cathode current efficiencies for copper deposition were obtained using the lowest cathode current densities. This was the case for both conventional and pulsed current electrolyses with the maximum efficiency values usually being obtained at a cathode current density of 5mA cm^{-2} (Figures 12 to 26).

The current efficiencies for tin deposition generally followed the same trend with the highest efficiencies being obtained at the lowest current densities. However, in the case of deposits produced by conventional electrolysis the maximum current efficiencies for tin deposition were obtained at cathode current densities of 20mA cm^{-2}. (Figures 12 to 16).

The maximum tin content in any deposit produced was obtained when using conventional electrolysis at between 20 to 30mA cm^{-2} which is in agreement with Menzies and Ng's work. When using pulsed electrolyses the maximum tin contents in deposits were obtained at current densities of

5mA cm^{-2}. (Figures 17 to 26).

Although the highest efficiencies with respect to metal deposition were obtained at the lowest current densities using a current density of 20 to 30mA cm^{-2} produces a faster plating rate.

This means that the optimum cathode current density employed in any controlled process would largely be determined by the mode of current being used. For conventional current this would be 20 to 30mA cm^{-2} and for pulsed electrolyses up to 10mA cm^{-2}.

4.3 Anode Material.

The selection of anode material is a complicated issue. In all cases investigated the use of inert anodes produced cathodic deposits having the highest tin contents. (Figures 55 to 57).

Bronze anodes produced deposits having slightly lower tin contents under corresponding conditions. At bath temperatures of 50°C and above the efficiency for bronze anodic dissolution was high. This was the case for each type of current and for all current densities investigated.

This is in broad agreement with the work of Baier and Macnaughton (16). However, they found that above a current density of 60mA cm^{-2} the bronze anodes passivated which was not found to be the case in the current work.

When copper anodes were used the efficiencies for copper dissolution were high. This was true irrespective of the temperature or the current density used, except for the case of long pulsed electrolysis at 30°C (Figure 31). Anodic efficiencies in all other cases were approximately

one hundred per cent.

The effect of using copper anodes upon the tin content of deposits obtained was however more complicated. Increasing anode current densities when using copper anodes had a complex effect upon the tin content in deposits. The tin content of the deposits exhibited a maxima with increasing current density before decreasing again with further increases in current density.

Deposits produced when using copper anodes had lower tin contents than deposits obtained when using bronze or inert anodes under corresponding plating conditions.

Tin anodes proved to be the least versatile of all the anode materials investigated.

The range of current densities employed when using tin anodes was small to avoid stannite formation and achieve an acceptable level of efficiency for anodic dissolution (3), (17),(20). Although the anode current density was kept within the range of 15 to 25mA cm^{-2} to achieve this end the resultant efficiencies and deposit compositions were not as promising as those obtained when using other anode materials.

The efficiencies for dissolution of tin anodes were generally low and some anomalous efficiencies were observed see (Figures 42 to 45). At 30°C no tin dissolution occurred at any current density investigated irrespective of the current mode used. With increasing temperature the anodic efficiencies generally increased. However, when long pulsed current was used at 60°C and 70°C no anodic dissolution occurred. Indeed all the tin anodes passivated under these

conditions with some of the anodes actually showing a gain in weight. Furthermore extremely high current efficiencies were observed when using short pulsed current at temperatures above 50°C and low current densities of 15mA cm^{-2} (Figures 43 to 45). The calculated efficiencies were twice the magnitude that could be expected if the tin was entering solution at one hundred per cent efficiency as the stannate ion with a valency of four. However, if tin were entering solution as the di-valent stannite ion at one hundred per cent efficiency this would explain the experimental data (20). This is in some ways in line with the findings of previous workers in this area who state that stannite formation occurs when using current densities less than 14mA cm^{-2}. However, their work involved the use of conventional current electrolyses only (17).

The anodic efficiencies for tin dissolution increased with increasing temperature when conventional current was used. The efficiency reached a maximum value of 50 per cent at a bath temperature of 70°C and an anodic current density of 15 to 20mA cm^{-2}. This is in agreement with the findings of Bechard who recorded efficiencies up to 60 per cent when using tin anodes.

The tin content of deposits obtained using tin anodes was low. Whether using conventional current or long or short pulsed electrolyses the tin content of deposits as a function of temperature is complicated. Using conventional or short pulsed current produced deposits having maximum tin contents of only approximately five per cent. Electrolyses using long pulsed current yielded deposits

having higher tin contents of up to ten per cent. However, this was probably due to the high potentials required to maintain a preset current density as the tin anodes began to passivate.

The variation in composition of the deposits obtained when using different anode material under given conditions is interesting. This might be explained to some extent by the fact that each anode material will have a different effect upon the cell overvoltage. Each particular anode material will require a different cell voltage to produce a given cathodic current density since plating was performed under galvanostatic conditions. This no doubt results in the actual cathode potential varying in accordance with the type of anode being used. Since the structure and composition of deposits is influenced by both the potential and current density the observations made in the present work may not be so surprising.

Of the anode materials investigated inert and bronze anodes best fulfilled the criteria for both a high anodic efficiency and the production of deposits with high tin contents. Deposits with high tin contents are those which are best suited to commercial practice.

A combination of copper, tin or bronze anodes could be used in conjunction with an inert anode. Conceivably this would produce deposits with adequate tin contents and also replenish the metal levels in the bath. Although ideally all of the metals would be replaced in this way it is envisaged that on a practical basis some of the metal content would have to be replaced by chemical additions.

A difficulty encountered when attempting to define the optimum plating conditions is that the optimum conditions for cathodic efficiency and deposit composition do not always coincide with the optimum conditions for the anodic processes. This is particularly true with respect to the use of different current modes. Also, in plating operations anodes are required to have a high limiting current. This can be achieved by having a large anode surface area and plating systems are commonly operated with an anode to cathode surface area of up to two and a half to one.

Another factor which would have to be considered is the difference between the true and apparent anodic efficiencies which occur when using soluble anodes. This phenomena was most evident when using copper or bronze anodes. These two types of anodes often exhibited apparent anodic efficiencies in excess of one hundred per cent when calculated on a purely weight loss basis. This was however shown to be due to physical disintegration of the anodes. When the anodes were bagged and the anode material which had dropped off into the bag was analysed the true efficiencies for copper and bronze anodes although high, were found to be less than one hundred per cent.

Conditions which fulfil the optimum criteria for both the anodic and cathodic processes using the basic plating solution would be typically:

1. Conventional current electrolysis.

2. Bath Temperature 60°C to 70°C.

3. Cathode current density 20 to 30mA cm^{-2}.

4. Anode current density up to 15mA cm^{-2}.

5. Anode material, inert plus a combination of copper, tin or bronze.

6. pH 12.9.

4.4 Dilution of the Basic Plating Solution.

The effect upon deposit composition produced by simple dilution of the basic plating solution and using diluted solutions in which the cyanide and hydroxide levels had been adjusted to their original values was similar.

In all cases the tin content of the deposits obtained was much less than in the deposits produced under corresponding conditions using the undiluted plating solution.

This would suggest that the tin content of the basic bronze solution is of utmost importance. Production of deposits having high tin contents requires a high tin content in the plating bath.

4.5 Effect of Varying Pulse Frequency.

Varying the frequency employed for pulsed electrolysis showed that a frequency of 1000Hz gave deposits having higher tin contents than those obtained using lower or higher frequencies. The efficiencies for copper and tin deposition also peaked at a frequency of 1000Hz although similar efficiencies were obtained at frequencies higher than this value.

4.6 Effect of Adding Zinc to the Basic Bronze Solution.

Replacing some of the copper in the basic bronze solution with zinc had an interesting effect upon deposit composition.

The deposits obtained from these solutions had much

higher tin contents than those deposits obtained using the basic plating solution under corresponding conditions. This was true for deposits obtained using both conventional and pulsed electrolyses. However, the amount of zinc in these deposits was not as high as might be expected from the amount of zinc in the plating solution. A typical increase in the tin content of these deposits above that in the equivalent deposits produced from the base solution would be an additional five or six per cent. The maximum zinc content of any deposit produced from these zinc / bronze plating solutions was however only two per cent.

This phenomena might be explained by the relative differences in the energies required for the nucleation and growth of tin and zinc.

If the energy required for tin nucleation is greater than that for zinc nucleation, then initially zinc will nucleate preferentially to tin. This will provide additional nucleation sites. However, if the energy required for subsequent growth of tin deposits is low compared to that for zinc, tin may deposit and grow on both the tin and zinc nuclei once formed.

This may be possible as the crystal structures of tin rich phases and zinc are hexagonal close packed (51). This means that if tin were to deposit on zinc nuclei the surface energy would be minimised relative to its deposition on copper which has a face centre cubic crystal structure. However, much more work is required to fully quantify the effect of zinc additions upon deposit composition and the structure of deposits obtained from

bronze plating solutions.

4.7 Effect of the Current Mode Employed upon Structure.

Using pulsed current as opposed to conventional current did not greatly affect the structures of the deposits. The most obvious result of using any pulsed current was that the deposits produced had lower tin contents than the corresponding deposits produced by conventional current. Thus, structures of pulse plated deposits consisted primarily of the alpha phase. Deposits obtained by conventional current electrolysis exhibited a wider range of tin contents and consequently more phases were present in their structures (Figures 58-68). However, deposits obtained using pulse and having the same chemical composition as those produced by conventional current electrolysis did not always exhibit the same structure.

The preferred orientation of pulsed deposits differed from those of the conventional deposits even though the phases present were the same.

Deposits produced by conventional current electrolysis exhibited alpha, beta and epsilon phases, the amount of each phase present depended upon the tin content of the deposit. At low tin contents the major phase present was alpha and as the tin content of deposits increased both beta and epsilon phases became more evident. Deposits having tin contents in excess of ten per cent consisted mainly of beta and epsilon phases with little or no alpha phase present. This is in agreement with structural work on bronze deposits performed by Raub and Sautter (37) and later by Menzies and Ng (36). They observed the presence of

non - equilibrium phases in electroplated deposits which on a purely compositional basis should not have been present. Indeed, examination of the copper-tin equilibrium diagram (Figure 1) suggests that the epsilon phase should not be present in deposits which have less than about thirty per cent tin.

This phenomena cannot be explained by the existence of small areas having high tin concentrations and thereby exhibiting these other phases. In deposits which had the highest tin content, around thirteen per cent, no alpha phase was observed. The structure of these deposits being predominantly beta or epsilon.

Although this phenomena has been observed previously no attempt has been made to suggest why these phases should exist when compositionally they would not be expected. This aspect requires much more in depth study using more advanced techniques such as transmission electron microscopy, electron diffraction and compositional analysis.

4.8 Development of a Control Model.

In order to develop a control system the baths operating characteristics must be known and the plating conditions must be specified. These conditions and characteristics include, bath temperature, anode and cathode current densities together with the respective efficiencies, current mode, anode material, work load and the bath configuration to be used. Once these parameters have been fixed the amount of alloy plating out at the cathode in a given time can be calculated. These parameters

also fix the amount of solution and water lost due to drag-out and evaporation respectively and the amount of metal replenishment by anodic dissolution where soluble anodes are used. A mass balance of the system as a whole may be constructed.

Using experimental data obtained for a plating bath operated at 70°C with conventional current at a cathode current density of 20mA cm^{-2} a rudimentary mass balance may be derived. In performing this operation certain considerations have to be taken into account. These are as follows:

1. The ultimate aim of alloy plating is to control the plating bath in order to obtain deposits having known and consistent properties.

2. In order to run these baths on an other than " ad hoc" basis it is necessary to develop a predictive control system. This must be based upon a fundamental understanding of the chemistry of the bath and the actual chemical / electrochemical reactions taking place.

3. In an ideal situation all the metal deposited at the cathode would be replaced by that dissolved from the anodes. To achieve this would require a single cathode operated using a multi-anode system with one component of the anode system being inert. This would be the case unless by chance the metals dissolving from the anodes did so in the same proportions and with the same efficiencies as those metals being deposited at the cathode.

4. The control circuitry for the power supply must allow the current output at each of the anodes to be controlled

separately.

It is evident from the results of the present work that all possible modes of operation of the bronze bath will require an inert component to be present as part of the overall anode system. This inert component would have a twofold function of: a) balancing the differences in anodic / cathodic efficiencies for dissolution and deposition and b) increasing the tin content of deposits to the desired levels. The use of inert anodes to specifically increase tin content of deposits during bronze plating does not appear to have been commented upon in previous work.

The simplest control system envisaged would involve an inert anode together with a single soluble anode component. The function of the soluble anode would be to replenish the bath with respect to the major component of the alloy being deposited. In the current work this would be copper. This would require the addition of chemicals to maintain a constant bath composition.

A more complete control system would involve the use of a multi-component anode comprising an inert plus two or more soluble anodes. The tin content of the bath being replenished by using either a bronze or a pure tin anode with the addition of chemicals to maintain fine control of the bath composition.

It is possible to derive a rudimentary mass balance for the bronze plating system using the simple two anode configuration shown in Figure 71. This may be accomplished by applying experimental data from the present work to an

anode system comprising of one copper and one inert anode.

The cathode to anode current relationship and that of the metals deposited at the cathode to those dissolved at the anode can be written as:

$$I_{CATHODE} = I_{ANODE1} + I_{ANODE2} \qquad (i)$$

Where;

$I_{CATHODE}$ = Total cathode current.

I_{ANODE1} = Partial anodic current passed via the inert anode.

I_{ANODE2} = Partial anodic current passed via soluble anode.

Therefore, assuming that anode 1 is the inert component the above may be rewritten as:

$$I_{C\,Cu} + I_{C\,Sn} + I_{C\,H2} = I_{A1\,O2} + (I_{A2\,S} + I_{A2\,Cu}) \qquad (ii)$$

Where;

$I_{C\,Cu}$ = Cathodic current used for copper deposition.

$I_{C\,Sn}$ = Cathodic current used for tin deposition.

$I_{C\,H2}$ = Cathodic current used for hydrogen evolution.

$I_{A1\,O2}$= Anodic current via inert anode.

$I_{A2\,Cu}$= Current used for the dissolution of copper from the soluble copper anode.

$I_{A2\,S}$ = Current associated with secondary reactions occurring at the anode.

The balance between the total metal deposited at the cathode and that being added to the bath by anodic dissolution and chemicals may be written as:

$$W_{C\,M1} + W_{C\,M2} = W_{A2\,M1} + W_{M1+M2\,\text{ADDED AS CHEMICALS}} \qquad \text{(iii)}$$

Where;

$W_{C\,M1}$ = Weight of metal 1 deposited at the cathode.

$W_{C\,M2}$ = Weight of metal 2 deposited at the cathode.

$W_{A2\,M1}$ = Weight of metal 1 replaced from soluble anode.

By application of Faraday's laws the following can be written:

$$W_{C\,M1} = z_{M1}\, i\, t\, e_{M1} \qquad \text{(iv)}$$

$$W_{C\,M2} = z_{M2}\, i\, t\, e_{M2} \qquad \text{(v)}$$

$$W_{A2\,M1} = z_{M1}\, i_{A2\,M1}\, t\, e_{A2\,M1} \qquad \text{(vi)}$$

Therefore where the efficiencies for copper and tin deposition and hydrogen evolution associated with each particular anode, and the anodic efficiencies for metal dissolution associated with the corresponding conditions are known, a rudimentary mass balance for bronze deposition can be calculated.

At this stage another assumption must be made. In the absence of experimental data concerning the effects due to the interaction of different anodes in a multi- anode system upon the cathodic process it must be assumed that the equivalent cathode current associated with each anode behaves in a similar manner to that found for the single anode systems. Only when data becomes available for complex anode systems will the development of a more sophisticated control model of the bath become feasible.

For the present purposes to obtain a deposit of

suitable composition a split in the anodic current will be considered. This will be seventy per cent to the inert anode and thirty per cent to the soluble copper anode.

If all the anode current passed via the inert anode a deposit containing over thirteen per cent tin would be obtained. If all the current passed via the copper anode a deposit of just over three per cent tin would be obtained. Thus by splitting the current in the above manner a deposit of suitable composition would be produced while at the same time achieving some metal replenishment.

The following procedure may be adopted to calculate a metal balance which ignores losses due to drag-out and evaporation.

Mass Balance for metals.

By application of equations (i to vi) to the experimental data obtained, see (Figure 16), a mass balance can be calculated for the following conditions:

1. Dual anode (copper and inert).

2. Cathode surface area $1m^2$.

3. Anode surface area $2m^2$.

4. Cathode current density 20mA cm^{-2}.

5. Anode current density 10mA cm^{-2}.

6. Seventy per cent of current via inert anode.

7. Thirty per cent of current via copper anode.

8. Plating time 1 minute.

9. Total current passed, 200 Amps.(Cathode area x cathode current density). Using a 70/30 split this equates to 140 Amps to inert anode and 60 Amps to copper anode, to obtain

a deposit of suitable composition .

The cathode current efficiencies using inert anodes at 20mA cm^{-2} cathode current density were, see (Figure 16).

Copper   =   65.47%

Tin   =   21.13%

Hydrogen   =   13.40%

Calculation of copper deposited due to inert anode.

The weight of copper deposited at the cathode (w_{Cu}) due to the current passed via the inert anode may be calculated using Faraday's Law :

$$w = z \ i \ t \ e$$

Thus;

$$w_{Cu} = \frac{63.546 \times 140 \times 60 \times 65.47}{100 \times 1 \times 96,500} = \underline{3.621 \ grams}$$

Calculation of tin deposited due to inert anode.

The weight of tin deposited at the cathode (w_{Sn}) by this cathode current may be similarly calculated:

$$w_{Sn} = \frac{118.71 \times 23.13 \times 140 \times 60}{100 \times 4 \times 96,500} = \underline{0.598 \ grams}$$

Metal deposition due to soluble copper anode.

The cathodic efficiencies obtained when using copper anodes at a cathode current density of 20mA cm^{-2} were, see

(Figure 55):

Copper   = 41.466%

Tin   = 3.43%

Hydrogen = 55.1%

Calculation of copper deposited due to copper anode.

The amount of copper deposited at the cathode (w_{Cu}) as a result of the current passed through the copper anode is:

$$w_{Cu} = \frac{63.546 \times 41.466 \times 60 \times 60}{100 \times 1 \times 96,500} = \underline{0.983 \text{ grams}}$$

Calculation of tin deposited due to copper anode.

The weight of tin deposited (w_{Sn}) will be:

$$w_{Sn} = \frac{118.71 \times 3.43 \times 60 \times 60}{100 \times 4 \times 96,500} = \underline{37.97 \times 10^{-3} \text{ grams}}$$

The total amount of copper and tin deposited is that due to the current associated with both the inert and copper anode systems, thus:-

Total copper deposited = 3.621 + 0.983   = $\underline{4.604 \text{ grams}}$

Total tin deposited = 0.598 + 37.97 $\times 10^{-3}$ = $\underline{0.636 \text{ grams}}$

This would give a cathodic deposit with a composition of 12.14% Tin , 87.86% Copper.

The above gives the masses of copper and tin removed from the plating solution in one minute due to cathodic deposition.

Copper replenishment by anodic dissolution.

The amount of copper entering solution as a result of dissolution of the soluble copper anode can be calculated using Faraday's Law. Assuming an anodic efficiency of one hundred per cent and a current of sixty amps passing through the copper anode the weight of copper dissolving (w_{Cu}) is :

$$w = \frac{63.546 \times 60 \times 60 \times 100}{100 \times 1 \times 96,500} = \underline{2.37 \text{ grams}}$$

Overall Metal Balance:

Copper deposited less copper dissolved = 4.604 - 2.37
    = 2.234 grams.

Tin deposited = 0.636 grams.

This indicates that each minute 2.234 grams of copper and 0.636 grams of tin must be added to the plating bath to maintain a constant composition.

To achieve this metals must be replenished by dissolution of the soluble anode, plus the addition of any necessary chemicals to make up the balance.

Two methods of metal replacement are possible, these being:

1. By additions of potassium stannate to replace the tin content and copper cyanide to replace the copper content of

the bath.

2. By copper stannate additions (52), which would effect replacement of both all of the tin and some of the copper.

Method 1: Chemical Additions.

The metal content of the bath can be adjusted to the desired levels by the addition of copper and tin as copper cyanide and potassium stannate respectively.

One gram of copper cyanide (CuCN) contains 0.7095 grams of copper, therefore to fully replace 2.234 grams of copper by this method would require the addition to the plating solution of;

$$\frac{2.234}{0.7095} = \underline{3.15\ grams\ Copper\ Cyanide}$$

One gram of potassium stannate $K_2SnO_3.3H_2O$ contains 0.398 grams of tin, therefore to replace 0.636 grams of tin in the bath would require the addition of;

$$\frac{0.636}{0.398} = \underline{1.6\ grams\ Potassium\ Stannate}$$

Method 2: Chemical Additions.

It is possible to replace both some of the tin and some of the copper simultaneously by additions of copper stannate (52) which has the formula $CuSn(OH)_6$. Thus one gram of copper stannate contains 0.4176 grams of tin and 0.2236 grams of copper.

Therefore to replace 0.636 grams of tin by additions of

copper stannate the following amount must be added.

$$\frac{0.636}{0.4176} = \underline{1.523 \text{ grams}}$$

Associated with this 1.523 grams of copper stannate there would be:

$$1.523 \times 0.2236 = \underline{0.3405 \text{ grams of Copper.}}$$

This means that to fully replace all the copper further additions have to be made. The amount of copper still required to fully replenish the bath is now:

$$2.234 - 0.3405 = \underline{1.894 \text{ grams.}}$$

This could be achieved by adding further copper in the form of copper cyanide. Since one gram of copper cyanide contains 0.7095 grams of copper the amount of this which would have to be added to the bath to fully correct the copper content is:

$$\frac{1.894}{0.7095} = \underline{2.67 \text{ grams of Copper cyanide.}}$$

A complication which could arise from additions of copper stannate is that the copper is being added in the di-valent state whereas copper is present in the original bath in the mono-valent state. However, past experience shows that this

does not appear to have a detrimental effect (52).

Any predictive control model would however have to take into account changes in cathode current efficiency for the copper deposition process as a result of introducing divalent copper into the bath.

It is interesting to note that even when using copper anodes as part of the above anode system and no tin containing anode that copper containing chemicals in addition to tin containing chemicals must be added to the bath to maintain a balance.

Further Considerations.

Some additional factors have to be considered to achieve a fully balanced system.

1. The water lost due to both drag-out and evaporation needs to be replaced.

2. The chemical losses due to drag-out must be accounted for and corrected.

Usually most of the drag-out would be removed by washing the plated work in a "drag-out" tank. The contents of this tank would be used to maintain the level of the plating solution. However, as the drag-out might contain excess carbonate and other "impurities" it would be beneficial to treat the drag-out solution with suitable chemicals to remove the excess carbonate.

3. Carbonate build up in the plating bath would have to be dealt with.

Carbonate can form by reaction of carbon dioxide from the atmosphere with the bath surface.

Since the carbon dioxide has to pass through the bath surface the amount of carbonate formed will be dependent upon the bath's surface area. It may also form as a result of secondary anodic reactions as well as through the decomposition and hydrolysis of cyanides (21).

$$2KOH + CO_2 = K_2CO_3 + 3H_2O$$

$$KCN + H_2O = KOH + HCN$$

$$HCN + 2H_2O = NH_4HCO$$

THEN $$NH_4HCO + 2H_2O = 2NH_3 + H_2CO_3$$
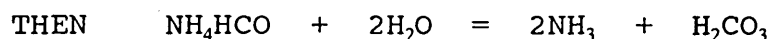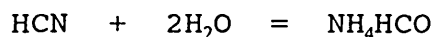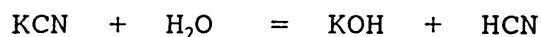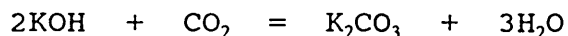
The "carbonate" factor was overcome in the present work by only using freshly prepared solutions for short periods.

Carbonate is not detrimental in small concentrations but excessive build up of carbonate in the bath is not desirable. This problem might be solved by continuous treatment of the drag-out solution with a suitable reagent such as barium hydroxide to precipitate out the carbonate (Figure 72). This would be followed by filtration prior to its return to the main plating bath.

4. The build up of hydroxyl ions in the bath from the deposition of tin needs could lead to variations in pH and perhaps more importantly changes in the hydroxide to cyanide ratio.

Hydroxide is formed during bronze plating as a result of the tin deposition reaction (1).

$$SnO_3^{2-} + 3H_2O + 4e = Sn^0 + 6OH^-$$
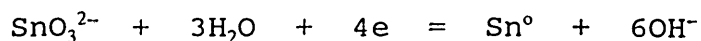
In commercially operated bronze baths the problem of

hydroxide build up is not as great as might be expected (42). This could be due to hydroxide in the bath reacting with carbon dioxide in the air to form carbonates. This theory is enhanced by the fact that in India silver plating baths operated at high temperatures need frequent additions of potassium hydroxide to maintain their alkalinity (62). This is accompanied by frequent treatment to remove the excess carbonate which builds up.

The above discussion suggests that it would be feasible to develop a predictive control model for the bronze plating system. A prototype model would contain the following components.

1. An inert anode.

2. A soluble copper anode.

3. Individual current control to each anode.

4. Chemical additions to effect overall balance.

5. A continuous dosing / filtration system to remove excess carbonate.

6. A continuous dosing system for addition of necessary chemicals.

5.0 Conclusions.

1. The optimum bath temperature required to achieve high efficiency for metal deposition and deposits having a suitable composition and physical properties was found to be 60°C to 70°C. This was the case for all modes of plating investigated.

2. Deposits having the highest tin contents were obtained using conventional current electrolysis. Deposits obtained using pulsed electrolyses had lower tin contents than conventional deposits produced under corresponding conditions.

3. The highest current efficiencies for copper deposition were obtained at a cathode current density of 5mA cm^{-2}, this was the case for all modes of plating investigated.

4. The highest current efficiencies for tin deposition were obtained at a cathode current density of 5mA cm^{-2} when using pulsed electrolyses and 10 to 20mA cm^{-2} cathode current density when using conventional electrolyses.

5. Increasing current density at any given bath temperature caused an increase in hydrogen discharge. This was the case irrespective of bath temperature or mode of electrolysis employed.

6. The highest tin content (13%), of any deposits produced when using the basic bronze plating solution was obtained using cathode current densities of 20 to 40mA cm^{-2} and conventional current electrolyses at 70°C.

7. Deposits produced by diluting the basic plating solution had lower tin contents than those deposits obtained from the undiluted solution under corresponding conditions. This

was also the case in diluted solutions with cyanide and hydroxide levels corrected to their original values.

8. An optimum frequency for pulsed electrolyses was found to be 1000Hertz. At this frequency both the efficiencies for copper and tin deposition attained a maximum. Deposits produced using this frequency also had the highest tin content of any deposits produced using pulsed electrolyses.

9. The composition of cathodic deposits was highly dependent upon the anode material used to produce the deposits. Using corresponding plating conditions inert anodes always produced cathodic deposits with higher tin contents than when soluble anodes were used.

10. Apparent anodic efficiencies for dissolution of copper and bronze anodes were extremely high and often in excess of one hundred per cent. This was shown to be due to physical disintegration of the anodes by bagging the anodes during operation.

11. The anodic efficiency for dissolution of tin anodes was low except at the highest bath temperatures when efficiencies of up to fifty per cent were attained. No dissolution occurred at a bath temperature of 30°C in any of the current modes investigated.

12. When long pulsed electrolyses were used in conjunction with tin anodes the anodes developed a permanent black film on their surface. This was due to passivation of the tin anode. The anodes actually gaining weight during these electrolyses.

13. When short pulsed electrolyses were used in conjunction with tin anodes at an anode current density of $15mA$ cm^{-2}

extremely high anodic efficiencies were obtained of approximately two hundred per cent. This was possibly due to tin entering solution as the stannite ion and not the preferred stannate ion. The anodes developed a mossy black deposit during electrolysis which was readily washed off after use.

14. Having relatively large amounts of zinc in the plating solution leads to bronze deposits containing only small amounts of zinc of up to two per cent.

15. The addition of zinc to the basic bronze solution had an interesting effect upon the composition of the deposits obtained. For any given plating conditions investigated the deposits obtained from solutions containing zinc had higher tin contents than those deposits obtained from corresponding solutions containing no zinc.

16. The structure of bronze deposits examined during the course of this work was highly dependant upon the chemical composition of the deposits.

17. Deposits produced by pulsed electrolysis generally had tin contents less than eight per cent and structures consisting mainly of the alpha phase.

18. Deposits produced by conventional electrolysis had a wide range of tin contents and exhibited alpha, beta and epsilon phases.

19. The structures exhibited by bronze deposits would not be those expected from simple inspection of the copper - tin thermal equilibrium diagram. Phases such as epsilon were present in deposits having much lower tin contents than would be predicted from the equilibrium diagram.

20. The optimum operating conditions for a bronze bath using the basic plating solution were found to be:

a). Bath temperature 60° to 70°C.

b). Conventional current electrolysis.

c). Cathode current density range 10 to 30mA cm^{-2}.

21. The optimum conditions for the cathodic and anodic processes differ when using pulsed electrolysis and therefore preclude the use of a control system based upon pulsed electrolysis.

22. It would be advantageous to operate a bronze plating bath using a prototype control system based upon the use of:

a). An dual anode system based upon an inert plus a copper anode.

b). Individual current control for each anode.

c). Chemical additions to control bath composition.

d). A continuous dosing and filtration system. This would enable the removal of excess carbonate and facilitate the addition of all necessary chemicals.

23. The model upon which the control system is based would have to be refined with further knowledge and understanding of the system. This would include :

a). The rate of change of bath composition due to the electrode reactions.

b). The rate of carbonate formation and removal within the bath.

c). The effects of anode interaction within a multi – anode system upon the cathodic process.

6.0 Further Work.

The present work indicates that it would be feasible to develop a model to control a bronze plating bath and the characteristics of deposits obtained from such a bath. However, the scope of the present work only permits the construction of a rudimentary model to give a balance of the metal levels involved.

To achieve a more complete understanding of the processes involved from both a fundamental and practical point of view certain avenues of research should be pursued:

1. A bronze plating bath of more commercial dimensions should be constructed to test the validity of models using multi - anode systems. These would typically consist of an inert anode plus a combination of soluble anodes to achieve adequate metal replenishment. Each anode used having independent current control.

2. Construction of a prototype bronze plating bath to be operated using the control system previously discussed.

3. To use this prototype control system to study the effects of anode interaction upon the composition of the cathodic deposits.

4. To study the bath chemistry and rate of carbonate formation due to:

a). Anodic breakdown of cyanide.

b). Tin deposition at the cathode.

c). Reaction between the bath and atmospheric carbon dioxide.

5. To refine the control model to take into account the results of any further work.

6. To investigate further the effect of introducing zinc into the bronze plating bath and its effect upon the resultant deposit composition.

7. The results of the present work suggest that deposits having high tin contents cannot be produced by using pulsed electrolysis and the basic bronze plating solution. However, if pulsed electrolysis has the same effect upon bronze solutions having higher tin contents as in speculum baths then it might be possible to produce deposits with acceptably high tin contents. Thus, it would be of interest to study the effects of pulsed electrolysis upon deposits obtained from a speculum type of bath.

8. Further studies into the physical structure of deposits is required. The phenomena of phases being present at compositions where they theoretically should not exist needs to be explained. This may be achieved to some extent by detailed study of deposits using transmission electron microscopy. Analysis of deposits by electron diffraction and quantitative compositional analysis.

References:

1. D. R. Gabe

   Principles of Metal Surface Treatment and

   Protection.

   Published by Pergammon Press (1972).

2. E. Raub and K. Muller

   Fundamentals of Metal Deposition.

   Published by Elsevier (1967).

3. A. Brenner

   Electrodeposition of Alloys. Volume 1.

   Published by Academic Press (1963).

4. A. Brenner

   Electrodeposition of Alloys. Volume 2.

   Published by Academic Press (1963).

5. A. Coehn

   German Patent No. 75482. (1893).

6. Jean-Claude Puippe and Frank Leaman

   Theory and Practice of Pulse Plating.

   Published A.E.F.S. (1988).

7. J. Winkler

   German Patent No. 576585.cl 48a (May 13. 1933).

8. G. E. Gardam and M. E. Tidswell

   The Electrodeposition of Gold and other Alloys by a

   New Method.

   Fourth International Conference on Electrodeposition

   and Metal Finishing. London (1954).

9. Jean-Claude Puippe

   Investigation of the structure of an

   Electrodeposited Ternary alloy (Cu - Sn - Zn).

Interfinish 84. Metal Finishing Conference (1984).

10. C.C.Wan, H.Y.Cheh and H.B.Linford

    Plating 61. (6). 559. (1974).

11. M. Viswanathan and Ch. J. Raub

    Surface Technology 4. 339. (1976).

12. W. Sullivan

    Plating. 62. (2). 139. (1975).

13. M. De Roulz

    Upon the means by which one obtains bronze by

    deposition.

    Compt. rend. acad sci. 15. 280-283. 140. (1842).

14. W. D. Treadwell and E. Bekh

    Über elektrolytische Bronzfällung

    Z. Elektrochem. 21. 374-380. (1915).

15. R. Kremann

    Die elektrolytische Darstellung von Legierungen aus

    wässerigen Lösungen.

    Vieweg , Braunschweig. (1914).

16. S. Baier and D. J. Macnaughton

    The electrodeposition of bronze using bronze anodes.

    Journal of Electrodepositors Technical Society.

    Volume 11 p1-14 (1936).

17. R.M. Angeles, F.V. Jones, J.W. Price, J.W.

    Cuthbertson.

    The Electrodeposition of Speculum.

    Journal of Electrodepositors Technical Society.

    Volume 21. p19-44 (1946).

18. Gerd Hoffacker

    Miralloy. A chance against nickel allergy.

Demetron Gmbh, Schwäbisch Gmund (1992).

19. W. T. Lee

    Bronze Plating from modified cyanide-stannate baths.

    Trans Inst Met Finish. 36. p51-57 (1958-59).

20. C. Bechard

    Exposés d'electrochimie theoretique (IV). Formation

    et structure des alliages electrolytiques.

    Actualities sci et ind 844. (1939).

21. N. V. Mandlich

    Carbonate Formation and removal and cyanide

    decomposition from a cyanide plating solution.

    Trans Inst Met Finishing 70 (1), 24. (1991).

22. J. Horner

    51st Annual Proceedings of American Electroplating

    Society p71. (1964).

23. J.J.Batten, B.T.Moore and B.S. Smith

    A study of electrochemical efficiencies of aluminium

    galvanic anodes in sea water.

    Materials Forum 16. p69-79. (1992).

24. W.H.Safranek, W.J.Neill and D.E.Sellbach

    Bronze Plating solves design and corrosion problems.

    Steel 133. No 25. p102-109. (1953).

25. W.H.Safranek, W.G.Hespenheide and C.L.Faust

    Bronze and Speculum plates provide good protection

    for steel.

    Metal Finishing 52. p70-73. 78. (1954).

26. T. Yoneda

    A method of Plating Copper-Tin alloy.

    Japanese Patent 130,440. (1949).

27. M. A. Loshkarev and M. P. Grechykhina

Adsorptional chemical polarization and cathodic

deposition of alloys from non-complex electrolytes.

Zhur Fiz Khim. 24. p1502-1510. (1950).

28. J. Balachandra

Electrodeposition of copper-tin alloys from a

Fluoroborate Bath.

Current Sci (India) 20. 99. (1951).

29. R. J. Teichimann and L. J. Mayer

U.K. Patent Application No G.B. 2. 100 634 A

30. R. J. Teichimann and L. J. Mayer

U.K. Patent Application No G.B. 2. 096 175 A

31. J. Vaid and T. L. Rama Char

Electrodeposition of copper-tin alloys from a

pyrophosphate bath.

Current Sci (India) 22. 170-171. (1953).

32. G. Langbein and W. T. Brannt

'Electrodeposition of Metals'

7th Edition p363. (1913).

33. R. Kremann, C.T.Suchy, J.Lorber and R. Maas

Über Versuche zur Abscheidung von Kupfer-Zinn

bronzen.

Monatsh. 35. 219-288. (1914).

34. H. Yagi

Electrolysis of gold, electrolytic reduction of

silver chloride, bronze plating, cadmium plating and

the plating of copper-cadmium alloy.

J. Mint Japan 2. 56-57. (1929).

35. B. E. Curry

Electrolytic Precipitation of Bronzes.

Journal of Physical Chemistry. p515-520. (1906).

36. I. A. Menzies and C. S. Ng

A Study of the Electrodeposition of Bronze from a

Cyanide-Stannate Bath.

Trans Inst Met Finish. Vol 146. p137-143. (1968).

37. E. Raub and F. Sautter

The structure of electrodeposited alloys XII. The

copper-tin alloys.

Metalloberfläche 11. p249-252. (1957).

38. V. R. Ramanathan

Hardness of Electrodeposited Speculum metal and

other Tin-Copper alloys.

Transactions of the Institute of Metal Finishing.

36. No2. p48-56. (1958-59).

39. J. B. Kushner

A new instrument for measuring stress in

electrodeposits.

Plating 41, p1146 - 1153, (1954).

40. D.S.Rickerby, G.Eckold, K.T.Scott and I.M.Buckley-

Golder

The Interrelationship between internal stress,

processing parameters and microstructure of

Physically Vapour Deposited and Thermally Sprayed

Coatings.

Thin Solid Films 154. p125-141. (1987).

41. D. S. Rickerby

Internal Stress and adherence of titanium nitride

coatings.

J. Vac. Sci. Technol. A4. (6). Nov\Dec (1986).

42. A. Medlock

    C.A.T.R.A. Private Communication (1992).

43. J. Lovie and K. B. Misciocio

    Statistical Proces Control For Electronics and

    Electroplating Applications.

    A.E.S.F. 13th Symposium Kissimmee. Florida (1986).

44. D. R. Stewart

    Advanced Control System for Plating Lines.

    A.E.S.F. 13th Symposium Kissimmee. Florida (1986).

45. R. R. Herrscher and G. L. Tingwall

    Innovative Control Systems for Plating.

    Metal Finishing 86. p47-49 March (1986).

46. J. F. Fallot

    A Computer Control System for Electroplating.

    Metal Finishing 87. p35-36 March (1989).

47. G. Wilde

    Modern Electrolytic Process Control.

    Finishing p28-31   April (1986).

48. L. Brown

    Automatic Controls.

    Finishing 12. p20 November (1988).

49. W. H. Caplinger

    CCKS, A Knowledge Based Control System for Coatings

    Application.

    3rd International Symposium on Intelligent Control

    Arlington U.S.A. p700-702   (1988).

50. D. R. Stewart

   Advanced Control for Plating Lines.

   Products Finishing (US) Vol 51 p66-69 (1987).

51. C. J. Smithells

   Metals Reference Book. Volume 1. 4th Edition.

   Published by Butterworths London.   (1967).

52. F. A. Lowenheim

   Tin Alloy Plating. American Experience.

   Trans Inst Metal Finishing 31. p386-397 (1954).

53. N. V. Parthasaradhy

   Practical Electroplating Handbook.

   Published by Prentice Hall.

54. M. R. Hillis

   Treatment of Cyanide Wastes by Electrolysis.

   Trans Inst Met Finish. Vol 153. p65-73. (1975).

55. B. D. Cullity

   Elements of X-Ray Diffraction. 2nd Edition.

   Addison-Wesley Publishing Co Ltd (1978).

56. S. V. Allen

   B.Sc Project Thesis (1988).

57. J. M. West

   Electrodeposition and Corrosion Processes.

   Publishers Van Norstrand Reinhold Co (1970).

58. C. L. Wilson and D. L. Wilson

   Comprehensive Analytical Chemistry. Coulometric

   Analysis.

   Published by Elsevier (1975).

59. W. Canning and Company

   Handbook on Electroplating.

60. F. A. Lowenheim

Modern Electroplating. 3rd Edition.

Published by John Wiley and Sons   (1968).

61. Larry. G. Hargis

Analytical Chemistry. Principles and Techniques.

Prentice-Hall International   (1988).

62. G. W. Marshall

Private communication   September (1992).

Metal couple	E^0 (volts)	Metal couple	E^0 (volts)
Li^+/Li	-3.01	$2H^+/H_2$	0.00
Ca^{++}/Ca	-2.87	Cu^{2+}/Cu	$+0.337$
Na^+/Na	-2.713	O_2/OH^-	$+0.401$
Mg^{2+}/Mg	-2.37	Cu^+/Cu	$+0.52$
Be^{2+}/Be	-1.85	Hg_2^{2+}/Hg	$+0.798$
U^{3+}/U	-1.80	Ag^+/Ag	$+0.799$
Al^{3+}/Al	-1.66	Rh^{3+}/Rh	$+0.8$
Ti^{2+}/Ti	-1.63	Hg^{2+}/Hg	$+0.854$
Zr^{4+}/Zr	-1.53	Pt^{2+}/Pt	$+1.2$
Mn^{2+}/Mn	-1.18	Cl_2/Cl^-	$+1.358$
Zn^{2+}/Zn	-0.763	Au^{3+}/Au	$+1.50$
Cr^{3+}/Cr	-0.74	Au^+/Au	$+1.70$
Fe^{2+}/Fe	-0.44	Cr^{3+}/Cr^{2+}	-0.41
Cd^{2+}/Cd	-0.403	Sn^{4+}/Sn^{2+}	$+0.15$
Co^{2+}/Co	-0.277	Cu^{2+}/Cu^+	$+0.153$
Ni^{2+}/Ni	-0.25	Fe^{3+}/Fe^{2+}	$+0.77$
Sn^{2+}/Sn	-0.136	$Cr_2O_7^{2-}/Cr^{3+}$	$+1.33$
Pb^{2+}/Pb	-0.126		

Table 1.
Standard (Reduction) Electrode Potentials at 25°C.

Concentration	1 M	10^{-2} M	10^{-7} M	10^{-20} M
Potential (volts)	E^0	$(E^0 - 0.059)$	$(E^0 - 0.21)$	$(E^0 - 0.59)$

Table 2.
The change in electrode potential with ion concentration.

Complex ion	Instability constant	Complex ion	Instability constant
$Ag(CN)_2^-$	1.8×10^{-19}	$Fe(CN)_6^{3-}$	1×10^{-42}
$Au(CN)_2^-$	5×10^{-39}	$Mn(OH)_2$	2×10^{-13}
$Cd(CN)_4^{2-}$	1.4×10^{-19}	$Ni(CN)_4^{2-}$	1×10^{-22}
$Co(NH_3)_6^{2+}$	1.25×10^{-5}	$Ni(NH_3)_4^{2+}$	1×10^{-8}
$Co(NH_3)_6^{3+}$	2.2×10^{-34}	$Ni(NH_3)_6^{2+}$	1.8×10^{-9}
$Cu(CN)_2^-$	1×10^{-16}	$Sn(OH)_4$	1×10^{-57}
$Cu(CN)_3^{2-}$	5.6×10^{-28}	SnF	1×10^{-10}
$Cu(CN)_4^{3-}$	1×10^{-27}	SnF_4^{2-}	1×10^{-25}
$Cu(NH_3)_2^+$	1.35×10^{-11}	$Zn(CN)_4^{2-}$	1.3×10^{-17}
$Fe(CN)_6^-$	1×10^{-35}	$Zn(NH_3)^{2+}$	3.4×10^{-10}

Table 3.
The instability constants of some metal complexes.

Solution and Conditions

Sodium Cyanide	49 g/l
Copper Cyanide	30 g/l
Zinc Cyanide	7 g/l
Sodium Carbonate	4.7 g/l

on-time seconds	Current Density 0.32 A/dm^2	Current Density 0.64 A/dm^2
	Color of Deposit	
½	orange	red
¾	orange-yellow	orange-yellow
1	orange-yellow	yellow
1¼	yellow	yellow
1¾	green	orange-green

<u>Table 4.</u>
The colour of brass deposits as a function of current density and pulse "on" time.

Table 5.
The charge weights of pure copper and pure tin and chemical analysis of the bronze alloys produced for use as analytical standards.

Weight of metals charged (grams)		Chemical Analysis
Copper	Tin	
1900	100	3.29% Tin
1800	200	5.40% Tin
1700	300	12.16%Tin
1600	400	15.8% Tin
1400	600	27.4% Tin

Table 6.
Composition of the Basic Bronze Plating Solution used for Anodic and Cathodic Efficiency Determinations.

Composition of Bronze Plating Solution (Grams per litre)	
Potassium Stannate	43
Potassium Cyanide	72
Copper Cyanide	35
Potassium Hydroxide	10.5

Table 6a
Compositions of Plating Solutions having the same Relative Composition but in Increasing Dilution.

Chemical Constituent	Composition (Grams per Litre)			
	Dilution Per Cent			
	Base	15%	25%	35%
Potassium Stannate	43	36.55	32.25	27.95
Potassium Cyanide	72	61.2	54	46.8
Copper Cyanide	35	29.75	26.25	22.75
Potassium Hydroxide	10.5	8.93	7.88	6.83

Table 7.
Composition of Bronze Plating Solution used for Anodic and Cathodic Efficiency Determinations diluted by fifteen per cent. Cyanide to Hydroxide ratio corrected to its original value.

Composition of Bronze Plating Solution (Grams per litre)	
Potassium Stannate	36.55
Potassium Cyanide	63.97
Copper Cyanide	29.75
Potassium Hydroxide	10.3

Table 8.
Composition of Bronze Plating Solution used for Anodic and
Cathodic Efficiency Determinations diluted by twenty five
per cent.Cyanide to Hydroxide ratio corrected to its
original value.

Composition of Bronze Plating Solution (Grams per litre)	
Potassium Stannate	32.25
Potassium Cyanide	58.24
Copper Cyanide	26.25
Potassium Hydroxide	9.98

Table 9.
Composition of Bronze Plating Solution used for Anodic and
Cathodic Efficiency Determinations diluted by thirty five
per cent.Cyanide to Hydroxide ratio corrected to its
original value.

Composition of Bronze Plating Solution (Grams per litre)	
Potassium Stannate	27.95
Potassium Cyanide	52.26
Copper Cyanide	22.75
Potassium Hydroxide	9.55

Table 10.
Composition of Zinc-Bronze Plating Solution where fifteen mol% Copper in the basic bronze plating solution was replaced by Zinc.

Composition of Zinc-Bronze Plating Solution (Grams per Litre)	
Potassium Stannate	43
Potassium Cyanide	72
Copper Cyanide	29.74
Zinc Cyanide	5.43
Potassium Hydroxide	10.5

Table 11.
Composition of Original Zinc Plating Solution Diluted by Twenty Five Per Cent and Cyanide to Hydroxide ratio corrected to original its value.

Composition of Zinc-Bronze Plating Solution Diluted by 25% (Grams per Litre)	
Potassium Stannate	32.25
Potassium Cyanide	58.24
Copper Cyanide	22.30
Zinc Cyanide	4.07
Potassium Hydroxide	9.97

Table 12.
The results of conventional current electrolyses carried out
at 30°C using inert anodes and the basic bronze plating
solution.

Direct Current 30°C				
Number of Test	Current Density mA cm^{-2}	Plating Time (seconds)	Average Weight Gain (grams)	Analysis Weight % Tin
DC1 + 1A	50	360	0.0188	0.47
DC2 + 2A	40	450	0.0217	0.56
DC3 + 3A	10	1800	0.0541	1.26
DC4 + 4A	70	257	0.0160	0.43
DC5 + 5A	20	900	0.0378	0.89
DC6 + 6A	60	300	0.0190	0.51
DC7 + 7A	30	600	0.0313	0.78
DC8 + 8A	5	3600	0.0798	2.90

Table 13.
The results of conventional current electrolyses carried out
at 40°C using inert anodes and the basic bronze plating
solution.

Direct Current 40°C				
Number of Test	Current Density mA cm^{-2}	Plating Time (seconds)	Average Weight Gain (grams)	Analysis Weight % Tin
DC9 + 9A	50	360	0.0365	1.47
DC10+10A	40	450	0.0445	1.67
DC11+11A	10	1800	0.0846	5.34
DC12+12A	70	257	0.0278	1.06
DC13+13A	20	900	0.0667	3.64
DC14+14A	60	300	0.0310	1.25
DC15+15A	30	600	0.0533	2.67
DC16+16A	5	3600	0.0931	4.82

Table 14.
The results of conventional current electrolyses carried out at 50°C using inert anodes and the basic bronze plating solution.

Direct Current 50°C				
Number of Test	Current Density mA cm^{-2}	Plating Time (seconds)	Average Weight Gain (grams)	Analysis Weight % Tin
DC9 + 9A	50	360	0.0365	1.47
DC10+10A	40	450	0.0445	1.67
DC11+11A	10	1800	0.0846	5.34
DC12+12A	70	257	0.0278	1.06
DC13+13A	20	900	0.0667	3.64
DC14+14A	60	300	0.0310	1.25
DC15+15A	30	600	0.0533	2.67
DC16+16A	5	3600	0.0931	4.82

Table 15.
The results of conventional current electrolyses carried out at 60°C using inert anodes and the basic bronze plating solution.

Direct Current 60°C				
Number of Test	Current Density mA cm^{-2}	Plating Time (seconds)	Average Weight Gain (grams)	Analysis Weight % Tin
DC25+25A	50	360	0.0809	8.84
DC26+26A	40	450	0.0846	10.22
DC27+27A	10	1800	0.0960	9.09
DC28+28A	70	257	0.0731	7.17
DC29+29A	20	900	0.0893	10.47
DC30+30A	60	300	0.0774	8.41
DC31+31A	30	600	0.0862	11.51
DC32+32A	5	3600	0.0968	7.43

Table 16.
The results of conventional current electrolyses carried out at 70°C using inert anodes and the basic bronze plating solution.

Direct Current 70°C				
Number of Test	Current Density mA cm^{-2}	Plating Time (seconds)	Average Weight Gain (grams)	Analysis Weight % Tin
DC33+33A	50	360	0.0831	12.77
DC34+34A	40	450	0.0845	13.22
DC35+35A	10	1800	0.0958	8.78
DC36+36A	70	257	0.0793	11.92
DC37+37A	20	900	0.0893	13.15
DC38+38A	60	300	0.0824	12.57
DC39+39A	30	600	0.0863	12.51
DC40+40A	5	3600	0.0990	7.88

Table17.
The results of short pulsed (1000Hz) electrolyses at 30°C using inert anodes and the basic bronze plating solution.

Short Pulsed Current. 30°C				
Number of Test	Current Density mA cm^{-2}	Plating Time (seconds)	Average Weight Gain (grams)	Analysis Weight % Tin
PC33+33A	50	360	0.0169	0.60
PC34+34A	40	450	0.0209	0.55
PC35+35A	10	1800	0.0572	2.38
PC36+36A	70	257	0.0121	0.43
PC37+37A	20	900	0.0352	1.29
PC38+38A	60	300	0.0147	0.55
PC39+39A	30	600	0.0262	0.89
PC40+40A	5	3600	0.0813	4.35

Table 18.
The results of short pulsed electrolyses (1000Hz) at 40°C using inert anodes and the basic bronze plating solution.

Short Pulsed Current. 40°C				
Number of Test	Current Density mA cm^{-2}	Plating Time (seconds)	Average Weight Gain (grams)	Analysis Weight % Tin
PC25+25A	50	360	0.0302	1.09
PC26+26A	40	450	0.0343	2.42
PC27+27A	10	1800	0.0851	4.93
PC28+28A	70	257	0.0220	0.79
PC29+29A	20	900	0.0602	2.76
PC30+30A	60	300	0.0275	0.96
PC31+31A	30	600	0.0459	1.95
PC32+32A	5	3600	0.0947	4.61

Table 19.
The results of short pulsed electrolyses (1000Hz) at 50°C using inert anodes and the basic bronze plating solution.

Short Pulsed Current. 50°C				
Number of Test	Current Density mA cm^{-2}	Plating Time (seconds)	Average Weight Gain (grams)	Analysis Weight % Tin
PC1 + 1A	50	360	0.0444	1.94
PC2 + 2A	40	450	0.0506	2.42
PC3 + 3A	10	1800	0.1007	5.32
PC4 + 4A	70	257	0.0316	2.03
PC5 + 5A	20	900	0.0801	4.24
PC6 + 6A	60	300	0.0392	1.75
PC7 + 7A	30	600	0.0647	3.23
PC8 + 8A	5	3600	0.1005	8.10

Table 20.
The results of short pulsed electrolyses (1000Hz) at 60°C using inert anodes and the basic bronze plating solution.

Short Pulsed Current. 60°C				
Number of Test	Current Density mA cm^{-2}	Plating Time (seconds)	Average Weight Gain (grams)	Analysis Weight % Tin
PC9 + 9A	50	360	0.0604	3.55
PC10+10A	40	450	0.0732	4.71
PC11+11A	10	1800	0.1062	5.25
PC12+12A	70	257	0.0532	3.02
PC13+13A	20	900	0.0959	6.46
PC14+14A	60	300	0.0535	3.48
PC15+15A	30	600	0.0862	5.57
PC16+16A	5	3600	0.1005	6.61

Table 21.
The results of short pulsed electrolyses (1000Hz) at 70°C using inert anodes and the basic bronze plating solution.

Short Pulsed Current. 70°C				
Number of Test	Current Density mA cm^{-2}	Plating Time (seconds)	Average Weight Gain (grams)	Analysis Weight % Tin
PC17+17A	50	360	0.0852	4.86
PC18+18A	40	450	0.0896	5.44
PC19+19A	10	1800	0.1097	4.87
PC20+20A	70	257	0.0736	3.83
PC21+21A	20	900	0.1048	5.84
PC22+22A	60	300	0.0762	3.90
PC23+23A	30	600	0.0995	6.04
PC24+24A	5	3600	0.1102	4.80

Table 22.
The results of long pulsed electrolyses (100Hz) at 30°C using inert anodes and the basic bronze plating solution.

Long Pulsed Current. 30°C				
Number of Test	Current Density mA cm^{-2}	Plating Time (seconds)	Average Weight Gain (grams)	Analysis Weight % Tin
LP33+33A	50	360	0.0120	0.34
LP34+34A	40	450	0.0149	0.39
LP35+35A	10	1800	0.0454	1.50
LP36+36A	70	257	0.0086	0.27
LP37+37A	20	900	0.0235	0.75
LP38+38A	60	300	0.0088	0.27
LP39+39A	30	600	0.0187	0.60
LP40+40A	5	3600	0.0760	3.61

Table 23.
The results of long pulsed electrolyses (100Hz) at 40°C using inert anodes and the basic bronze plating solution.

Long Pulsed Current. 40°C				
Number of Test	Current Density mA cm^{-2}	Plating Time (seconds)	Average Weight Gain (grams)	Analysis Weight % Tin
LP9 + 9A	50	360	0.0186	0.36
LP10+10A	40	450	0.0249	0.43
LP11+11A	10	1800	0.0527	1.99
LP12+12A	70	257	0.0151	0.33
LP13+13A	20	900	0.0372	0.64
LP14+14A	60	300	0.0172	0.35
LP15+15A	30	600	0.0288	0.56
LP16+16A	5	3600	0.0877	2.84

Table 24.
The results of long pulsed electrolyses (100Hz) at 50°C using inert anodes and the basic bronze plating solution.

Long Pulsed Current. 50°C				
Number of Test	Current Density mA cm^{-2}	Plating Time (seconds)	Average Weight Gain (grams)	Analysis Weight % Tin
LP17+17A	50	360	0.0286	0.71
LP18+18A	40	450	0.0337	0.75
LP19+19A	10	1800	0.0865	3.65
LP20+20A	70	257	0.0222	0.57
LP21+21A	20	900	0.0574	2.30
LP22+22A	60	300	0.0257	0.72
LP23+23A	30	600	0.0447	1.51
LP24+24A	5	3600	0.0995	4.50

Table 25.
The results of long pulsed electrolyses (100Hz) at 60°C using inert anodes and the basic bronze plating solution.

Long Pulsed Current. 60°C				
Number of Test	Current Density mA cm^{-2}	Plating Time (seconds)	Average Weight Gain (grams)	Analysis Weight % Tin
LP25+25A	50	360	0.0433	1.68
LP26+26A	40	450	0.0552	2.50
LP27+27A	10	1800	0.1019	5.84
LP28+28A	70	257	0.0335	1.20
LP29+29A	20	900	0.0801	4.35
LP30+30A	60	300	0.0377	1.62
LP31+31A	30	600	0.0637	3.29
LP32+32A	5	3600	0.1031	6.51

Table 26.
The results of long pulsed electrolyses (100Hz) at 70°C using inert anodes and the basic bronze plating solution.

Long Pulsed Current. 70°C				
Number of Test	Current Density mA cm^{-2}	Plating Time (seconds)	Average Weight Gain (grams)	Analysis Weight % Tin
LP1 + 1A	50	360	0.0582	2.04
LP2 + 2A	40	450	0.0674	2.61
LP3 + 3A	10	1800	0.1016	4.68
LP4 + 4A	70	257	0.0484	1.34
LP5 + 5A	20	900	0.0925	4.05
LP6 + 6A	60	300	0.0505	1.40
LP7 + 7A	30	600	0.0765	3.28
LP8 + 8A	5	3600	0.1028	5.22

Table 27.
The cathode current efficiencies for copper and tin deposition and hydrogen evolution obtained from conventional current electrolysis at 30°C using inert anodes

Current Density mA cm^{-2}	% Efficiency 30°C			
	Copper	Tin	Overall	Hydrogen
5	65.38	4.15	69.53	30.47
10	45.05	1.23	46.28	53.72
20	31.6	0.61	32.21	67.79
30	26.19	0.45	26.64	73.36
40	18.2	0.22	18.42	81.58
50	15.8	0.18	15.98	84.02
60	15.95	0.18	16.13	83.87
70	13.41	0.18	13.59	86.41

Table 28.
The cathode current efficiencies for copper and tin
deposition and hydrogen evolution obtained from
conventional current electrolysis at 40°C using
inert anodes.

Current Density mA cm^{-2}	% Efficiency 40°C			
	Copper	Tin	Overall	Hydrogen
5	74.75	8.13	82.88	17.12
10	67.58	8.13	75.71	24.49
20	54.25	4.34	58.59	41.41
30	44.21	1.63	45.84	54.16
40	36.95	1.26	38.21	61.79
50	30.37	0.90	31.27	68.73
60	25.82	0.72	26.54	75.46
70	23.2	0.54	23.74	76.26

Table 29.
The cathode current efficiencies for copper and tin
deposition and hydrogen evolution obtained from
conventional current electrolysis at 50°C using
inert anodes.

Current Density mA cm^{-2}	% Efficiency 50°C			
	Copper	Tin	Overall	Hydrogen
5	78.88	9.57	88.43	11.57
10	75.59	12.65	88.24	11.76
20	67.24	11.38	78.62	21.38
30	62.09	8.85	70.94	29.06
40	56.02	6.5	62.52	37.48
50	51.88	5.06	56.94	43.06
60	46.06	3.79	49..85	50.15
70	40.75	3.07	43.82	56.18

Table 30.
The cathode current efficiencies for copper and tin deposition and hydrogen evolution obtained from conventional current electrolysis at 60°C using inert anodes.

Current Density mA cm^{-2}	% Efficiency 60°C			
	Copper	Tin	Overall	Hydrogen
5	75.59	13.0	88.59	11.41
10	73.65	15.72	89.37	10.63
20	67.49	16.8	84.29	15.71
30	64.37	17.88	82.25	17.75
40	64.03	15.72	79.75	20.25
50	62.18	13.0	75.18	24.82
60	59.81	11.74	71.55	28.45
70	57.28	9.39	66.67	33.33

Table 31.
The cathode current efficiencies for copper and tin deposition and hydrogen evolution obtained from conventional current electrolysis at 70°C using inert anodes.

Current Density mA cm^{-2}	% Efficiency 70°C			
	Copper	Tin	Overall	Hydrogen
5	76.94	14.09	91.03	8.97
10	73.74	15.17	88.91	11.09
20	65.47	21.13	86.6	13.4
30	63.7	19.5	83.2	16.8
40	61.84	20.23	82.07	17.93
50	61.17	19.15	80.32	19.68
60	60.74	18.6	79.04	20.96
70	58.97	16.98	75.95	24.05

Table 32.
The cathode current efficiencies for copper and tin
deposition and hydrogen evolution obtained from
short pulsed electrolysis (1000Hz) at 30°C using
inert anodes.

Current Density mA cm^{-2}	% Efficiency 30°C			
	Copper	Tin	Overall	Hydrogen
5	65.6	6.5	72.1	27.9
10	47.11	2.53	49.64	50.36
20	29.31	0.9	30.21	69.79
30	21.91	0.36	22.27	77.73
40	17.54	0.18	17.72	82.28
50	14.17	0.18	14.35	85.65
60	12.33	0.18	12.51	87.49
70	10.12	0.18	10.3	89.7

Table 33.
The cathode current efficiencies for copper and tin
deposition and hydrogen evolution obtained from
short pulsed electrolysis (1000Hz) at 40°C using
inert anodes.

Current Density mA cm^{-2}	% Efficiency 40°C			
	Copper	Tin	Overall	Hydrogen
5	76.21	7.95	84.17	15.83
10	68.26	7.59	75.85	24.15
20	49.39	3.07	52.46	47.54
30	37.97	1.63	39.6	60.4
40	28.24	1.45	29.69	70.31
50	25.48	0.54	26.02	73.98
60	22.98	0.54	23.52	76.48
70	18.41	0.36	18.77	81.23

Table 34.
The cathode current efficiencies for copper and tin
deposition and hydrogen evolution obtained from
short pulsed electrolysis (1000Hz) at 50°C using
inert anodes.

Current Density mA cm^{-2}	% Efficiency 50°C			
	Copper	Tin	Overall	Hydrogen
5	75.59	14.27	89.86	10.14
10	80.4	9.75	90.15	9.85
20	64.71	6.14	70.85	29.15
30	52.82	3.79	56.61	43.39
40	41.66	2.17	43.83	56.17
50	36.78	1.45	38.23	61.77
60	32.49	1.26	33.75	66.25
70	26.15	1.08	27.23	72.77

Table 35.
The cathode current efficiencies for copper and tin
deposition and hydrogen evolution obtained from
short pulsed electrolysis (1000Hz) at 60°C using
inert anodes.

Current Density mA cm^{-2}	% Efficiency 60°C			
	Copper	Tin	Overall	Hydrogen
5	78.88	11.92	90.8	9.2
10	84.87	10.12	94.99	5.01
20	75.68	11.2	86.88	13.12
30	68.67	8.67	77.34	22.66
40	58.88	6.14	65.02	34.98
50	49.19	3.79	52.98	47.02
60	43.53	3.43	46.96	53.04
70	43.53	2.89	46.42	53.58

Table 36.
The cathode current efficiencies for copper and tin deposition and hydrogen evolution obtained from short pulsed electrolysis (1000Hz) at 70°C using inert anodes.

Current Density mA cm^{-2}	% Efficiency 70°C			
	Copper	Tin	Overall	Hydrogen
5	88.5	9.57	98.07	1.93
10	88	9.75	97.75	2.25
20	83.27	11.02	94.29	5.71
30	78.88	10.84	89.72	10.28
40	71.46	8.85	80.31	19.69
50	68.34	7.59	75.93	24.07
60	61.76	5.42	67.18	32.82
70	59.73	5.06	64.79	35.21

Table 37.
The cathode current efficiencies for copper and tin deposition and hydrogen evolution obtained from long pulsed electrolysis (100Hz) at 30°C using inert anodes.

Current Density mA cm^{-2}	% Efficiency 30°C			
	Copper	Tin	Overall	Hydrogen
5	61.8	5.06	66.86	33.14
10	37.73	1.26	38.99	61.01
20	19.68	0.36	20.04	79.96
30	15.68	0.18	15.86	84.14
40	12.52	0.18	12.7	87.3
50	10.09	0.18	10.27	89.73
60	7.4	0.18	7.58	92.42
70	7.24	0.18	7.42	92.58

Table 38.
The cathode current efficiencies for copper and tin deposition and hydrogen evolution obtained from long pulsed electrolysis (100Hz) at 40°C using inert anodes.

Current Density mA cm^{-2}	% Efficiency 40°C			
	Copper	Tin	Overall	Hydrogen
5	76.21	7.95	84.17	15.83
10	68.26	7.59	75.85	24.15
20	49.39	3.07	52.46	47.54
30	37.97	1.63	39.6	60.4
40	28.24	1.45	29.69	70.31
50	25.48	0.54	26.02	73.98
60	22.98	0.54	23.52	76.48
70	18.41	0.36	18.77	81.23

Table 39.
The cathode current efficiencies for copper and tin deposition and hydrogen evolution obtained from long pulsed electrolysis (100Hz) at 50°C using inert anodes.

Current Density mA cm^{-2}	% Efficiency 50°C			
	Copper	Tin	Overall	Hydrogen
5	75.59	14.27	89.86	10.14
10	80.4	9.75	90.15	9.85
20	64.71	6.14	70.85	29.15
30	52.82	3.79	56.61	43.39
40	41.66	2.17	43.83	56.17
50	36.78	1.45	38.23	61.77
60	32.49	1.26	33.75	66.25
70	26.15	1.08	27.23	72.77

Table 40.
The cathode current efficiencies for copper and tin
deposition and hydrogen evolution obtained from
long pulsed electrolysis (100Hz) at 60°C using
inert anodes.

Current Density mA cm^{-2}	% Efficiency 60°C			
	Copper	Tin	Overall	Hydrogen
5	78.88	11.92	90.8	9.2
10	84.87	10.12	94.99	5.01
20	75.68	11.2	86.88	13.12
30	68.67	8.67	77.34	22.66
40	58.88	6.14	65.02	34.98
50	49.19	3.79	52.98	47.02
60	43.53	3.43	46.96	53.04
70	43.53	2.89	46.42	53.58

Table 41.
The cathode current efficiencies for copper and tin
deposition and hydrogen evolution obtained from
long pulsed electrolysis (100Hz) at 70°C using
inert anodes.

Current Density mA cm^{-2}	% Efficiency 70°C			
	Copper	Tin	Overall	Hydrogen
5	82.2	9.75	91.95	8.05
10	81.7	8.67	90.37	9.63
20	74.88	6.86	81.74	18.26
30	62.42	4.52	66.94	33.06
40	55.38	3.25	58.63	41.37
50	48.1	2.17	50.27	49.73
60	42.01	1.26	43.27	56.73
70	40.28	1.26	41.54	58.46

Table 42.
The apparent anodic efficiencies for dissolution of soluble copper anodes at 30°C using conventional current electrolysis at various anode current densities.

Copper Anodes 30°C (D.C)				
Test Number.	Current Density mA cm^{-2}	Test Duration (minutes)	Anode Weight Loss (g)	Efficiency %
14	5	120	0.2494	105
15	10	60	0.2457	104
16	20	30	0.2408	102
17	30	20	0.2390	100.9

Table 43.
The apparent anodic efficiencies for dissolution of soluble copper anodes at 40°C using conventional current electrolysis at various anode current densities.

Copper Anodes 40°C (D.C)				
Test Number.	Current Density mA cm^{-2}	Test Duration (minutes)	Anode Weight Loss (g)	Efficiency %
6	5	120	0.2421	102.2
7	10	60	0.2380	100.5
8	20	30	0.2387	100.8
9	30	20	0.2388	100.8

Table 44.

The apparent anodic efficiencies for dissolution of soluble copper anodes at 50°C using conventional current electrolysis at various anode current densities.

Copper Anodes 50°C (D.C)				
Test Number.	Current Density mA cm^{-2}	Test Duration (minutes)	Anode Weight Loss (g)	Efficiency %
18	5	120	0.2445	103.2
19	10	60	0.2439	103
20	20	30	0.2517	106.2
21	30	20	0.2416	102

Table 45.

The apparent anodic efficiencies for dissolution of soluble copper anodes at 60°C using conventional current electrolysis at various anode current densities.

Copper Anodes 60°C (D.C)				
Test Number.	Current Density mA cm^{-2}	Test Duration (minutes)	Anode Weight Loss (g)	Efficiency %
1	5	120	0.2507	105.8
2	10	60	0.2466	104.1
3	20	30	0.2487	105
4	30	20	0.2414	101.9

Table 46.

The apparent anodic efficiencies for dissolution of soluble copper anodes at 70°C using conventional current electrolysis at various anode current densities.

Copper Anodes 70°C (D.C)				
Test Number.	Current Density mA cm^{-2}	Test Duration (minutes)	Anode Weight Loss (g)	Efficiency %
10	5	120	0.2549	107.6
11	10	60	0.2519	106.3
12	20	30	0.2468	104.2
13	30	20	0.2436	102.9

Table 47.

The apparent anodic efficiencies for dissolution of soluble copper anodes at 30°C using short pulsed electrolysis (1000Hz) at various anode current densities.

Copper Anodes 30°C (Pulsed @1000Hz)				
Test Number.	Current Density mA cm^{-2}	Test Duration (minutes)	Anode Weight Loss(g)	Efficiency %
35	5	120	0.2515	106.2
36	10	60	0.2562	108.1
37	20	30	0.2409	101.7
38	30	20	0.2457	103.7

Table 48.

The apparent anodic efficiencies for dissolution of soluble copper anodes at 40°C using short pulsed electrolysis (1000Hz) at various anode current densities.

Copper Anodes 40°C (Pulsed @1000Hz)				
Test Number.	Current Density mA cm^{-2}	Test Duration (minutes)	Anode Weight Loss(g)	Efficiency %
27	5	120	0.2519	106.4
28	10	60	0.2328	98.3
29	20	30	0.2570	108.5
30	30	20	0.2408	101.7

Table 49.

The apparent anodic efficiencies for dissolution of soluble copper anodes at 50°C using short pulsed electrolysis (1000Hz) at various anode current densities.

Copper Anodes 50°C (Pulsed @1000Hz)				
Test Number.	Current Density mA cm^{-2}	Test Duration (minutes)	Anode Weight Loss(g)	Efficiency %
39	5	120	0.2479	104.7
40	10	60	0.2471	104.3
41	20	30	0.2581	109
42	30	20	0.2507	105.9

Table 50.

The apparent anodic efficiencies for dissolution of soluble copper anodes at 60°C using short pulsed electrolysis (1000Hz) at various anode current densities.

Copper Anodes 60°C (Pulsed @1000Hz)				
Test Number.	Current Density mA cm^{-2}	Test Duration (minutes)	Anode Weight Loss(g)	Efficiency %
23	5	120	0.2568	108.4
24	10	60	0.2462	103.9
25	20	30	0.2340	98.8
26	30	20	0.2460	103.9

Table 51.

The apparent anodic efficiencies for dissolution of soluble copper anodes at 70°C using short pulsed electrolysis (1000Hz) at various anode current densities.

Copper Anodes 70°C (Pulsed @1000Hz)				
Test Number.	Current Density mA cm^{-2}	Test Duration (minutes)	Anode Weight Loss(g)	Efficiency %
31	5	120	0.2522	106.5
32	10	60	0.2461	103.9
33	20	30	0.2527	106.7
34	30	20	0.2451	106.5

Table 52.

The apparent anodic efficiencies for dissolution of soluble copper anodes at 30°C using long pulsed electrolysis (100Hz) at various anode current densities.

Copper Anodes 30°C (Pulsed @100Hz)				
Test Number.	Current Density mA cm^{-2}	Test Duration (minutes)	Anode Weight Loss(g)	Efficiency %
55	5	120	0.2434	102.8
56	10	60	0.2458	103.8
57	20	30	0.2540	107.2
58	30	20	0.2030	85.7

Table 53.

The apparent anodic efficiencies for dissolution of soluble copper anodes at 40°C using long pulsed electrolysis (100Hz) at various anode current densities.

Copper Anodes 40°C (Pulsed @100Hz)				
Test Number.	Current Density mA cm^{-2}	Test Duration (minutes)	Anode Weight Loss(g)	Efficiency %
47	5	120	0.2509	105.9
48	10	60	0.2479	104.7
49	20	30	0.2443	103.1
50	30	20	0.2422	102.2

Table 54.

The apparent anodic efficiencies for dissolution of soluble copper anodes at 50°C using long pulsed electrolysis (100Hz) at various anode current densities.

Copper Anodes 50°C (Pulsed @100Hz)				
Test Number.	Current Density mA cm^{-2}	Test Duration (minutes)	Anode Weight Loss(g)	Efficiency %
59	5	120	0.2516	106.3
60	10	60	0.2491	105.2
61	20	30	0.2434	102.8
62	30	20	0.2517	106.3

Table 55.

The apparent anodic efficiencies for dissolution of soluble copper anodes at 60°C using long pulsed electrolysis (100Hz) at various anode current densities.

Copper Anodes 60°C (Pulsed @100Hz)				
Test Number.	Current Density mA cm^{-2}	Test Duration (minutes)	Anode Weight Loss(g)	Efficiency %
43	5	120	0.2493	105.3
44	10	60	0.2450	103.5
45	20	30	0.2414	101.9
46	30	20	0.2388	100.8

Table 56.
The apparent anodic efficiencies for dissolution of soluble copper anodes at 70°C using long pulsed electrolysis (100Hz) at various anode current densities.

Copper Anodes 70°C (Pulsed @100Hz)				
Test Number.	Current Density mA cm^{-2}	Test Duration (minutes)	Anode Weight Loss(g)	Efficiency %
51	5	120	0.2562	111.9
52	10	60	0.2496	105.4
53	20	30	0.2460	103.8
54	30	20	0.2428	102.5

Table 57.
The apparent anodic efficiencies for dissolution of soluble bronze anodes at 30°C using conventional current electrolysis at various anode current densities.

Bronze Anodes 30°C (D.C)				
Test Number.	Current Density mA cm^{-2}	Test Duration (minutes)	Anode Weight Loss(g)	Efficiency %
BA19	5	120	0.2376	111.63
BA18	10	60	0.0554	26.02
BA21	20	30	−	−
BA20	30	20	−	−

Table 58.

The apparent anodic efficiencies for dissolution of soluble bronze anodes at 40°C using conventional current electrolysis at various anode current densities.

Bronze Anodes 40°C (D.C)				
Test Number.	Current Density mA cm^{-2}	Test Duration (minutes)	Anode Weight Loss(g)	Efficiency %
BA11	5	120	0.2430	114
BA10	10	60	0.2328	109.32
BA13	20	30	0.0819	38.41
BA12	30	20	0.0270	12.69

Table 59.

The apparent anodic efficiencies for dissolution of soluble bronze anodes at 50°C using conventional current electrolysis at various anode current densities.

Bronze Anodes 50°C (D.C)				
Test Number.	Current Density mA cm^{-2}	Test Duration (minutes)	Anode Weight Loss(g)	Efficiency %
BA2	5	120	0.2306	117
BA1	10	60	0.2509	108.43
BA4	20	30	0.2254	105.88
BA3	30	20	0.0477	22.35

Table 60.

The apparent anodic efficiencies for dissolution of soluble bronze anodes at 60°C using conventional current electrolysis at various anode current densities.

Bronze Anodes 60°C (D.C)				
Test Number.	Current Density mA cm^{-2}	Test Duration (minutes)	Anode Weight Loss(g)	Efficiency %
BA7	5	120	0.2458	115.48
BA6	10	60	0.2361	110.9
BA9	20	30	0.2274	106.85
BA8	30	20	0.2124	99.8

Table 61.

The apparent anodic efficiencies for dissolution of soluble bronze anodes at 70°C using conventional current electrolysis at various anode current densities.

Bronze Anodes 70°C (D.C)				
Test Number.	Current Density mA cm^{-2}	Test Duration (minutes)	Anode Weight Loss(g)	Efficiency %
BA15	5	120	0.2419	113.6
BA14	10	60	0.2424	113.8
BA17	20	30	0.2065	97.02
BA16	30	20	0.1180	55.45

Table 62.
The apparent anodic efficiencies for dissolution of soluble bronze anodes at 30°C using short pulsed electrolysis (1000Hz) at various anode current densities.

Bronze Anodes 30°C (Pulsed@1000Hz)				
Test Number.	Current Density mA cm^{-2}	Test Duration (minutes)	Anode Weight Loss(g)	Efficiency %
PBA14	5	120	0.2292	107.6
PBA13	10	60	0.2259	106.1
PBA16	20	30	0.004	1.88
PBA15	30	20	–	–

Table 63.
The apparent anodic efficiencies for dissolution of soluble bronze anodes at 40°C using short pulsed electrolysis (1000Hz) at various anode current densities.

Bronze Anodes 40°C (Pulsed@1000Hz)				
Test Number.	Current Density mA cm^{-2}	Test Duration (minutes)	Anode Weight Loss(g)	Efficiency %
PBA6	5	120	0.2430	114.2
PBA5	10	60	0.2236	105.1
PBA8	20	30	0.0636	29.8
PBA7	30	20	0.0030	1.4

<u>Table 64.</u>
The apparent anodic efficiencies for dissolution of soluble
bronze anodes at 50°C using short pulsed electrolysis (1000Hz)
at various anode current densities.

Bronze Anodes 50°C (Pulsed@1000Hz)				
Test Number.	Current Density mA cm^{-2}	Test Duration (minutes)	Anode Weight Loss(g)	Efficiency %
PBA18	5	120	0.2540	119.3
PBA17	10	60	0.2342	110.01
PBA20	20	30	0.2096	98.6
PBA19	30	20	0.0108	5.1

<u>Table 65.</u>
The apparent anodic efficiencies for dissolution of soluble
bronze anodes at 60°C using short pulsed electrolysis (1000Hz)
at various anode current densities.

Bronze Anodes 60°C (Pulsed@1000Hz)				
Test Number.	Current Density mA cm^{-2}	Test Duration (minutes)	Anode Weight Loss(g)	Efficiency %
PBA2	5	120	0.2600	122.18
PBA1	10	60	0.2378	111.95
PBA4	20	30	0.2290	107.67
PBA3	30	20	0.2090	97.36

Table 66.

The apparent anodic efficiencies for dissolution of soluble bronze anodes at 70°C using short pulsed electrolysis (1000Hz) at various anode current densities.

Bronze Anodes 70°C (Pulsed@1000Hz)				
Test Number.	Current Density mA cm^{-2}	Test Duration (minutes)	Anode Weight Loss(g)	Efficiency %
PBA10	5	120	0.2622	122.9
PBA9	10	60	0.2377	111.7
PBA12	20	30	0.2267	106.45
PBA11	30	20	0.2216	113.84

Table 67.

The apparent anodic efficiencies for dissolution of soluble bronze anodes at 30°C using long pulsed electrolysis (100Hz) at various anode current densities.

Bronze Anodes 30°C (Pulsed@100Hz)				
Test Number.	Current Density mA cm^{-2}	Test Duration (minutes)	Anode Weight Loss(g)	Efficiency %
PBA34	5	120	0.2214	104.04
PBA33	10	60	0.0559	26.28
PBA36	20	30	0.0044	2.05
PBA35	30	20	–	–

Table 68.

The apparent anodic efficiencies for dissolution of soluble bronze anodes at 40°C using long pulsed electrolysis (100Hz) at various anode current densities.

Bronze Anodes 40°C (Pulsed@100Hz)				
Test Number.	Current Density mA cm^{-2}	Test Duration (minutes)	Anode Weight Loss(g)	Efficiency %
PBA26	5	120	0.2419	113.66
PBA25	10	60	0.0847	39.78
PBA28	20	30	0.0396	18.63
PBA27	30	20	0.0106	5.03

Table 69.

The apparent anodic efficiencies for dissolution of soluble bronze anodes at 50°C using long pulsed electrolysis (100Hz) at various anode current densities.

Bronze Anodes 50°C (Pulsed@100Hz)				
Test Number.	Current Density mA cm^{-2}	Test Duration (minutes)	Anode Weight Loss(g)	Efficiency %
PBA38	5	120	0.2591	121.78
PBA37	10	60	0.2260	106.21
PBA40	20	30	0.0670	31.09
PBA39	30	20	0.0058	2.73

Table 70.

The apparent anodic efficiencies for dissolution of soluble bronze anodes at 60°C using long pulsed electrolysis (100Hz) at various anode current densities.

Bronze Anodes 60°C (Pulsed@100Hz)				
Test Number.	Current Density mA cm^{-2}	Test Duration (minutes)	Anode Weight Loss(g)	Efficiency %
PBA22	5	120	0.2586	121.5
PBA21	10	60	0.2363	111.05
PBA24	20	30	0.2132	100.21
PBA23	30	20	0.1023	48.06

Table 71.

The apparent anodic efficiencies for dissolution of soluble bronze anodes at 70°C using long pulsed electrolysis (100Hz) at various anode current densities.

Bronze Anodes 70°C (Pulsed@100Hz)				
Test Number.	Current Density mA cm^{-2}	Test Duration (minutes)	Anode Weight Loss(g)	Efficiency %
PBA30	5	120	0.2370	111.4
PBA29	10	60	0.2369	111.3
PBA32	20	30	0.2257	106.03
PBA31	30	20	0.2160	101.54

Table 72.

The apparent anodic efficiencies for dissolution of soluble tin anodes at 40°C using conventional current electrolysis at various anode current densities.

Tin Anodes 40°C (D.C)				
Test Number.	Current Density mA cm^{-2}	Test Duration (minutes)	Anode Weight Loss(g)	Efficiency %
TIN10	15	40	0.0033	2.98
TIN12	17.5	34.3	0.0002	1.8
TIN9	20	30	-	-
TIN11	25	24	-	-

Table 73.

The apparent anodic efficiencies for dissolution of soluble tin anodes at 50°C using conventional current electrolysis at various anode current densities.

Tin Anodes 50°C (D.C)				
Test Number.	Current Density mA cm^{-2}	Test Duration (minutes)	Anode Weight Loss(g)	Efficiency %
TIN14	15	40	0.0110	9.94
TIN16	17.5	34.3	0.0072	6.5
TIN13	20	30	-	-
TIN15	25	24	-	-

Table 74.
The apparent anodic efficiencies for dissolution of soluble tin anodes at 60°C using conventional current electrolysis at various anode current densities.

Tin Anodes 60°C (D.C)				
Test Number.	Current Density mA cm^{-2}	Test Duration (minutes)	Anode Weight Loss(g)	Efficiency %
TIN2	15	40	0.0326	29.45
TIN4	17.5	34.3	0.0276	24.93
TIN1	20	30	0.0165	14.9
TIN3	25	24	0.0133	12.0

Table 75.
The apparent anodic efficiencies for dissolution of soluble tin anodes at 70°C using conventional current electrolysis at various anode current densities.

Tin Anodes 70°C (D.C)				
Test Number.	Current Density mA cm^{-2}	Test Duration (minutes)	Anode Weight Loss(g)	Efficiency %
TIN6	15	40	0.0538	48.7
TIN8	17.5	34.3	0.0590	53.3
TIN5	20	30	0.0347	31.3
TIN7	25	24	0.0348	31.4

Table 76.
The apparent anodic efficiencies for dissolution of soluble tin
anodes at 40°C using short pulsed electrolysis (1000Hz) at
various anode current densities.

Tin Anodes 40°C (Pulsed@1000Hz)				
Test Number.	Current Density mA cm^{-2}	Test Duration (minutes)	Anode Weight Loss(g)	Efficiency %
TIN29	15	40	0.0037	3.34
TIN31	17.5	34.3	0.0014	1.26
TIN30	20	30	0.0012	1.08
TIN32	25	24	-	-

Table 77.
The apparent anodic efficiencies for dissolution of soluble tin
anodes at 50°C using short pulsed electrolysis (1000Hz) at
various anode current densities.

Tin Anodes 50°C (Pulsed@1000Hz)				
Test Number.	Current Density mA cm^{-2}	Test Duration (minutes)	Anode Weight Loss(g)	Efficiency %
TIN25	15	40	0.2215	200
TIN27	17.5	34.3	0.0131	11.8
TIN26	20	30	0.0107	9.66
TIN28	25	24	0.0075	6.78

Table 78.
The apparent anodic efficiencies for dissolution of soluble tin anodes at 60°C using short pulsed electrolysis (1000Hz) at various anode current densities.

Tin Anodes 60°C (Pulsed@1000Hz)				
Test Number.	Current Density mA cm^{-2}	Test Duration (minutes)	Anode Weight Loss(g)	Efficiency %
TIN17	15	40	0.2240	202
TIN19	17.5	34.3	0.0270	24.4
TIN18	20	30	0.0251	22.7
TIN20	25	24	0.0166	15.0

Table 79.
The apparent anodic efficiencies for dissolution of soluble tin anodes at 70°C using short pulsed electrolysis (1000Hz) at various anode current densities.

Tin Anodes 70°C (Pulsed@1000Hz)				
Test Number.	Current Density mA cm^{-2}	Test Duration (minutes)	Anode Weight Loss(g)	Efficiency %
TIN21	15	40	0.2254	203
TIN23	17.5	34.3	0.0484	43.7
TIN22	20	30	0.0482	43.5
TIN24	25	24	0.0278	25.1

Table 80.

The apparent anodic efficiencies for dissolution of soluble tin anodes at 40°C using long pulsed electrolysis (100Hz) at various anode current densities.

Tin Anodes 40°C (Pulsed@100Hz)				
Test Number.	Current Density mA cm^{-2}	Test Duration (minutes)	Anode Weight Loss(g)	Efficiency %
TIN33	15	40	0.0044	3.97
TIN35	17.5	34.3	0.0008	0.09
TIN34	20	30	0.001	0.09
TIN36	25	24	-	Passivated

Table 81.

The apparent anodic efficiencies for dissolution of soluble tin anodes at 50°C using long pulsed electrolysis (100Hz) at various anode current densities.

Tin Anodes 50°C (Pulsed@100Hz)				
Test Number.	Current Density mA cm^{-2}	Test Duration (minutes)	Anode Weight Loss(g)	Efficiency %
TIN37	15	40	0.0053	4.79
TIN39	17.5	34.3	-	Passivated
TIN38	20	30	-	Passivated
TIN40	25	24	-	Passivated

Table 82.

The apparent anodic efficiencies for dissolution of soluble tin anodes at 60°C using long pulsed electrolysis (100Hz) at various anode current densities.

Tin Anodes 60°C(Pulsed@100Hz)				
Test Number.	Current Density mA cm^{-2}	Test Duration (minutes)	Anode Weight Loss(g)	Efficiency %
TIN41	15	40	All anodes passivated	
TIN43	17.5	34.3		
TIN42	20	30		
TIN44	25	24		

Table 83.

The apparent anodic efficiencies for dissolution of soluble tin anodes at 70°C using long pulsed electrolysis (100Hz) at various anode current densities.

Tin Anodes 70°C(Pulsed@100Hz)				
Test Number.	Current Density mA cm^{-2}	Test Duration (minutes)	Anode Weight Loss(g)	Efficiency %
TIN41	15	40	All anodes passivated	
TIN43	17.5	34.3		
TIN42	20	30		
TIN44	25	24		

Table 84.

The apparent and true efficiencies of soluble copper and bronze anodes determined from bagged anodic tests at 60°C using conventional current electrolysis at 10mA cm^{-2} anode current density.

Bagged Anodic Tests at 60°C				
Anode Material	Weight Lost (g)	Apparent Efficiency (%)	Total Metal in Bag (g)	True Efficiency (%)
Copper	0.7470	105	0.065	95.85
Bronze	0.6129	96	0.052	87.92

Table 85.

The effect upon deposit composition of using increasingly diluted plating solutions of 15, 25 and 35% dilution. Deposits obtained from solutions at 60°C using conventional and pulsed electrolyses at 20mA cm^{-2} average cathode current density.

Diluted Plating Solutions at 60°C				
Test Number	Dilution %	Current Density mA cm^{-2}	Frequency (Hz)	Weight % Tin
DS15DC	15	20	D.C	3.35
DS15SP	15	20	1000	3.15
DS15LP	15	20	100	1.55
DS25DC	25	20	D.C	3.5
DS25SP	25	20	1000	3.0
DS25LP	25	20	100	1.45
DS35DC	35	20	D.C	3.3
DS35SP	35	20	1000	2.85
DS35LP	35	20	100	1.33

Table 86.

The effect upon deposit composition of using increasingly diluted plating solutions of 15, 25 and 35% dilution with cyanide to hydroxide ratios adjusted to that in the basic plating solution. Deposits obtained from baths at 60°C using conventional and pulsed electrolyses at 20mA cm^{-2} average cathode current density.

Adjusted Diluted Plating Solutions at 60°C				
Test Number	Dilution %	Current Density mA cm^{-2}	Frequency (Hz)	Weight % Tin
CD15DC	15	20	D.C	3.80
CD15SP	15	20	1000	3.06
CD15LP	15	20	100	1.55
CD25DC	25	20	D.C	3.5
CD25SP	25	20	1000	2.93
CD25LP	25	20	100	1.50
CD35DC	35	20	D.C	3.25
CD35SP	35	20	1000	2.65
CD35LP	35	20	100	1.55

Table 87.

The effect upon deposit composition of replacing 15mol% copper in the basic plating solution with zinc. Deposits obtained from baths at 60°C and 70°C using conventional and short pulsed electrolyses at an average cathode current density of 20mA cm^{-2}.

Zinc Bronze Platiing Solution					
Test Number	Frequency (Hz)	Current Density mA cm^{-2}	(°C)	Weight % Zinc	Weight % Tin
ZDC2	D.C	20	70	1.7	22.7
ZSP2	1000	20	70	0.9	18.5
ZDC1	D.C	20	60	1.2	18.7
ZSP1	1000	20	60	0.8	15.0

Table 88.
The effect upon deposit composition of using the zinc - bronze plating solution diluted by 25%. Deposits obtained from baths at 60°C and 70°C using conventional and short pulsed electrolyses at an average cathode current density of 20mA cm^{-2}.

Diluted Zinc Bronze Platiing Solution					
Test Number	Frequency (Hz)	Current Density mA cm^{-2}	(°C)	Weight % Zinc	Weight % Tin
DZDC2	D.C	20	70	1.7	13.1
DZSP2	1000	20	70	1.5	12.7
DZDC1	D.C	20	60	1.6	14.0
DZSP1	1000	20	60	1.6	13.1

Table 89.
The analyses of some commercially produced bronze deposits.

Analysis of Commercially Produced Bronzes					
Number	%Sn	%Cu	%Zn	%Ni	%Si
BA1	10.8	67.5	19.5	2.1	0.1
BA2	8.3	89.2	1.8	0.6	0.1
BA3	18.6	79.9	0.4	0.9	0.1
BA5	12.3	86.7	0.7	0.2	0.1

Table 90.
The calculated lattice parameter of bronze deposits as a function of deposit composition.

Weight % Tin	Lattice Parameter ($\overset{\circ}{A}$)
0.75	3.635
1.2	3.641
2.3	3.648
3.29	3.658
4.35	3.665
6.51	3.68
8.0	3.694
8.84	3.70
9.09	3.698
10.47	3.705
12.51	3.705

COPPER–TIN

Point °C. Sn, %	A 1083 0	B 798 13·5	C 798 22·0	D 798 25·5	E 755 25·9	F 755 27·0	G 755 30·6	H 586 15·8	I 586 24·6	J 586 25·4	K 520 15·8	L 520 27·0	M 520 32·4	N′ 200 1·2
Point °C. Sn, %	N 350 11·0	O 350 32·55	P 350 37·8	P′ 640 37·8	Q 676 38·3	R 640 34·2	S 640 35·2	T 590 31·6	U 590 32·3	V 590 33·1	W 582 32·9	X 582 34·1	Y 640 39·5	Z 415 38·3

Figure 1.
The Copper–Tin Thermal Equilibrium Diagram.
(After G.V.Raynor)
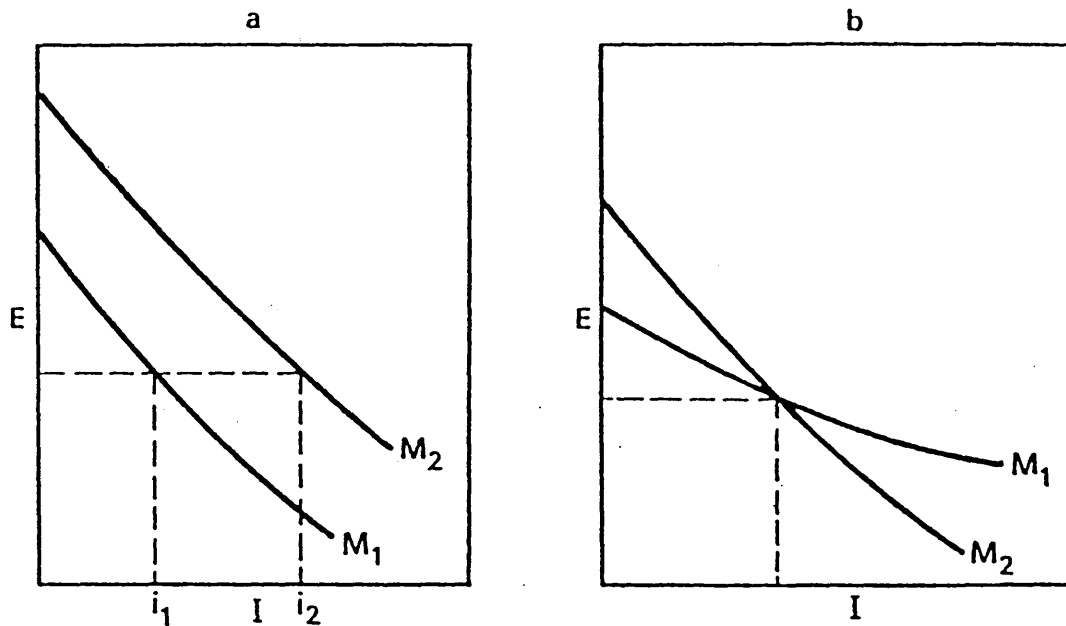
Figure 2.
Conditions of Polarization for co-deposition
of metals M_1 and M_2. (a) M_1 and M_2 having similar
E/i curves. (b) M_2 polarizing more than M_1.(2).
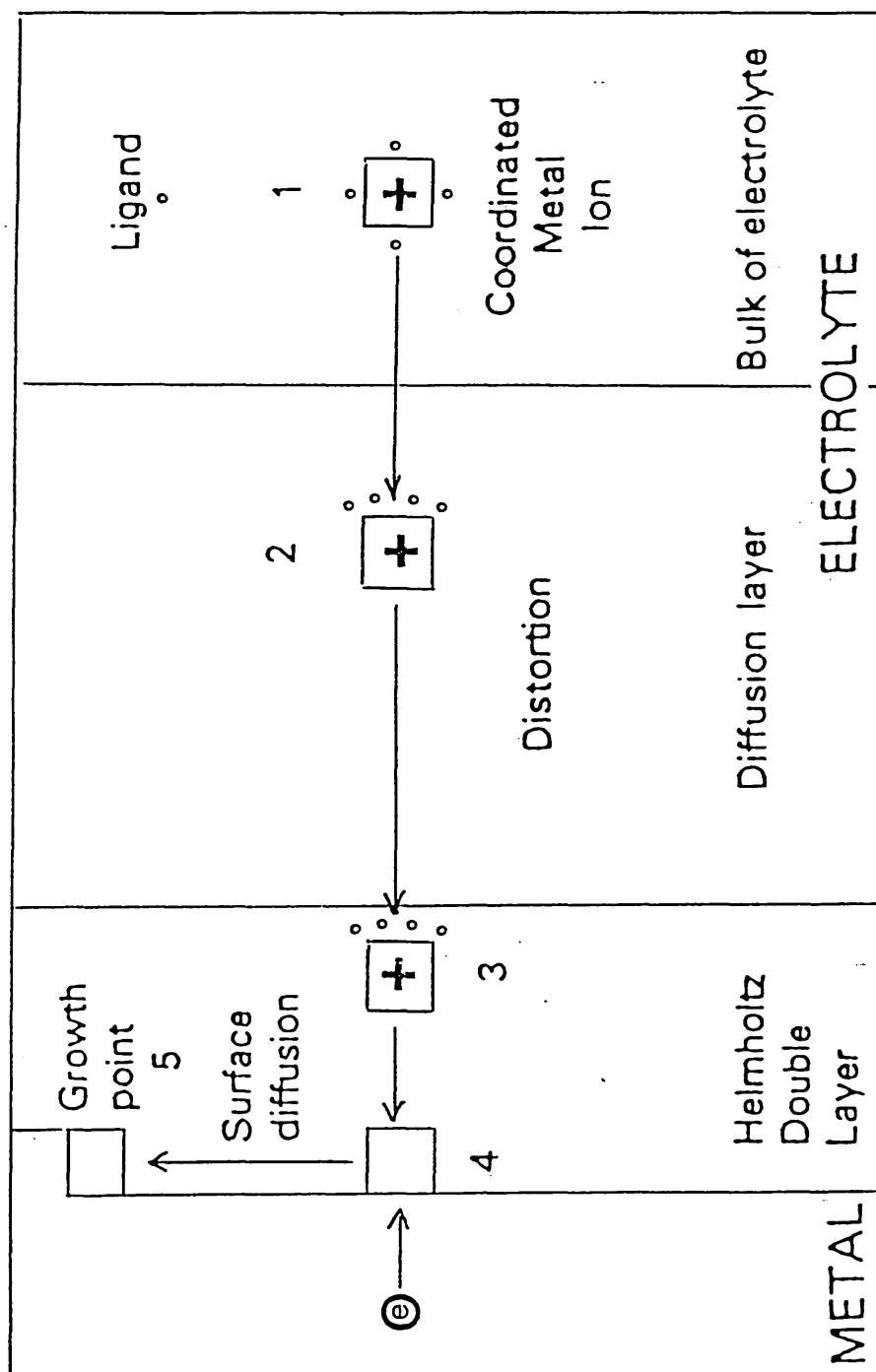
Figure 3.

Schematic representation of deposition process.
1. The metal ion in its ligand field.
2. The ligand field becomes distorted.
3. The metal ion is stripped from its ligand field.
4. The metal ion is neutralised.
5. The metal atom migrates to the nearest growth point.
(After H.Gerischer)

UNIPOLAR

Pulse

T_{on} T_{off}

j_p

0

Superimposed Pulse

T_{on} T_{off}

j_p

0 j_b

Duplex Pulse

T_1 T_2

$T_{on(1)}$ $T_{off(1)}$ $T_{on(2)}$ $T_{off(2)}$

$j_{p(1)}$ $j_{p(2)}$

0

Pulsed Pulse

T_{on} T_{off} T' T

j_p

0

Pulse-On-Pulse

T_{on} T_{off} T' T

j_p

j_b

0

BIPOLAR

Pulse Reverse

$T_{on(c)}$ $T_{on(a)}$

$j_{p(c)}$

0

$j_{p(a)}$

Pulse Reverse (with off-time)

$T_{on(c)}$ $T_{on(a)}$ $T_{off(c)}$ $T_{off(a)}$

$j_{p(c)}$

0

$j_{p(a)}$

Pulsed Pulse Reverse

T_c T_a

$T_{on(c)}$ $T_{off(c)}$ $T_{on(a)}$ $T_{off(a)}$

$j_{p(c)}$

0

$j_{p(a)}$

Pulse-On-Pulse Reverse

T_c T'_c T_a T'_a

$T_{on(c)}$ $T_{off(c)}$ $T_{on(a)}$ $T_{off(a)}$

$j_{b(c)}$ $j_{p(c)}$

0

$j_{b(a)}$

$j_{p(a)}$

Figure 4.

Schematic representation and suggested nomenclature for some square wave modulated current systems, and definition of related parameters.(6).

- 160 -
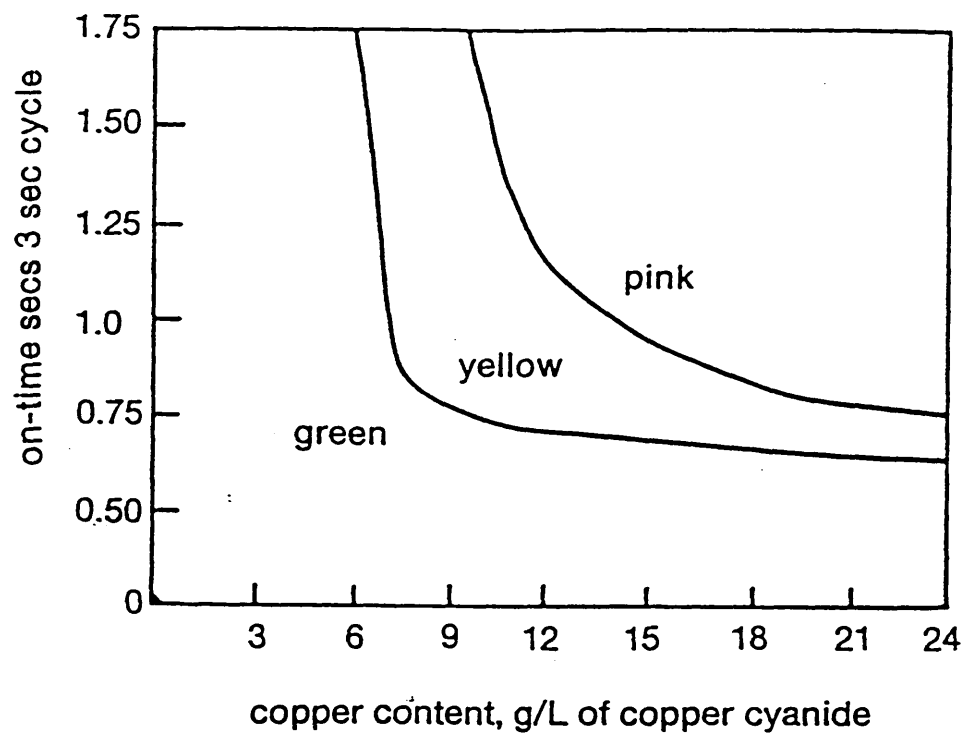
Figure 5.
The Influence of Copper content and Plating cycle on
the colour of Gold Deposits.(8).
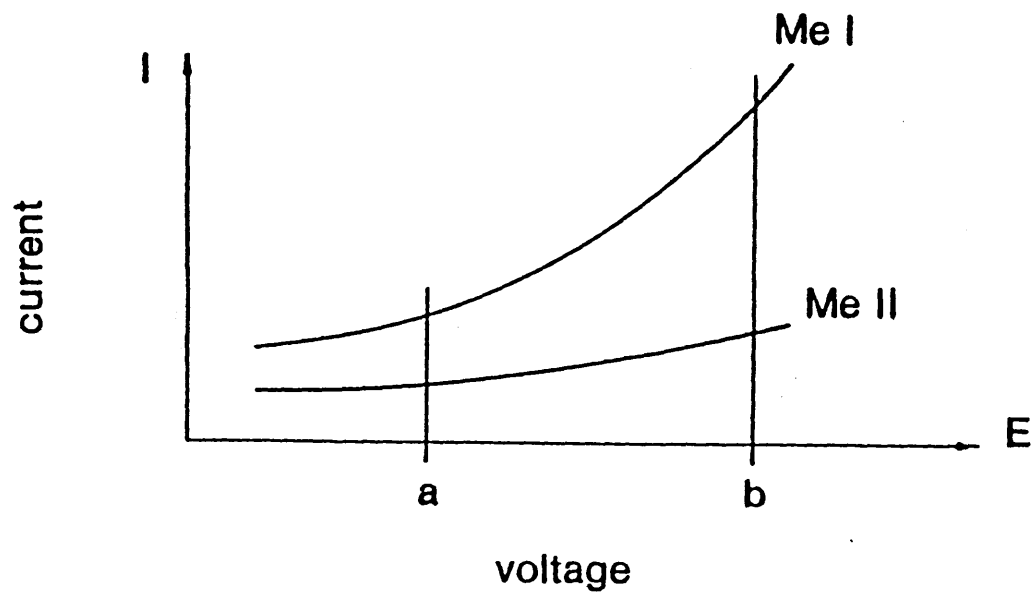
<u>Figure 6.</u>
Current-voltage curves for two competing reactions with
different kinetics. An increase in voltage from a to b
produces a change in current efficiency for reaction 1
(MeI) and reaction 2 (MeII). (6).

a) build-up of existing crystals
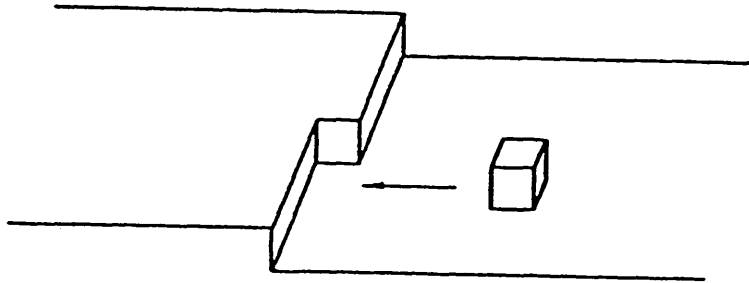
b) nucleation and formation of new crystals
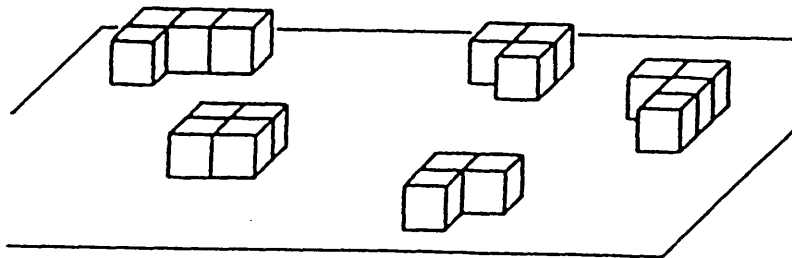
Figure 7.
Schematic representation of competing crystallisation mechanisms. (a) Growth of existing crystals. (b) Nucleation and formation of new crystals. (6).
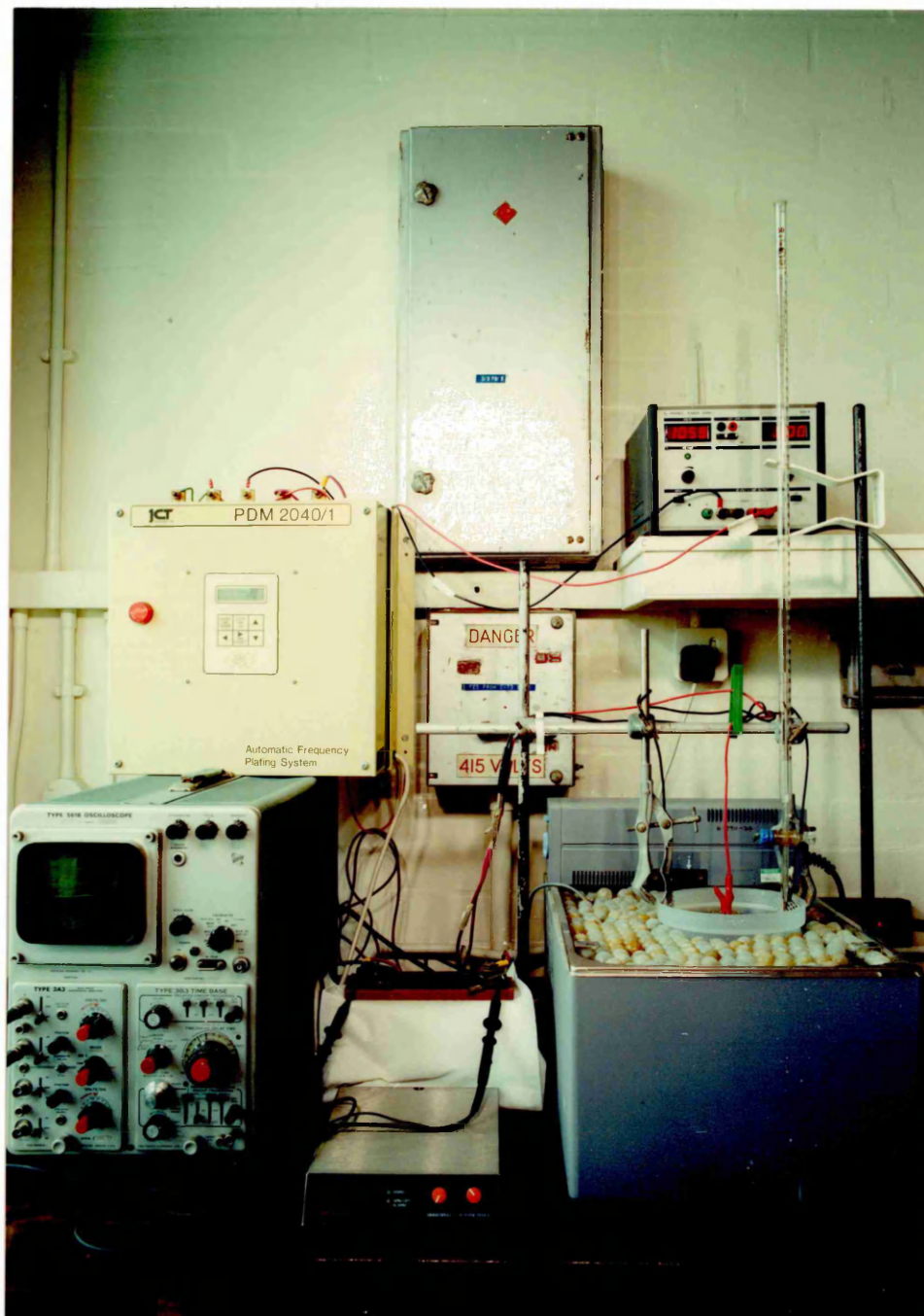
Figure 8.
Apparatus used for the production of bronze deposits.
(Original in Colour)
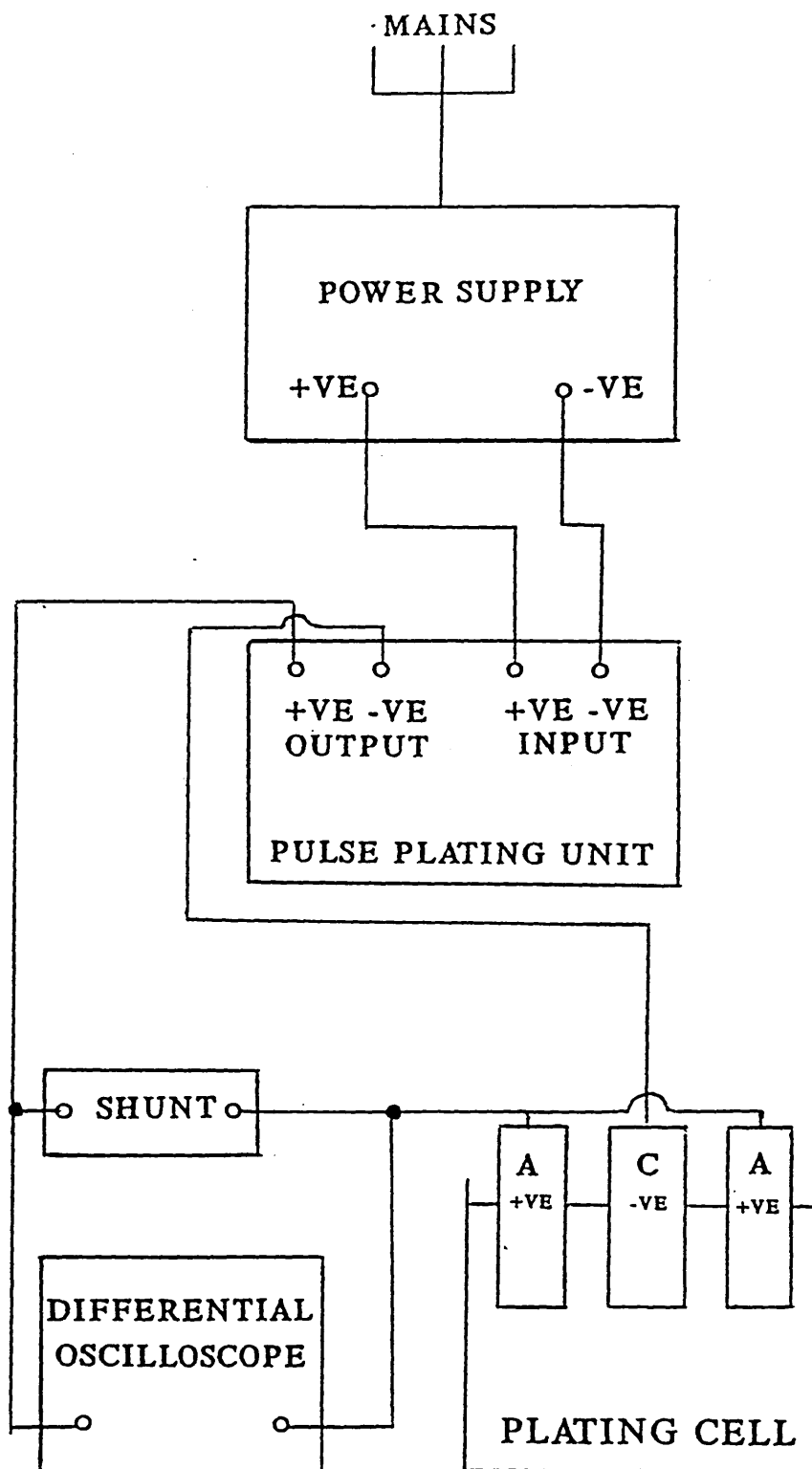
Figure 9.
Circuit diagram for the plating rig which was used to
produce bronze deposits.
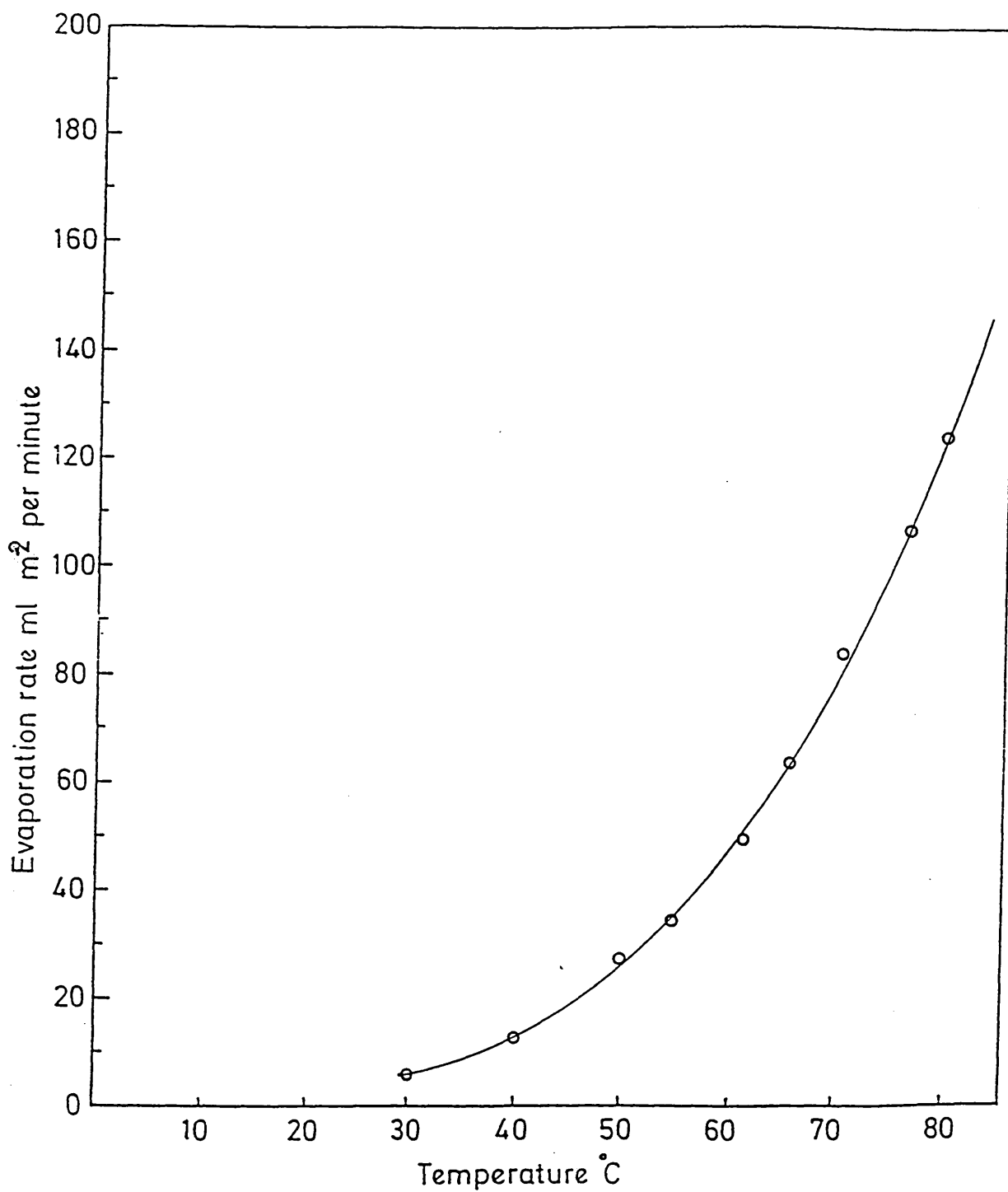
Figure 10.
Evaporation rate from a bronze plating bath at a
constant humidity as a function of bath temperature.
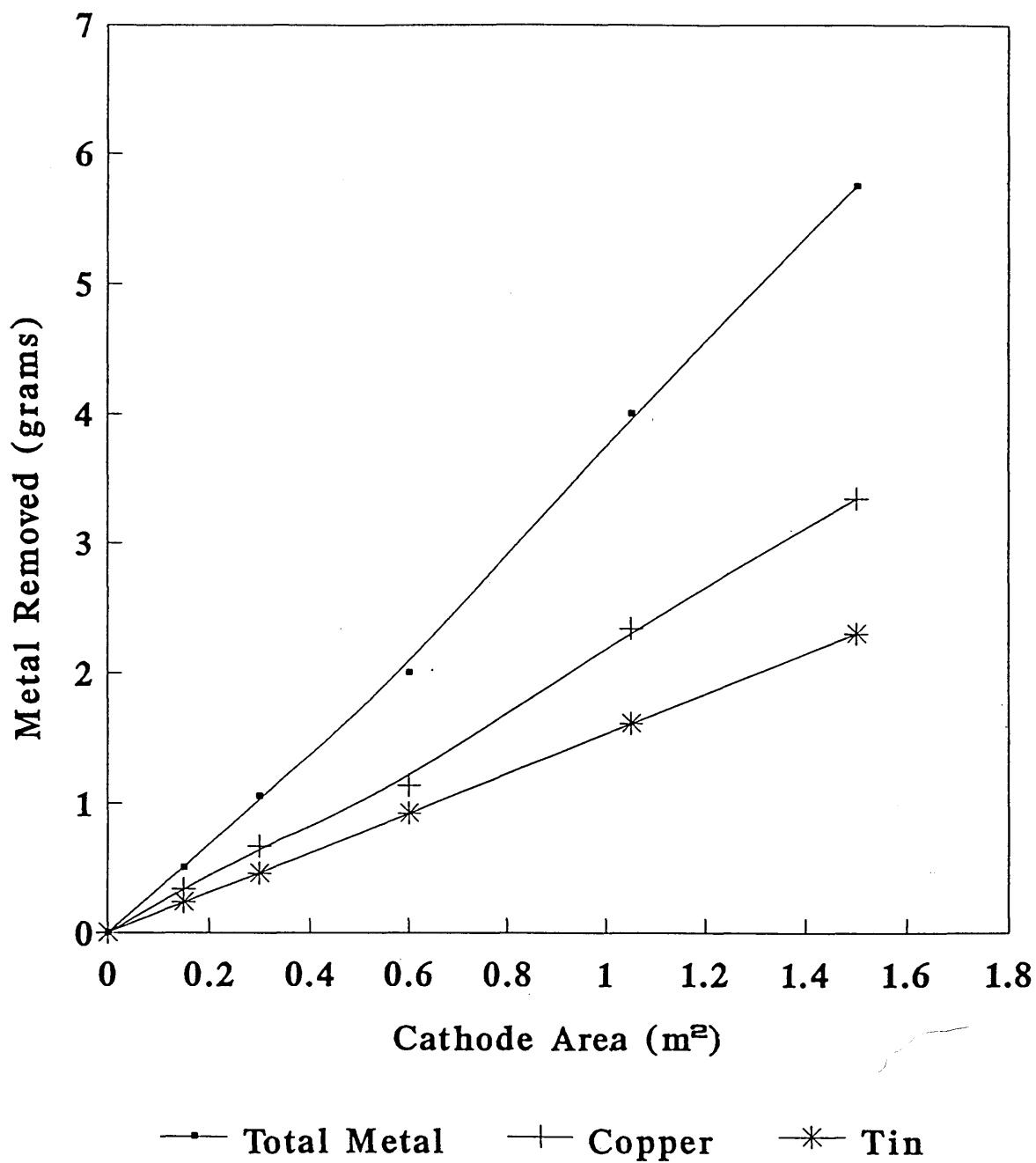
<u>Figure 11.</u>
The amount of metal removed from the basic bronze
plating solution at 70°C due to drag-out, as a function
of the cathode surface area removed.
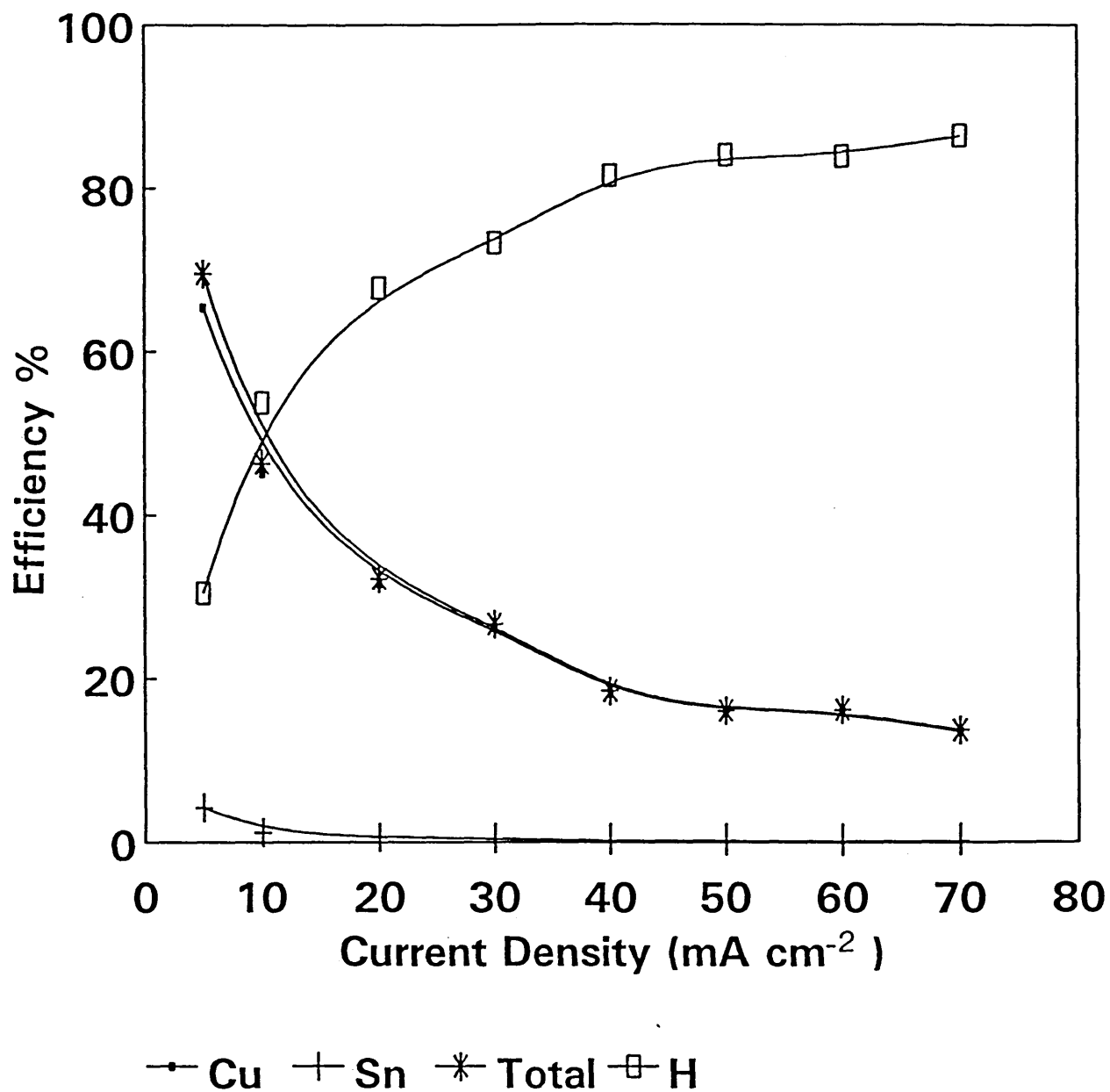
Figure 12.
The cathode current efficiencies for metal deposition
and hydrogen evolution as a function of cathode current
density. The deposits were obtained from a plating bath
operated at 30°C using conventional direct current and
inert anodes.
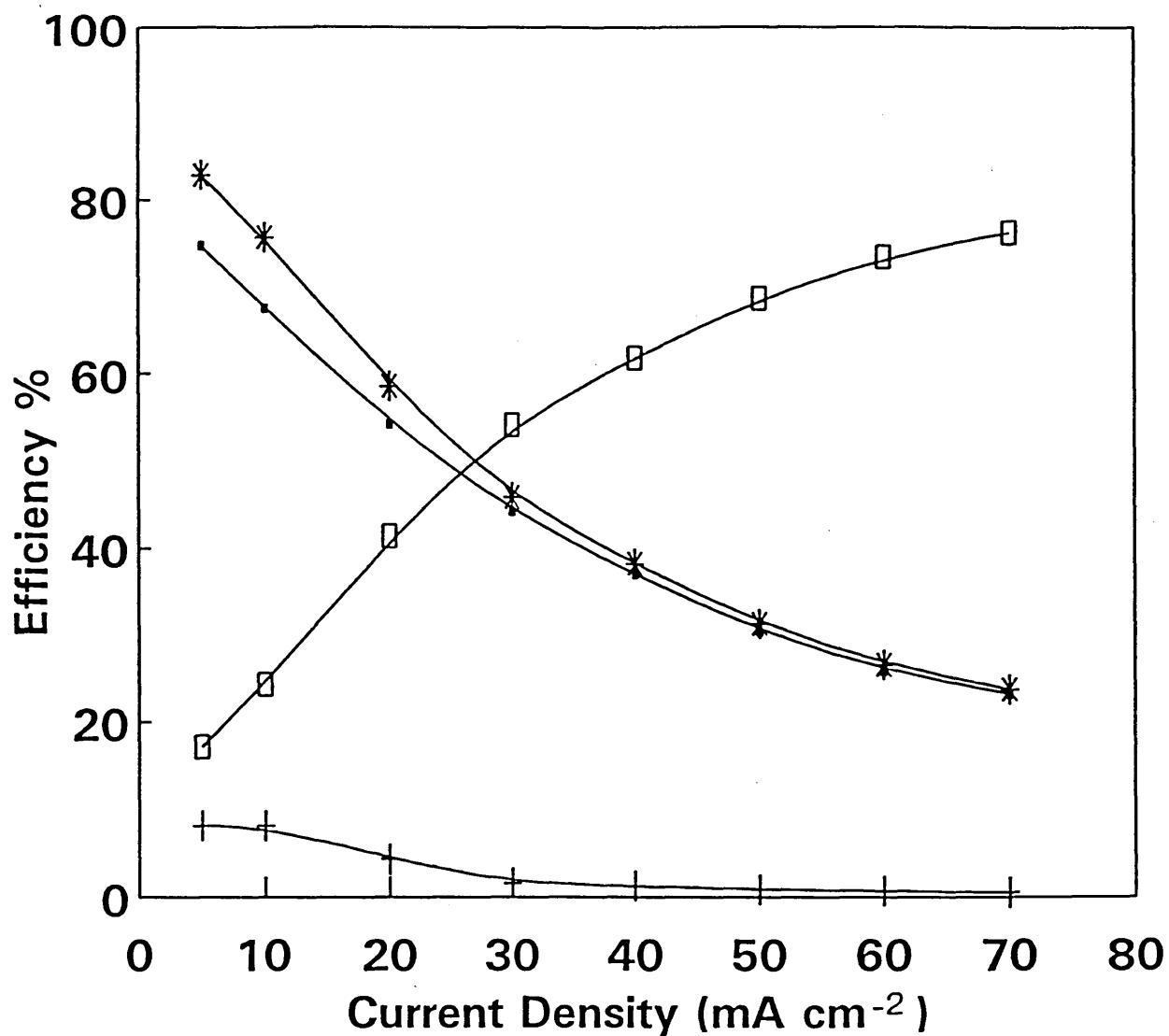
<u>Figure 13.</u>
The cathode current efficiencies for metal deposition
and hydrogen evolution as a function of cathode current
density. The deposits were obtained from a plating bath
operated at 40°C using conventional direct current and
inert anodes.
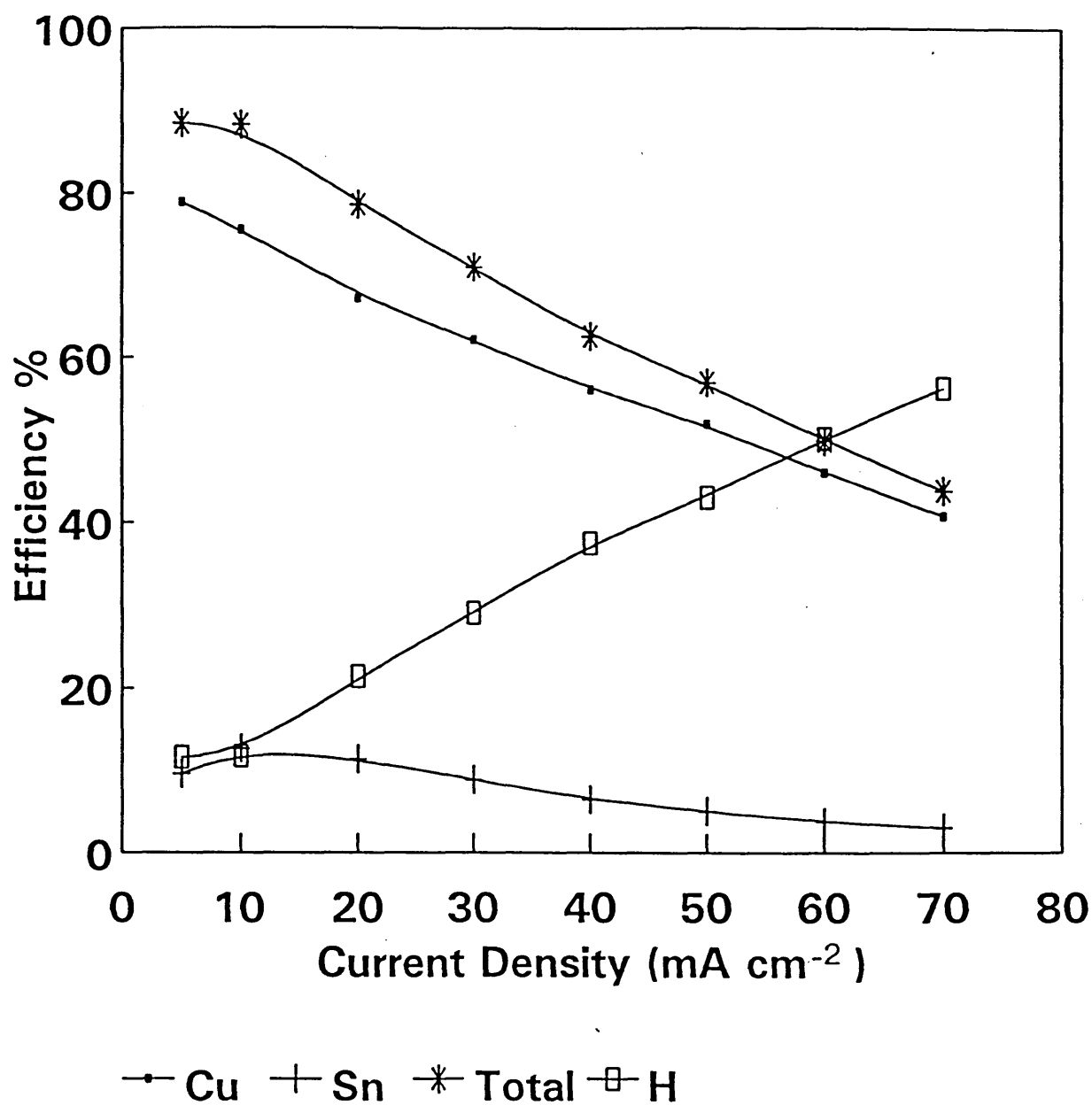
<u>Figure 14.</u>
The cathode current efficiencies for metal deposition and hydrogen evolution as a function of cathode current density. The deposits were obtained from a plating bath operated at 50°C using conventional direct current and inert anodes.
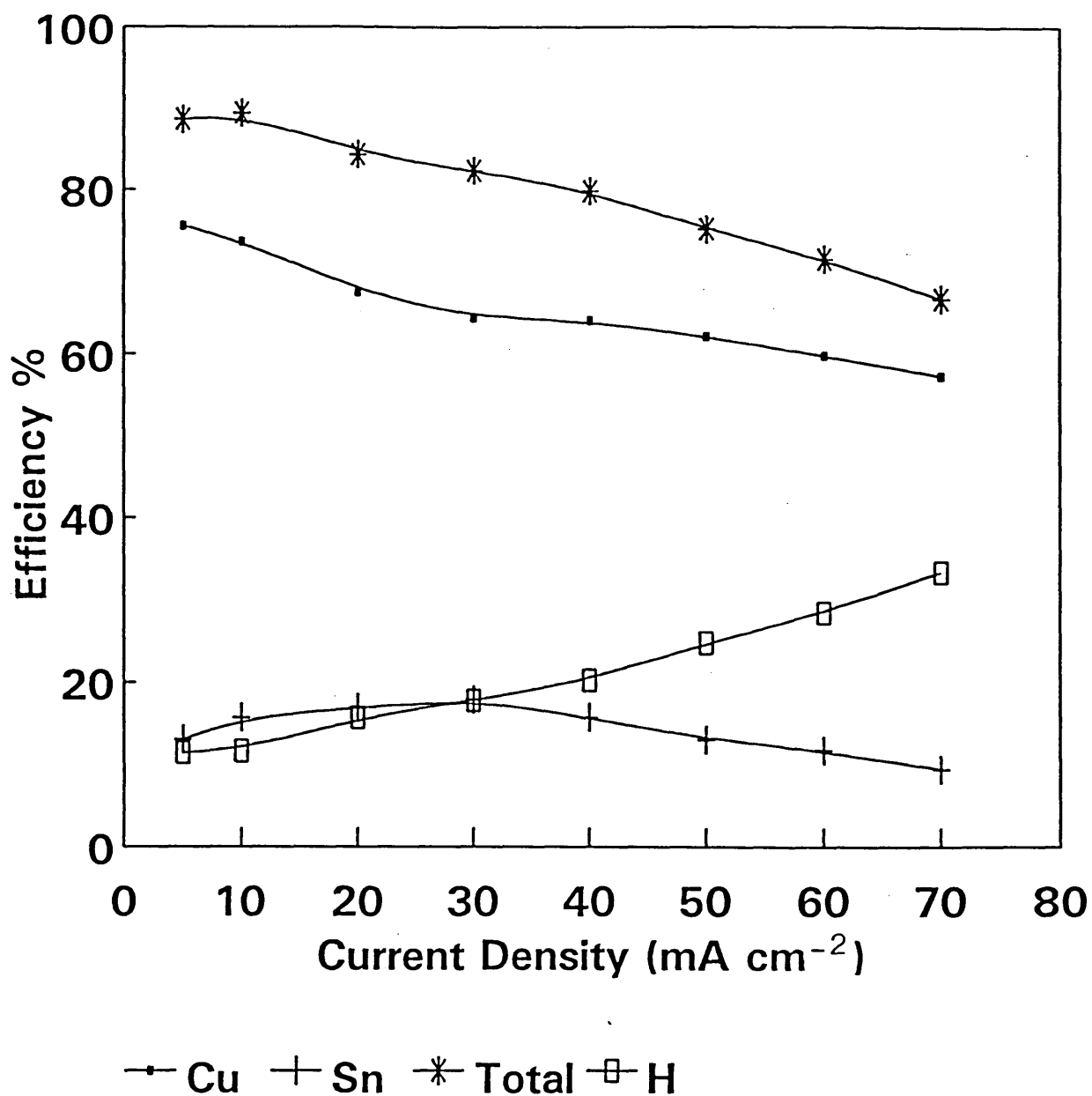
Figure 15.
The cathode current efficiencies for metal deposition
and hydrogen evolution as a function of cathode current
density. The deposits were obtained from a plating bath
operated at 60°C using conventional direct current and
inert anodes.
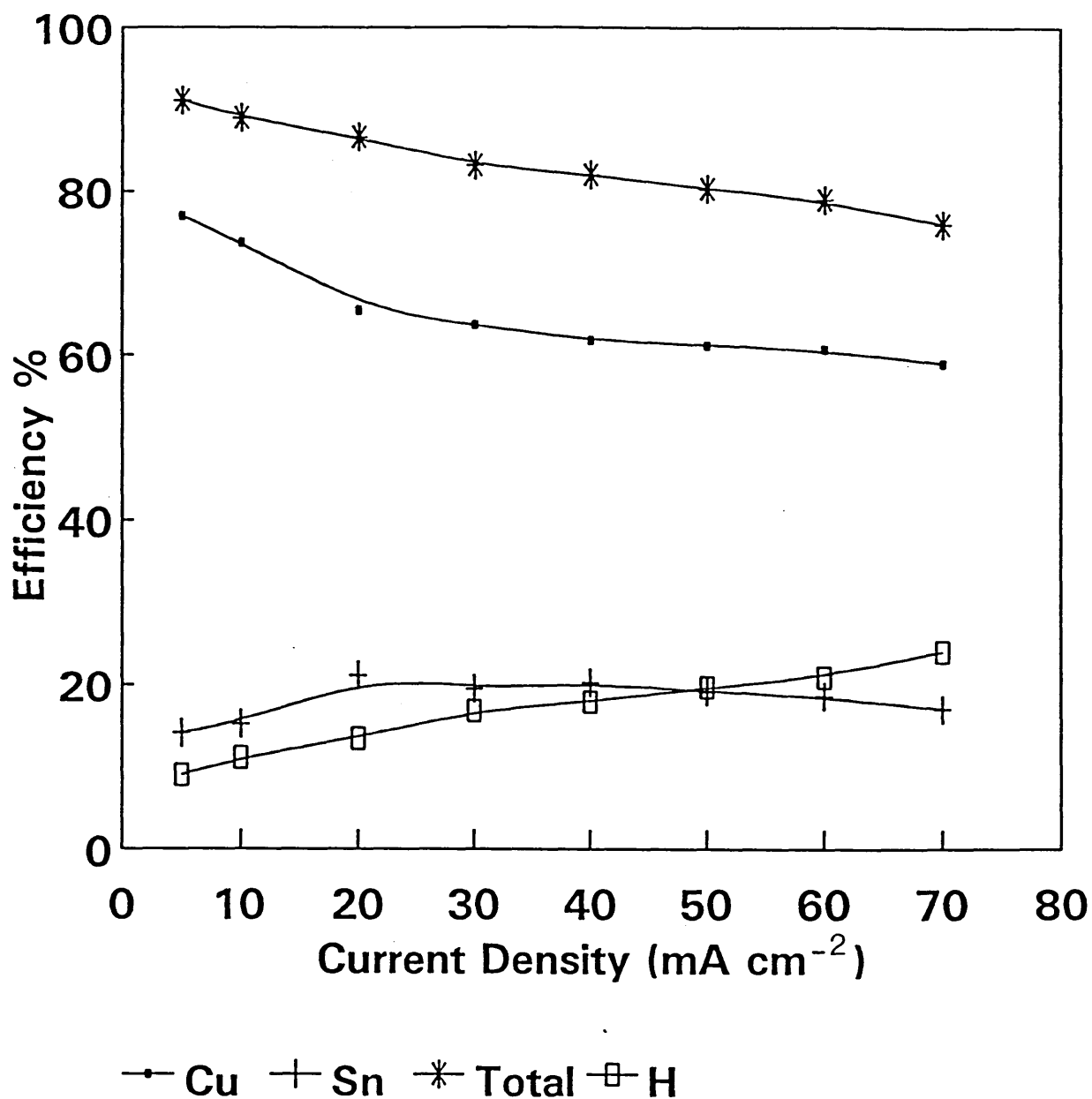
Figure 16.

The cathode current efficiencies for metal deposition and hydrogen evolution as a function of cathode current density. The deposits were obtained from a plating bath operated at 70°C using conventional direct current and inert anodes.
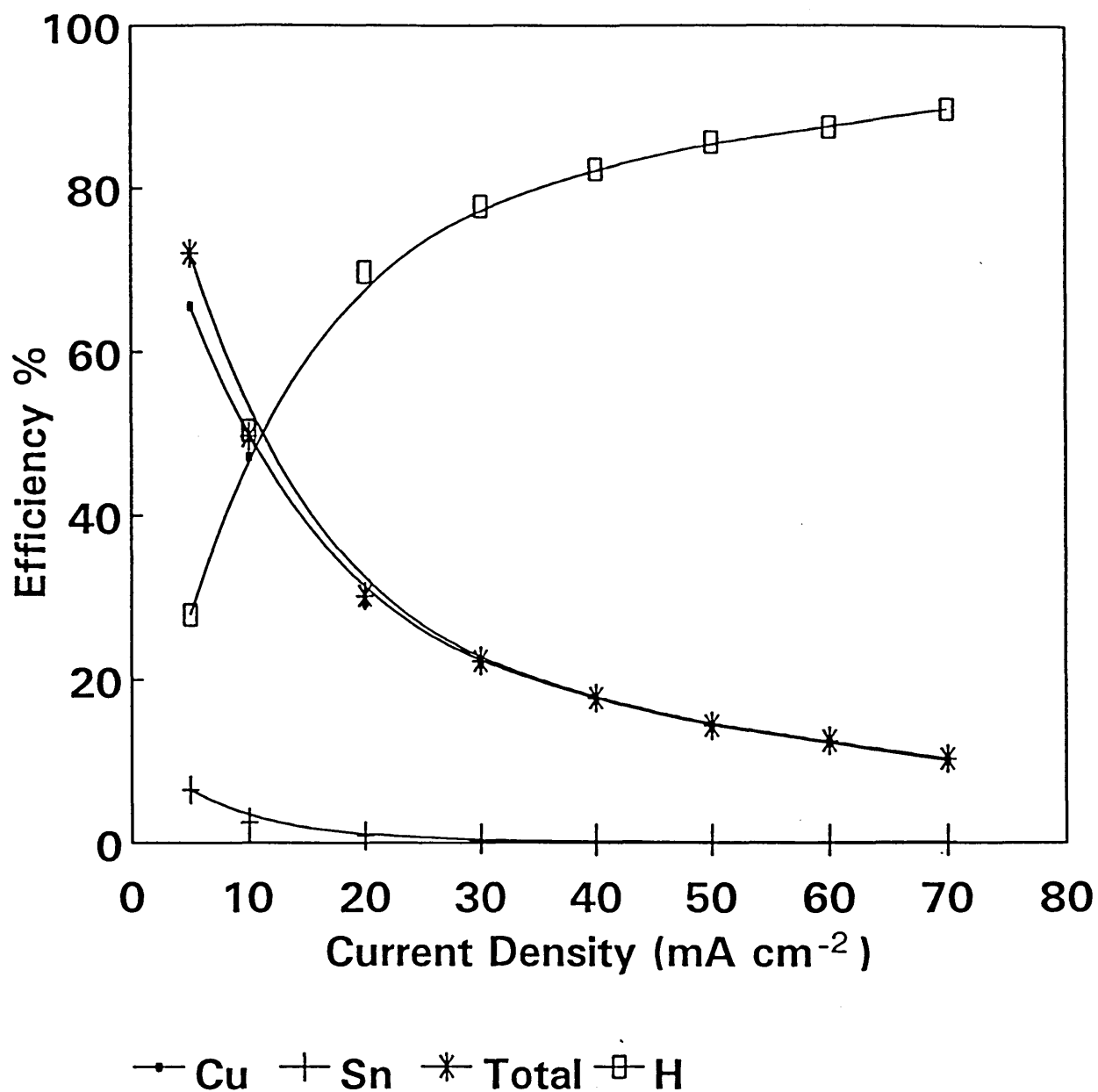
Figure 17.
The cathode current efficiencies for metal deposition
and hydrogen evolution as a function of cathode current
density. The deposits were obtained from a plating bath
operated at 30°C using short pulsed current (1000Hz)
and inert anodes.
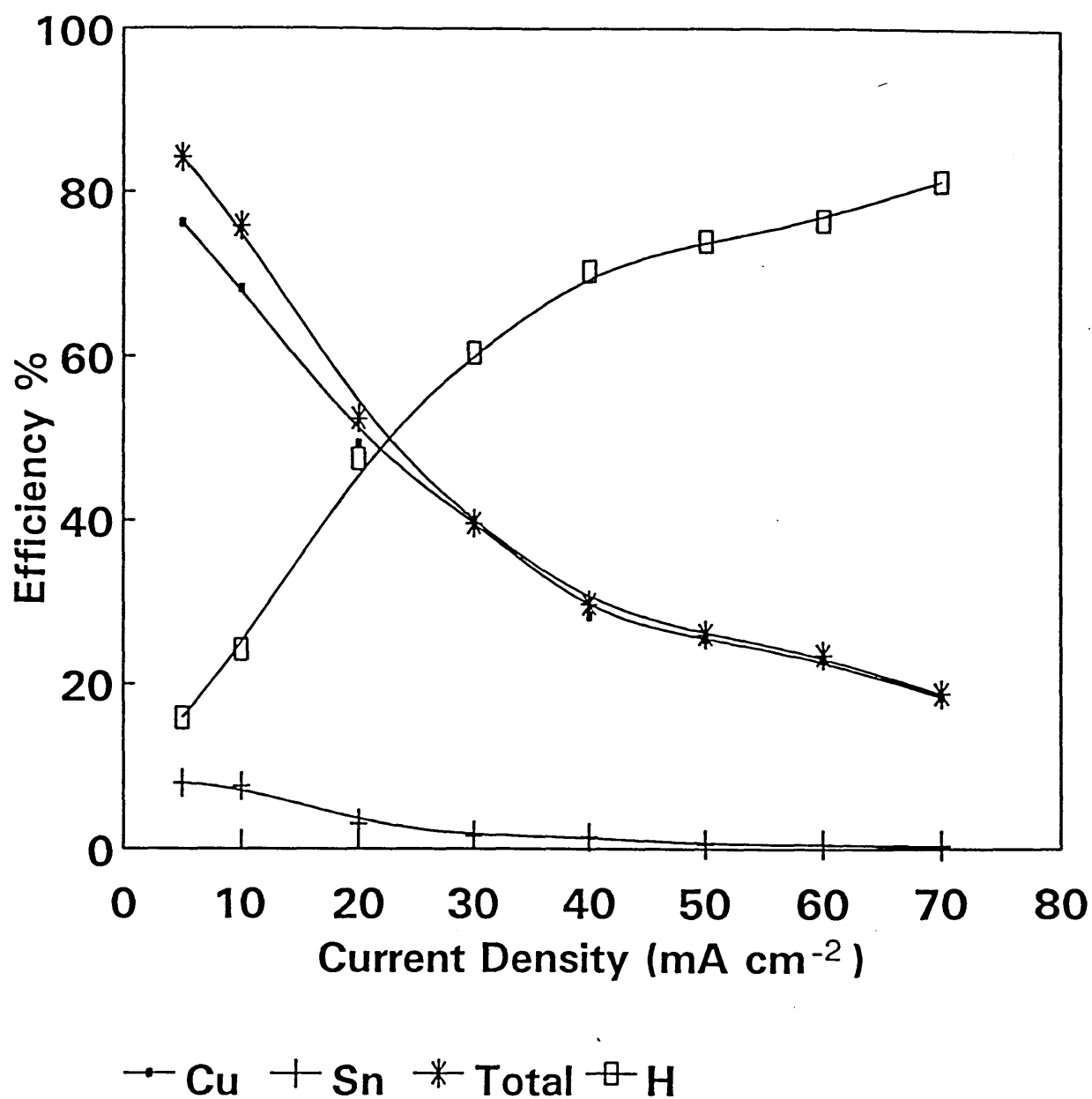
Figure 18.
The cathode current efficiencies for metal deposition
and hydrogen evolution as a function of cathode current
density. The deposits were obtained from a plating bath
operated at 40°C using short pulsed current (1000Hz)
and inert anodes.
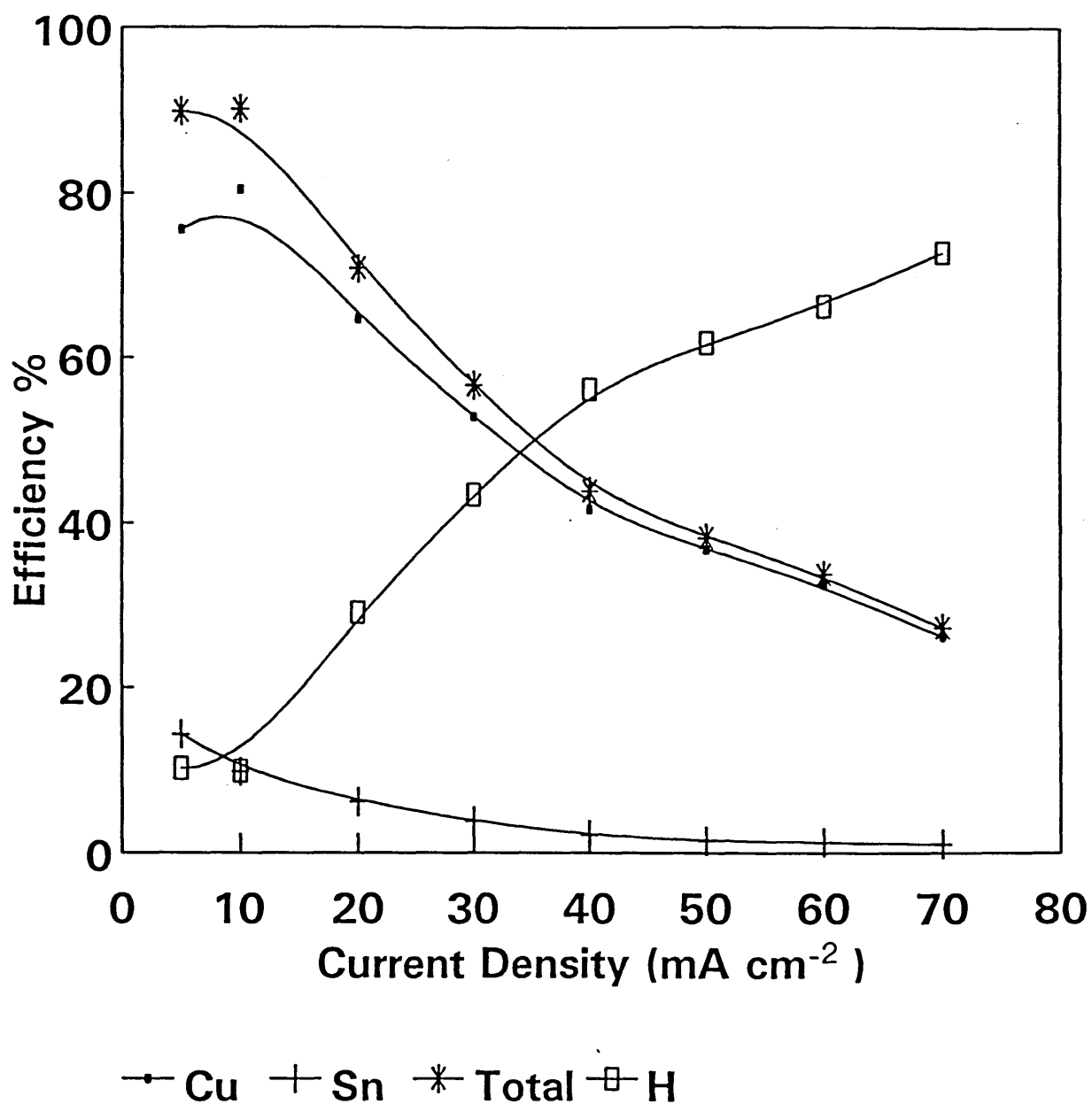
Figure 19.

The cathode current efficiencies for metal deposition and hydrogen evolution as a function of cathode current density. The deposits were obtained from a plating bath operated at 50°C using short pulsed current (1000Hz) and inert anodes.
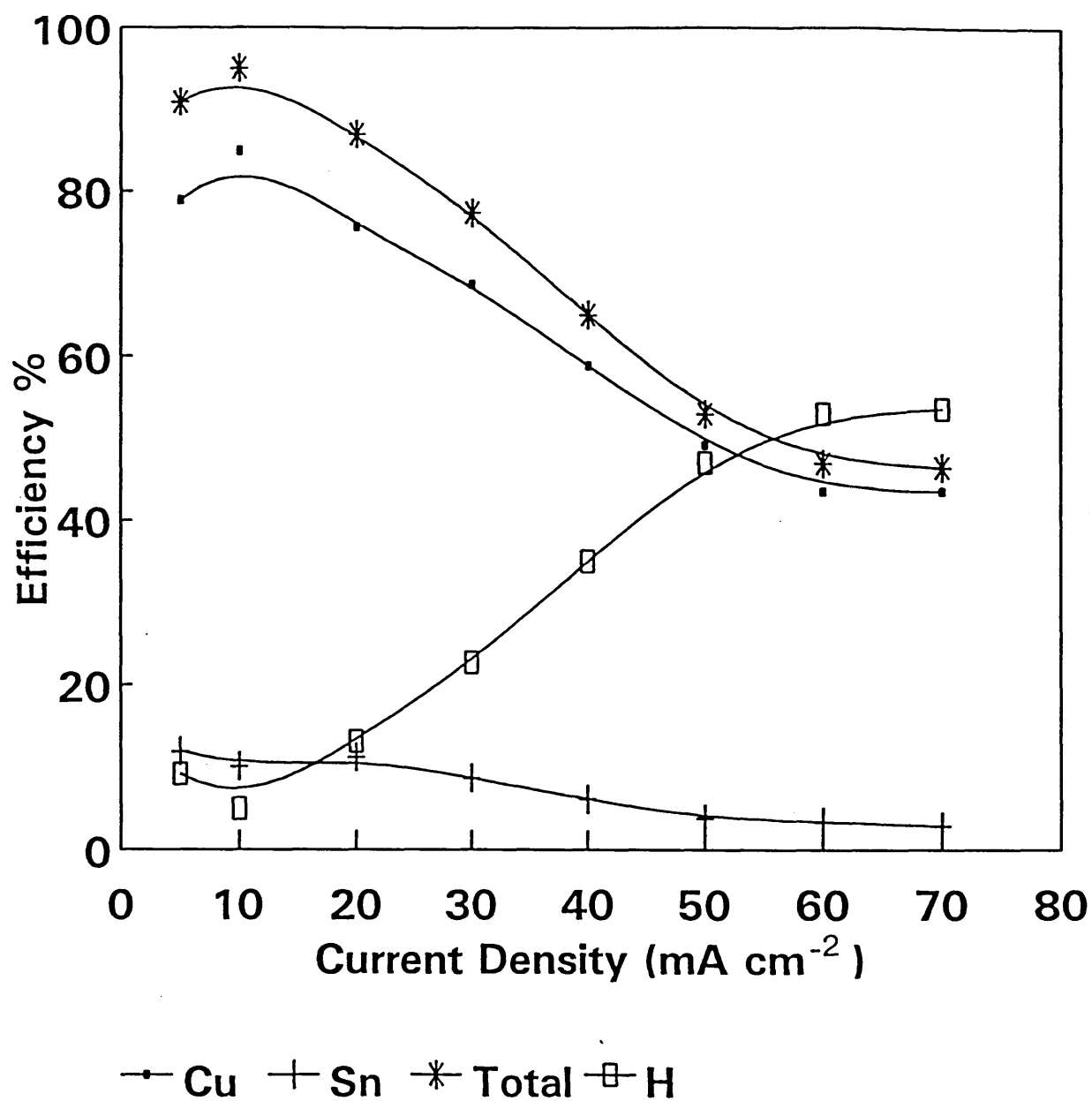
Figure 20.
The cathode current efficiencies for metal deposition
and hydrogen evolution as a function of cathode current
density. The deposits were obtained from a plating bath
operated at 60°C using short pulsed current (1000Hz)
and inert anodes.
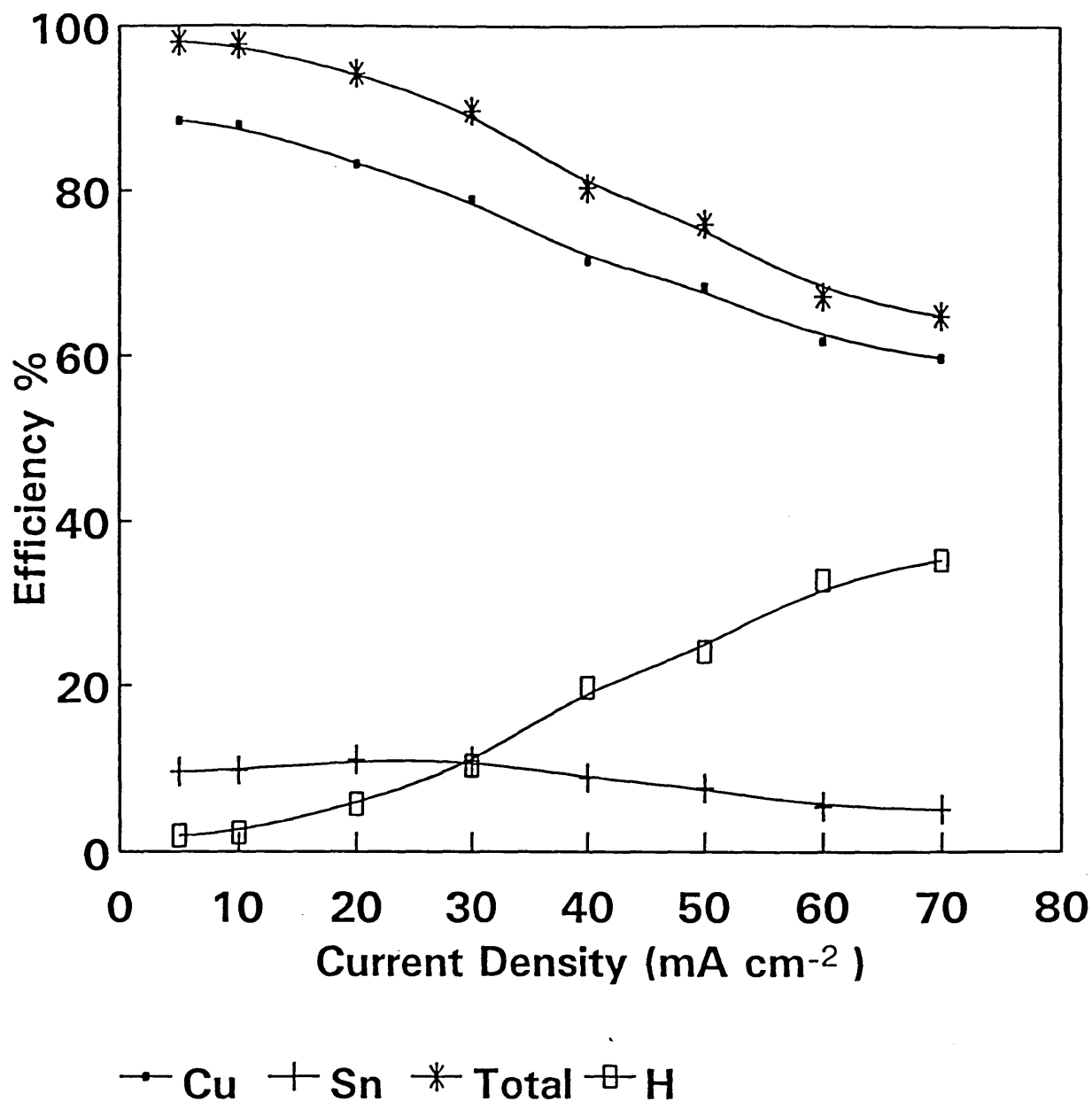
Figure 21.
The cathode current efficiencies for metal deposition and hydrogen evolution as a function of cathode current density. The deposits were obtained from a plating bath operated at 70°C using short pulsed current (1000Hz) and inert anodes.
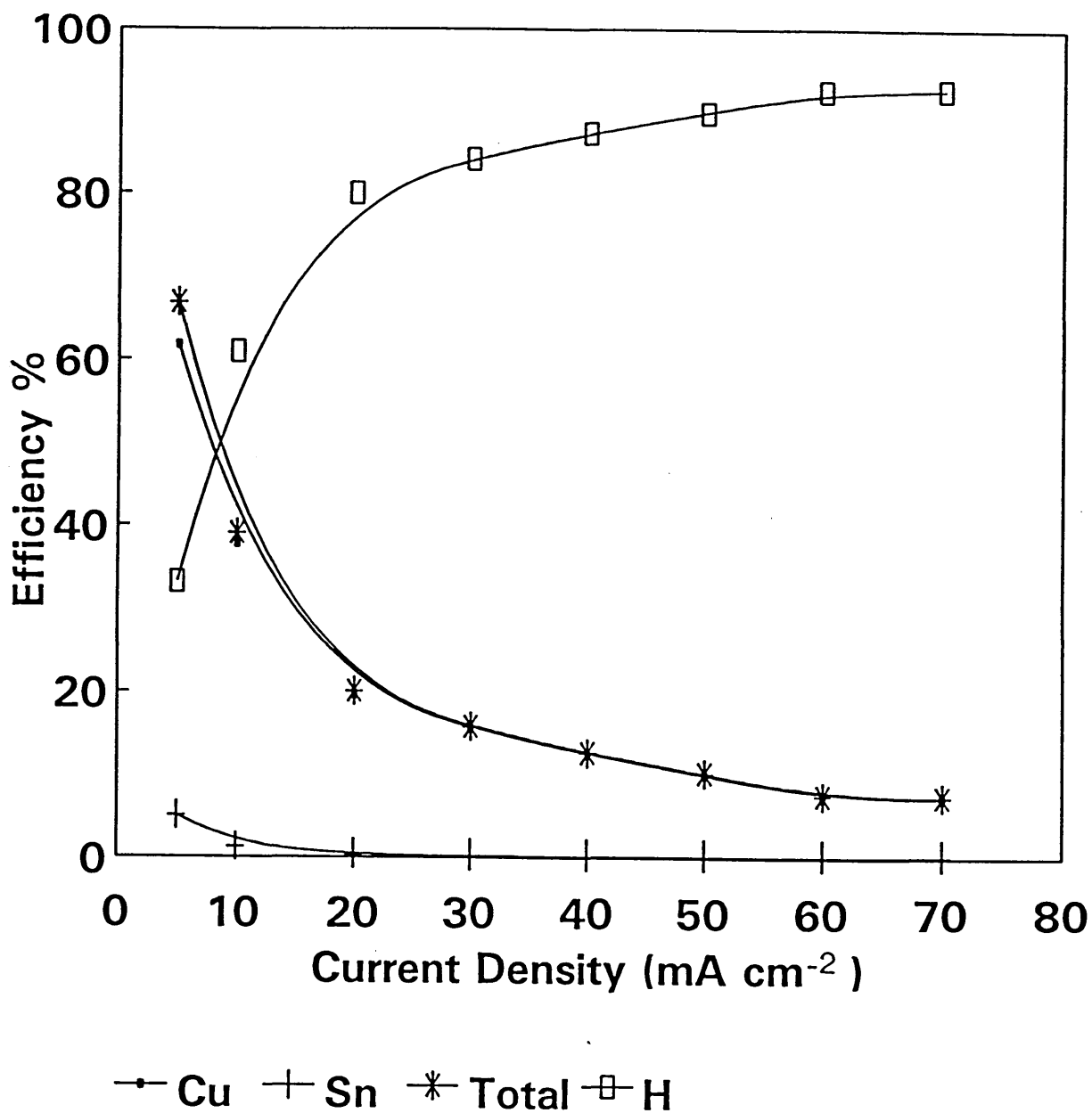
Figure 22.
The cathode current efficiencies for metal deposition
and hydrogen evolution as a function of cathode current
density. The deposits were obtained from a plating bath
operated at 30°C using long pulsed current (100Hz)
and inert anodes.
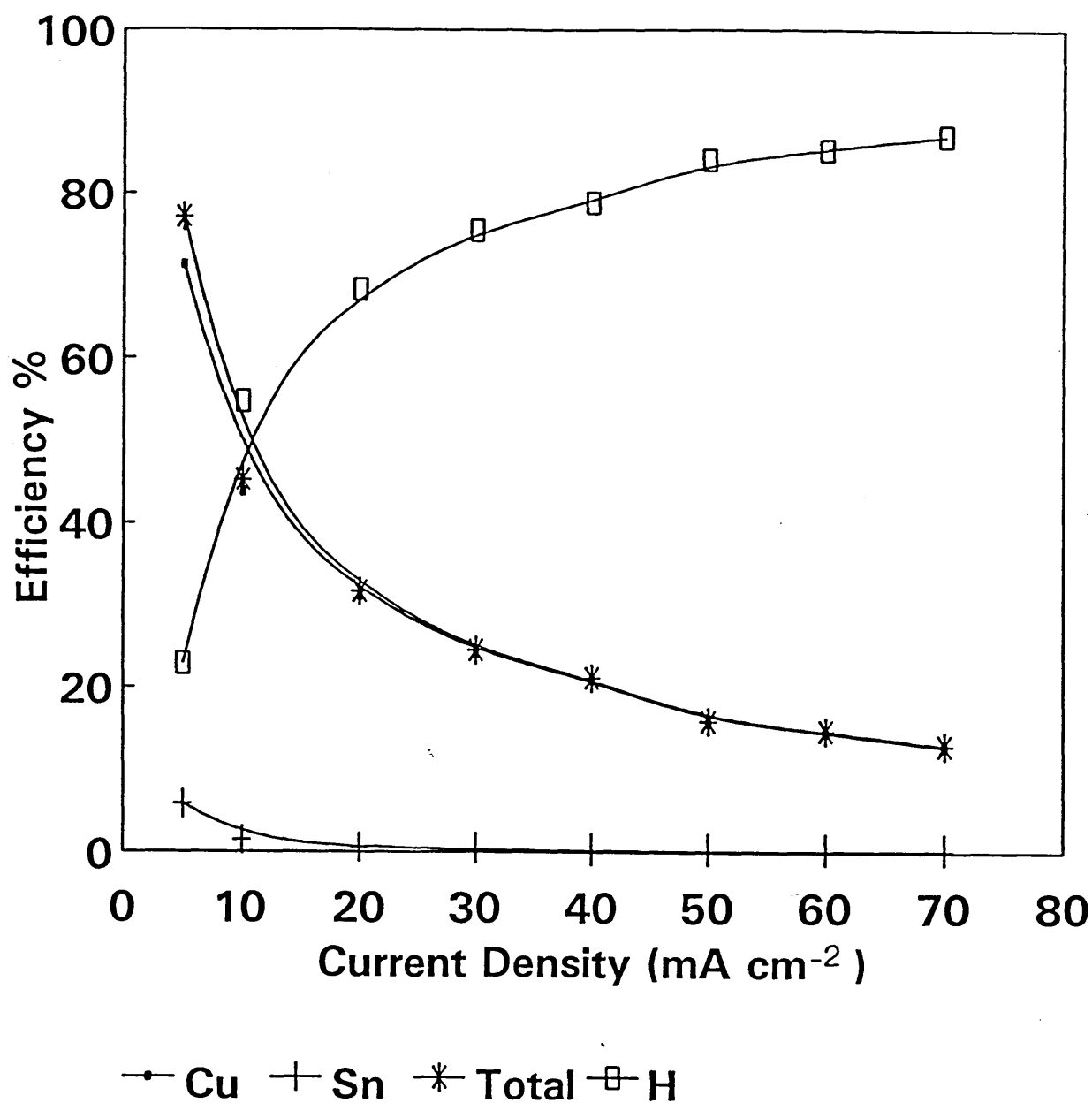
Figure 23.
The cathode current efficiencies for metal deposition
and hydrogen evolution as a function of cathode current
density. The deposits were obtained from a plating bath
operated at 40°C using long pulsed current (100Hz)
and inert anodes.
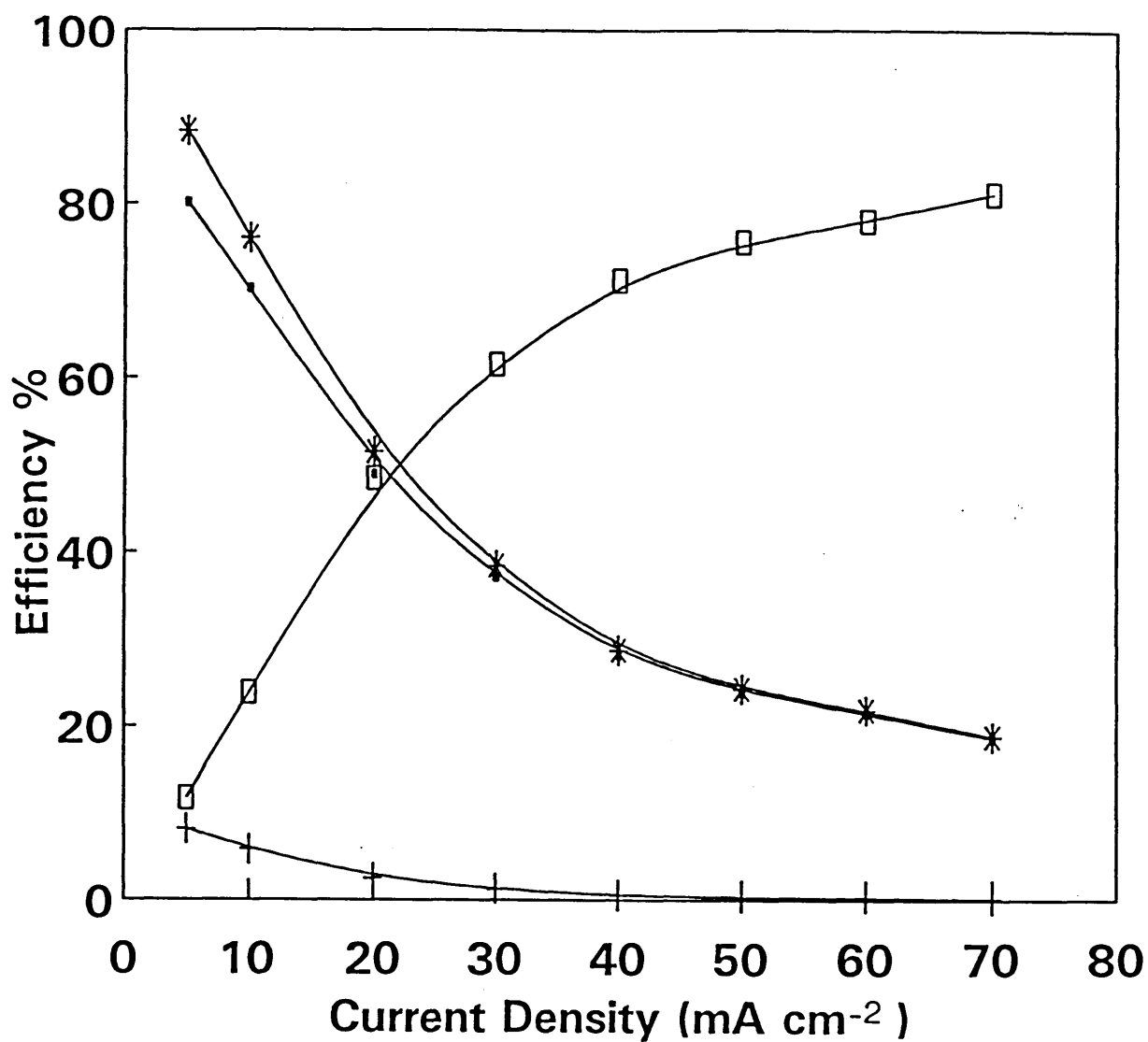
Figure 24.

The cathode current efficiencies for metal deposition
and hydrogen evolution as a function of cathode current
density. The deposits were obtained from a plating bath
operated at 50°C using long pulsed current (100Hz)
and inert anodes.
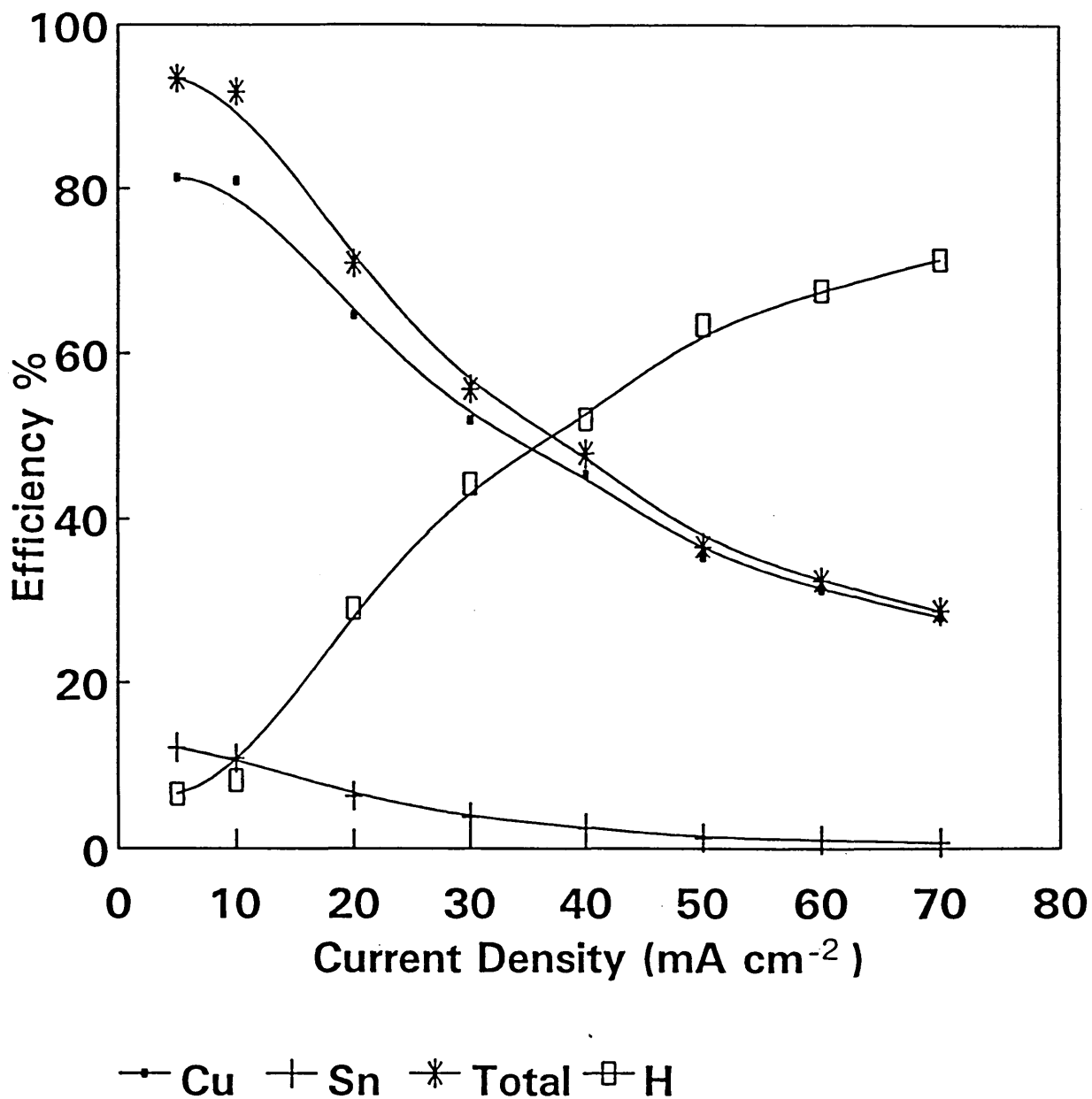
<u>Figure 25.</u>
The cathode current efficiencies for metal deposition and hydrogen evolution as a function of cathode current density. The deposits were obtained from a plating bath operated at 60°C using long pulsed current (100Hz) and inert anodes.
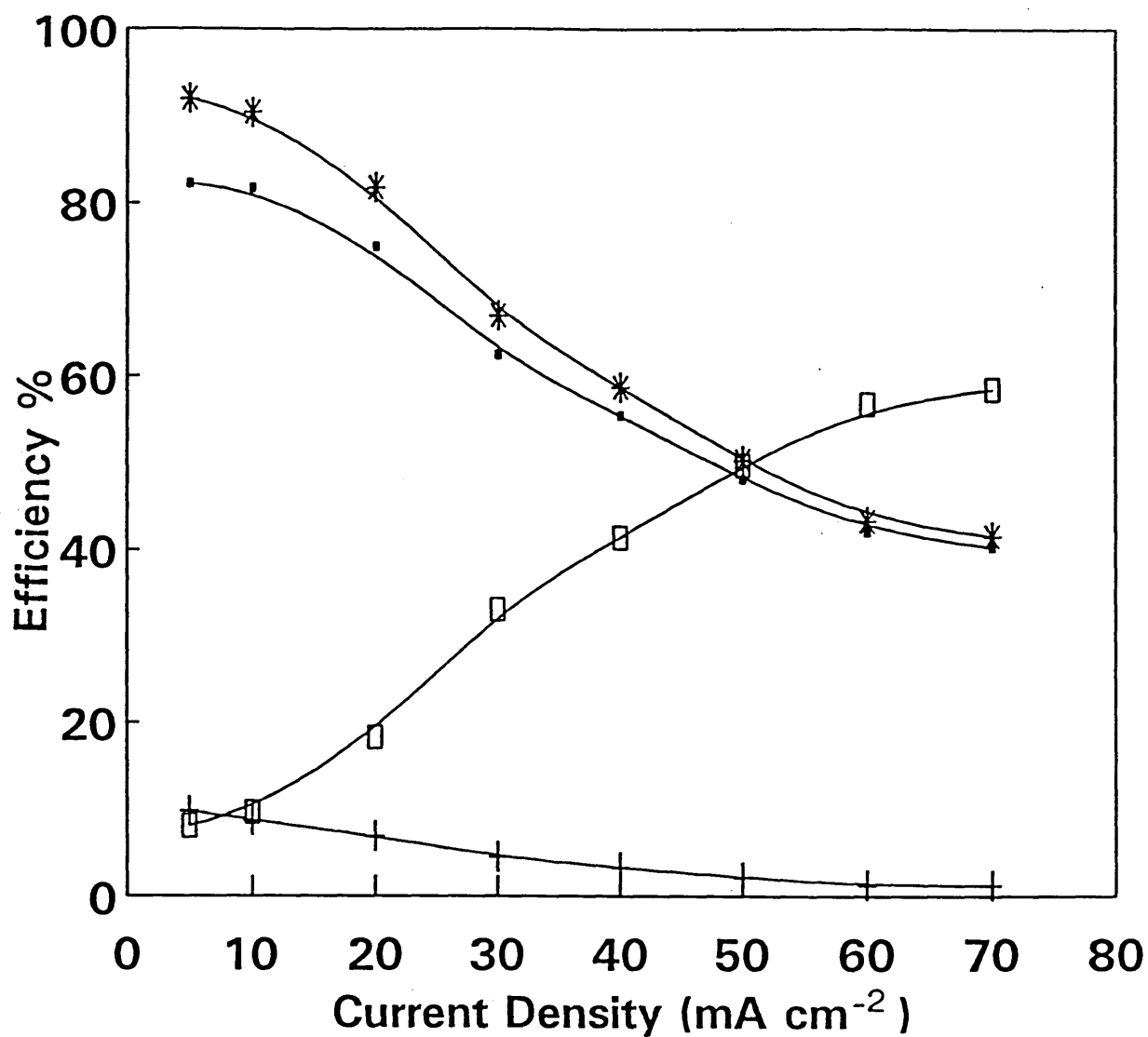
Figure 26.
The cathode current efficiencies for metal deposition
and hydrogen evolution as a function of cathode current
density. The deposits were obtained from a plating bath
operated at 70°C using long pulsed current (100Hz)
and inert anodes.
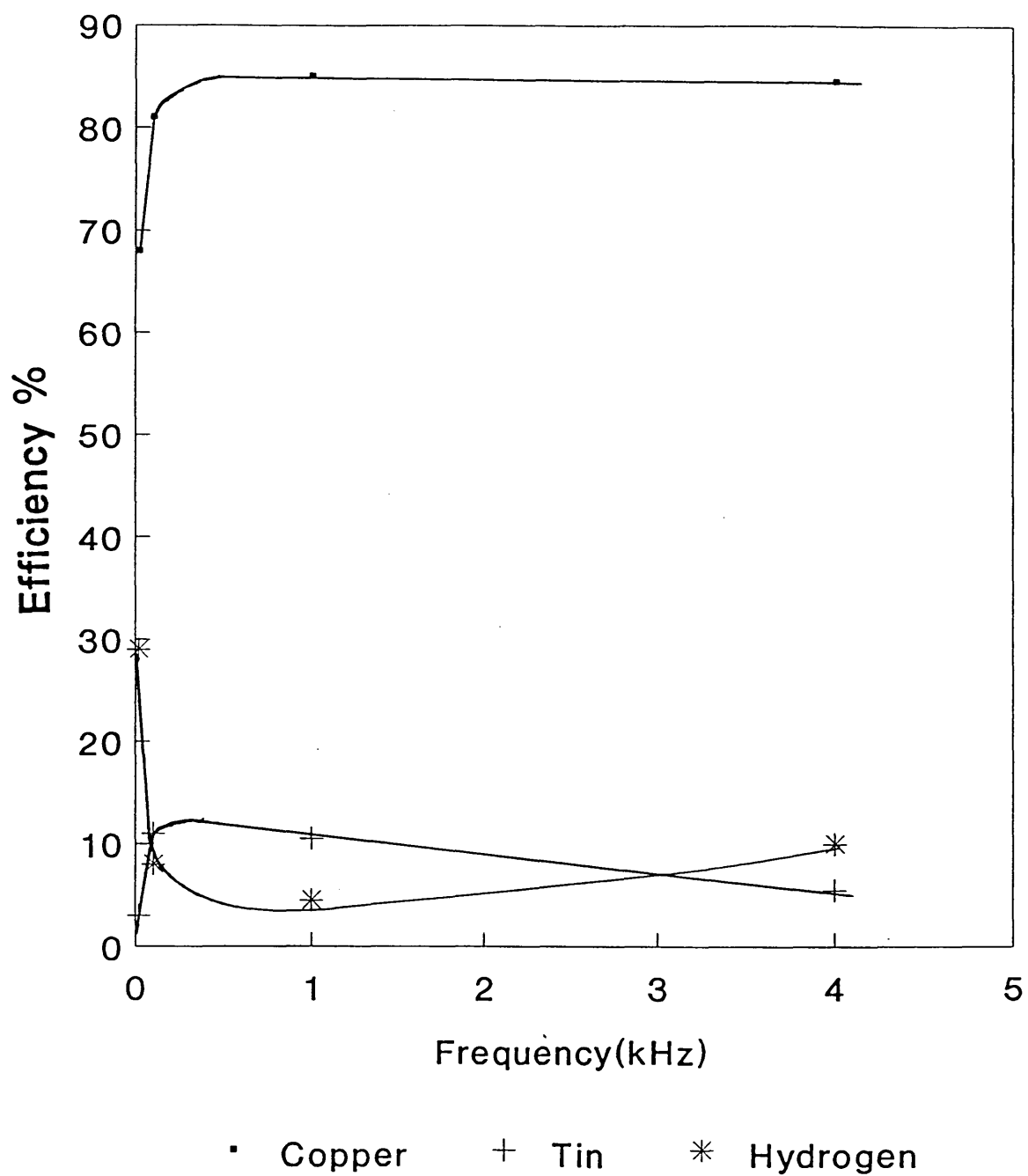
Figure 27.
The cathode current efficiencies for copper and tin
deposition and hydrogen evolution as a function of
pulse frequency. Conditions used were, bath temperature
60°C, cathode current density 10mA cm^{-2}, inert anodes.
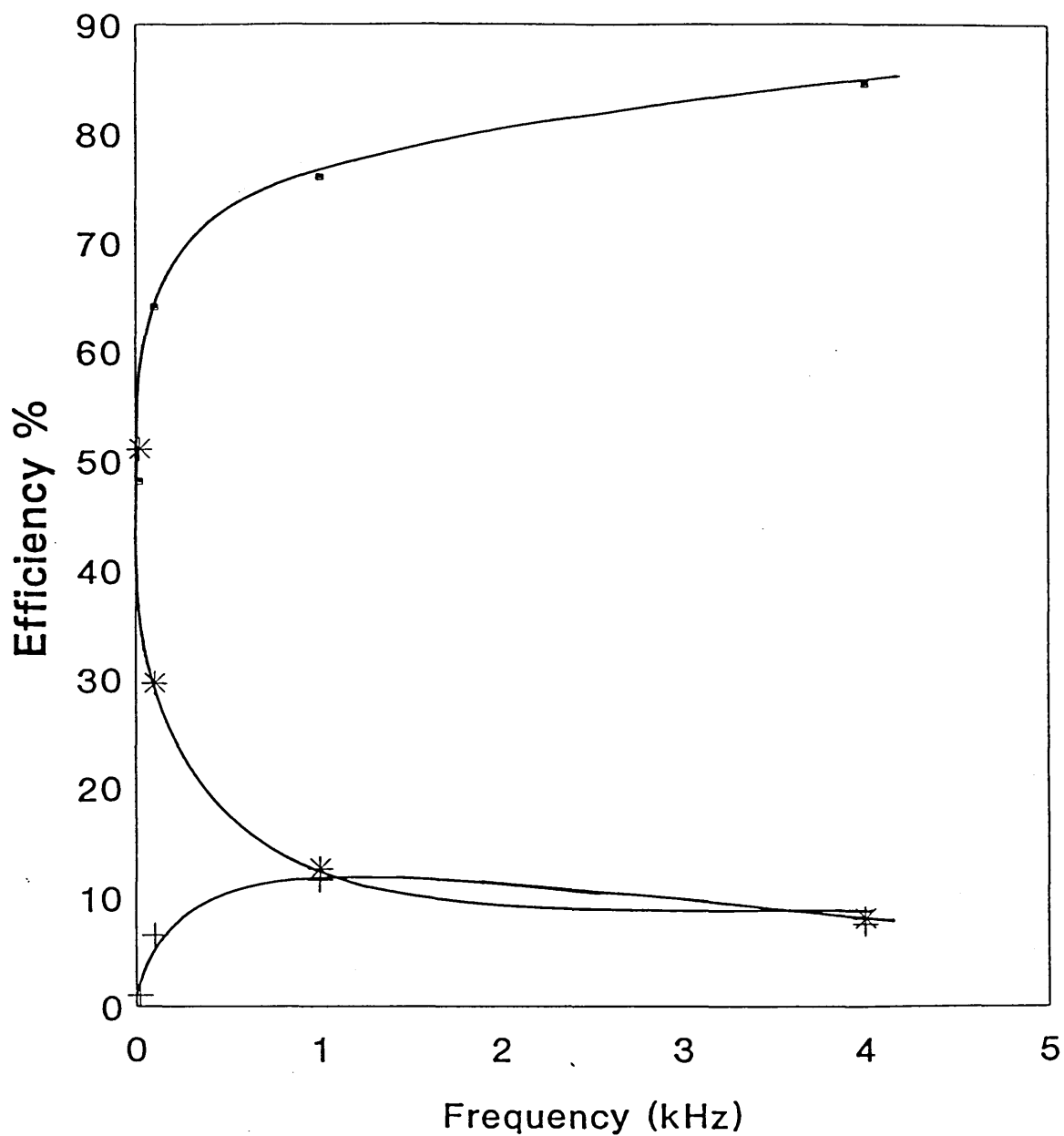
Figure 28.
The cathode current efficiencies for copper and tin deposition and hydrogen evolution as a function of pulse frequency. Conditions used were, bath temperature 60°C, cathode current density 20mA cm^{-2}, inert anodes.
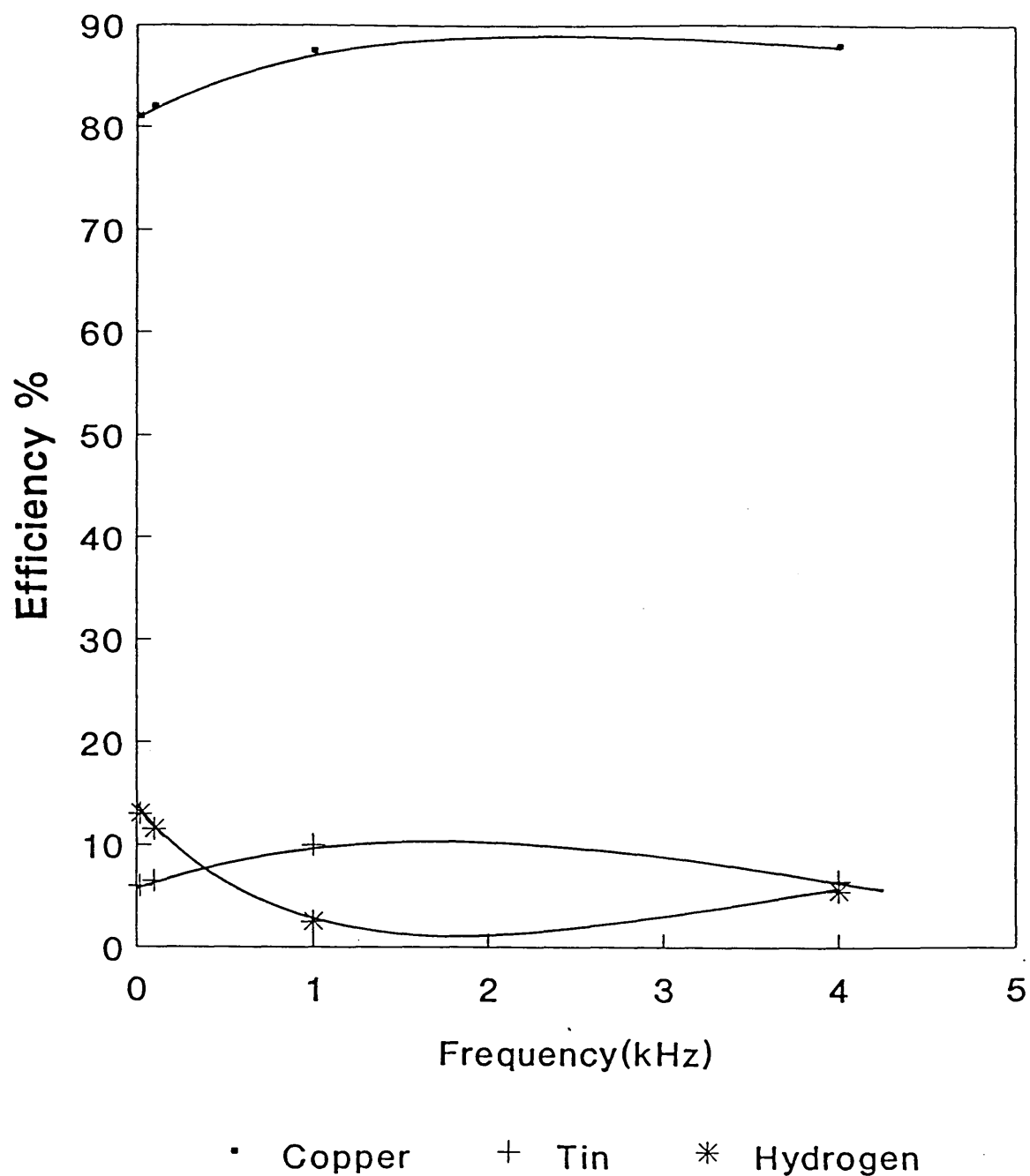
Figure 29.
The cathode current efficiencies for copper and tin
deposition and hydrogen evolution as a function of
pulse frequency. Conditions used were, bath temperature
70°C, cathode current density 10mA cm^{-2}, inert anodes.
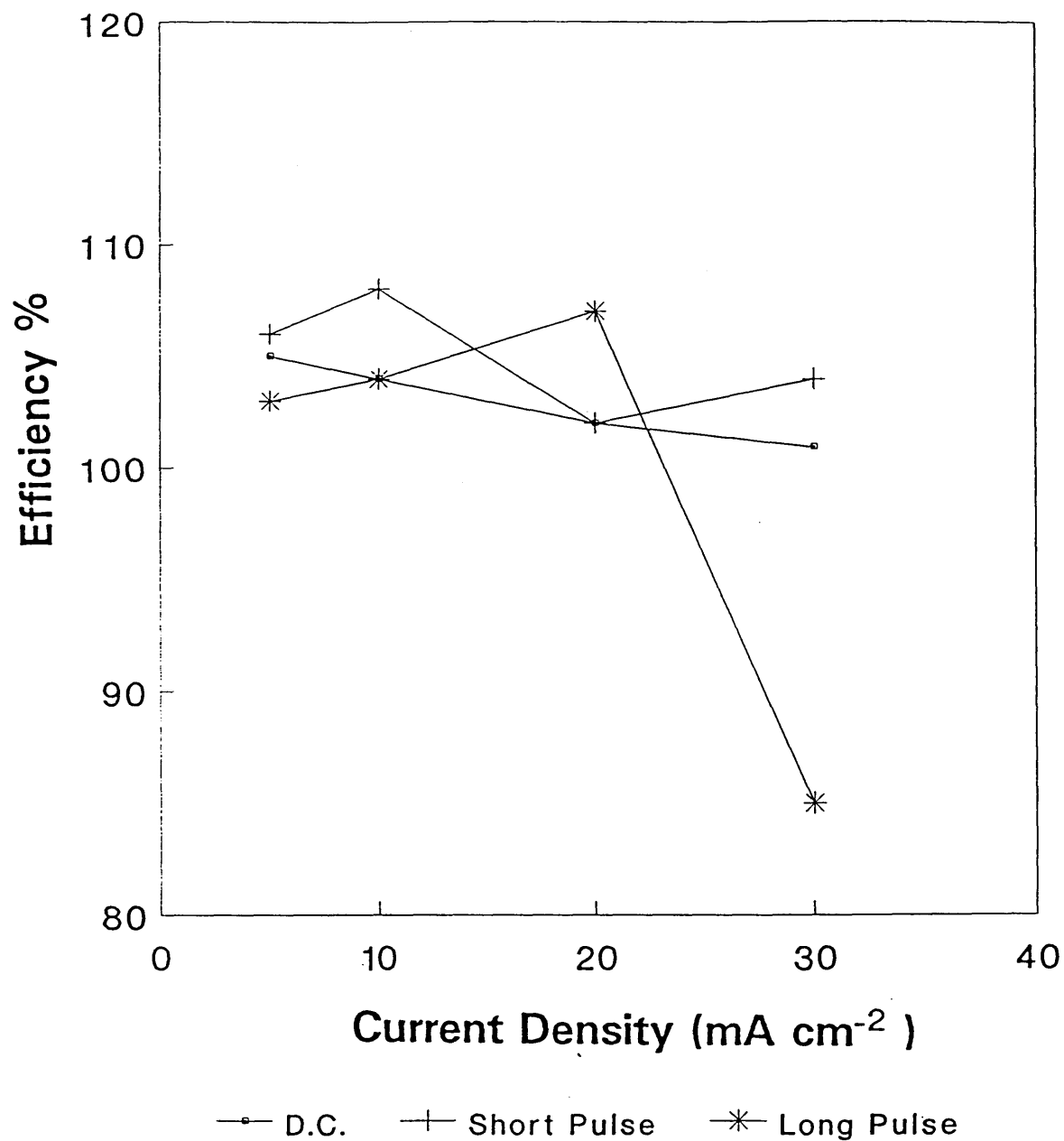
<u>Figure 31.</u>
The apparent anodic efficienies for dissolution of copper anodes as a function of anode current density. Conditions used; bath temperature 30°C, conventional direct current, short pulsed current (1000Hz) and long pulsed current (100Hz).
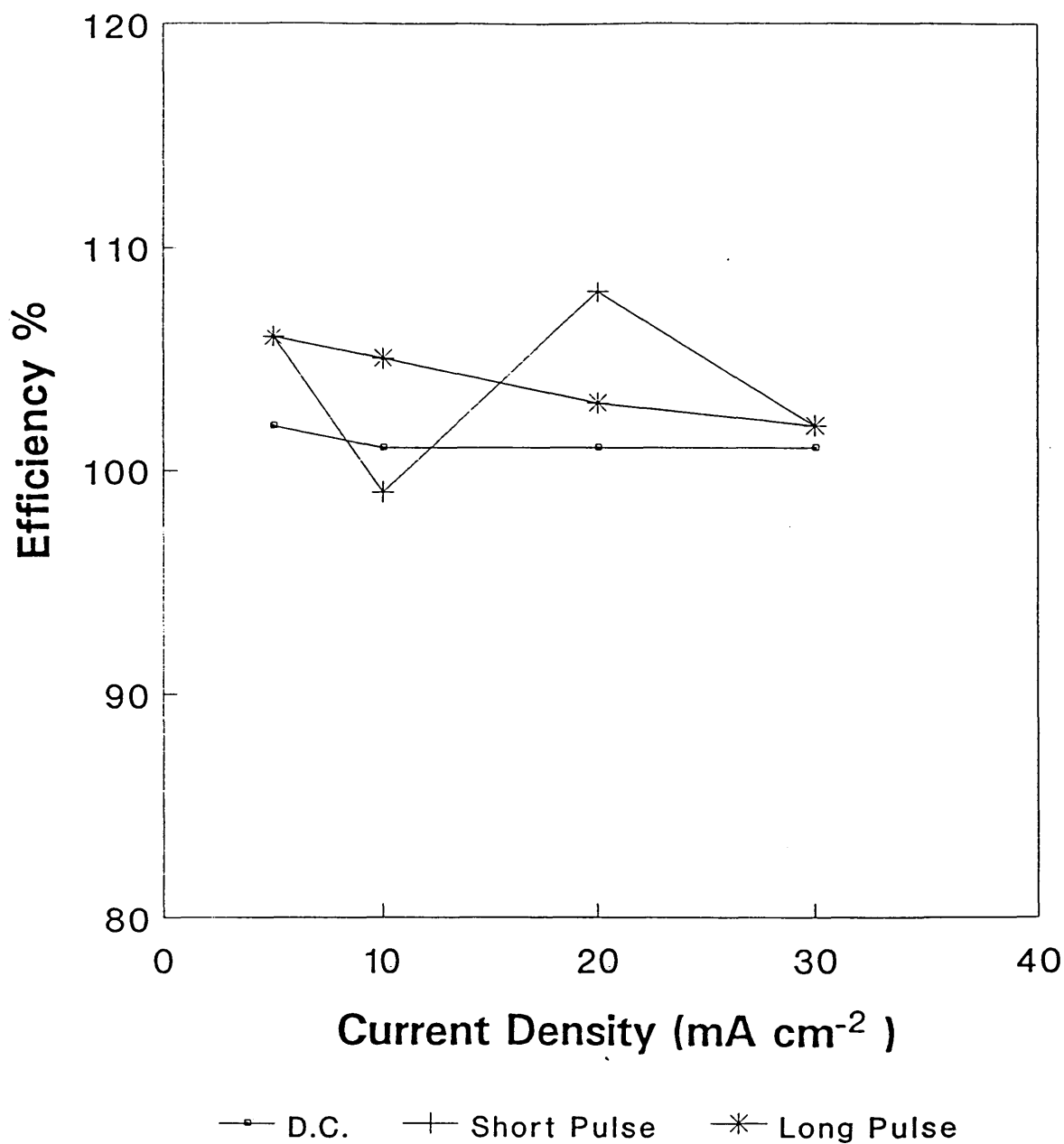
Figure 32.

The apparent anodic efficienies for dissolution of
copper anodes as a function of anode current density.
Conditions used; bath temperature 40°C, conventional
direct current, short pulsed current (1000Hz) and long
pulsed current (100Hz).
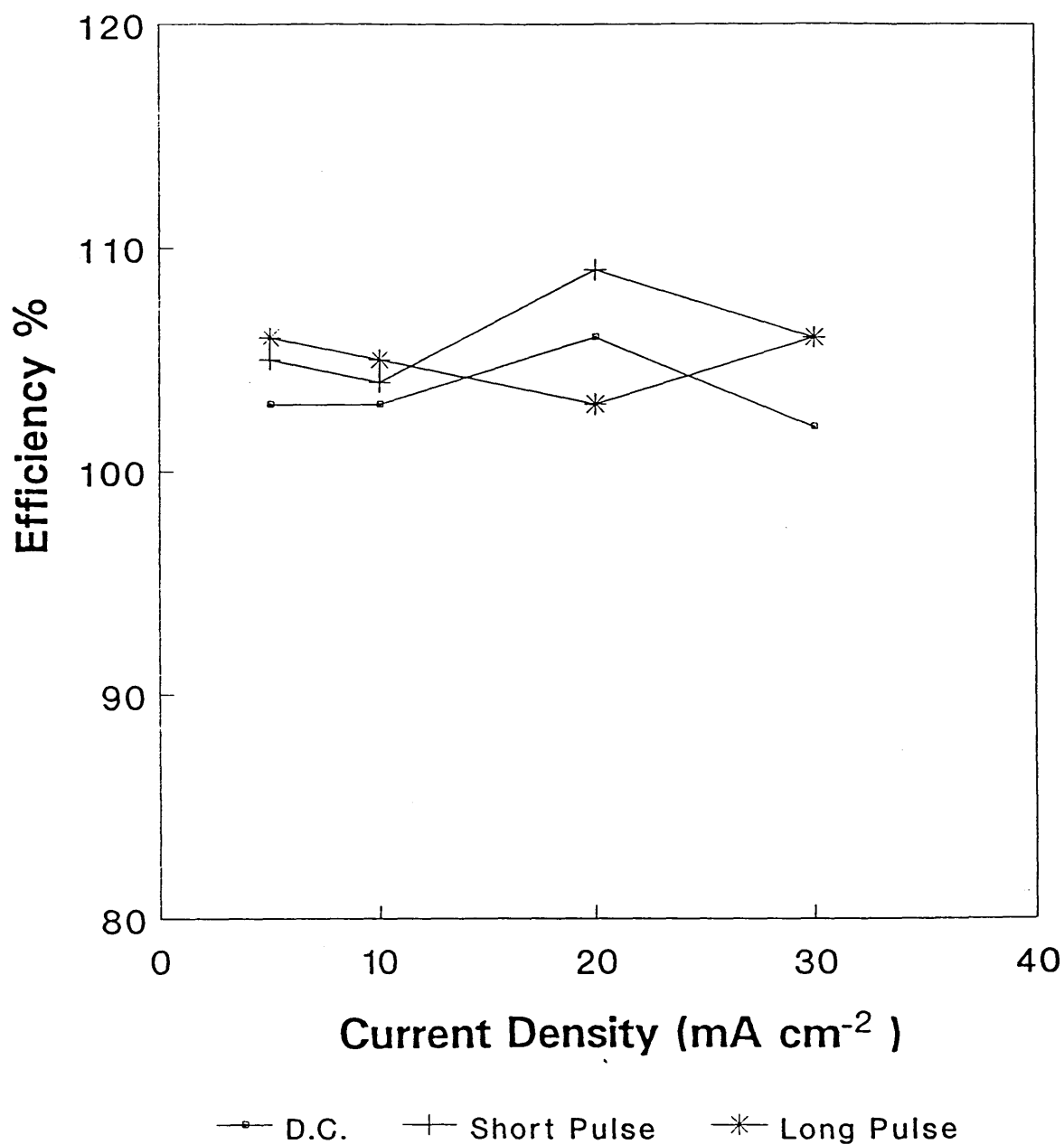
Figure 33.
The apparent anodic efficienies for dissolution of
copper anodes as a function of anode current density.
Conditions used; bath temperature 50°C, conventional
direct current, short pulsed current (1000Hz) and long
pulsed current (100Hz).
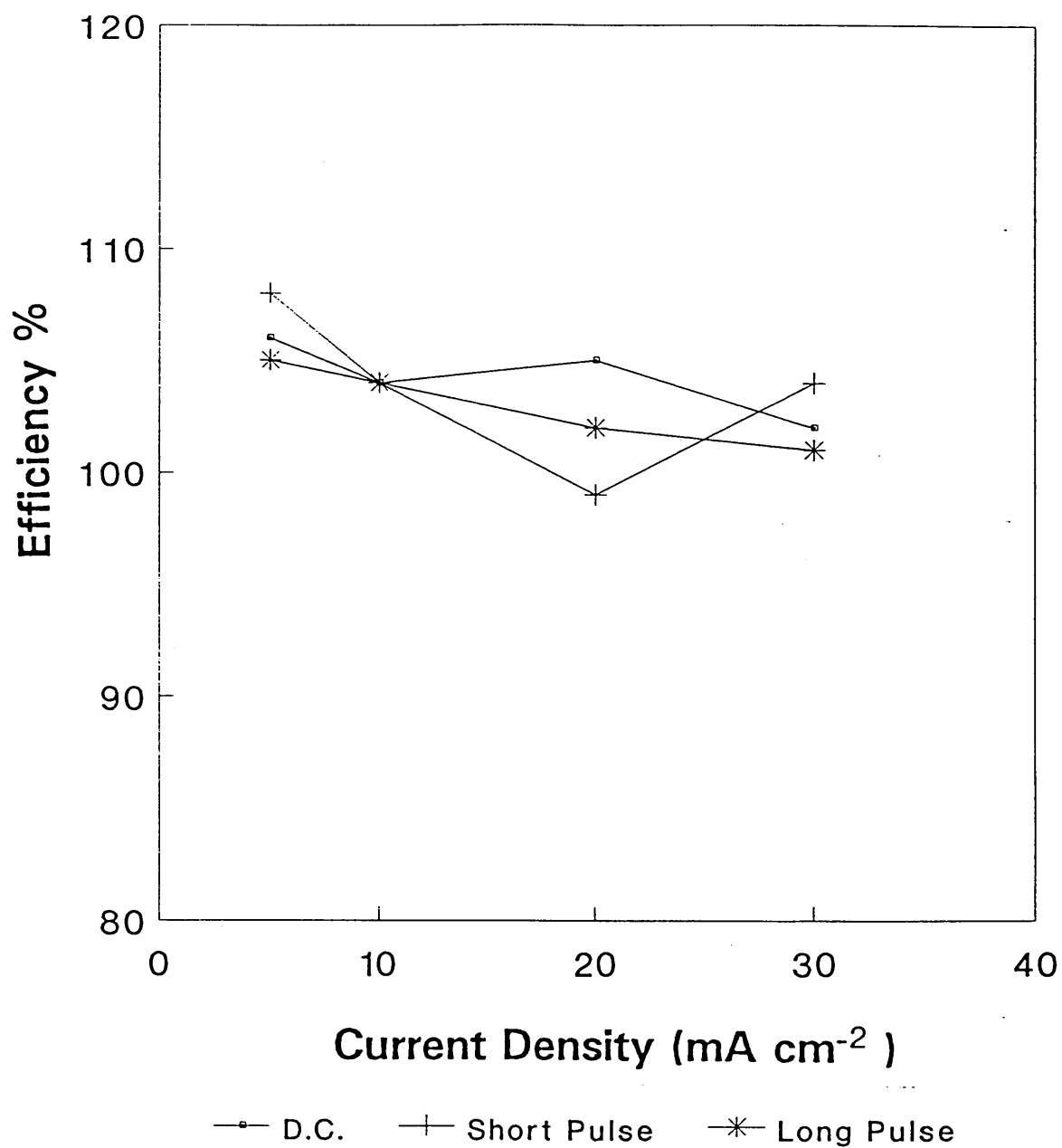
Figure 34.
The apparent anodic efficienies for dissolution of
copper anodes as a function of anode current density.
Conditions used; bath temperature 60°C, conventional
direct current, short pulsed current (1000Hz) and long
pulsed current (100Hz).
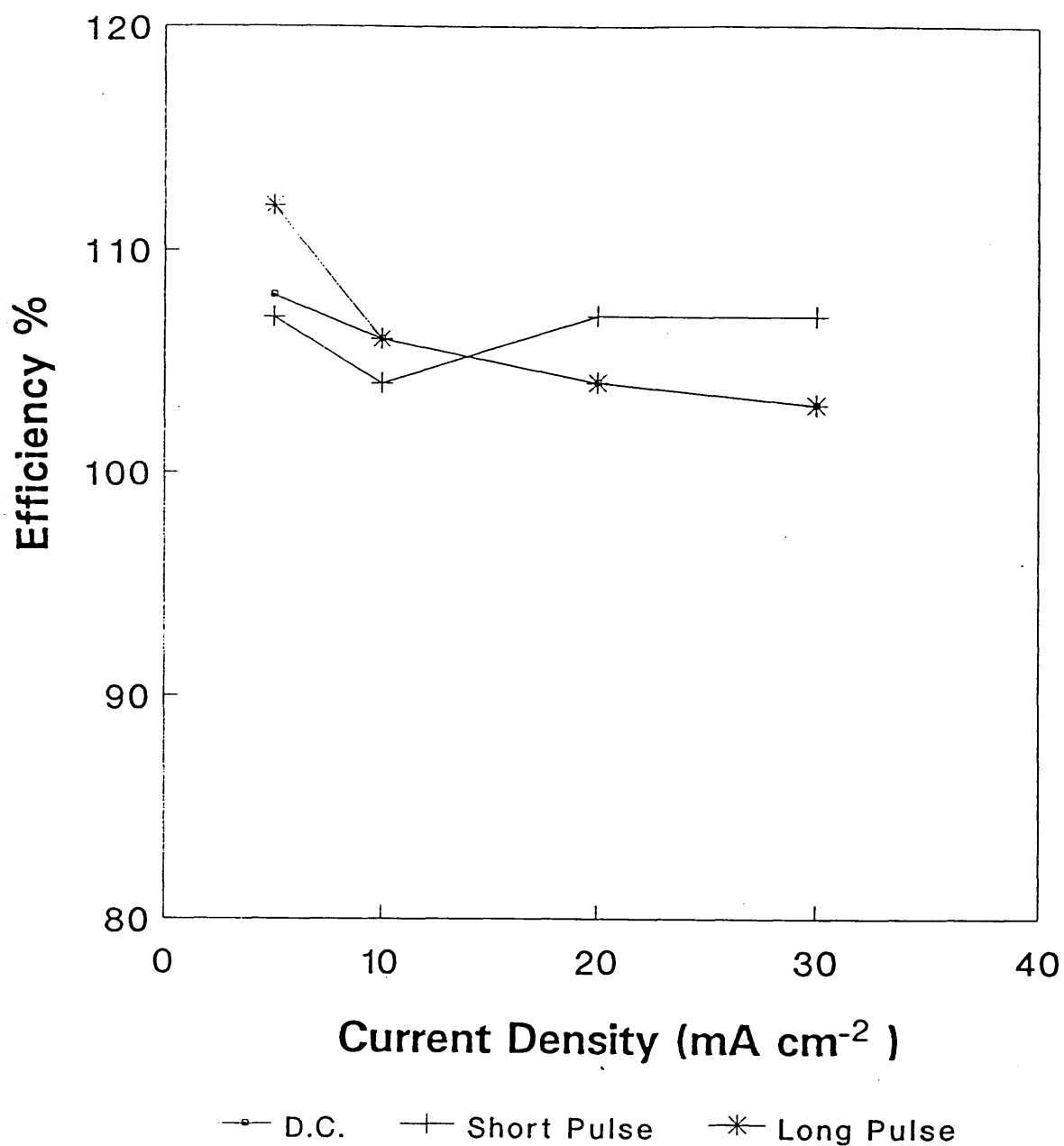
<u>Figure 35.</u>
The apparent anodic efficienies for dissolution of
copper anodes as a function of anode current density.
Conditions used; bath temperature 70°C, conventional
direct current, short pulsed current (1000Hz) and long
pulsed current (100Hz).
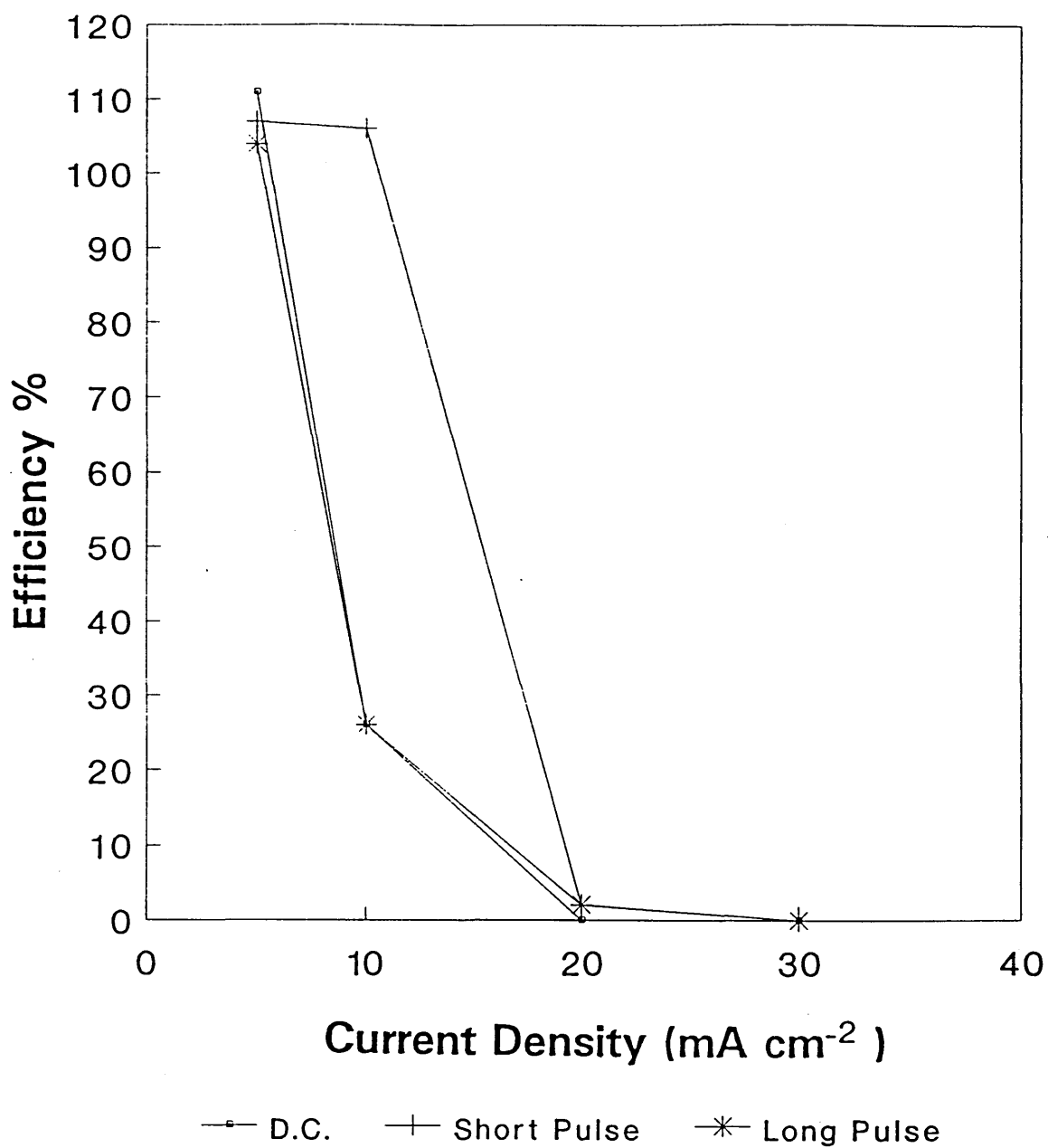
Figure 36.
The apparent anodic efficienies for dissolution of bronze anodes as a function of anode current density. Conditions used; bath temperature 30°C, conventional direct current, short pulsed current (1000Hz) and long pulsed current (100Hz).
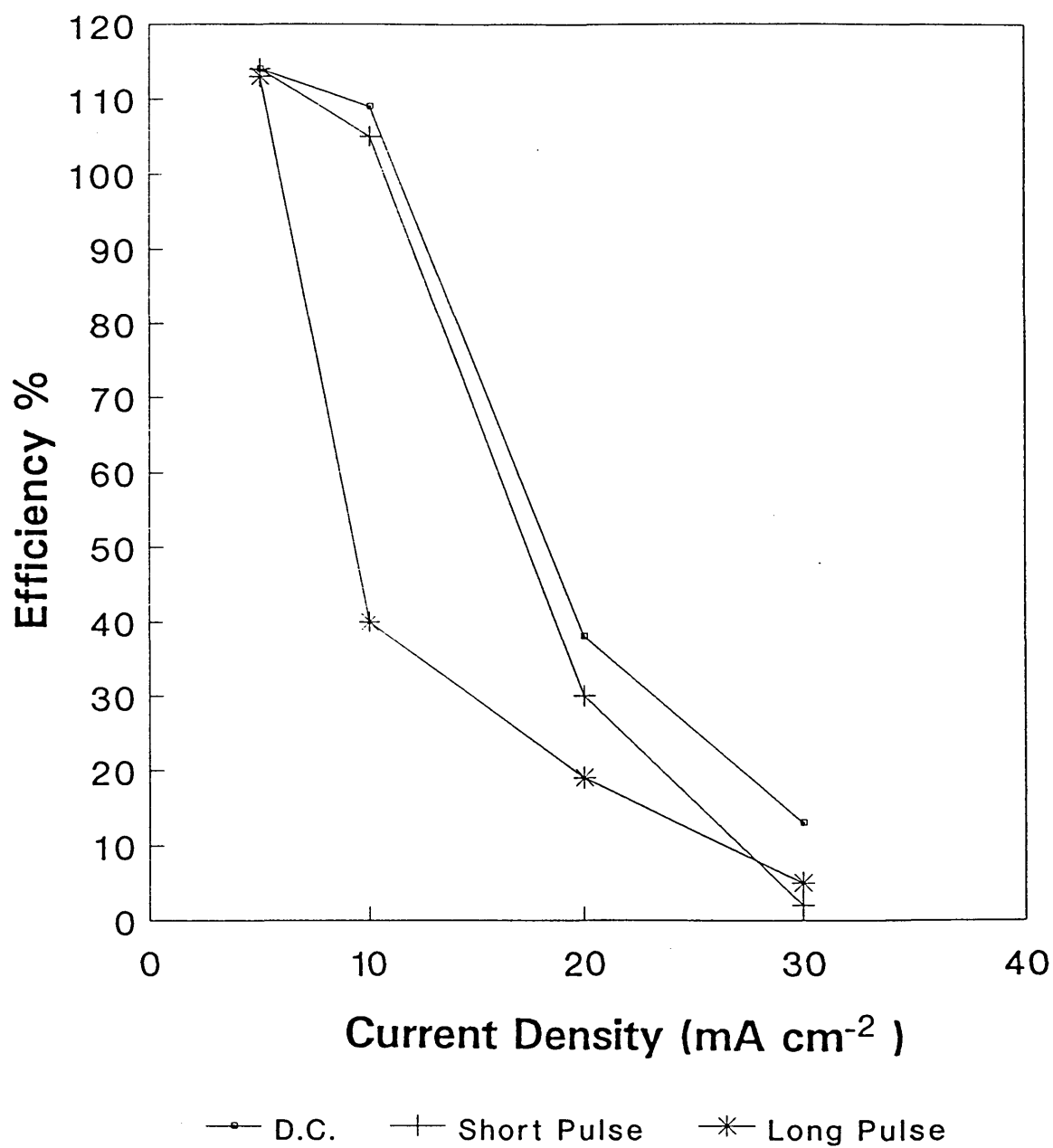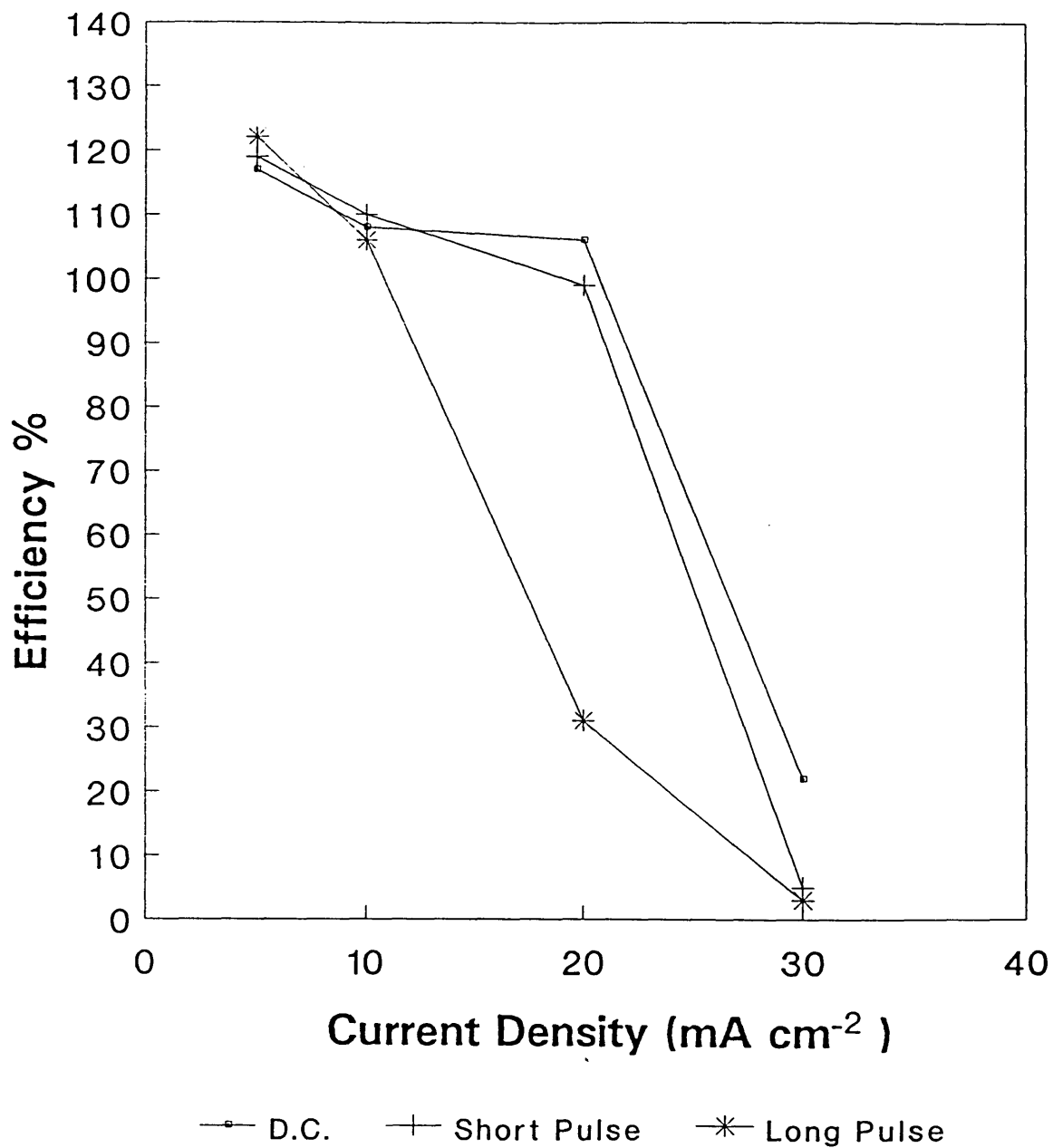
<u>Figure 38.</u>
The apparent anodic efficienies for dissolution of
bronze anodes as a function of anode current density.
Conditions used; bath temperature 50°C, conventional
direct current, short pulsed current (1000Hz) and long
pulsed current (100Hz).
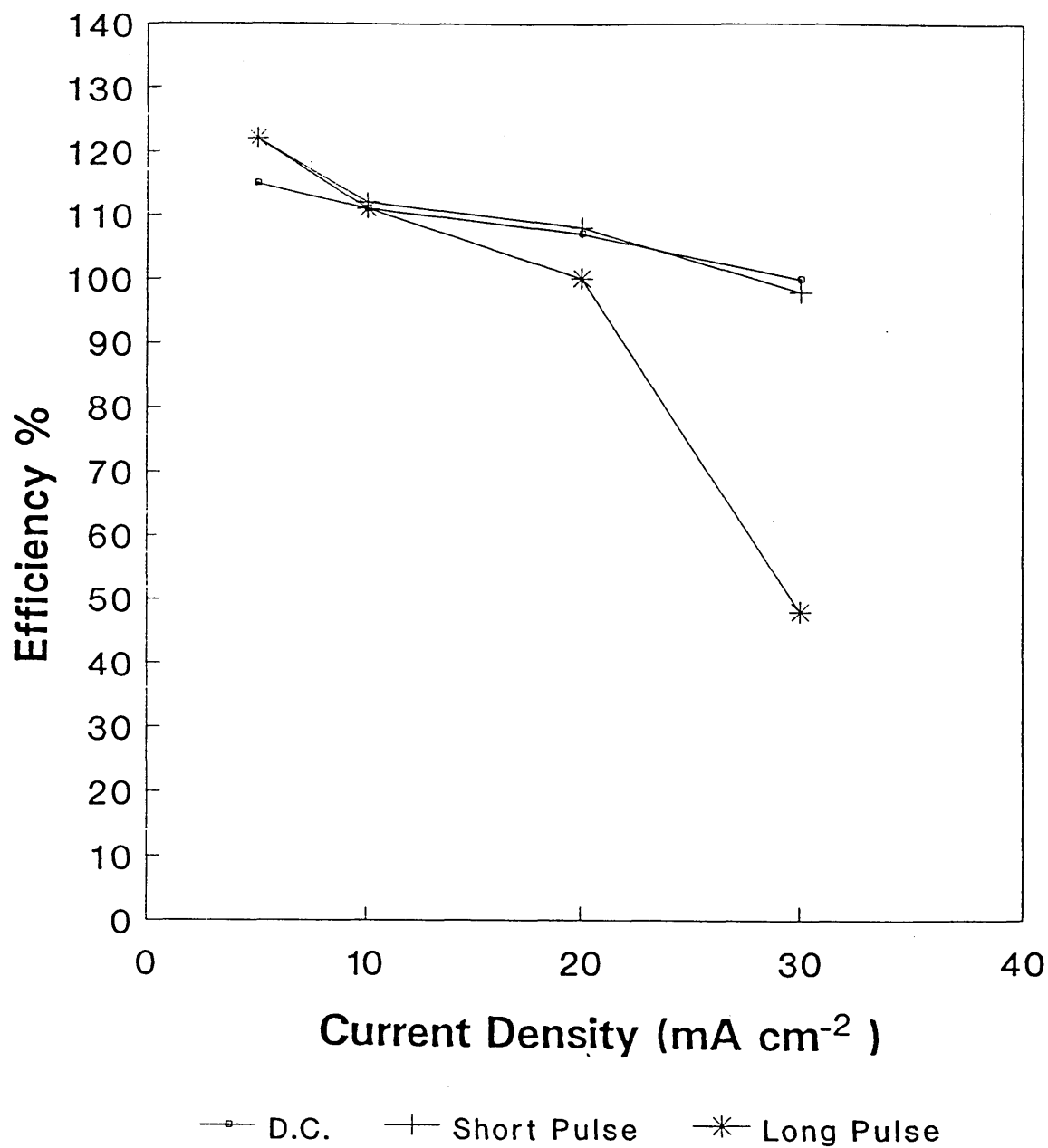
Figure 39.
The apparent anodic efficienies for dissolution of
bronze anodes as a function of anode current density.
Conditions used; bath temperature 60°C, conventional
direct current, short pulsed current (1000Hz) and long
pulsed current (100Hz).
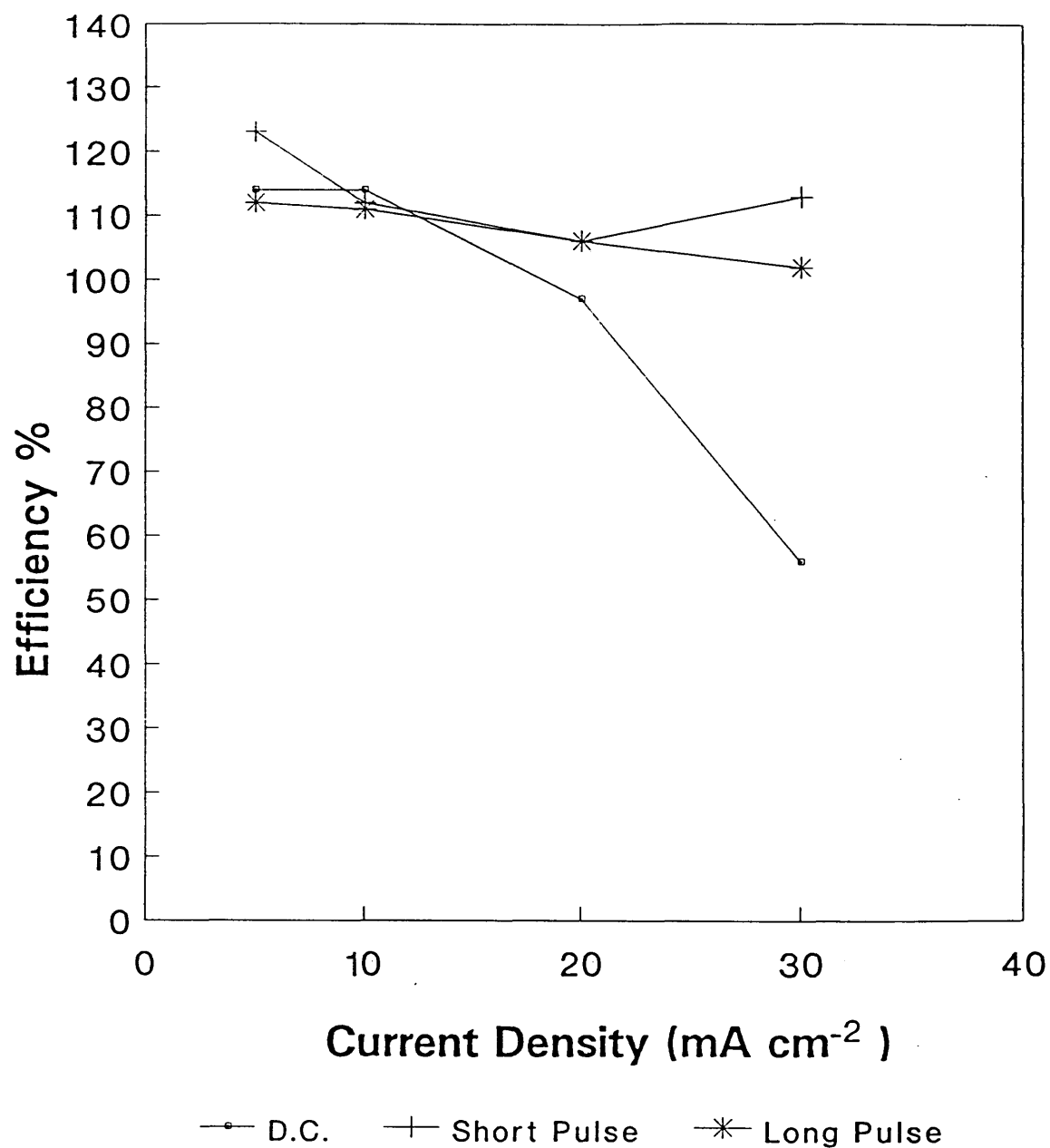
Figure 40.
The apparent anodic efficienies for dissolution of
bronze anodes as a function of anode current density.
Conditions used; bath temperature 70°C, conventional
direct current, short pulsed current (1000Hz) and long
pulsed current (100Hz).
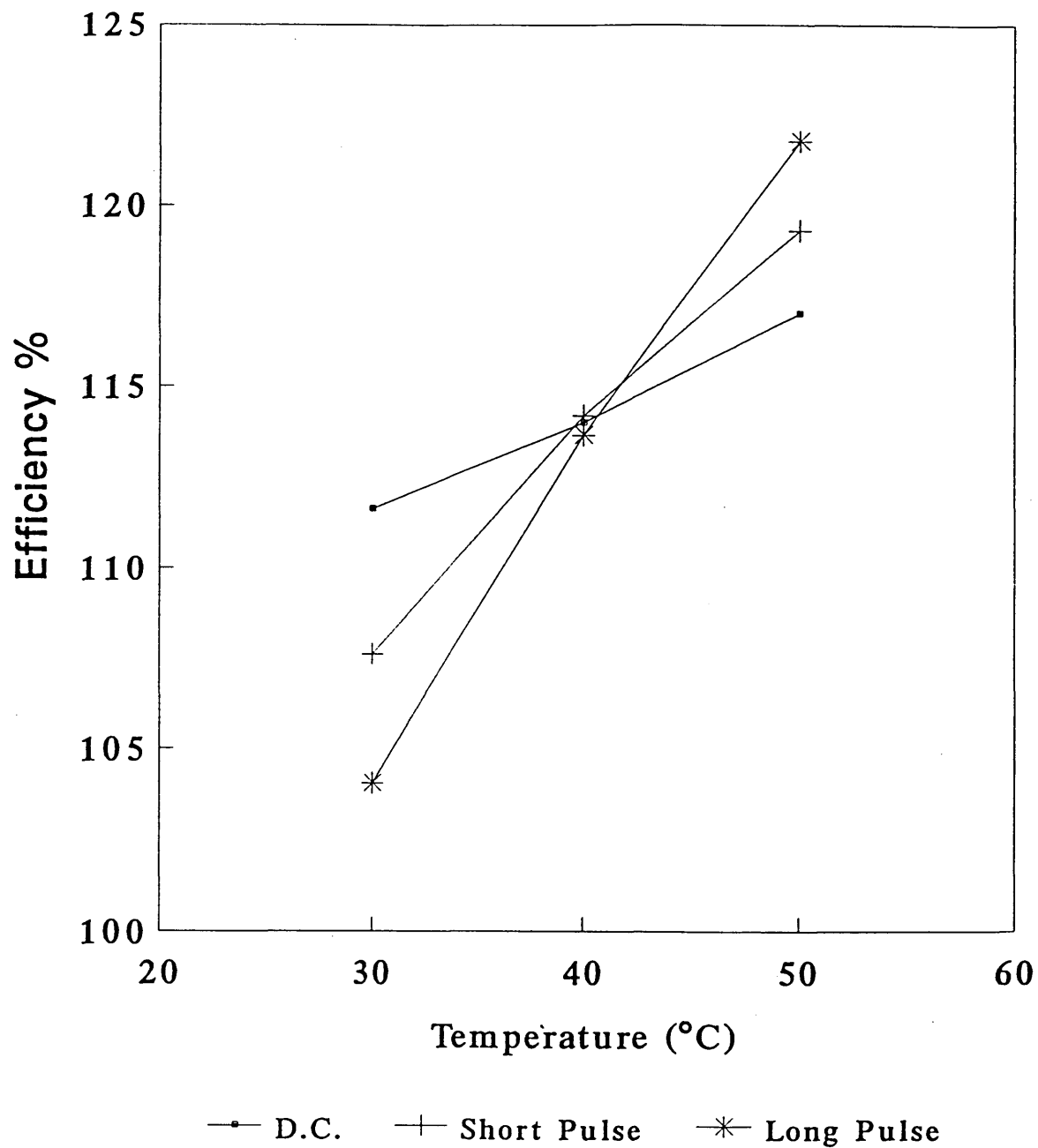
Figure 41.
The increase in apparent efficiency above one hundred
per cent for dissolution of bronze anodes with
increasing temperature between 30°C and 50°C.
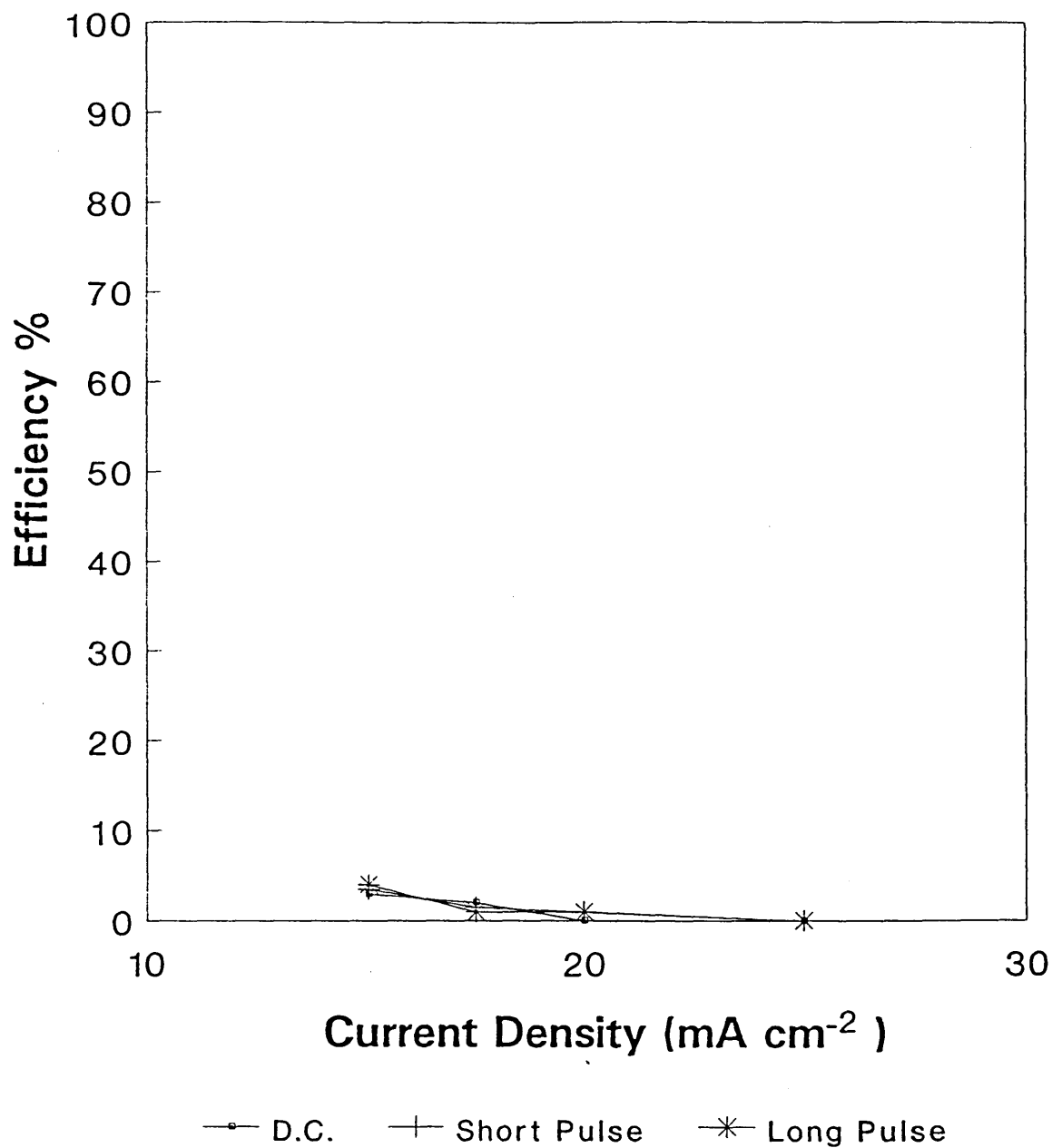
Figure 42.
The apparent anodic efficiencies for dissolution of tin anodes as a function of anode current density. Conditions used; bath temperature 40°C, conventional direct current, short pulsed current (1000Hz) and long pulsed current (100Hz).
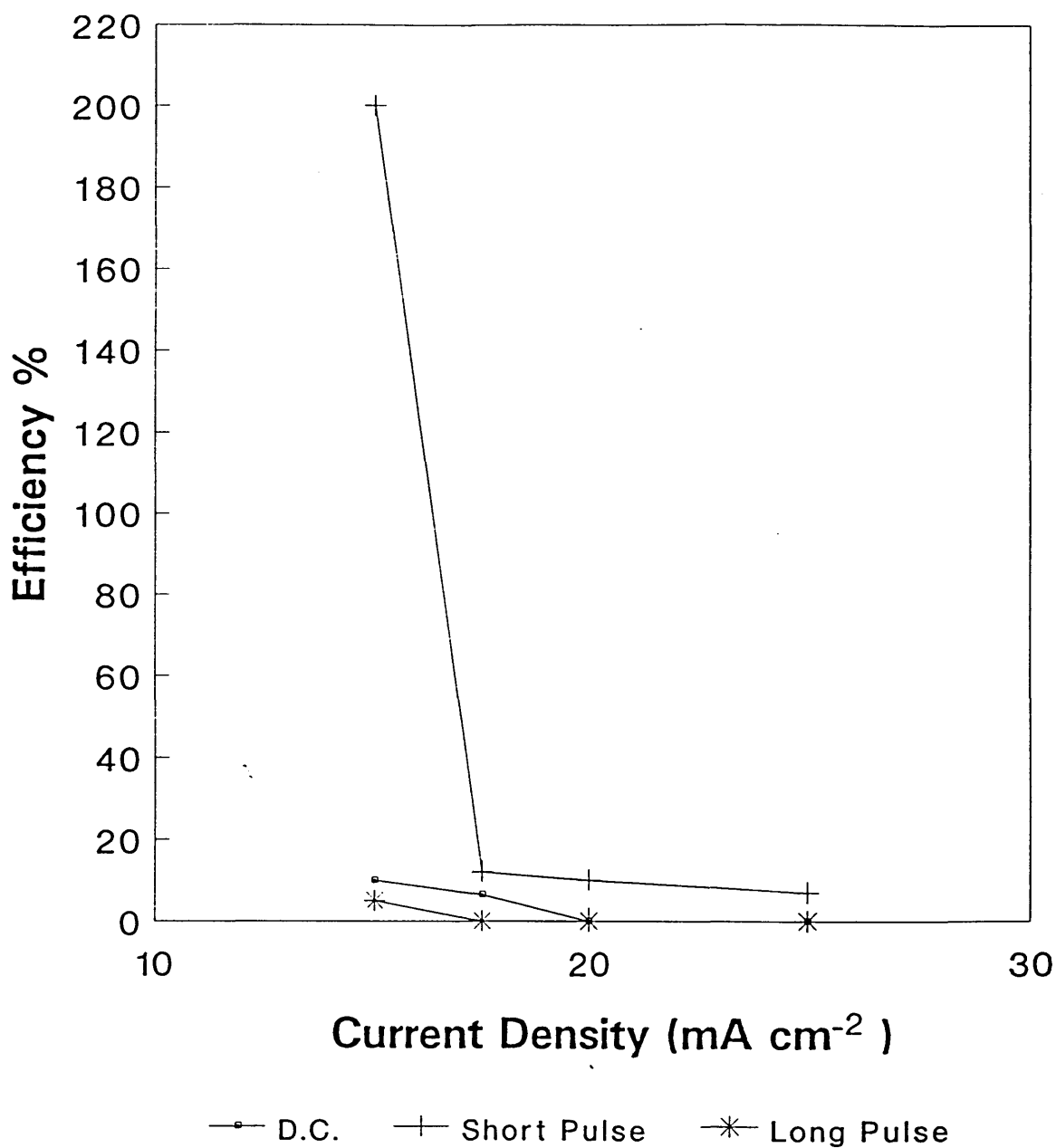
Figure 43.
The apparent anodic efficiencies for dissolution of tin
anodes as a function of anode current density.
Conditions used; bath temperature 50°C, conventional
direct current, short pulsed current (1000Hz) and long
pulsed current (100Hz).
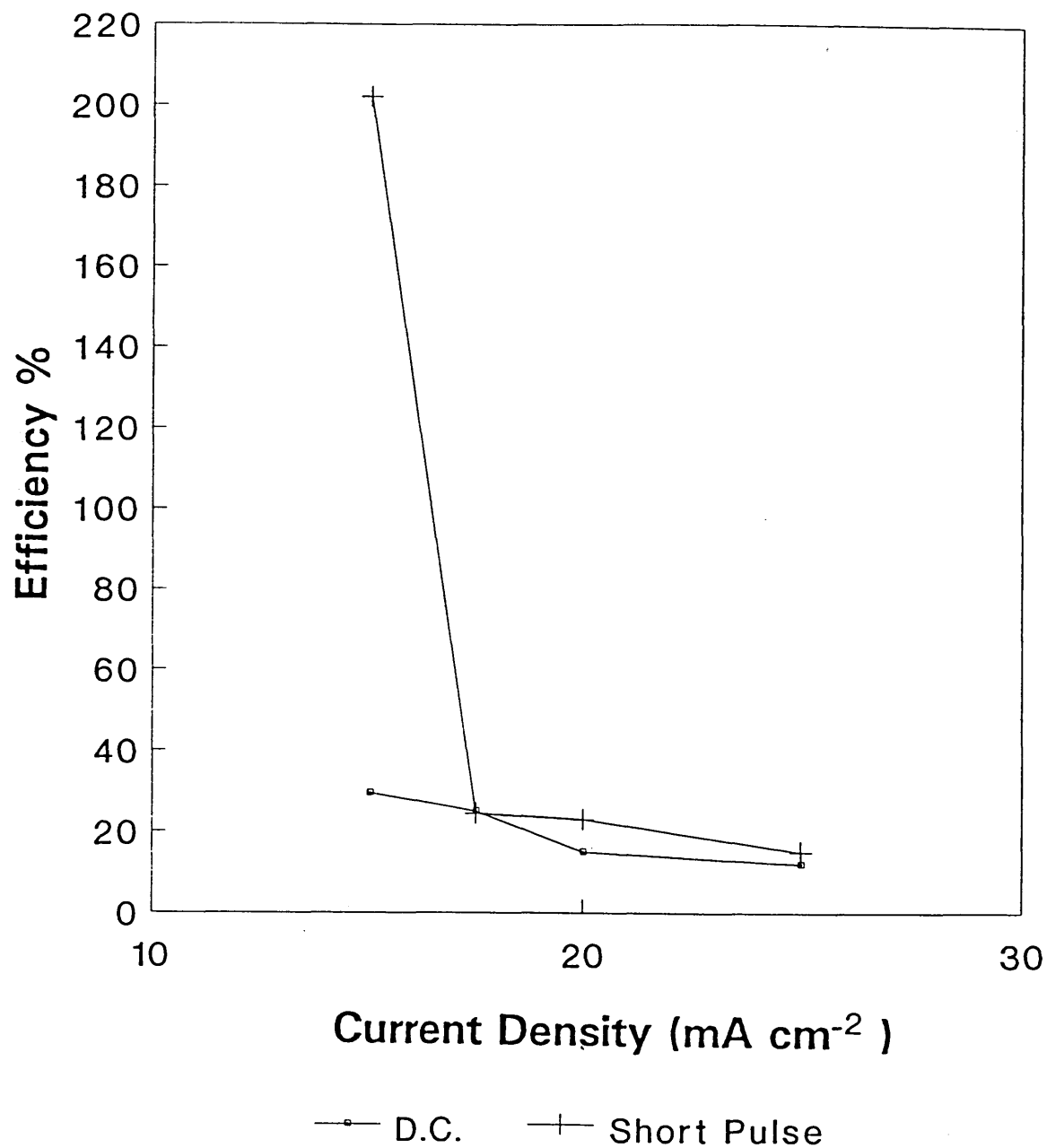
Figure 44.
The apparent anodic efficiencies for dissolution of tin anodes as a function of anode current density. Conditions used; bath temperature 60°C, conventional direct current, short pulsed current (1000Hz) and long pulsed current (100Hz).
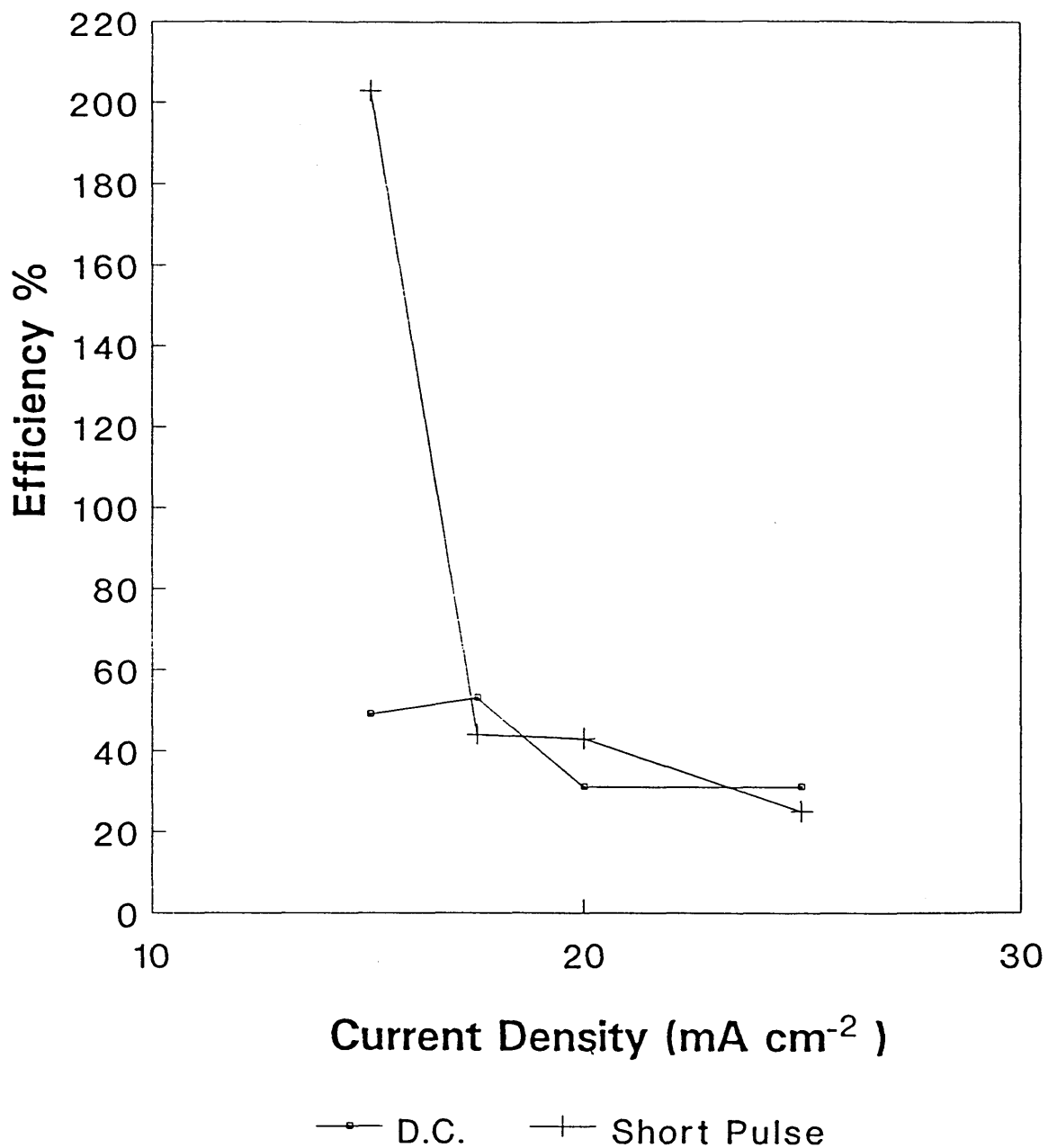
Figure 45.
The apparent anodic efficiencies for dissolution of tin
anodes as a function of anode current density.
Conditions used; bath temperature 70°C, conventional
direct current, short pulsed current (1000Hz) and long
pulsed current (100Hz).
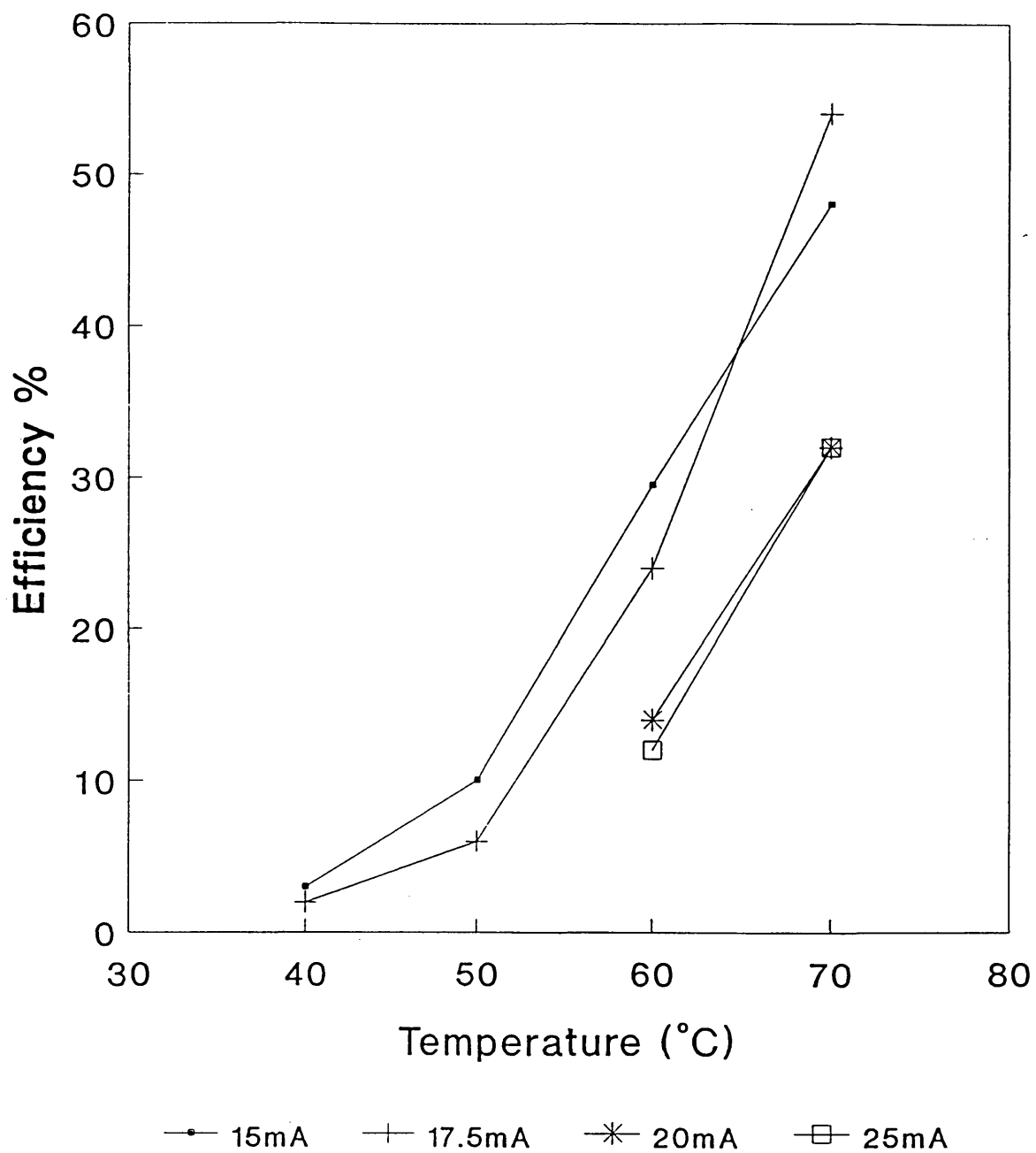
Figure 46.
The apparent anodic efficiencies for dissolution of tin anodes as a function of plating bath temperature, using conventional direct current at different current densities.
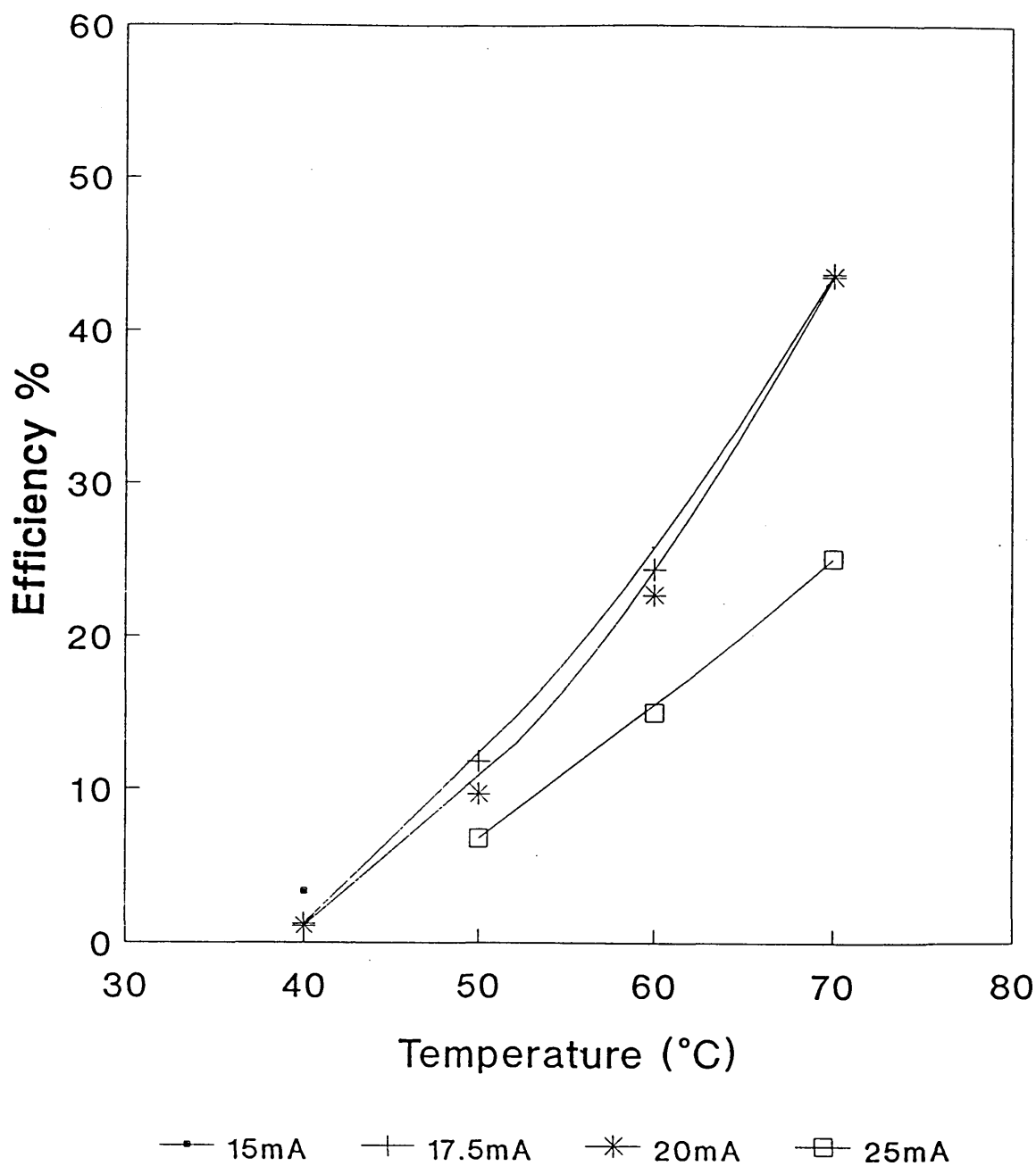
<u>Figure 47.</u>
The apparent anodic efficiencies for dissolution of tin
anodes as a function of plating bath temperature, using
short pulsed current (1000Hz) at different current
densities.
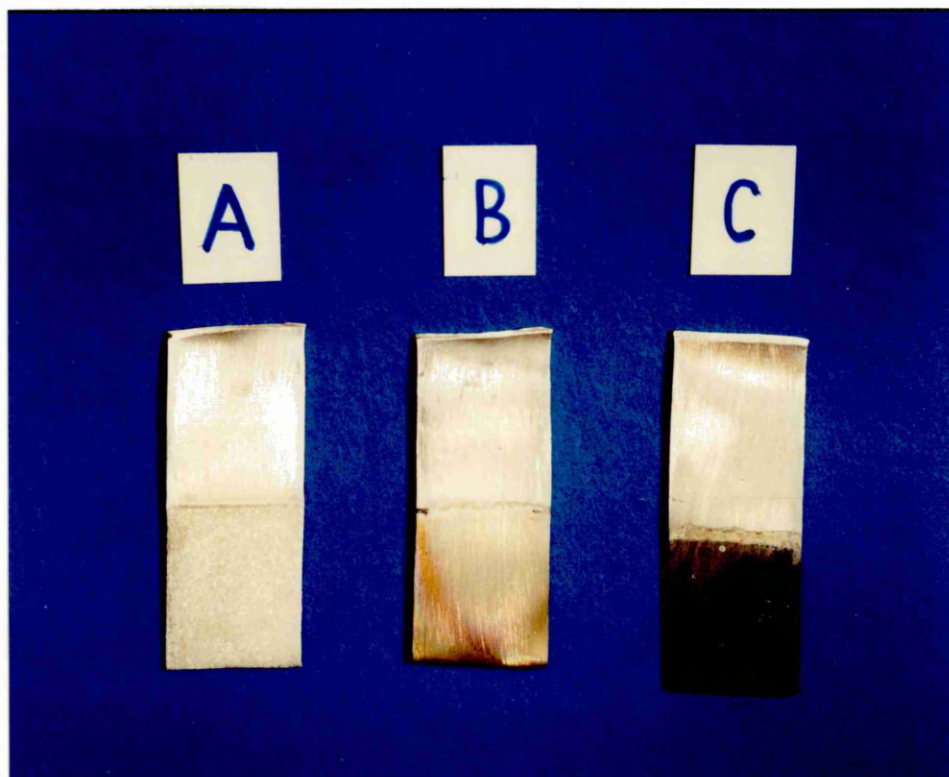
<u>Figure 48.</u>
Tin anodes used for dissolution experiments.
A) Acceptable anode surface with slight yellow film.
B) Anode which developed a black mossy deposit during
   testing. The deposit could be washed off easily.
C) Anode which passivated during testing and developed
   a permanent black oxide layer.
             (Original in Colour)
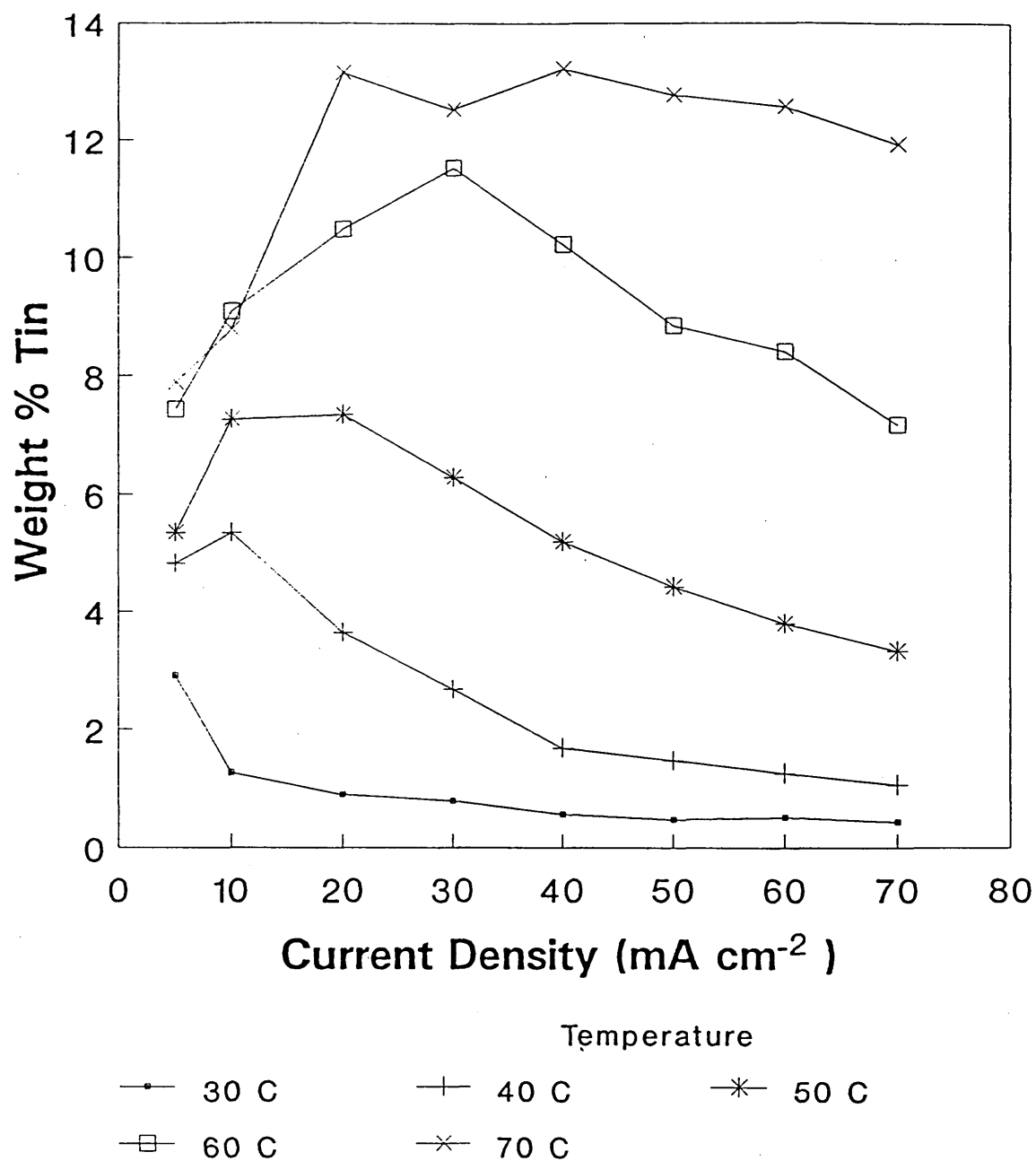
<u>Figure 49.</u>
The variation in Tin content of deposits as a function
of cathode current density, for bath temperatures from
30°C to 70°C using conventional direct current.
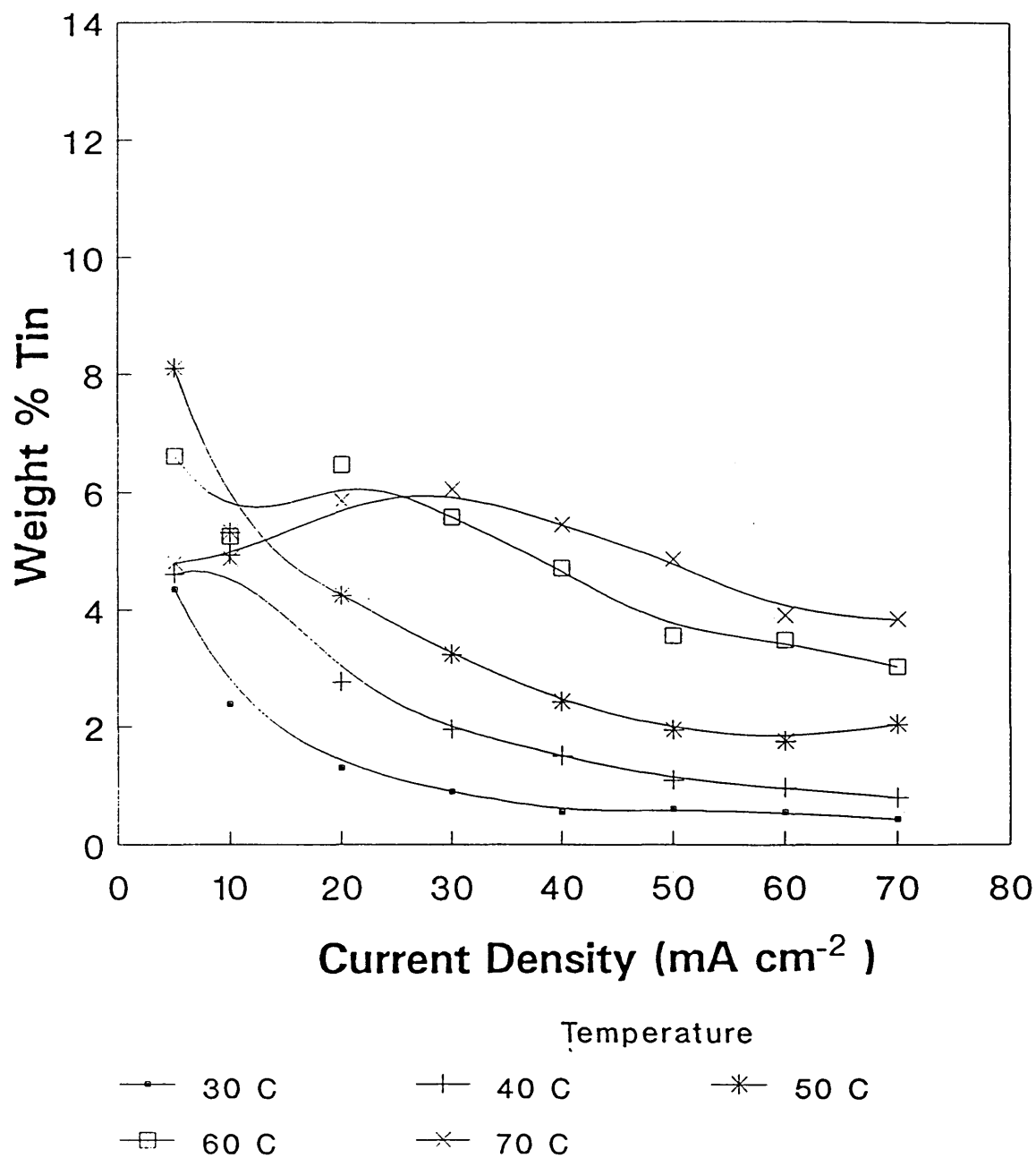
<u>Figure 50.</u>
The variation in Tin content of deposits as a function
of average cathode current density, for bath
temperatures from 30°C to 70°C using short pulsed
current (1000Hz).
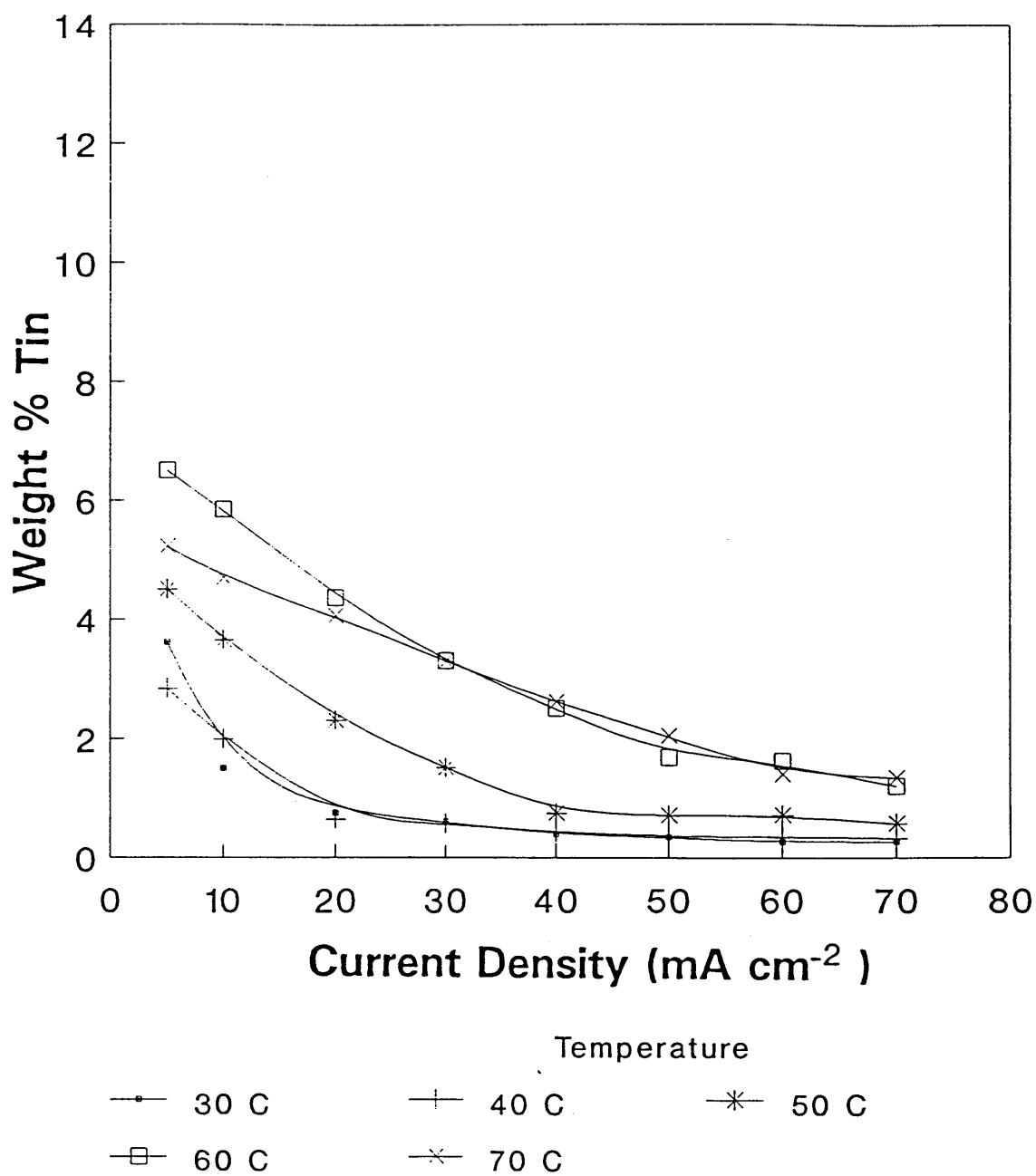
<u>Figure 51.</u>
The variation in Tin content of deposits as a function
of average cathode current density, for bath
temperatures from 30°C to 70°C using long pulsed
current (100Hz).
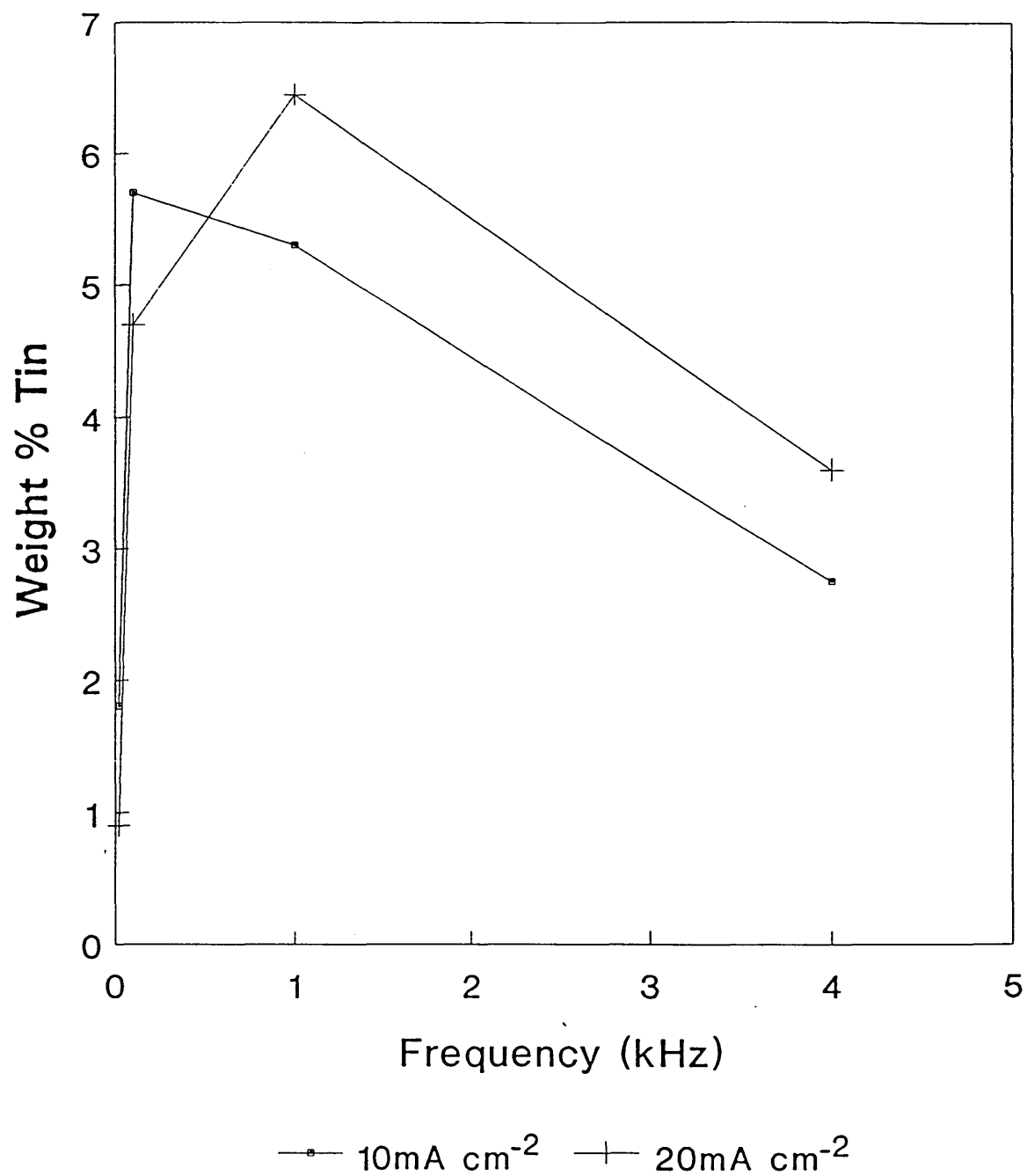
Figure 52.
The variation in Tin content of deposits as a function
of pulse frequency, for average current densities of
10mA cm^{-2} and 20mA cm^{-2} and a bath temperature of 60°C.
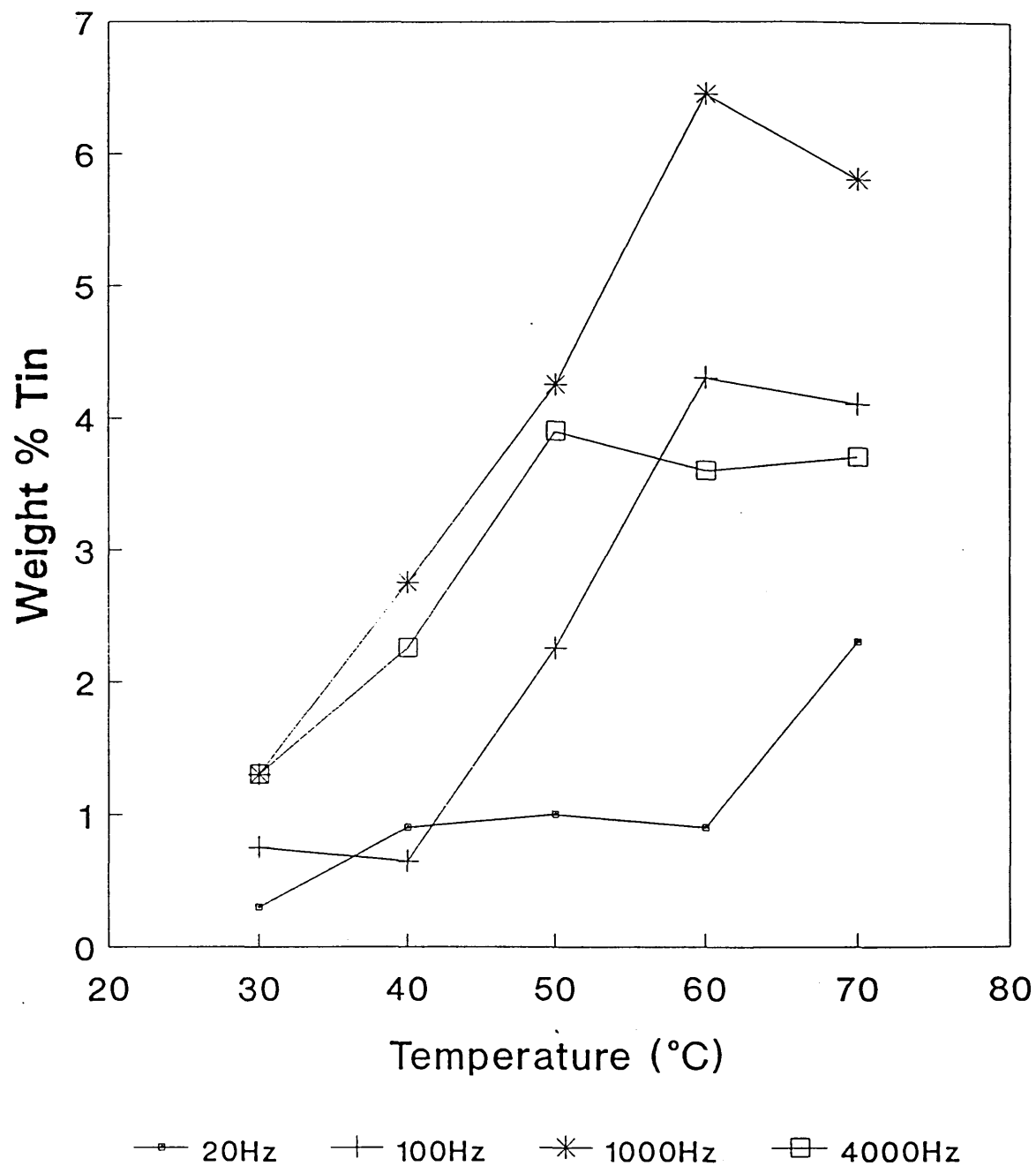
Figure 54.
The variation in Tin content of deposits as a function
of temperature, for different pulse frequencies at an
average current density of 20mA cm^{-2}.
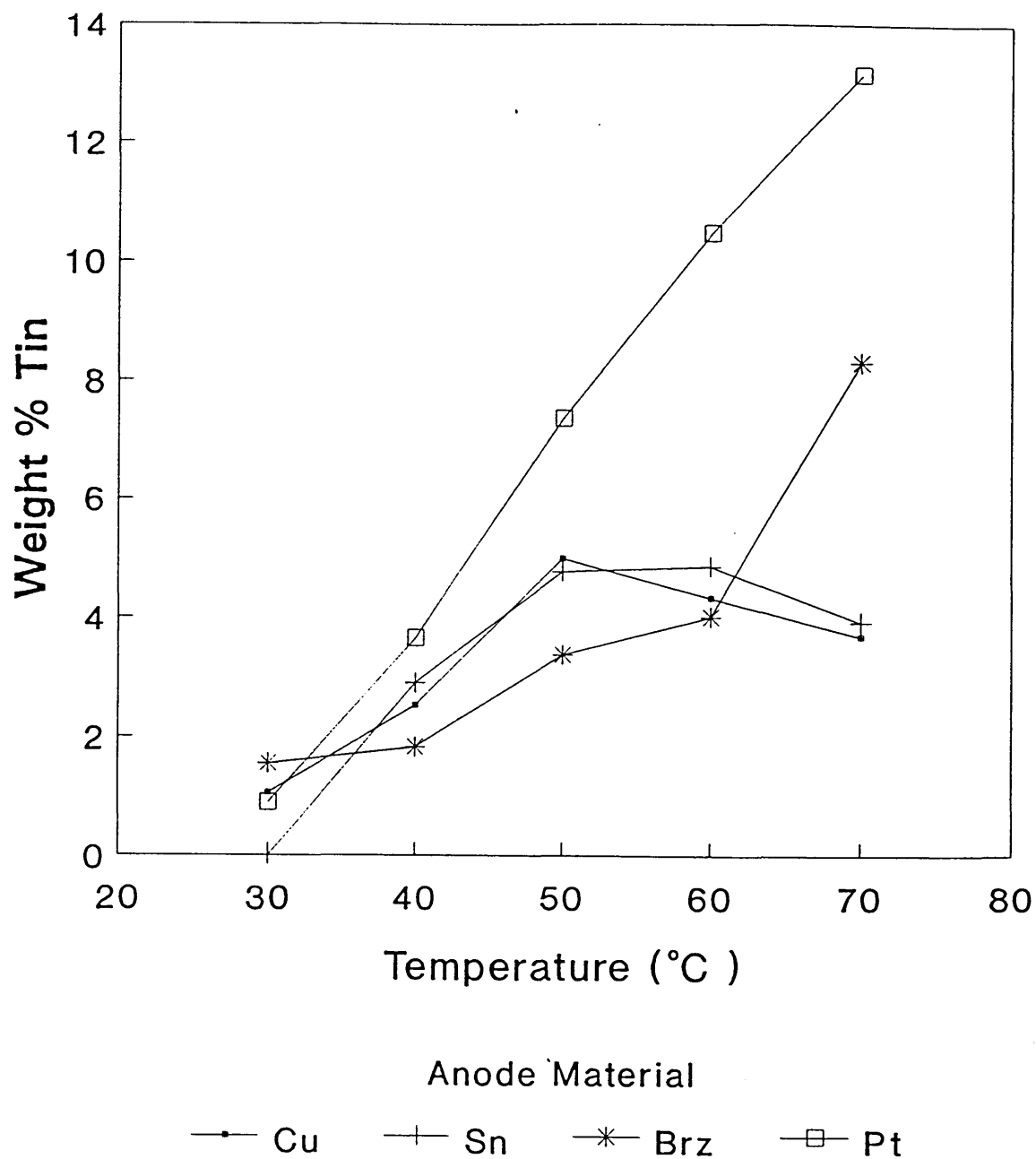
<u>Figure 55.</u>
The variation in Tin content of deposits as a function
of temperature, for different anode materials using
conventional direct current at 20mA cm^{-2} current
density.
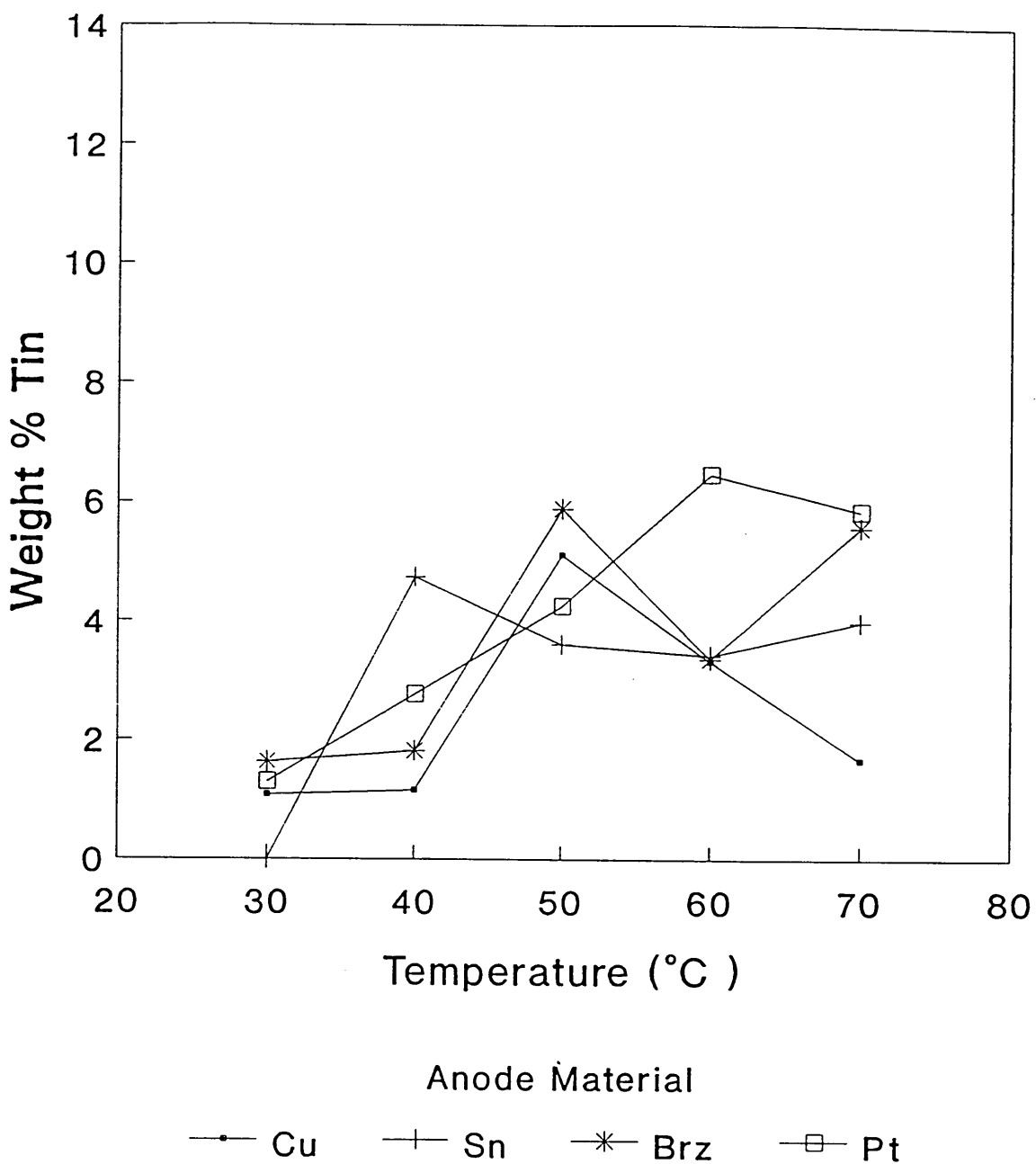
Figure 56.
The variation in Tin content of deposits as a function
of temperature, for different anode materials using
short pulsed current (1000Hz) at 20mA cm^{-2} average
current density.
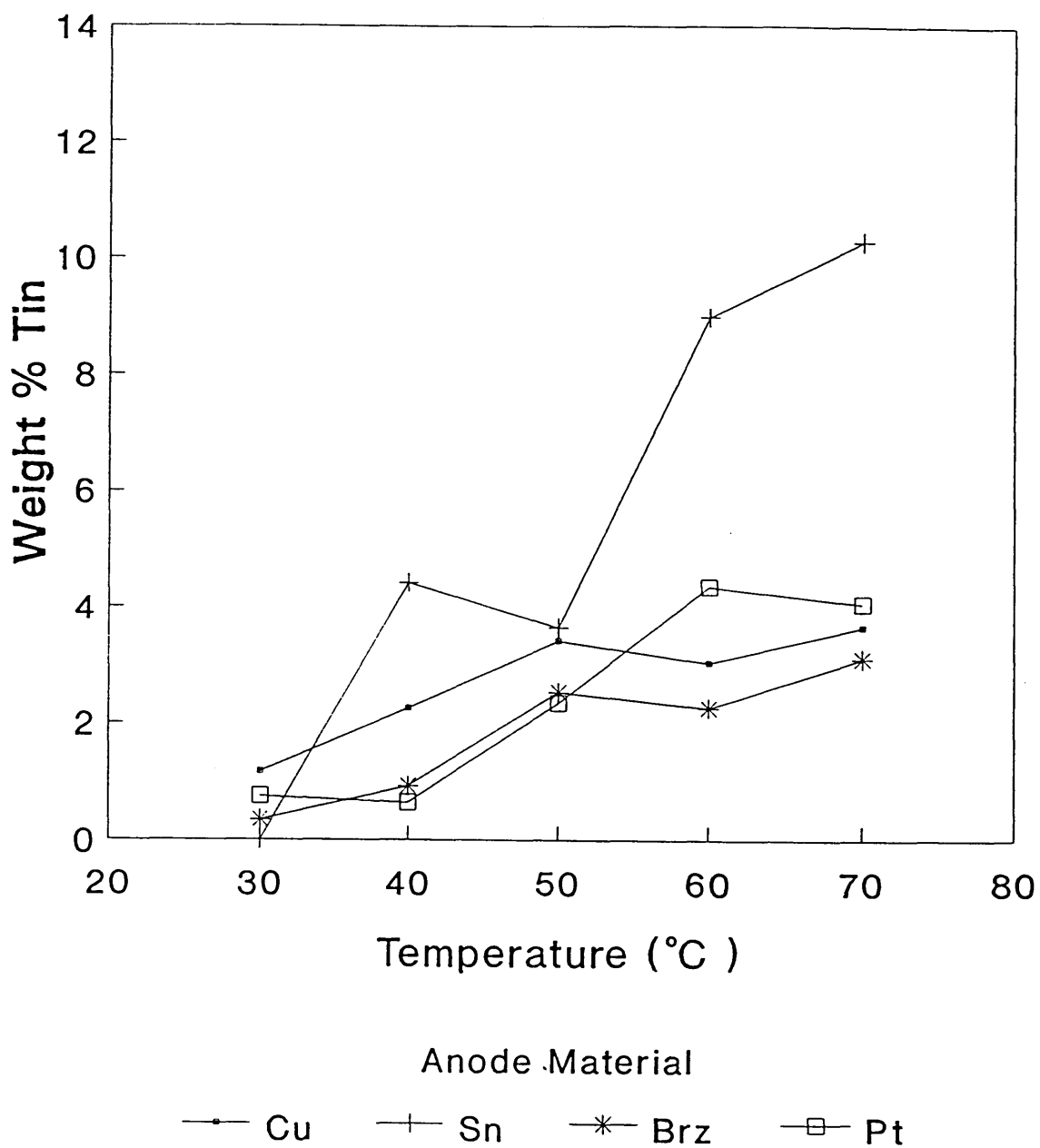
Figure 57.
The variation in Tin content of deposits as a function
of temperature, for different anode materials using
long pulsed current (100Hz) at 20mA cm^{-2} average
current density.
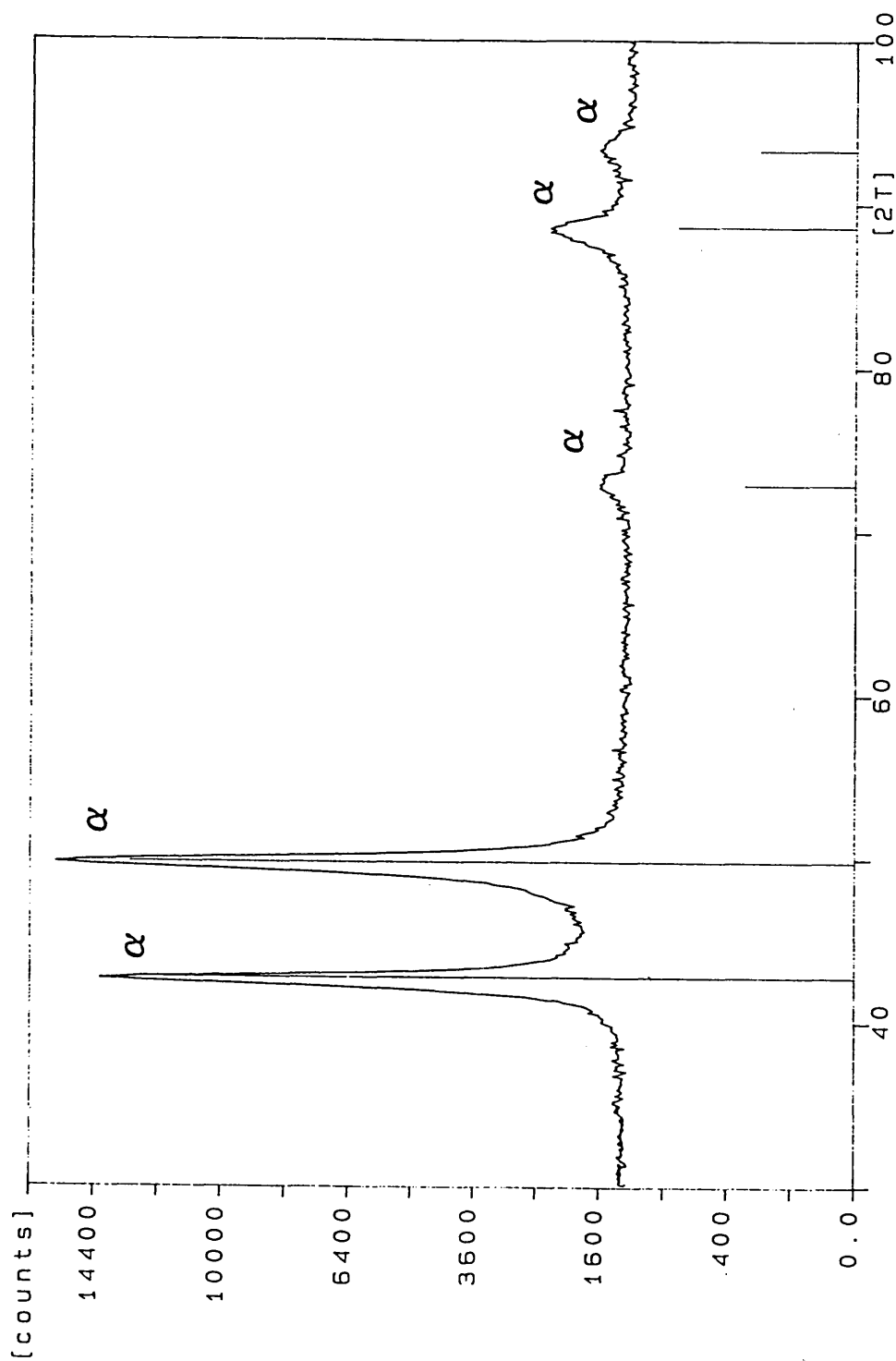
Figure 58.

X-Ray Diffraction trace of a bronze deposit containing 5.84% Tin. The deposit was produced from a bath at 60°C using long pulsed electrolysis (100Hz), at an average cathode current density of 10mA cm^{-2}.
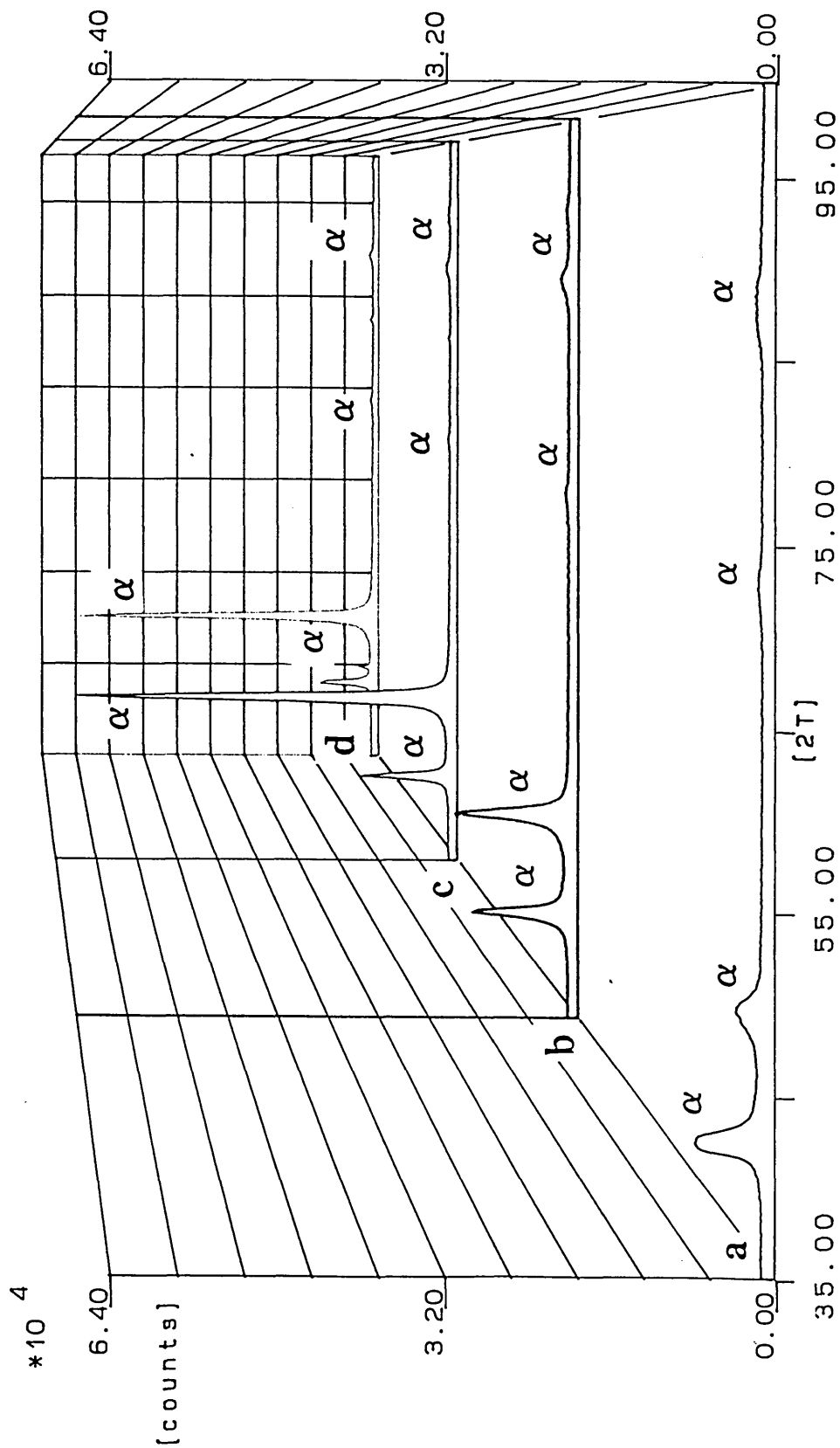
Figure 59.

X-Ray Diffraction traces of deposits obtained from a bath at 60°C using long pulsed electrolysis at different average cathode current densities.(a) 5mA cm^{-2}(composition 6.51% Tin).(b) 10mA cm^{-2}(composition 5.84% Tin).(c) 30mA cm^{-2} (composition 3.29% Tin).(d) 70mA cm^{-2}(composition 1.2% Tin).
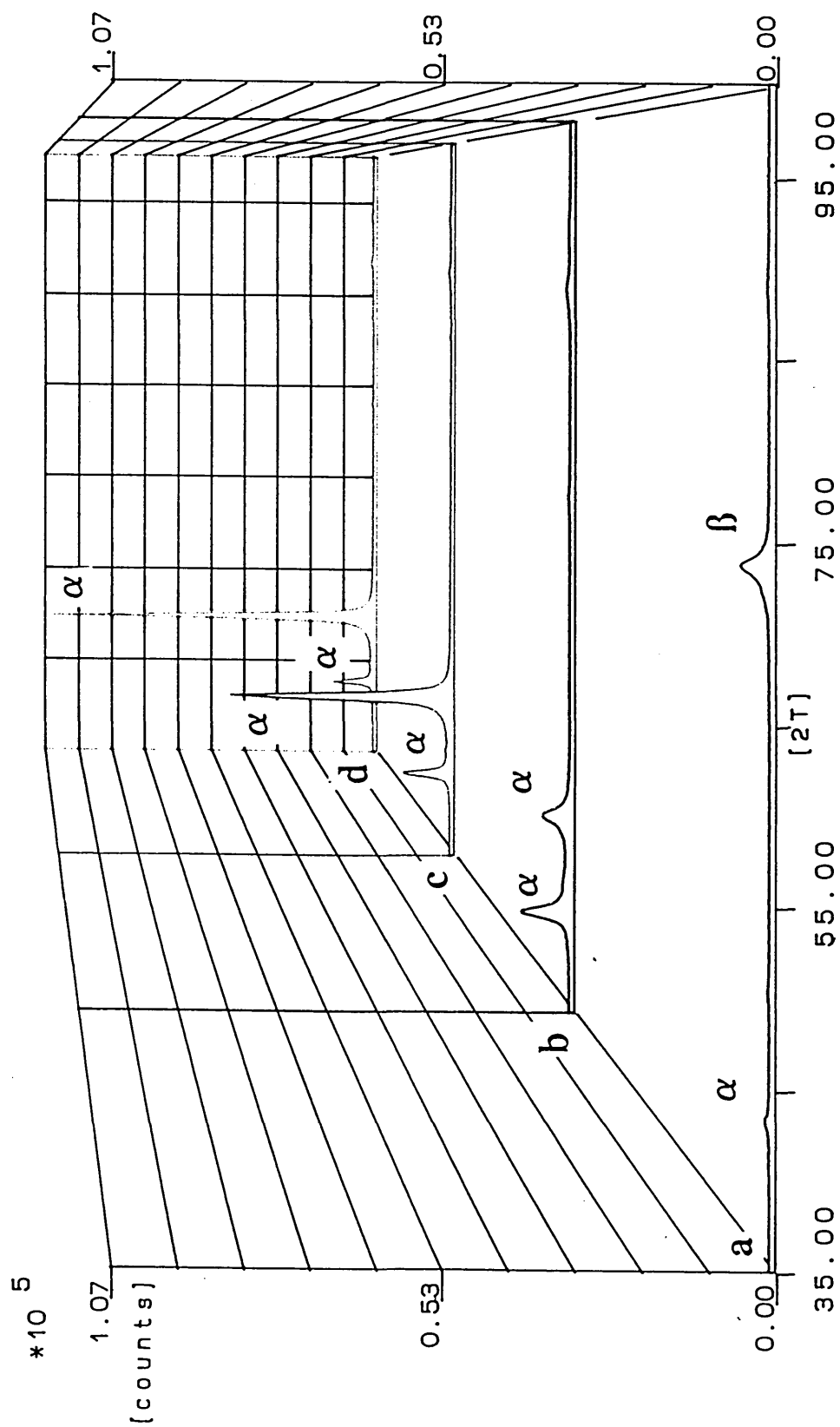
Figure 60.

X-Ray Diffraction traces of deposits obtained from a bath at 60°C using short pulsed electrolysis at different average cathode current densities. (a) 5mA cm^{-2}(composition 6.61% Tin). (b) 20mA cm^{-2}(composition 6.46% Tin). (c) 50mA cm^{-2} (composition 3.55% Tin). (d) 70mA cm^{-2}(composition3.02% Tin).
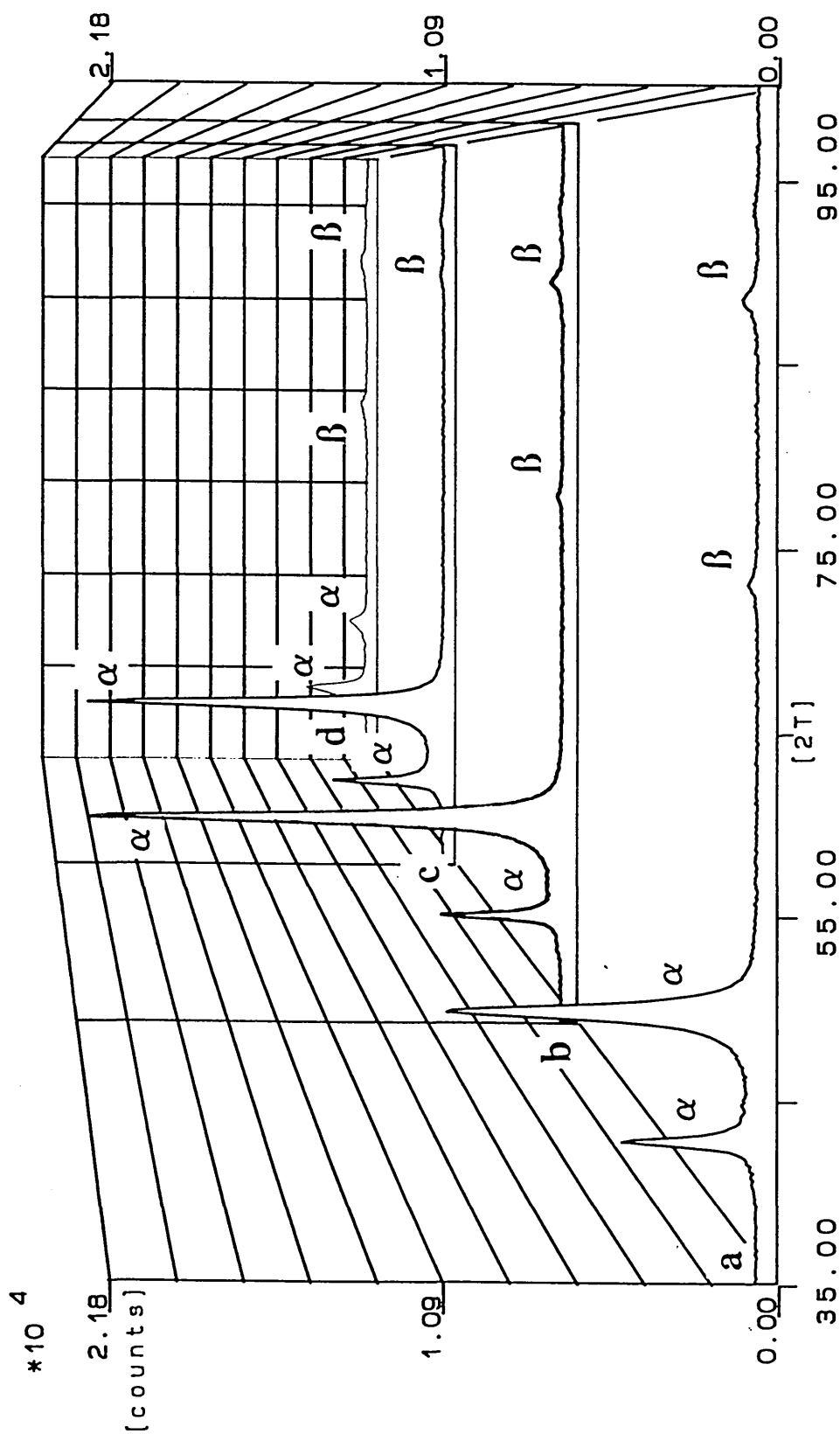
Figure 61.

X-Ray Diffraction traces of deposits obtained using short pulsed electrolysis at an average cathode current density of 5mA cm^{-2} and different bath temperatures.(a) 30°C (composition 4.35% Tin).(b) 40°C(composition 4.61% Tin).(c) 50°C(composition 8.1% Tin).(d) 70°C(composition 4.8% Tin).
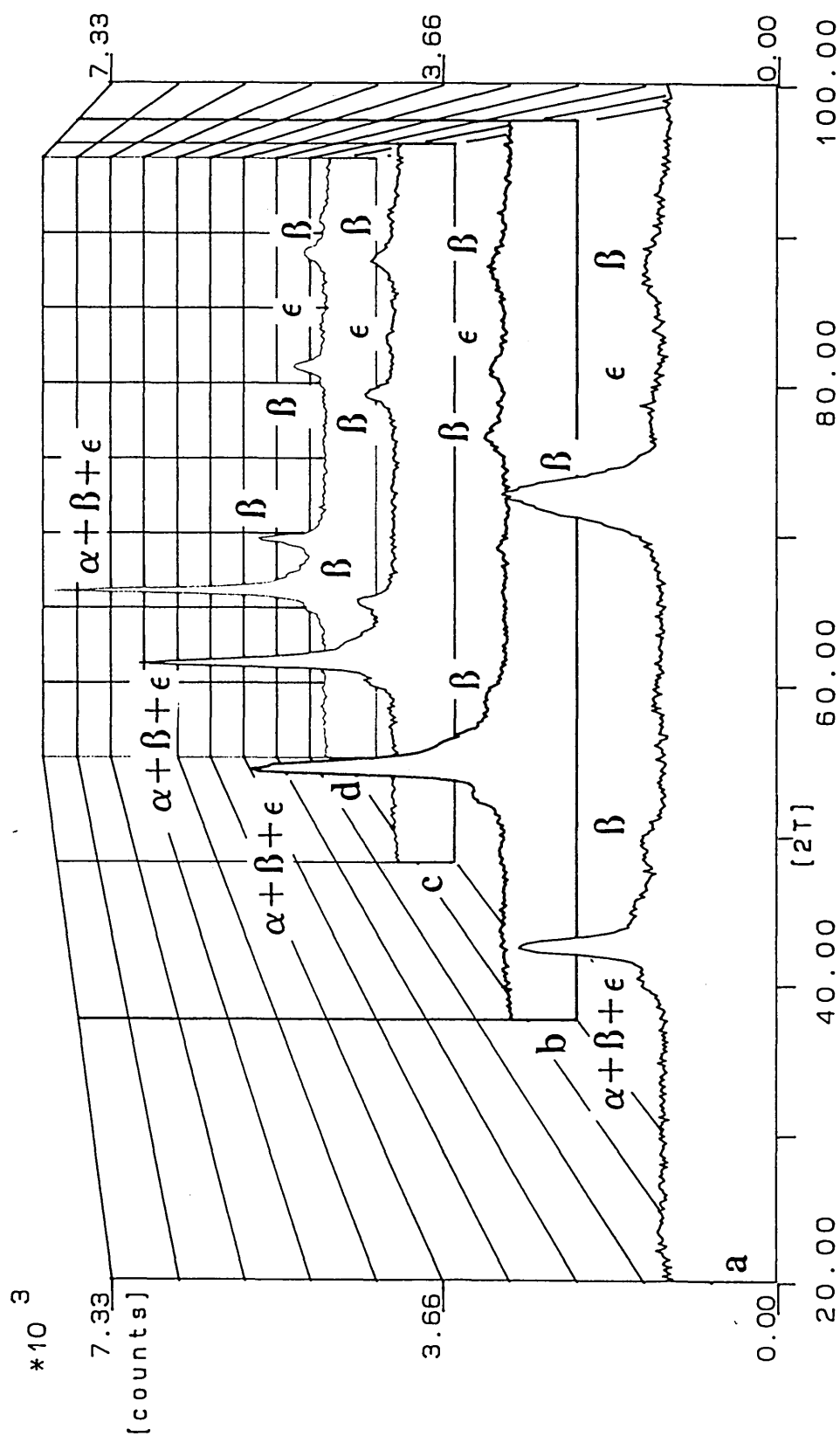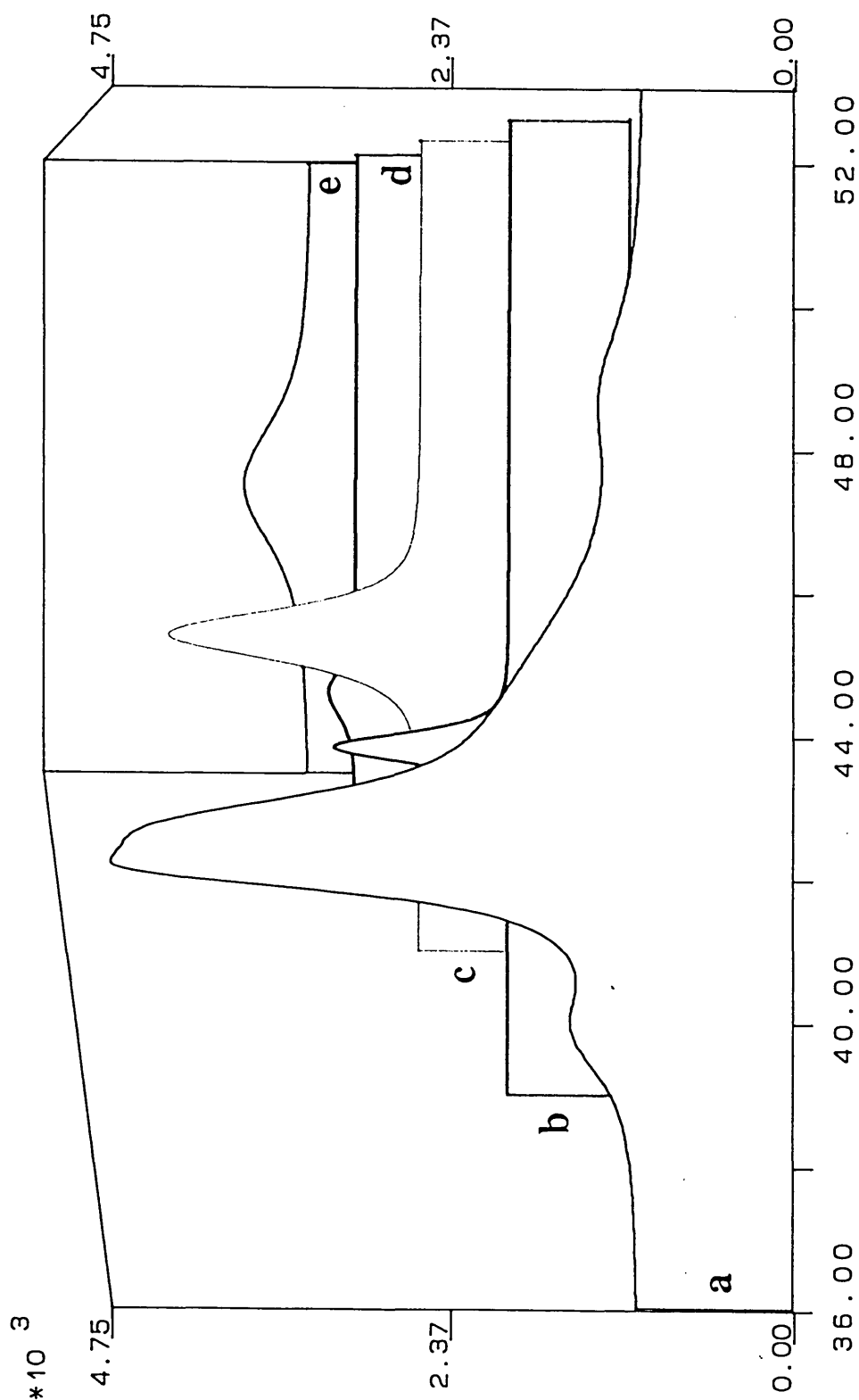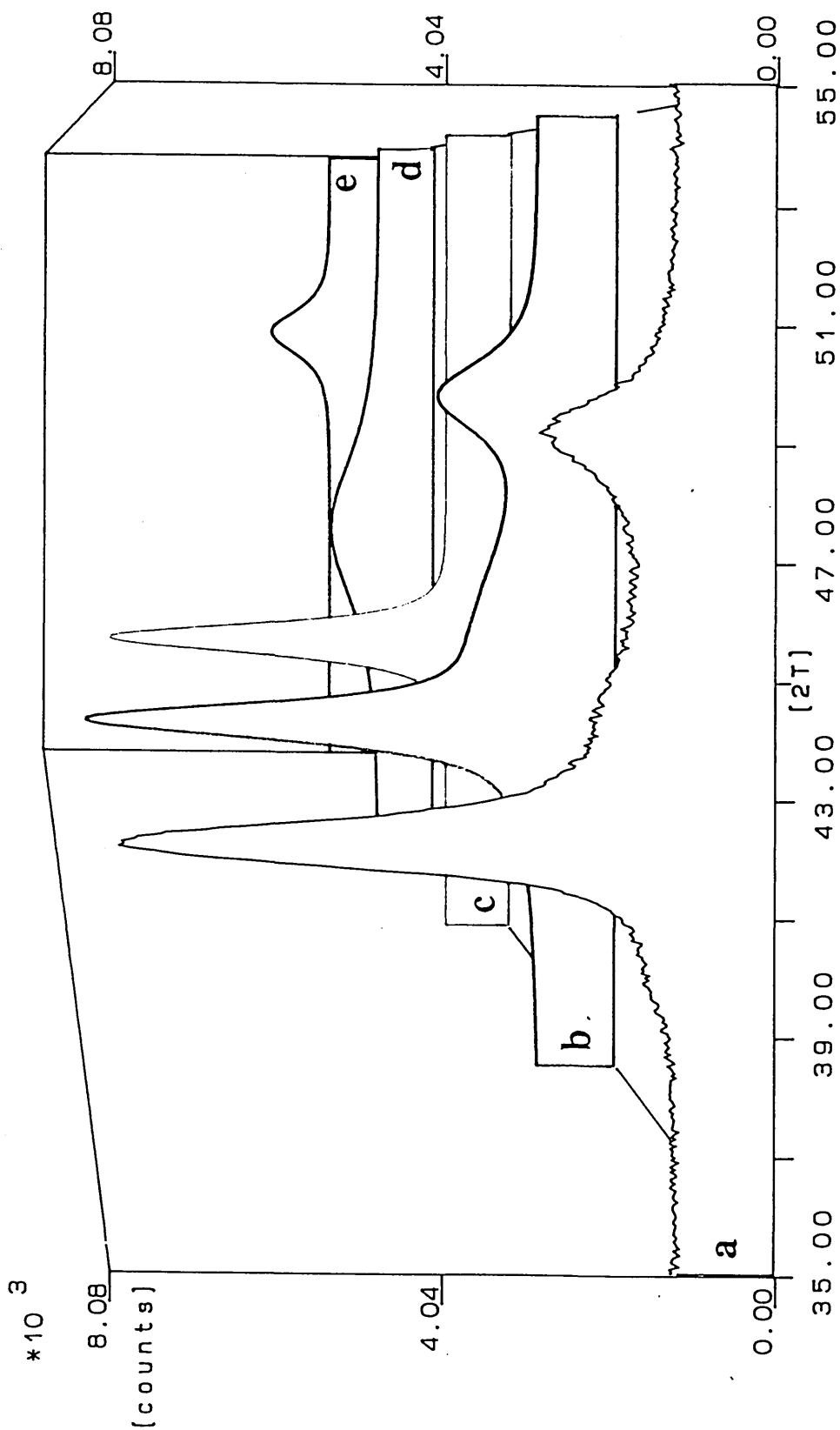
Figure 62.

X-Ray Diffraction traces of deposits obtained from a bath at 60°C using conventional current electrolysis at different cathode current densities.(a) 5mA cm^{-2}(composition 7.43% Tin).(b) 30mA cm^{-2}(composition 11.51% Tin).(c) 50mA cm^{-2}(composition 8.84% Tin).(d) 70mA cm^{-2}(composition 7.17%Tin).
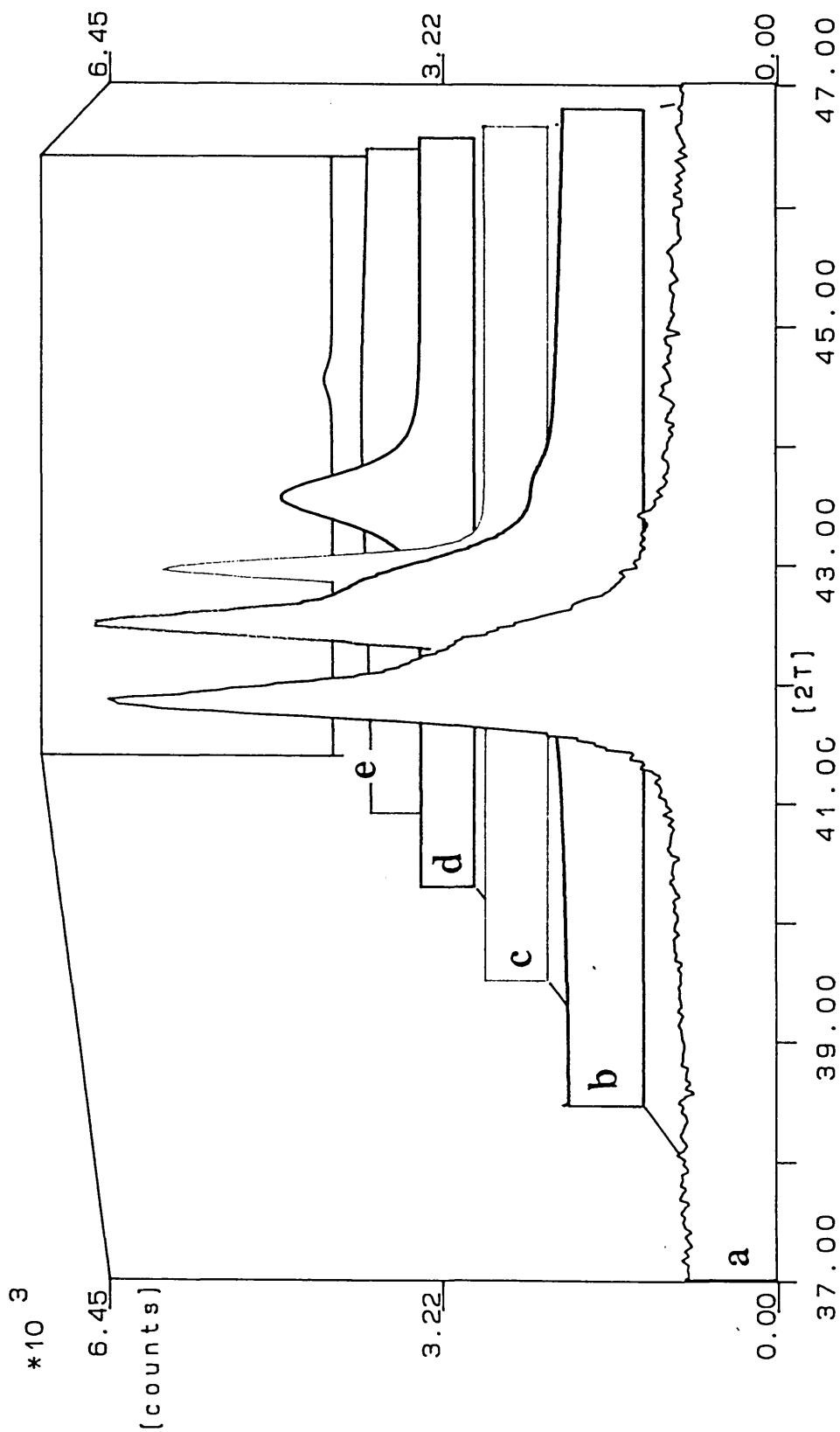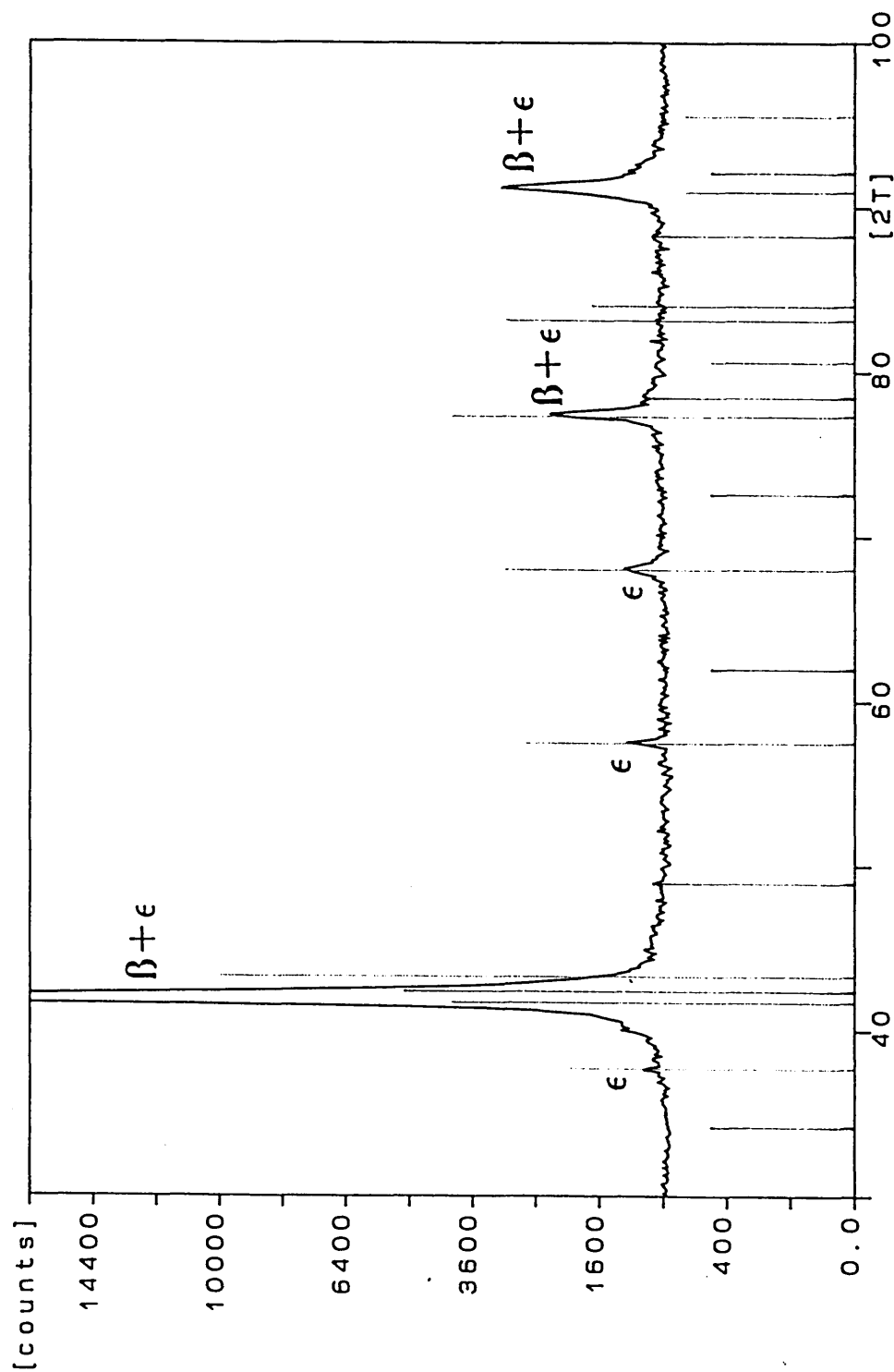
Figure 63.

Fitted X-Ray Diffraction trace of a deposit obtained from a bath at 60°C using conventional current electrolysis at 10mA cm^{-2} cathode current density(composition 9.09% Tin). The peaks shown are (a) Raw data peak.(b) Smoothed data peak. (c) Beta.(d) Epsilon.(e) Beta. The peaks are resolved from the complex peak present at a two theta value of 42°.

Figure 64.

Fitted X-Ray Diffraction trace of a deposit obtained from a bath at 60°C using conventional current electrolysis at 30mA cm^{-2} cathode current density (composition 11.51% Tin). The peaks shown are (a) Smoothed data.(b) Beta.(c) Epsilon. (d) Beta.(e) Amorphous.

Figure 65.

Fitted X-Ray Diffraction trace of a deposit obtained from
a bath at 50°C using conventional current electrolysis at
20mA cm^{-2} cathode current density (composition 3.64% Tin).
The peaks shown are (a) Raw data. (b) Smoothed data. (c) Beta.
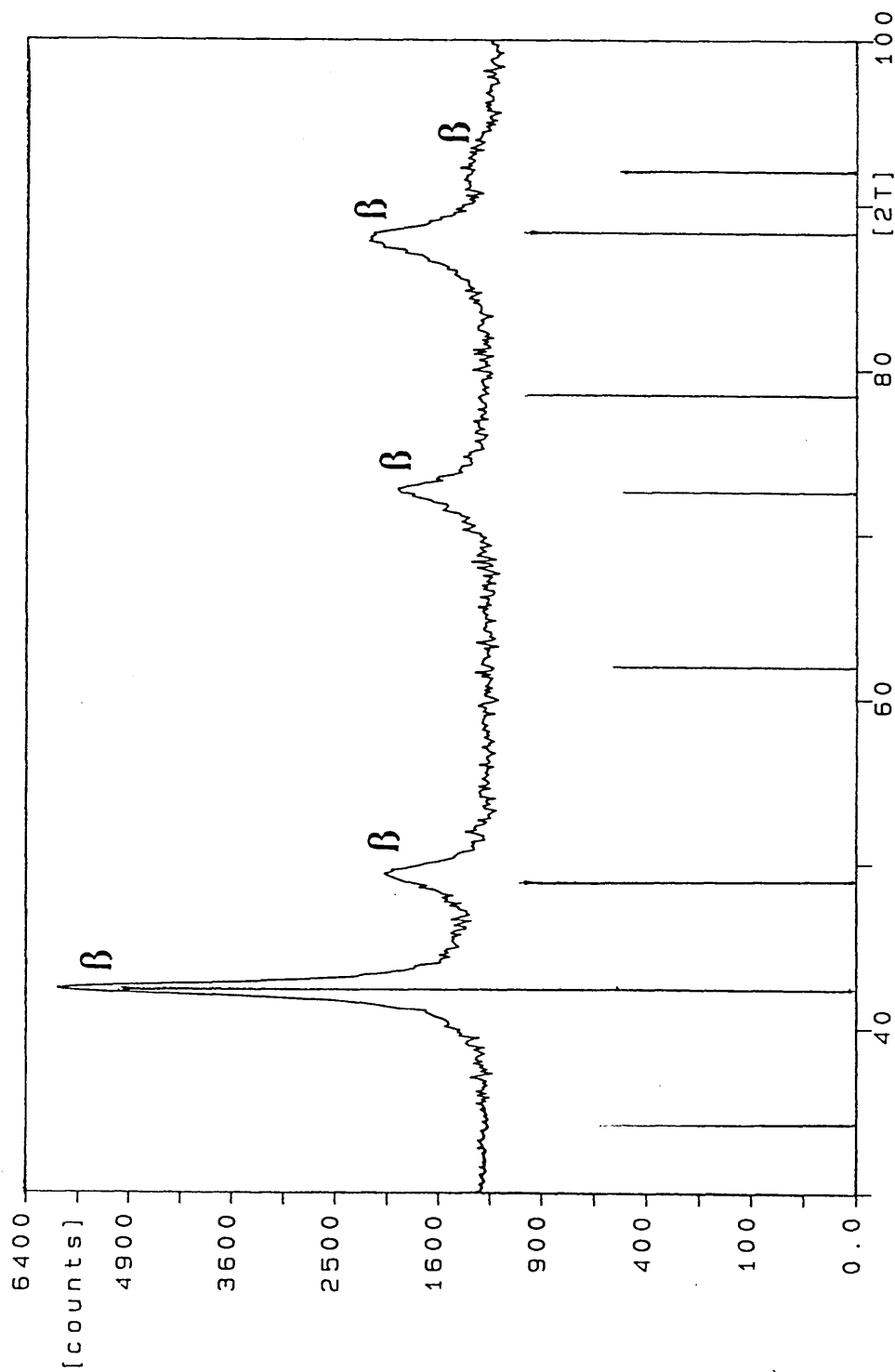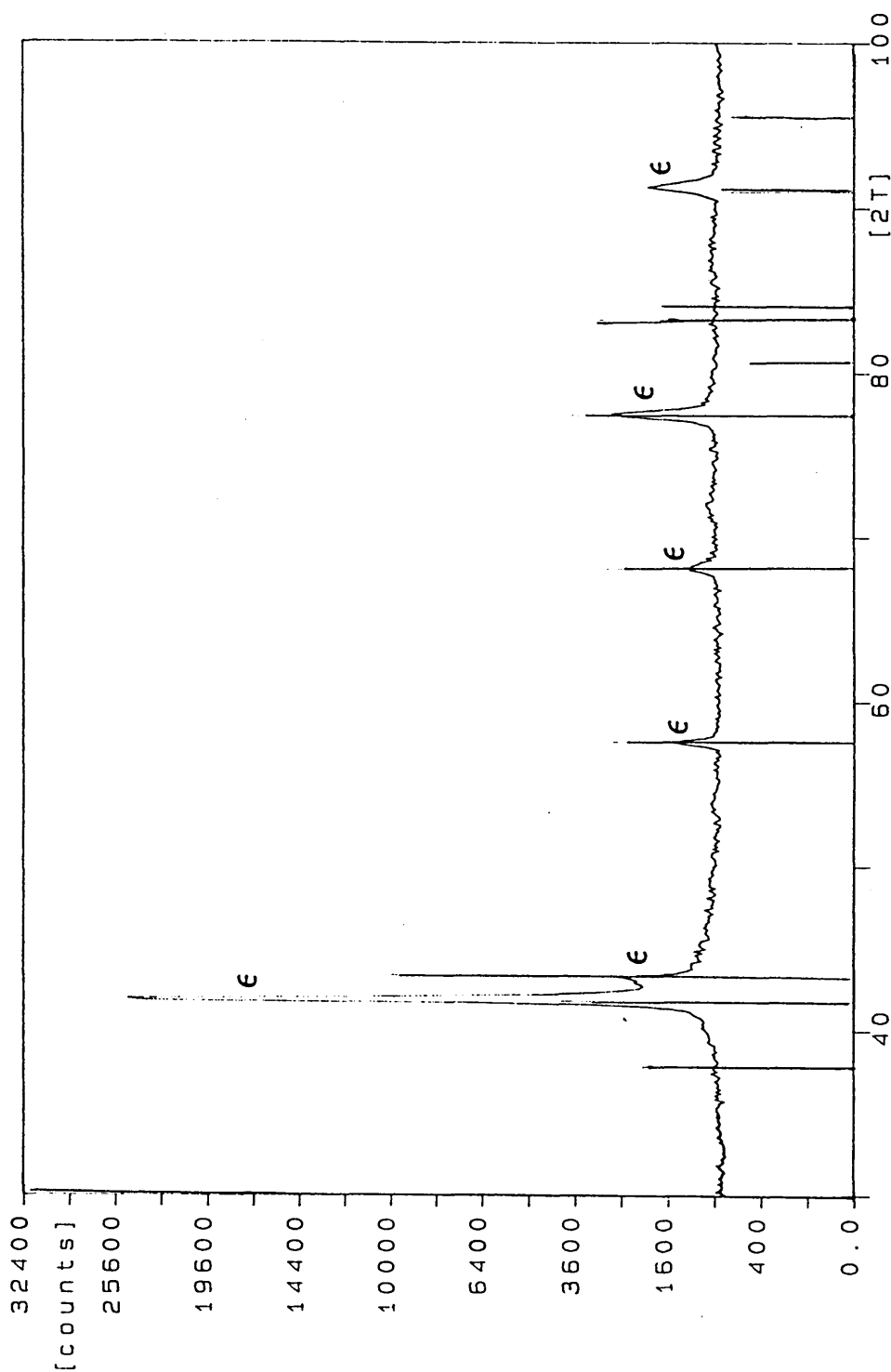(d) Amorphous. (e) Beta.

Figure 66.

X-Ray Diffraction trace of a deposit obtained from a bath at 70°C using conventional current electrolysis at a cathode current density of 20mA cm^{-2}(composition 13.15%Tin) The peak markers clearly show the deposit to consist of beta and epsilon phases.

Figure 67.

X-Ray Diffraction trace of a deposit obtained from a bath at 50°C using conventional current electrolysis at a cathode current density of 10mA cm^{-2} (composition 5.34%Tin) The peak markers clearly show the deposit to consist of mainly the beta phase.

Figure 68.

X-Ray Diffraction trace of a deposit obtained from a bath at 70°C using conventional current electrolysis at a cathode current density of 30mA cm^{-2} (composition 12.51%Tin) The peak markers clearly show the deposit to consist of mainly the epsilon phase.
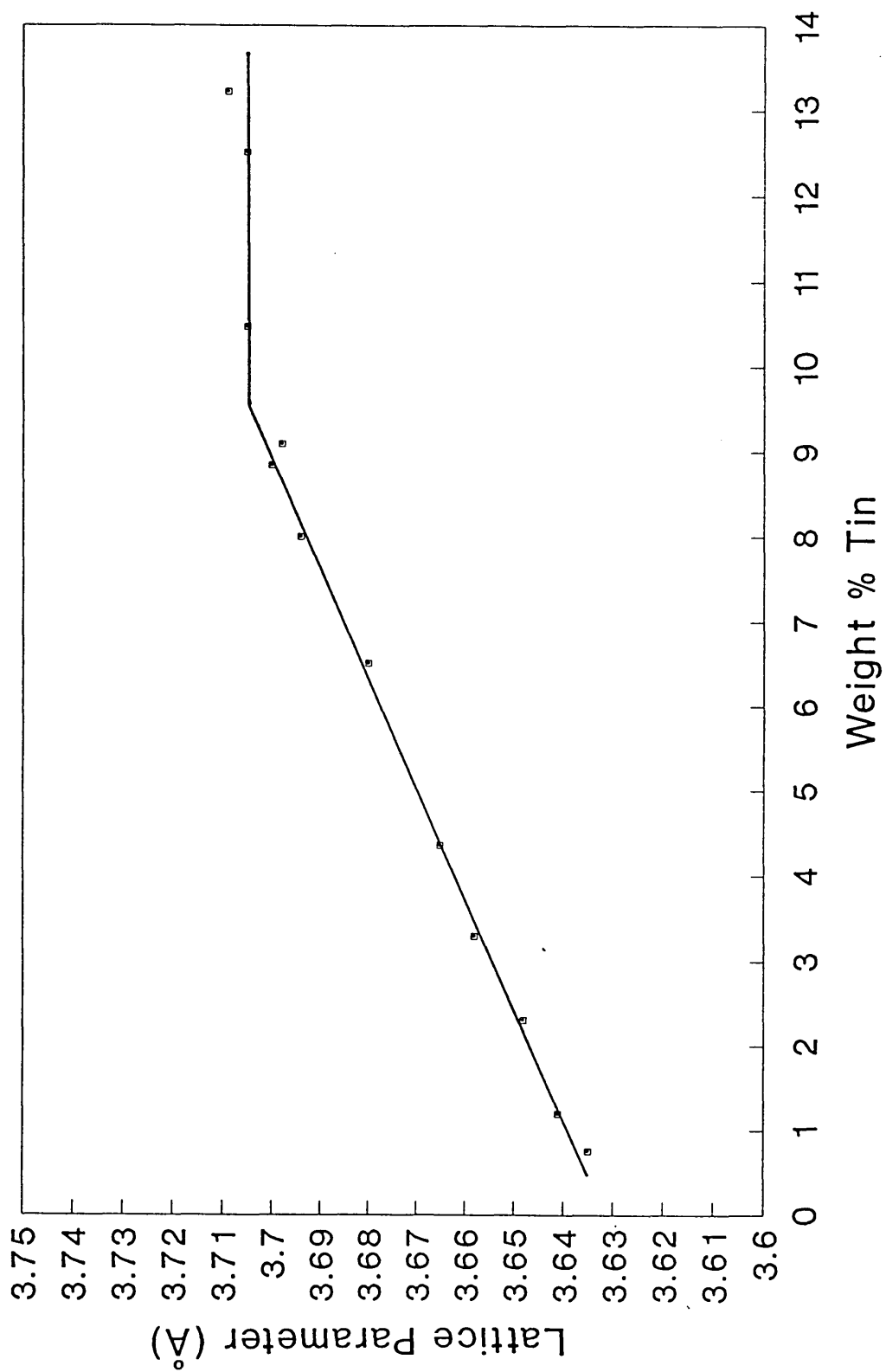
Figure 69.

Increase in lattice parameter of the alpha phase in bronze deposits as a function of the deposits tin content. The change in slope at a tin content of nine per cent suggests the presence of a phase boundary.
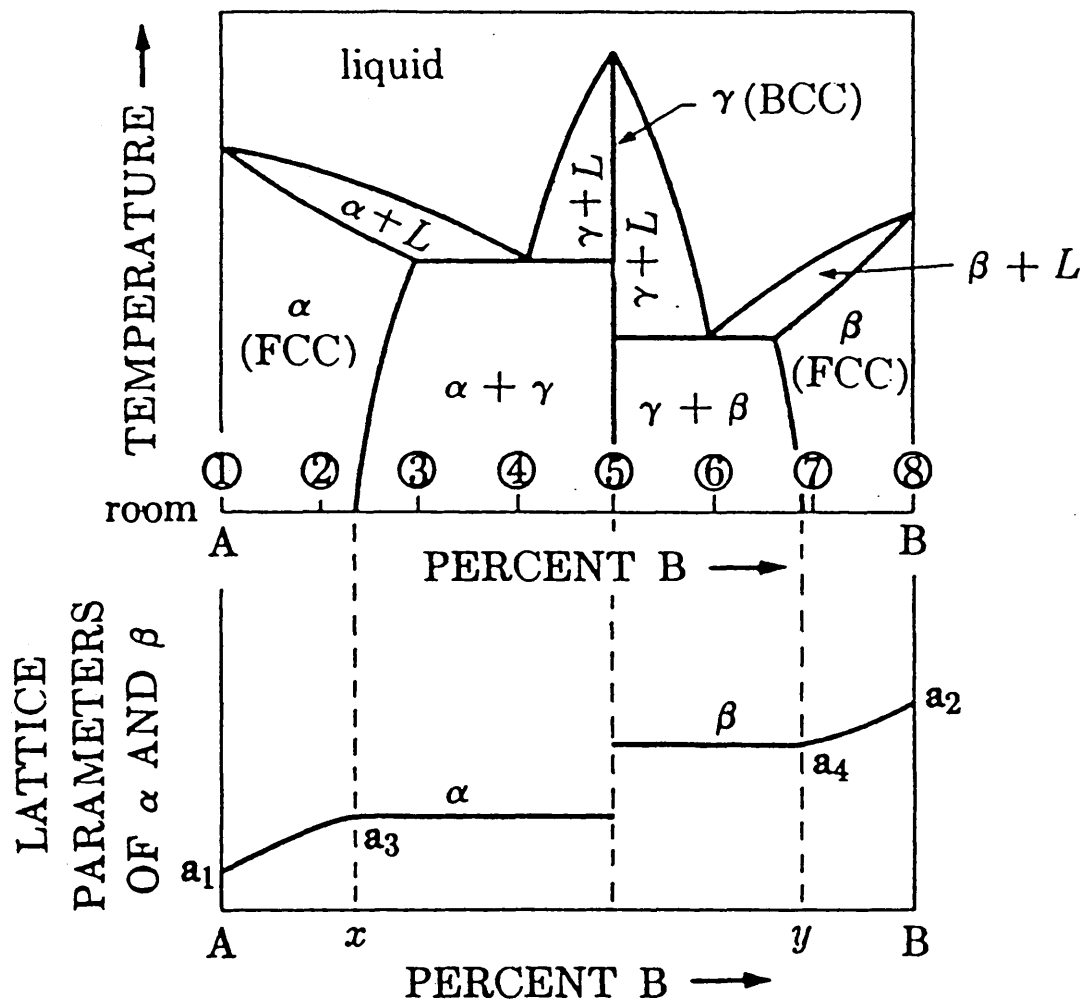
Figure 70.
Schematic representation of the relationship between
lattice parameter and phase boundaries showing how the
lattice parameter changes with composition.
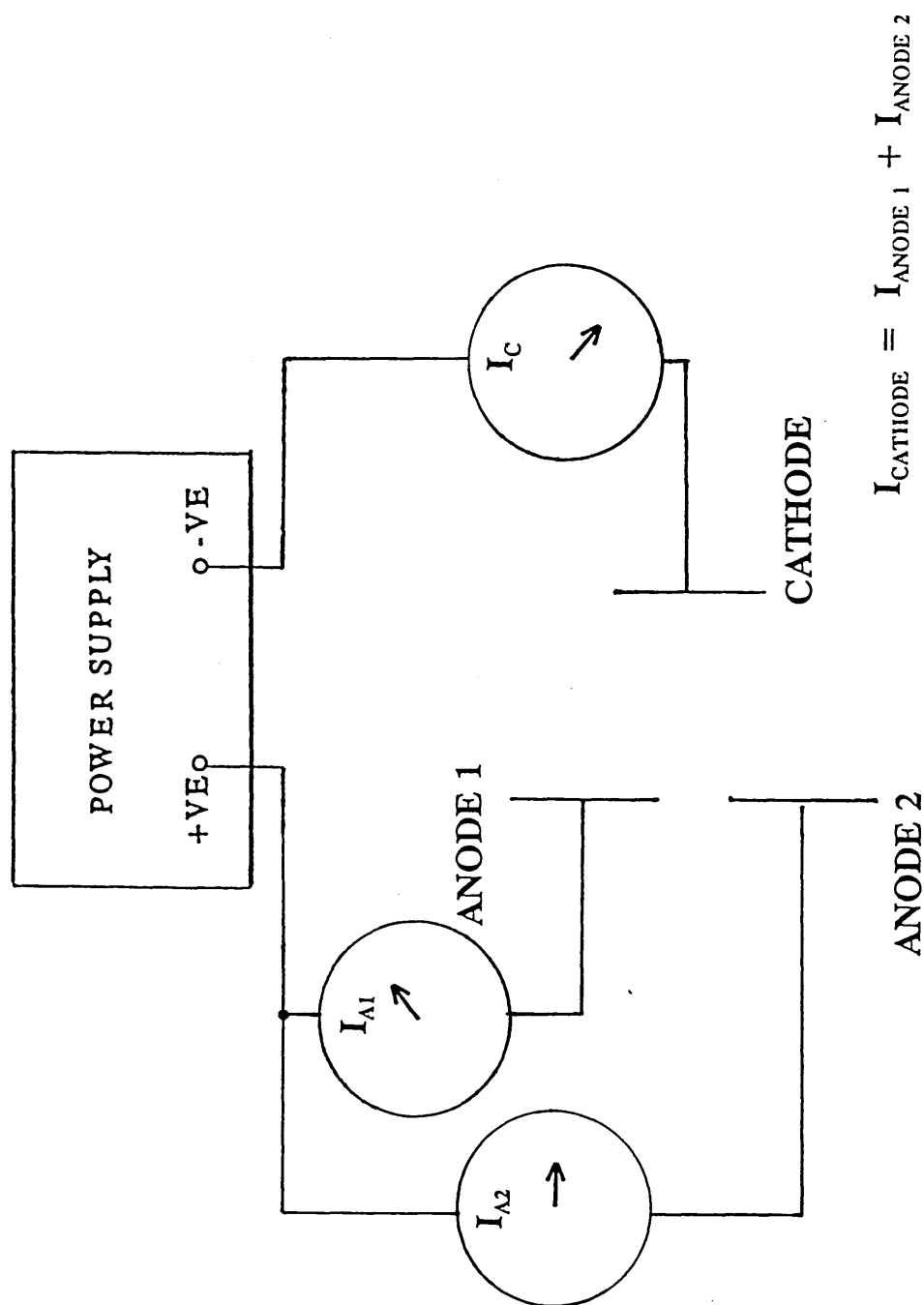(After Cullity (ref 55))

POWER SUPPLY

+VE

-VE

I_{A1}

I_{A2}

I_C

ANODE 1

ANODE 2

CATHODE

$$I_{CATHODE} = I_{ANODE\ 1} + I_{ANODE\ 2}$$

Figure 71.

Schematic representation of a plating system employing
a dual anodic system with the current split between the
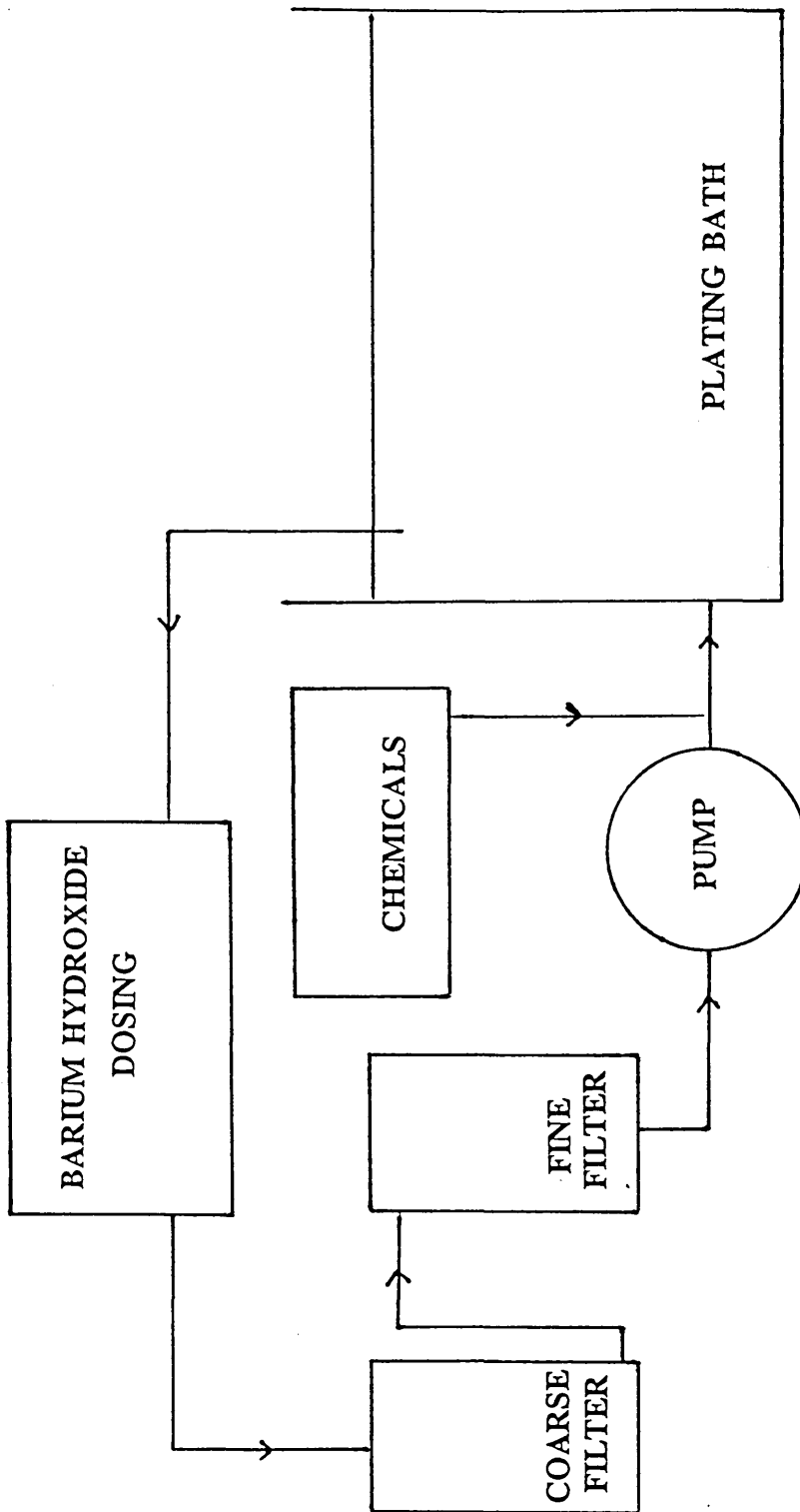individual anodes.

Figure 72.

Schematic representation of an envisaged plating system
including filters for removal of impurities and excess
carbonate.